MAR 12 1929

BUREAU OF STANDARDS JOURNAL OF RESEARCH

Vol. 1 NOVEMBER, 1928 No. 5

CONTENTS

RP. No.	TITLE AND AUTHOR	Page
24	Mutual inductance and torque between two concentric solenoids. Chester Snow	685
25	A study of the hydrogen-antimony-tin method for the determination of oxygen in cast irons. Bengt Kjerrman and Louis Jordan	701
26	Note on the effect of repeated stresses on the magnetic properties of steel. M. F. Fischer	721
27	Effect of twist on cotton yarns. A. A. Mercier and Charles W. Schoffstall	733
28	Design of tuned reed course indicators for aircraft radiobeacon. F. W. Dunmore	751
29	Thermal expansion of magnesium and some of its alloys. Peter Hidnert and W. T. Sweeney	771
30	Equipment for routine spectral transmission and reflection measurements. H. J. McNicholas	793
31	Effect of temperature change on the color of red and yellow Lovibond glasses. Deane B. Judd	859

BUREAU OF STANDARDS JOURNAL OF RESEARCH

CONTENTS OF PREVIOUS ISSUES

July, 1928 (Vol. 1, No. 1)

RP1. Accelerated tests of organic protective coatings. Percy H. Walker and E. F. Hickson.

RP2. Measurement of the tread movement of pneumatic tires and a discussion of the probable relation to tread wear. W. L. Holt and C. M. Cook.

RP3. Absolute methods in reflectometry. H. J. McNicholas.

RP4. Interferometer measurements of wave lengths in the vacuum arc spectra of titanium and other elements. C. C. Kiess.

RP5. Analysis of bauxite and of refractories of high alumina content. G. E. F. Lundell and J. I. Hoffman.

August, 1928 (Vol. 1, No. 2)

RP6. Some measurements of the transmission of ultra-violet radiation through various kinds of fabrics. W. W. Coblentz, R. Stair, and C. W. Schoffstall.

RP7. Tinting strength of pigments. H. D. Bruce.

RP8. Wave-length measurements in the arc and spark spectra of hafnium. William F. Meggers.

RP9. Tests of the effect of brackets in reinforced concrete rigid frames. Frank E. Richart.

RP10. Accelerated laboratory corrosion test methods for zinc-coated steel. Edward C. Groesbeck and William A. Tucker.

September, 1928 (Vol. 1, No. 3)

RP11. Stanoard solar wave lengths (3592-7148A). Keivin Burns, William F. Meggers, and C. C. Kiess.

RP12. Wave lengths and Zeeman effects in yttrium spectra. William F. Meggers.

RP13. Wear and mechanical properties of railroad bearing bronzes at different temperatures. H. J. French, S. J. Rosenberg, W. LeC. Harbaugh, and H. C. Cross.

RP14. Steel for casehardening—normal and abnormal steel. S. Epstein and H. S. Rawdon.

RP15. Strain markings in mild steel under tension. H. S. Rawdon.

October, 1928 (Vol. 1, No. 4)

RP16. Methods for the derivation and expansion of formulas for the mutual inductance of coaxial circles and for the inductance of single-layer solenoids. Frederick W. Grover.

RP17. Effect of clearance and displacement of attracted disk, and also of a certain arrangement of conducting hoops upon the constant of an electrometer. Chester Snow.

RP18. Mutual inductance of any two circles. Chester Snow.

RP19. Receiving sets for aircraft beacon and telephony. Haraden Pratt and Harry Diamond.

RP20. Sensitization of photographic emulsions by colloidal materials. Burt H. Carroll and Donald Hubbard.

RP21. An experimental study of the corona voltmeter. H. B. Brooks and F. M. Defandorf.

RP22. The International temperature scale. George K. Burgess.

RP23. Tables of theoretical Zeeman effects. C. C. Kiess and W. F. Meggers.

These are available as separates for purchase from the Superintendent of Documents, United States Government Printing Office, Washington, D. C.

DEPARTMENT OF COMMERCE
BUREAU OF STANDARDS
George K. Burgess, Director

BUREAU OF STANDARDS JOURNAL OF RESEARCH

November, 1928
Vol. 1, No. 5

PRICE 25 CENTS
$2.75 PER YEAR ON SUBSCRIPTION
Sold only by the Superintendent of Documents, U. S. Government Printing Office
Washington, D. C.

UNITED STATES
GOVERNMENT PRINTING OFFICE
WASHINGTON
1928

MUTUAL INDUCTANCE AND TORQUE BETWEEN TWO CONCENTRIC SOLENOIDS

By Chester Snow

ABSTRACT

By integrating a certain form of expression for the magnetic field due to a circular current, an expression equation (25) involving zonal harmonics is obtained for the r-component of magnetic field within a solenoid, where r is the radius vector from an origin lying on the axis of the solenoid. By means of a theorem derived in Research Paper No. 18 this component alone enables us to obtain the flux of this field through a circular element perpendicular to r, and, thence, by integration the mutual inductance of the two solenoids is obtained in a rapidly converging series. The axes of the solenoids make an angle θ, and by differentiating with respect to this angle the torque between the two is obtained when each carries an electric current. The effect of the discrete nature of the windings of both solenoids is investigated, and correction terms obtained for this effect.

CONTENTS

	Page
I. Introduction	685
II. The magnetic field within a solenoidal current sheet	686
III. The flux of an external field through a solenoidal current sheet	690
IV. The mutual inductance between two solenoidal current sheets whose axes intersect—one solenoid within the other	692
V. Mutual inductance of two concentric solenoids not necessarily parallel	694
VI. The torque on the inner solenoid	695
1. Correction factor when inner solenoid is a single layer helical wire of radius ρ^2	696
2. Field of endless helical filament—Uniformity of field within it	696
VII. Summary	699

I. INTRODUCTION

In a certain type of current balance for absolute measurements a large solenoid incloses a smaller one, the two being concentric and having their axes perpendicular. The torque on the inner one when they both carry electric currents may be found by first finding their mutual inductance when their axes make an angle θ, and then differentiating this with respect to θ. In the derivation of an accurate formula for this mutual inductance it will be assumed that the two solenoids are each current sheets. Correction terms will then be found which take account of the discrete nature of the windings in each solenoid.

A section of the two solenoidal current sheets by a plane containing the axes of both is shown in Figure 1.

109851°—28

II. THE MAGNETIC FIELD WITHIN A SOLENOIDAL CURRENT SHEET

The magnetic potential $\Delta\Omega\ (x, y)$ at $P\ (x, y)$ (fig. 1), due to the circular current of amount $n_1\ dx_1$ in the circle whose center is at (x_1, o) and whose axis is the x-axis, its radius being a_1, is obtained in Research Paper No. 18, equation (12) as

$$\Delta\Omega\ (x, y) = 2\pi n_1 a_1 dx_1 \int_0^\infty e^{-s\,(x-x_1)}\ J_1\ (a_1 s)\ J_o\ (ys)\ ds \text{ if } x_1 < x$$
$$= -2\pi n_1 a_1 dx_1 \int_0^\infty e^{s\,(x-x_1)}\ J_1\ (a_1\, s)\ J_o\ (ys)\ ds \text{ if } x_1 > x \tag{1}$$

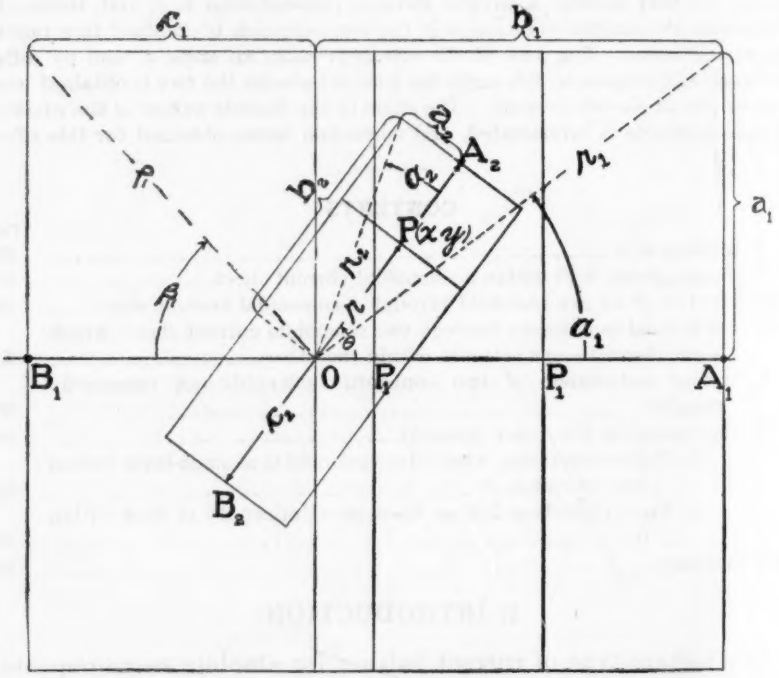

FIG. 1.—*A principal section of two solenoids whose axes intersect*

where J_o and J_1 are Bessel's functions. First differentiating with respect to x and y, respectively, and then integrating with respect to x_1, from $-c_1$ to b_1, gives for the field components at P, due to a unit current circulating around the large solenoid (a cylindrical current sheet),

$$H_x = -\frac{\delta\Omega\ (x, y)}{\delta x} = 2\pi n_1 a_1 \int_0^\infty ds\ J_1\ (a_1 s) J_o\ (ys)\ \{2 - e^{-s\,(b_1-x)} - e^{-s\,(c_1+x)}\} \tag{2}$$

$$H_y = -\frac{\delta\Omega\ (x, y)}{\delta x} = 2\pi n_1 a_1 \int_0^\infty ds\ J_1\ (a_1 s)\ J_1\ (ys)\ \{e^{-s\,(b_1-x)} - e^{-s\,(c_1+x)}\} \tag{3}$$

These are the magnetic field components (due to unit current in the large solenoid with n_1 turns per cm) at any point x, y inside or outside this solenoid provided $-c_1<x<b_1$. For the case where $P(x, y)$ lies within the large solenoid $y^2<a_1^2$. It is known that

$$\int_0^\infty e^{-sx} J_n(ys)\, ds = \frac{[(x^2+y^2)^{\frac{1}{2}}-x]^n}{y^n (x^2+y^2)^{\frac{1}{2}}} \text{ if } x>0 \tag{4}$$

and

$$\begin{aligned} a_1\int_0^\infty ds\, J_1(a_1 s)\, J_0(ys) &= 1 \text{ if } y<a_1 \\ &= 0 \text{ if } y>a_1 \end{aligned} \tag{5}$$

Hence, for internal point the equation (2) may be replaced by the following when $y<a_1$ and $-c_1<x<b_1$.

$$\begin{aligned} H_x(x, y) &= 4\pi n_1 - 2\pi n_1 a_1 \int_0^\infty ds\, J_1(a_1 s)\, J_0(ys)\, \{e^{-s(b_1-x)} - e^{-s(c_1+x)}\} \\ &= 4\pi n_1 + 2\pi n_1 a_1 \Big[J_1(a_1 D_{b_1}) \int_0^\infty e^{-s(b_1-x)} J_0(ys)\, ds \\ &\quad + J_1(a_1 D_{c_1}) \int_0^\infty e^{-s(c_1+x)} J_0(ys)\, ds \Big] \end{aligned} \tag{6}$$

or, making use of equation (4) for $n=0$.

$$\begin{aligned} H_x(x, y) = 4\pi n_1 + 2\pi n_1 a_1 \Big[& J_1(a_1 D_{b_1}) \frac{1}{\sqrt{(b_1-x)^2+y^2}} \\ & + J_1(a_1 D_{c_1}) \frac{1}{\sqrt{(c_1+x)^2+y^2}} \Big] \end{aligned} \tag{7}$$

Similarly equation (3) leads to

$$\begin{aligned} H_y(x, y) = -2\pi n_1 a_1 \Big[& J_1(a_1 D_{b_1}) \int_0^\infty e^{-s(b_1-x)} J_1(ys)\, ds \\ & - J_1(a_1 D_{c_1}) \int_0^\infty e^{-s(c_1+x)} J_1(ys)\, ds \Big] \end{aligned}$$

or, by equation (4) for $n=1$.

$$H_y(x, y) = \frac{2\pi n_1 a_1}{y} \Big[J_1(a_1 D_{b_1}) \frac{b_1-x}{\sqrt{(b_1-x)^2+y^2}} - J_1(a_1 D_{c_1}) \frac{c_1+x}{\sqrt{(c_1+x)^2+y^2}} \Big] \tag{8}$$

Here J_1 is a Bessel's function in the symbolic sense, its argument being a differentiating operator.

If $H_r(r, \theta)$ denotes that component of field at any point in the plane whose polar coordinates are (r, θ), which is reckoned in the

direction of increasing r, then from (7) and (8) (placing $x=r\cos\theta$ and $y=r\sin\theta$)

$$H_r(r,\theta)=H_x\cos\theta+H_y\sin\theta$$

$$=4\pi n_1\cos\theta+2\pi n_1 a_1\left[J_1(a_1D_{b_1})\frac{1}{r\sqrt{1-2\frac{r}{b_1}\cos\theta+\frac{r^2}{b_1^2}}}\right.$$

$$\left.-J_1(a_1D_{c_1})\frac{1}{r\sqrt{1+2\frac{r}{c_1}\cos\theta+\frac{r_1^2}{c^2}}}\right] \tag{9}$$

One form of expansion for this may be obtained by using the series of zonal harmonics

$$\frac{1}{r\sqrt{1-2\frac{r}{b_1}\cos\theta+\frac{r^2}{b_1^2}}}=\frac{1}{r}+\sum_{s=0}^{\infty}\frac{r^s}{b_1^{s+1}}P_{s+1}(\cos\theta)\text{ when }r<b_1 \tag{10}$$

Operating on this with

$$J_1(a_1D_{b_1})\equiv\sum_{k=0}^{\infty}\frac{(-1)^k\left(\frac{a_1}{2}\right)^{2k+1}}{k!\,(k+1)!}D_{b_1}^{2k+1} \tag{11}$$

and noting that

$$D_{b_1}^{2k+1}\frac{1}{b_1^{s+1}}=-\frac{\Gamma(s+2k+2)}{\Gamma(s+1)}\frac{1}{b_1^{s+2k+2}} \tag{12}$$

one finds

$$J_1(a_1D_{b_1})\frac{1}{r\sqrt{1-2\frac{r}{b_1}\cos\theta+\frac{r^2}{b_1^2}}}$$

$$=-\sum_{k=0}^{\infty}\sum_{s=0}^{\infty}\frac{(-1)^k\Gamma(s+2k+2)P_{s+1}(\cos\theta)}{\Gamma(k+1)\Gamma(k+2)\Gamma(s+1)}\left(\frac{a_1}{2b_1}\right)^{2k+1}\frac{r^s}{b_1^{s+1}} \tag{13}$$

Similarly if r is also less than c_1

$$-J_1(a_1D_{c_1})\frac{1}{r\sqrt{1+2\frac{r}{c_1}\cos\theta+\frac{r^2}{c_1^2}}}$$

$$=-\sum_{k=0}^{\infty}\sum_{s=0}^{\infty}\frac{(-1)^k\Gamma(s+2k+2)P_{s+1}(\cos\theta)}{\Gamma(k+1)\Gamma(k+2)\Gamma(s+1)}\left(\frac{a_1}{2c_1}\right)^{2k+1}(-1)^s\frac{r^s}{c_1^{s+1}} \tag{14}$$

Using the equations (13) and (14) in (9) gives

$$H_r(r,\theta) = 4\pi n_1 \cos\theta$$

$$-\pi n_1 a_1^2 \sum_{k=0}^{\infty}\sum_{s=0}^{\infty} \frac{(-1)^k \Gamma(s+2k+2) P_{s+1}(\cos\theta)}{\Gamma(k+1)\Gamma(k+2)\Gamma(s+1)} \left(\frac{a_1}{2}\right)^{2k}\left[\frac{1}{b_1^{s+2k+2}} + \frac{(-1)^s}{c_1^{s+2k+2}}\right] \tag{15}$$

If in this formula we sum first with respect to k making use of the formula

$$\Gamma(s+2k+2) = \frac{2^{2k+s+1}}{\sqrt{\pi}} \Gamma\left(k+\frac{s+2}{2}\right)\Gamma\left(k+\frac{s+3}{2}\right) \tag{16}$$

it becomes, letting $\mu = \cos\theta$

$$H_r(r,\theta) = 4\pi n_1 \mu - n_1 \pi a_1^2 D_r[\psi(r,\mu,b_1) - \psi(r,-\mu,c_1)] \tag{17}$$

where

$$\psi(r,\mu,b_1) \equiv \sum_{k=1}^{\infty} \frac{r^k}{b_1^{k+1}} P_k(\mu) F\left(\frac{k+1}{2}, \frac{k+2}{2}, 2, -\frac{a_1^2}{b_1^2}\right) \tag{18}$$

where F denotes the hypergeometric function, which has a meaning only if $\frac{a_1}{b_1}$ and $\frac{a_1}{c_1}$ are less than unity, which is the case for the applications to be made here. By applying Euler's transformation

$$F\left(\frac{k+1}{2}, \frac{k+2}{2}, 2, -\frac{a_1^2}{b_1^2}\right) = \left(\frac{b_1^2}{a_1^2+b_1^2}\right)^{1+\frac{k}{2}} F\left(\frac{2+k}{2}, \frac{3-k}{2}, 2, \frac{a_1^2}{a_1^2+b_1^2}\right) \tag{19}$$

This reduces equation (18) to

$$\psi(r,\mu,b_1) = \cos\alpha_1 \sum_{k=1}^{\infty} \frac{r^k P_k(\mu) F\left(\frac{2+k}{2}, \frac{3-k}{2}, 2, \sin^2\alpha_1\right)}{r_1^{k+1}} \tag{20}$$

where

$$r_1 \equiv \sqrt{a_1^2+b_1^2} \text{ and } \tan\alpha_1 = \frac{a_1}{b_1} \text{ and } \alpha_1 \text{ is a positive} \tag{21}$$

acute angle shown in Figure 1. Similarly, if we let

$$\rho_1 \equiv \sqrt{a_1^2+c_1^2} \text{ and } \tan\beta_1 = \frac{a_1}{c_1}$$

where β_1 is the positive acute angle shown in Figure 1, then

$$\psi(r,-\mu,c_1) = \cos\beta_1 \sum_{k=1}^{\infty} \frac{r^k P_k(-\mu) F\left(\frac{2+k}{2}, \frac{3-k}{2}, 2, \sin^2\beta_1\right)}{\rho_1^{k+1}} \tag{22}$$

By the use of (20) and (22), the expression (17) becomes

$$H_r(r,\mu)=4\pi n_1\mu$$

$$-n_1\pi a_1^2 D_{r_1}\sum_{k=1}^{\infty} r^k\left\{P_k(\mu)\frac{\cos\alpha_1 F\left(\frac{2+k}{2},\frac{3-k}{2},2,\sin^2\alpha_1\right)}{r_1^{k+1}}\right. \tag{23}$$

$$\left.-P_k(-\mu)\frac{\cos\beta_1 F\left(\frac{2+k}{2},\frac{3-k}{2},2,\sin^2\beta_1\right)}{\rho_1^{k+1}}\right\}$$

If Gauss's transformation be applied to these hypergeometric functions, one finds that

$$F\left(\frac{1+k}{2},\frac{2-k}{2},2,\sin^2\alpha_1\right)$$

$$=\cos\alpha_1 F\left(\frac{2+k}{2},\frac{3-k}{2},2,\sin^2\alpha_1\right)=\frac{2(1-\cos\alpha_1)}{\sin^2\alpha_1}\text{ if }k=1 \tag{24}$$

$$=\frac{2P'_{k-1}(\cos\alpha_1)}{k(k-1)}\text{ if }k>1$$

where P'_k denotes the derivative of P_k with respect to its argument. Hence, the expression (23) for $H_r(r,\mu)$ becomes

$$H_r(r,\mu)=2\pi n_1\left\{(\cos\alpha_1+\cos\alpha_2)\mu\right.$$

$$-D_r\sin^2\alpha_1\sum_{k=1}^{\infty}\frac{r^{k+1}P_{k+1}(\mu)P'_k(\cos\alpha_1)}{r_1^k k(k+1)} \tag{25}$$

$$\left.+D_r\sin^2\beta_1\sum_{k=1}^{\infty}\frac{r^{k+1}P_{k+1}(-\mu)P'_k(\cos\beta_1)}{\rho_1^k k(k+1)}\right\}$$

This r-component of the field is all that will be required in what follows. If the θ-component is desired it may be found by projection of H_x and H_y which are given in equations (7) and (8).

III. THE FLUX OF AN EXTERNAL FIELD THROUGH A SOLENOIDAL CURRENT SHEET

The magnetic flux through a circle of radius a_2 whose center is at $P(x, y)$ and whose plane is perpendicular to r has been obtained in Research Paper No. 18, equation (10) as

$$\Delta M=-2\pi a_2 J_1(a_2 D_r)\Omega(x,y)$$

$$=2\pi a_2\left\{\frac{a_2}{2}H_r(r,\theta)+\sum_{n=1}^{\infty}(-1)^n\frac{\left(\frac{a_2}{2}\right)^{2n+1}}{\Gamma(n+1)\Gamma(n+2)}D_r^{2n}H_r(r,\theta)\right\} \tag{26}$$

The mutual energy between this magnetic field and a solenoid or cylindrical current sheet made up of a series of continuously distributed circles, all parallel, coaxial, and of equal radius a_2, the axis entending from $r=c_2$ to $r=b_2>c_2$ $\left(0\leqq\theta\leqq\frac{\pi}{2}\right)$ and carrying a circulating current n_2 per unit length (which is constant) may be derived from equation (26) by multiplying by n_2dr and integrating with respect to r from c_2 to b_2 (holding θ constant at some value between zero and $\frac{\pi}{2}$). This energy W_1 is given by

$$W_1=2\pi n_2a_2\left\{\frac{a_2}{2}\int_{c_2}^{b_2}H_rdr+\sum_{n=1}^{\infty}\frac{(-1)^n\left(\frac{a_2}{2}\right)^{2n+1}}{\Gamma(n+1)\Gamma(n+2)}[(D_r^{2n-1}H_r)_{r=b_2}-(D_r^{2n-1}H_r)_{r=c_2}]\right\} \tag{27}$$

It is important to notice that this formula, although it makes no assumption as to the origin of the magnetic field H, does not apply to the case shown in Figure 1, where the axis of the small solenoid extends beyond the origin. It only applies to the case where both ends of the axis of this solenoid lie in the direction of the acute angle θ from the origin. On account of the peculiar character of the polar coordinates it must be modified as follows to fit the case of a solenoid shown in Figure 1. In the first place, it is evident that the integral $\int_{c_2}^{b_2}H_rdr$ must be replaced by $\int_{B_2}^{A_2}H_sds$ where s is the distance from B_2 to any point on the axis of the solenoid and H_s is the field component in the direction *from* B_2 *to* A_2. Its value will of course be independent of the path from B_2 to A_2. In the second place, if it is agreed that the polar coordinates of the point A_2 are (b_2, θ) where θ is the positive angle between zero and π (shown in the fig. 1 as acute), then the polar coordinates of B_2 will be $(c_2, \theta-\pi)$ making the convention that all polar angles shall lie between $-\pi$ and π. With this understanding the term in (27), namely, $(D_r^{2n-1}H_r)_{r=c_2}$ for $n=1, 2, 3$ (which is the derivative of odd order in the direction B_2A_2 of the field component in this same direction, taken at the point whose polar coordinates are c_2, θ where $0<\theta<\pi$) must be replaced by $D_{c_2}^{2n-1}H_{c2}$ $(c_2, \pi-\theta)$ when B_2 lies on the opposite side of the origin from A_2 and where H_{c_2} $(c_2, \pi-\theta)$ denotes the field component at B_2 in the direction of increasing c_2; that is, away from the origin. The modification of (27), which gives the mutual inductance between the unit current with n_2 turns per cm in the cylindrical sheet No. 2 and the external

field, for the case shown in Figure 1 where the faces of the cylinder lie on opposite sides of the origin, is (using μ for $\cos\theta$)

$$M = n_2 \pi a_2^2 \left\{ \int_0^{b_2} H_r(r, \mu)\, dr + \sum_{n=1}^{\infty} \frac{(-1)^n \left(\frac{a_2}{2}\right)^{2n}}{\Gamma(n+1)\,\Gamma(n+2)} D_{b_2}{}^{2n-1} H_{b_2}(b_2, \mu) \right.$$

$$\left. - \int_0^{c_2} H_r(r, -\mu)\, dr - \sum_{n=1}^{\infty} \frac{(-1)^n \left(\frac{a_2}{2}\right)^{2n}}{\Gamma(n+1)\,\Gamma(n+2)} D_{c_2}{}^{2n-1} H_{c_2}(c_2, -\mu) \right\} \quad (28)$$

This formulation of the flux through the cylindrical sheet of radius a_2 is independent of the particular source of the field. It is to be understood that b_2 and c_2 are the positive real radii vectors from the origin to the points A_2 and B_2, respectively, the corresponding angles being θ and $\pi - \theta$, and the subscript, b_2 or c_2 indicate that the component of field is reckoned in the direction of increasing b_2 or c_2, respectively.

It is in a form suitable for those applications in which the field at the points A_2 and B_2 is given in terms of the plane polar coordinates of these points, by expressions which hold for all values of r and of θ in the range between $-\pi$ and π.

IV. THE MUTUAL INDUCTANCE BETWEEN TWO SOLENOIDAL CURRENT SHEETS WHOSE AXES INTERSECT—ONE SOLENOID WITHIN THE OTHER

The two field components which occur in (28); namely, $H_{b_2}(b_2, \mu)$ and $H_{c_2}(c_2, -\mu)$ are obtainable from (25) and are

$$H_{b_2}(b_2, \mu) = 2\pi n_1 \left\{ (\cos\alpha_1 + \cos\beta_1)\,\mu - D_{b_2} \sin^2\alpha_1 \sum_{k=1}^{\infty} \frac{b_2{}^{k+1} P_{k+1}(\mu) P'_k(\cos\alpha_1)}{k(k+1) r_1{}^k} \right.$$

$$\left. + D_{b_2} \sin^2\beta_1 \sum_{k=1}^{\infty} \frac{b_2{}^{k+1} P_{k+1}(-\mu) P'_k(\cos\beta_1)}{k(k+1)\rho_1{}^k} \right\} \quad (29)$$

$$H_{c_2}(c_2, -\mu) = 2\pi n_1 \left\{ -(\cos\alpha_1 + \cos\beta)\mu \right.$$

$$- D_{c_2} \sin^2\alpha_1 \sum_{k=1}^{\infty} \frac{c_2{}^{k+1} P_{k+1}(-\mu) P'_k(\cos\alpha_1)}{k(k+1) r_1{}^k} \quad (30)$$

$$\left. + D_{c_2} \sin^2\beta_1 \sum_{k=1}^{\infty} \frac{c_2{}^{k+1} P_{k+1}(\mu) P'_k(\cos\beta_1)}{k(k+1)\rho_1{}^k} \right\}$$

Making use of (25), (29), and (30) in (28) gives

$$M = 2\pi n_1 n_2 \pi a_2^2 \{ (b_2 + c_2) \ (\cos \alpha_1 + \cos \beta_1)\mu$$

$$- u(b_2, \mu, r_1, \alpha_1) + u(b_2, -\mu, \rho_1, \beta_1) + u(c_2, -\mu, r_1, \alpha_1) - u(c_2, \mu, \rho_1, \beta_1) \} \quad (31)$$

where

$$u(b_2,\mu,r_1,\alpha_1) \equiv \sin^2 \alpha_1 \sum_{n=0}^{\infty} (-1)^n \frac{\left(\frac{a_2}{2}\right)^{2n} D_{b_2}{}^{2n}}{\Gamma(n+1)\,\Gamma(n+2)} \sum_{k=1}^{\infty} \frac{b_2{}^{k+1} P_{k+1}(\mu) P'_k(\cos \alpha_1)}{k(k+1) r_1{}^k}$$

$$= b_2 \sin^2 \alpha_1 \sum_{n=0}^{\infty} \frac{(-1)^n \left(\frac{a_2}{2b_2}\right)^2}{\Gamma(n+1)\Gamma(n+2)} \sum_{k=1}^{\infty} \frac{b_2{}^k \Gamma(k) P_{k+1}(\mu) P'_k(\cos \alpha_1)}{r_1{}^k \Gamma(k+2-2n)} \quad (32)$$

$$= b_2 \sin^2 \alpha_1 \sum_{k=1}^{\infty} \left(\frac{b_2}{r_1}\right)^k P_{k+1}(\mu) P_k(\cos \alpha_1) \Gamma(k) \sum_{n=0}^{\infty} \frac{(-1)^n \left(\frac{a_2}{2b_2}\right)^{2n}}{\Gamma(n+1)\Gamma(n+2)\Gamma(k+2-2n)}$$

But when k is a positive integer

$$\Gamma(k) \sum_{n=0}^{\infty} \frac{(-1)^n \left(\frac{a_2}{2b_2}\right)^{2n}}{\Gamma(n+1)\,\Gamma(n+2)\Gamma(k+2-2n)} = \frac{F\left(\frac{-k}{2}, -\frac{k+1}{2}, 2, -\tan^2 \alpha_2\right)}{k(k+1)}$$

$$= \frac{F\left(\frac{5+k}{2}, \frac{-k}{2}, 2, \sin^2 \alpha_2\right)}{k(k+1)\cos^k \alpha_2} = \frac{2P'_{k+2}(\cos \alpha_2)}{k(k+1)(k+2)(k+3)\cos^{k+1} \alpha_2} \quad (33)$$

if $r_2^2 = a_2^2 + b_2^2$ and $\tan \alpha_2 = \frac{a_2}{b_2}$. Hence

$$u(b_2, \mu, r_1, \alpha_1) = 2r_2 \sin^2 \alpha_1 \sum_{k=1}^{\infty} \left(\frac{r_2}{r_1}\right)^k \frac{P'_k(\cos\alpha_1) P_{k+1}(\mu) P'_{k+2}(\cos\alpha_2)}{k(k+1)(k+2)(k+3)}$$

$$= \frac{2r_2}{\sin^2 \alpha_2} \sum_{k=1}^{\infty} \left(\frac{r_2}{r_1}\right)^k \left[\frac{P_{k-1}(\cos\alpha_1) - P_{k+1}(\cos\alpha_1)}{2k+1}\right] P_{k+1}(\mu) \quad (34)$$

$$\left[\frac{P_{k+1}(\cos\alpha_2) - P_{k+3}(\cos\alpha_2)}{2k+5}\right]$$

For the other functions u one may adopt a similar notation; namely, $\rho_2^2 = a_2^2 + c_2^2$, $\tan \beta_2 = \frac{a_2}{c_2}$.

V. MUTUAL INDUCTANCE OF TWO CONCENTRIC SOLENOIDS NOT NECESSARILY PARALLEL

In this case $c_1=b_1$, $\beta_1=\alpha_1=\tan^{-1}\frac{a_1}{b_1}$, $\rho_1=r_1=\sqrt{a_1^2+b_1^2}$, $c_2=b_2$, $\beta_2=\alpha_2=\tan^{-1}\frac{a_2}{b_2}$, $\rho_2=r_2=\sqrt{a_2^2+b_2^2}$, $\mu=\cos\theta$, where θ is the angle between their axes. The formula (31) then reduces to

$$M=4\pi n_1 n_2 \pi a_2^2 2b_2\left\{\mu\cos\alpha_1 - 2\sin^2\alpha_1\cos\alpha_2\sum_{s=1}^{\infty}\frac{P_{2s+1}(\mu)\,P'_{2s}(\cos\alpha_1)\,P'_{2s+2}(\cos\alpha_2)}{2s(2s+1)(2s+2)(2s+3)}\left(\frac{r_2}{r_1}\right)^{2s}\right\}$$

$$=8\pi n_1 n_2 \pi a_2^2 b_2\cos\alpha_1\left\{\mu-\frac{\sin^2\alpha_1\cos^2\alpha_2}{2}\cdot\sum_{s=1}^{\infty}C_s(\alpha_1)\,C_{s+1}(\alpha_2)\,P_{2s+1}(\mu)\left(\frac{r_2}{r_1}\right)^{2s}\right\} \tag{35}$$

where

$$C_s(\alpha)=\frac{2P'_{2s}(\cos\alpha)}{2s(2s+1)\cos\alpha}=\frac{2\left[P_{2s-1}(\cos\alpha)-P_{2s+1}(\cos\alpha)\right]}{(4s+1)\sin^2\alpha\cos\alpha}$$

$$=F\left(1-s,s+\frac{3}{2},2,\sin^2\alpha\right)=\frac{\Gamma(s)}{\Gamma\left(s+\frac{3}{2}\right)}\sum_{k=0}^{s-1}\frac{\Gamma\left(k+s+\frac{3}{2}\right)(-\sin^2\alpha)^k}{\Gamma(k+1)\,\Gamma(k+2)\,\Gamma(s-k)} \tag{36}$$

$$=1+\frac{(1-s)}{2}\cdot\frac{\left(s+\frac{3}{2}\right)}{1}\sin^2\alpha + \frac{(1-s)}{2}\cdot\frac{(2-s)}{3}\cdot\frac{\left(s+\frac{3}{2}\right)\left(s+\frac{5}{2}\right)}{1\cdot 2}\sin^4\alpha+\cdots$$

For accurate computation the polynomials C_s for low orders of s, ($s=1, 2, 3, 4$) may be computed conveniently by this formla, which gives the special cases

$$C_1(\alpha)=1$$

$$C_2(\alpha)=1-\frac{7}{4}\sin^2\alpha$$

$$C_3(\alpha)=1-\frac{9}{2}\sin^2\alpha+\frac{33}{8}\sin^4\alpha$$

$$C_4(\alpha)=1-\frac{33}{4}\sin^2\alpha+\frac{143}{8}\sin^4\alpha-\frac{715}{64}\sin^6\alpha$$

etc., etc.

For large values of s the values of C_s might be more readily obtained (with sufficient accuracy) by interpolation from a table or curves for zonal harmonies or their derivatives.

VI. THE TORQUE ON THE INNER SOLENOID

If the two solenoids carry currents I_1 and I_2, respectively, the couple or torque T, on the inner one, tending to decrease θ is found from (35) to be

$$T = -I_1 I_2 \frac{\delta M}{\delta \theta} = I_1 I_2 \frac{\delta M}{\delta \mu} \tag{37}$$

or

$$T = 4\pi n_1 I_1 (2b_2 n_2 I_2)\, \pi a_2^2 \cos \alpha_1 \sin \theta$$

$$\left\{1 - \frac{\sin^2 \alpha_1 \cos^2 \alpha_2}{2} \sum_{s=1}^{\infty} C_s(\alpha_1) C_{s+1}(\alpha_2) P'_{2s+1}(\mu) \left(\frac{r_1}{r_2}\right)^{2s}\right\}$$

This torque is a maximum T_s when $\theta = \frac{\pi}{2}$, and $\mu = 0$, in which case

$$P'_{2s+1}(0) = \frac{2}{\sqrt{\pi}} (-1)^s \frac{\Gamma\left(s + \frac{3}{2}\right)}{\Gamma(s+1)}$$

and

$$T_s = 4\pi n_1 I_1 (2b_2 n_2 I_2)\, \pi a_2^2 \cos \alpha_1$$

$$\left\{1 + \frac{\sin^2 \alpha_1 \cos^2 \alpha_2}{\sqrt{\pi}} \sum_{s=1}^{\infty} (-1)^{s+1} C_s(\alpha_1) C_{s+1}(\alpha_2) \frac{\Gamma\left(s + \frac{3}{2}\right)}{\Gamma(s+1)} \left(\frac{r_2}{r_1}\right)^{2s}\right\} \tag{38}$$

$$= 4\pi n_1 I_1 N_2 I_2 \pi a_2^2 \cos \alpha_1 (1 + S) .$$

where $N_2 I_2 = 2b_2 n_2 I_2 =$ total current circulating around the inner solenoid, and where

$$S = \sin^2 \alpha_1 \cos \alpha_2 \sum_{s=1}^{\infty} (-1)^{s+1} \left(\frac{r_2}{r_1}\right)^{2s} \tag{39}$$

$$C_s(\alpha_1)\, C_{s+1}(\alpha_2) \left(s + \frac{1}{2}\right) \left(\frac{(1.3.5 \cdots (2s-1)}{2.4.6 \cdots\cdots (2s)}\right)$$

In equation (38) the factor $4\pi n_1 I_1$ represents the uniform field which would exist if the outer solenoid were infinite in length. Hence, the factor $\cos \alpha_1 (1 + S)$ is the end-correction factor, which reduces to 1 when $\alpha_1 = 0$; that is, when the outer solenoid is infinitely long.

In case this solenoid is 100 cm long and 30 cm in diameter, $\cos \alpha_1 = 0.957826$. If the length and diameter of the inner solenoid is 10 cm, then $S = 0.000054$, so that the end correction factor $\cos \alpha_1 (1 + S) = 0.957879$, showing that the torque on the inner solenoid is about 4

per cent less than if the outer one were infinitely long. Evidently the small solenoid lies in a field which is practically uniform in this case.

1. CORRECTION FACTOR WHEN INNER SOLENOID IS A SINGLE LAYER HELICAL WIRE OF RADIUS ρ_2

If the inner solenoid (lying in a uniform field $4\pi n_1 I_1$) be not a continuous-current sheet as previously assumed, but consists rather of any number of strips or rings of no cross section, the torque upon it remains the same as before if their radii remain the same and the total current $N_2 I_2$ be the same. The torque on each ring is unaltered by giving it a parallel displacement. Hence, it is evident that in those cases where the inner solenoid lies in an approximately uniform field, but consists of N_2 circular turns of mean radius a_2, whose circular cross section is ρ_2, the factor πa_2^2 which occurs in (38) must be replaced by $\frac{1}{\pi\rho_2^2}\int\int \pi a^2 dS$ where the integration is taken over the circular section of the wire of radius ρ_2 whose center is a distance a_2 from the axis of the solenoid, and where a is the distance of any point in this section from that axis. (This assumes uniform current distribution over the section of the wire.) For a circular section

$$\frac{\pi}{\pi\rho_2^2}\int\int a^2 dS = \pi a_2^2\left(1+\frac{\rho_2^2}{4a_2^2}\right)$$

Hence, when the inner solenoid consists of N_2 parallel circular rings of wire, of mean radius a_2, with wire section of radius ρ_2, it experiences a torque

$$T = 4\pi n_1 I_1 \pi a_2^2 (N_2 I_2)\left(1+\frac{\rho_2^2}{4a_2^2}\right)\cos\alpha_1\,(1+S) \qquad (40)$$

The N_2 parallel turns might be spaced irregularly in any manner without affecting the validity of this formula if the field $4\pi n_1 I_1$ is uniform as assumed. Moreover, since this field is perpendicular to the axis of the small solenoid, this formula for N_2 parallel circles could also be used for a helix of N_2 turns, since the torque due to the axial component of current in the helix could have no component of the type represented by T. Furthermore, if the return lead wires of this helix lie in the vertical plane containing the knife-edge upon which the helix is balanced, they would contribute nothing to the component of torque about that knife-edge.

2. FIELD OF AN ENDLESS HELICAL FILAMENT—UNIFORMITY OF FIELD WITHIN IT

Although the lack of uniformity of the field of the outer solenoid over the space occupied by the inner one, may be small due to the end-correction factor $\cos\alpha_1\,(1+S)$ being very nearly unity, there will be

in any actual case another source of nonuniformity; namely, that due to the fact that the outer solenoid is not a current sheet but a helix. It is evident that if the number of turns per cm is large the field may be made very uniform over the region in which the inner coil lies, provided all parts of the latter are sufficiently distant from the windings of the former. What assurance have we that this condition is realized in any actual case, and to such an extent that (40) may be regarded as a precision formula?

The answer may be found in an examination of the field within and near the first solenoid, when it is considered endless though not a current sheet but a helical current filament wound upon a cylinder of radius a_1, whose axis is the x axis. If any point in space P has the cylindrical coordinates x, r, θ (where r is now its distance from the x axis) then the magnetic field at P is the curl of a vector potential A, and its cylindrical components are given by

$$H_x = \frac{1}{r}\left[\frac{\delta}{\delta r}(rA_\theta) - \frac{\delta A_r}{\delta \theta}\right], H_r = \frac{1}{r}\frac{\delta A_x}{\delta \theta} - \frac{\delta A_\theta}{\delta_x}, H_\theta = \frac{\delta A_r}{\delta x} - \frac{\delta A_x}{\delta r} \qquad (41)$$

Let the number of turns of the helix be n_1 (not necessarily integral) and let the trace of this helical filament on the upper part of the plane $z=0$, for which $y=+a_1$, be the points whose x coordinates are $-\infty, \ldots\ldots -\frac{2}{n}, -\frac{1}{n}, 0, \frac{1}{n}, \frac{2}{n}, \frac{3}{n} \ldots\ldots +\infty$. It may be shown that if $r<a_1$

$$A_x = 2I_1\left\{\log\frac{1}{a_1} + \pi i\sum_{k=1}^{\infty} J_k(2\pi n_1 rki)H_k(2\pi n_1 a_1 ki)\cos k(2\pi n_1 x - \theta)\right\}$$

$$A_r = 4\pi n_1 a_1 I_1\left\{\frac{\pi i}{2}\sum_{k=1}^{\infty}[J_{k+1}(2\pi n_1 rki)H_{k+1}(2\pi n_1 a_1 ki)\right.$$

$$\left. - J_{k-1}(2\pi n_1 rki)H_{k-1}(2\pi n_1 a_1 ki)\,]\sin k(2\pi n_1 x - \theta)\right\} \qquad (42)$$

$$A_\theta = 4\pi n_1 a_1 I_1\left\{\frac{r}{2a_1} + \frac{\pi i}{2}\sum_{k=1}^{\infty}[J_{k+1}(2\pi n_1 rki)H_{k+1}(2\pi n_1 a_1 ki)\right.$$

$$\left. - J_{k-1}(2\pi n_1 rki)H_{k-1}(2\pi n_1 a_1 ki)]\cos k(2\pi n_1 x - \theta)\right\}$$

where H_k denotes Hankel's function of the first kind whose asymptotic expansion when x is a large positive real is

$$H_k(ix) \simeq \sqrt{\frac{2}{\pi x}}\, e^{-x - i\frac{\pi}{2}(k+1)}$$

The corresponding expansion for the Bessel's function is

$$iJ_k(ix) \simeq \frac{1}{\sqrt{2\pi x}} e^{x+1\frac{\pi}{2}(k+1)}$$

When the point is outside the helix, $r>a_1$, the corresponding values of A_x, A_r, A_θ are obtainable from (42) by interchanging a_1 and r where they occur inside the braces. These exact expressions may be simplified, and, in fact, the series may be summed, in case the number of turns n_1 per cm of the winding is sufficiently great, and the radius a_1 of the winding so large that $2\pi n_1 a_1$ is large enough to make the foregoing asymptotic expansions valid. In this case (42) reduces in case r is slightly less than a_1 to

$$\begin{aligned} A_x &= 2I_1\left\{\log\frac{1}{a_1} - \frac{\log\psi}{4\pi n_1\sqrt{a_1 r}}\right\} \\ A_r &= 0 \qquad (43) \\ A_\theta &= 4\pi n_1 a_1 I_1\left\{\frac{r}{2a_1} - \frac{\log\psi}{4\pi n_1\sqrt{a_1 r}}\right\} \end{aligned}$$

where

$$\psi = 1 - 2e^{-2\pi n_1(a_1-r)}\cos(2\pi n_1 x-\theta) + e^{-4\pi n_1(a_1-r)} \qquad (44)$$

For outside points ($r>a_1$) the quantities a_1 and r must be interchanged in (44) and within the braces of (43). If $e^{-2\pi n_1(a_1-r)}$ is very small one finds from (43) and (44) the approximations for $r<a_1$

$$\begin{aligned} A_x &= 2I_1\left\{\log\frac{1}{a_1} + \frac{e^{-2\pi n_1(a_1-r)}\cos(2\pi n_1 x-\theta)}{2\pi n_1 a_1}\right\} \\ A_r &= 0 \\ A_\theta &= 4\pi n_1 a_1 I_1\left\{\frac{r}{2a_1} + \frac{e^{-2\pi n_1(a_1-r)}\cos(2\pi n_1 x-\theta)}{2\pi n_1 a_1}\right\} \end{aligned}$$

This gives for the field components

$$\begin{aligned} H_x &= 4\pi n_1 I_1\{1 + e^{-2\pi n_1(a_1-r)}\cos(2\pi n_1 x-\theta)\} \\ H_r &= 4\pi n_1 I_1\, e^{-2\pi n_1(a_1-r)}\sin(2\pi n_1 x-\theta) \qquad (45) \\ H_\theta &= -\frac{2I_1}{a_1} e^{-2\pi n_1(a_1-r)}\cos(2\pi n_1 x-\theta) \end{aligned}$$

In case $n_1 \geqq 3$, $a_1 \geqq 5$ cm, then $2\pi n_1 a_1$ is approximately 100, and the asymptotic expansion may be used to obtain a good approximation. An inspection of (45) shows that the nonuniform component field will be less than one-millionth of the uniform value provided $2\pi n_1(a_1-r) \geqq 15$, which would be the case if $a_1-r=1$ cm, so that in this case the assumption that the field is uniform is amply justified.

VII. SUMMARY

The formula (35) gives the mutual inductance of the two concentric solenoids shown in Figure 1, where n_1 and n_2 are the number of turns per cm and μ is cos θ, θ being the angle between their axes. The formula presumes a strip winding so that the solenoids constitute current sheets in which the axial component of current is neglected. a_1 is the radius of the outer solenoid, 2 b_1 is length, and 2 a_1 the angle subtended at the center by its end diameter, and 2 r_1 the diagonal of a principal section. The inner solenoid is characterized by the similar quantities a_2, b_2, a_2, and r_2.

The torque in the inner solenoid is given by equation (37) in general, and by equation (38) when the axes are perpendicular. The latter expression is modified in equation (40) to take account of the finite cross section and discrete nature of the windings of the inner solenoid. The effect of the discrete nature of the windings of the outer solenoid is investigated in VI, 2, and is found to be negligible for certain relative dimensions of the two solenoids.

WASHINGTON, April 26, 1928.

A STUDY OF THE HYDROGEN-ANTIMONY-TIN METHOD FOR THE DETERMINATION OF OXYGEN IN CAST IRONS

By Bengt Kjerrman and Louis Jordan

ABSTRACT

A comparison of the vacuum fusion and the hydrogen-antimony-tin reduction methods for the determination of oxygen in cast-iron samples indicated that it is very important that lump samples rather than milled samples be used in either method in order to avoid erroneous results for oxygen due chiefly to the adsorption of air and moisture on milled samples and, in a lesser degree, to surface oxidation.

Within the precision of the method—namely, about 0.006 per cent oxygen—the hydrogen reduction procedure gave the same values for oxygen in cast-iron samples as the vacuum-fusion method. The precision of the latter method, however, was of the order of 0.001 per cent oxygen. For application to cast irons containing oxygen within the range of the samples used—namely, from 0.01 to 0.04 per cent—the vacuum-fusion method is to be preferred on the basis of its greater precision.

The complexity of the "blank" corrections necessary in the application of the hydrogen reduction method to high-carbon iron alloys is pointed out and discussed.

The limitation of the hydrogen-antimony-tin method to low silicon materials, said to be necessary in the case of low-carbon iron alloys, appears not to hold in the case of high carbon alloys where the carbon plays a greater part than the hydrogen in the reduction of the oxides in the sample.

CONTENTS

	Page
I. Introduction	702
II. Cast-iron samples	703
III. Oxygen content of cast irons by the vacuum-fusion method	704
1. Lump samples	705
2. Milled samples	706
IV. Oxygen content of cast irons by the hydrogen-antimony-tin method	707
1. Apparatus	707
2. Antimony-tin alloy	709
3. Detailed procedure	709
4. Blanks	712
5. Application of method to cast-iron samples	714
V. Summary	718
VI. Conclusions	720

111999°—28——1

I. INTRODUCTION

The investigation described in the present report was undertaken in 1925 as a portion of the work on gases in metals which was carried out at the Bureau of Standards under a research fellowship of the Swedish Engineers' Academy of Science (Ingeniors Vetenskaps Akademien). The object of the research was to study the application to cast irons of the "hydrogen-antimony-tin" method [1] for the determination of oxygen and to compare the results given by this method with those given by the vacuum-fusion method generally used in the bureau's laboratories.

Oberhoffer [2] has briefly and clearly traced the evolution of the hydrogen-antimony-tin method from the original Ledebur method. Following the early modifications of the original Ledebur procedure, which were attempts to increase the accuracy and decrease the time required for the determination, it was shown that by changing the temperature of the reduction from 950° C. to above 1,200° C. the amount of oxygen found in a given steel was increased. This increase in operating temperature, however, introduced new difficulties and led to the addition of antimony and tin to the steel sample in order to lower the melting point to a range in which readily available refractory tubes and furnaces were serviceable. It appeared that the reduction of manganous oxide was aided by the addition of antimony and tin, and that a partial reduction of ferrous silicates was also secured.

However, further study of the method showed that the presence of carbon in the sample caused an error, in that a very considerable reduction of the oxides in the sample by this carbon took place, with the evolution of large proportions of the oxygen as carbon dioxide and carbon monoxide, gases which were not determined in the regular procedure. Thereupon the method was modified [3] to provide for the recovery of carbon dioxide and carbon monoxide in addition to water vapor. The conclusions were, however, that the modified method was very complicated, and that the simple hydrogen-reduction method (in which there is the addition of an alloying metal or metals and the recovery only of water vapor) was best retained, with the understanding that it was applicable only to samples low in carbon and not containing any considerable amounts of difficulty reducible oxides, such as silica and alumina.

---

[1] J. Keutman and P. Oberhoffer, "II. Bestimmung des Sauerstoffs nach dem Wasserstoffverfahren unter Zuschlag von Zinn-Antimon-Legierung," Stahl und Eisen, **45**, pp. 1557–1559; 1925.

[2] P. Oberhoffer, "Sauerstoff im Eisen," Stahl und Eisen, **45**, pp. 1379–1384; 1925.

[3] P. Oberhoffer, E. Piwowarsky, A. Pfeifer-Schiessl and H. Stein, "Ueber Gas und Sauerstoffbestimmungen im Eisen, Insbesondere Gusseisen," Stahl und Eisen, **44**, pp. 113–116; 1924.

Very recently, and since the completion of the experimental work to be described in this report, Thanheiser and Müller [4] and Bardenheuer and Müller [5] have published two papers dealing with the limitations of the hydrogen reduction method. Thanheiser and Müller stated that the hydrogen-reduction method, using antimony alone as the alloying addition, is further limited to low-carbon irons containing little or no silicon. This, they indicate, is because during the determination, ferrous and manganous oxides are in large part reduced by the silicon in the steel with the formation of silica. The oxygen thus combined with silicon escapes determination. Even with as little as 0.05 per cent silicon in a steel containing 0.02 per cent carbon, less than 50 per cent of the 0.03 per cent oxygen present in the sample was found by the hydrogen reduction method. Bardenheuer and Müller add to these limitations the requirement of a low phosphorus content.

Oberhoffer and his collaborators [6] have considered that the modification of the hydrogen-antimony-tin method, which provides for the recovery of carbon dioxide and carbon monoxide, yields accurate results for oxygen in high-carbon alloys. On account, however, of the complicated train and procedure required in this method, they state that it is best to resort to a vacuum-fusion method for determining oxygen in a high-carbon iron alloy.

In the present work it was desired to study critically the hydrogen-antimony-tin method as applied to a high-carbon iron alloy, specifically cast irons, with suitable provision for recovering carbon dioxide and carbon monoxide in addition to the water vapor, and to compare such a procedure with the graphite-crucible vacuum-fusion determination of oxygen as applied to the same iron samples.

II. CAST-IRON SAMPLES

The material upon which the analyses were made was a pig iron of the following composition as represented by a single vertical cross-section slice (slice No. 3):

	Per cent
Carbon	3.68
Manganese	.73
Phosphorus	.115
Sulphur	.038
Silicon	1.31

All samples were taken from a single pig, designated as No. 4, which was cut into a number of vertical cross section slices, each

[4] G. Thanheiser and C. A. Müller, "Der Einfluss des Siliziums auf die Sauerstoffbestimmung im Wasserstoffstrom," Mitt. Kaiser-Wilhelm Inst. Eisenforsch. Düsseldorf, **9**, pp. 211-213; 1927.

[5] P. Bardenheuer and C. A. Müller, "Einfluss einiger Begleitelemente des Eisens auf die Sauerstoffbestimmung im Stahl nach dem Wasserstoffreduktionsverfahren," Archiv. Eisenhüttenwesen **1**, pp. 707-709; 1928.

[6] See footnote 3.

about 10 mm thick. These slices were numbered consecutively from one end of the pig. Thus, "4–3" indicates the third slice of the No. 4 pig. The location of the samples in the cross-section slice was designated by the letters *a*, *b*, and *c*, as shown in Figure 1.

At the conclusion of the work analyses were also made on a special cast iron containing high manganese and silicon.

III. OXYGEN CONTENT OF CAST IRONS BY THE VACUUM-FUSION METHOD

The vacuum-fusion method for oxygen, as described by Jordan and Eckman,[7] was employed for determining the total oxygen content of the pig iron. The results obtained by Jordan and Eckman in their development of this method indicate that it should yield the oxygen present in a ferrous alloy, including that combined as silica or as manganous oxide. Further, the presence of large amounts of carbon in the iron sample is an essential factor of the vacuum-fusion method and should be expected to cause no interference, as in the case of the hydrogen-antimony-tin method. The vacuum-fusion method should, therefore, be suitable for the determination of oxygen in cast-iron samples.[8] The blanks determined for the vacuum-fusion analyses are given in Table 1.

TABLE 1.—*Blanks for vacuum-fusion method*

Test No.	Oxygen blank	Hydrogen blank
	g	*g*
1	0.0048	0.00050
2	.0044	.00044
3	.0052	.00041
4	.0046	.00034
Average	.0048	.00042

In order to test the performance of the entire apparatus before starting the analyses of the pig-iron sample, duplicate determinations were made on a pure iron ingot, made from electrolytic iron, the oxygen content of which had previously been determined by the vacuum-fusion method to be 0.14 per cent. The new determinations gave 0.124 and 0.116 per cent, an average of 0.120 per cent.

[7] Louis Jordan and James R. Eckman, Gases in Metals: II. The Determination of Oxygen and Hydrogen in Metals by Fusion in Vacuum, B. S. Sci. Paper No. 514; 1925.

[8] Recent results obtained in the course of the modification and improvement of the vacuum-fusion method have indicated that the gases delivered to the gas analysis train from the fusion of ferrous materials containing free manganese may not be a true measure of the total oxygen content of the sample.

1. LUMP SAMPLES

The analyses of lump samples of pig iron No. 4 were then made, with the results given in Table 2.

TABLE 2.—*Oxygen in pig iron No. 4 by vacuum-fusion analysis of lump sample*

Pig-iron sample No.	Weight of sample	Total oxygen found	Total hydrogen found	Blank corrections		Corrected values	
				Oxygen	Hydrogen	Oxygen	Hydrogen
	g	*g*	*g*	*g*	*g*	*Per cent*	*Per cent*
4-a-2	28.24	0.0066	0.00038	0.0048	0.00042	0.006	
4-a-2	32.86	.0074	.00047	.0048	.00042	.008	0.0002
4-a-3	38.75	.0074	.00049	.0048	.00042	.007	.0002
4-a-3	31.90	.0078	.00051	.0048	.00042	.009	.0003
4-c-3	35.04	.0039	.00030	[1].0017	[1].0002	.006	.0002
4-c-3	30.76	.0034	.00025	.0012	.0001	.007	.0002
4-c-3	30.17	.0057	.00035	.0010	.0002	.015	.0005
4-c-3	25.85	.0054	.00032	.0012	.0002	.014	.0005
4-b-3	41.77	.0048	.00024	.0006	.0001	.010	.0003
4-b-3	41.15	.0061	.00035	.0010	.0001	.013	.0005

[1] The last 6 determinations listed in this table were made by an improved form of the vacuum-fusion method in which the magnitude of the blank has been materially reduced.

The analyses originally made were only those on the 4–a–2 and 4–a–3 samples. (Fig. 1.) Subsequently, additional determinations were made on four samples cut from the "c" section of the third slice of pig iron No. 4 (the 4-c-3 samples) in the position indicated by the dotted lines on section "c" in Figure 1. Unfortunately, the rela-

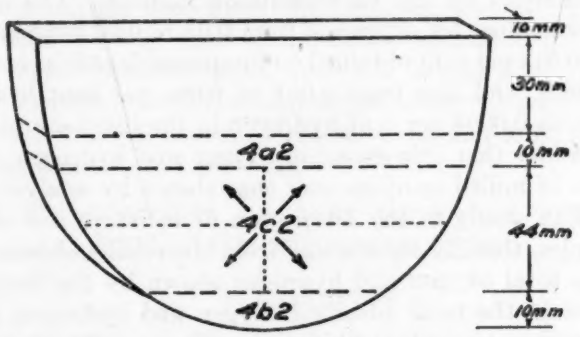

FIG. 1.—*Location of analytical samples in cross section of pig iron No. 4*

tive positions of these four samples were not recorded. Two of the four samples checked the oxygen result obtained on the "a" samples of slices 2 and 3, giving 0.006 and 0.007 per cent as compared with an average of 0.008 for the four "a" samples. The other two samples, however, were very much higher in oxygen; namely, 0.015 and 0.014 per cent. Two additional analyses made on samples from the "b" section of slice 3 gave 0.010 and 0.013 per cent oxygen. It thus appears that appreciable segregation of oxygen

occurred near the bottom of the "c" section in each cross-section slice of the pig. The milled sample of this pig iron, which was subsequently used in analyses both by vacuum-fusion and by hydrogen-reduction methods, was the entire "c" section of slice 2. The true oxygen content of this section is then to be considered as the average of the vaccuum-fusion analyses of the four 4-c-3 samples of Table 2, namely, 0.011 per cent oxygen and 0.0004 per cent hydrogen.

2. MILLED SAMPLES

It has apparently been the usual procedure to use a milled sample in those methods for determining oxygen in iron and steel which are dependent on reduction by hydrogen. Eckman, Jordan, and Jominy [9] have pointed out that the use of a finely divided form of a cast-iron sample leads to very large errors in determining oxygen by the vacuum-fusion method. Presumably such errors are due to surface oxidation of the chips or to adsorption of moisture or of air. Oberhoffer and Keutmann [10] have also found differences of from 0.02 to 0.03 per cent oxygen between lump and milled samples in analyses by the hydrogen-reduction method.

The 4–c–2 sample of pig iron No. 4 was cut on a milling machine at a very slow speed and also with extreme care to prevent any contact of oil with the milled sample. The millings were not washed in any way. Portions of this 4–c–2 sample, after thorough mixing, were taken for analysis by the vacuum-fusion method. The first three analyses gave values for oxygen of from 0.05 to 0.06 per cent as compared with 0.011 per cent obtained on lump samples of the corresponding 4–c–3 iron, and also from 0.001 to 0.003 per cent hydrogen as compared with 0.0004 per cent hydrogen in the lump samples.

If we consider that this excess of oxygen and hydrogen shown by the analysis of milled samples over that shown by analysis of lump samples is due chiefly to the adsorption of moisture and air on the milled samples, then by subtracting from the results obtained on the millings the total oxygen and hydrogen shown by the lump sample we shall obtain the total adsorbed oxygen and hydrogen, including also oxygen due to surface oxidation. The weight of this excess oxygen should be at least eight times that of the adsorbed hydrogen (since the increase in hydrogen must be due to adsorbed water) and any oxygen in excess of the hydrogen equivalent should represent adsorbed air and surface oxidation. Such calculations are given below in Table 3 for eight analyses on the milled sample and taking 0.011 per cent oxygen and 0.0004 per cent hydrogen as the true values for those gases in the 4–c–2 pig-iron sample.

---

[9] J. R. Eckman, Louis Jordan, and W. E. Jominy, "The oxygen content of coke and charcoal cast irons," Trans. Am. Foundrymen's Assoc. **33** p. 431; 1926.

[10] P. Oberhoffer and J. Keutmann, "Zur Bestimmung des Sauerstoff im Eisen; Wasserstoffverfahren," Stahl und Eisen, **46**, pp. 1045–1046; 1926.

TABLE 3.—*Adsorbed oxygen in milled sample of pig iron No. 4–c–2*

Date of analysis	Weight of sample	Total gases from milled chips		Estimated adsorbed oxygen	
		Oxygen	Hydrogen	As water	As air
	g	*Per cent*	*Per cent*	*Per cent*	*Per cent*
Sept. 11	15.83	0.046	0.0030	0.021	0.014
Sept. 12	15.05	.060	.0029	.020	.029
Sept. 24	15.10	.063	.0012	.006	.046
Sept. 25	15.24	.080	.0029	.020	.049
Sept. 28	14.94	.070	.0024	.016	.043
Dec. 11	15.00	.091	.0039	.028	.052
Dec. 12	10.00	.076	.0020	.013	.052

The milled sample of pig iron 4–c–2 was cut on the day preceding the first analysis listed in Table 3. The remaining analyses followed on the dates indicated in the table.

The total oxygen obtained from the milled samples by the vacuum-fusion procedure was from 0.05 to 0.09 per cent, some four to eight times the true oxygen content of the pig iron as shown by vacuum-fusion analyses of lump samples. Of this amount the oxygen adsorbed as water was calculated to be from 0.02 to 0.03 per cent and that as air from 0.02 to 0.05 per cent.

Oberhoffer and E. Piwowarsky [11] have also lately shown that their vacuum-fusion procedure gave an oxygen value on millings of cast iron of from two to four times that obtained with lump samples.

The true oxygen content of the lump samples of pig iron 4–c–3 was therefore fixed by the vacuum-fusion method as 0.011 per cent. For the milled samples taken from the second slice at the corresponding position (4–c–2) the total oxygen content, including adsorbed air and moisture, was shown by the same method to be six times the true value; namely, 0.07 per cent.

IV. OXYGEN CONTENT OF CAST IRONS BY THE HYDROGEN-ANTIMONY-TIN METHOD

1. APPARATUS

A diagram of the apparatus assembled for carrying out the hydrogen-antimony-tin reduction method is shown in Figure 2. A cylinder of hydrogen is connected to the train through stopcock *A*; *B* is an open-end manometer for indicating the pressure of the incoming hydrogen and is also used for testing the tightness of the train; *C* is a bubble tube and guard tube containing sulphuric acid to indicate the rate of flow of the incoming gas; *D* is an electric resistance furnace operated at about 800° C. to heat a silica tube filled with

[11] P. Oberhoffer and E. Piwowarsky, "Ueber den Sauerstoff im Roh und Gusseisen," Stahl und Eisen, 47, p. 521; 1927.

copper chips. This furnace was designed to convert to water vapor the traces of oxygen in the hydrogen gas. The absorption tube *E* contains phosphorus pentoxide for absorbing water vapor formed in the catalyst furnace *D*. The three-way stopcock *F* permits the sweeping out of the train up to the furnace *G* with oxygen-free hydrogen before admitting the hydrogen to the furnace. The platinum wound electric resistance furnace *G* heats the porcelain (sillimanite) tube which contains the sample boat and sample. The weighed absorption tubes *I* and *J* contain, respectively, phosphorus pentoxide, for the absorption of water vapor, and ascarite, which is

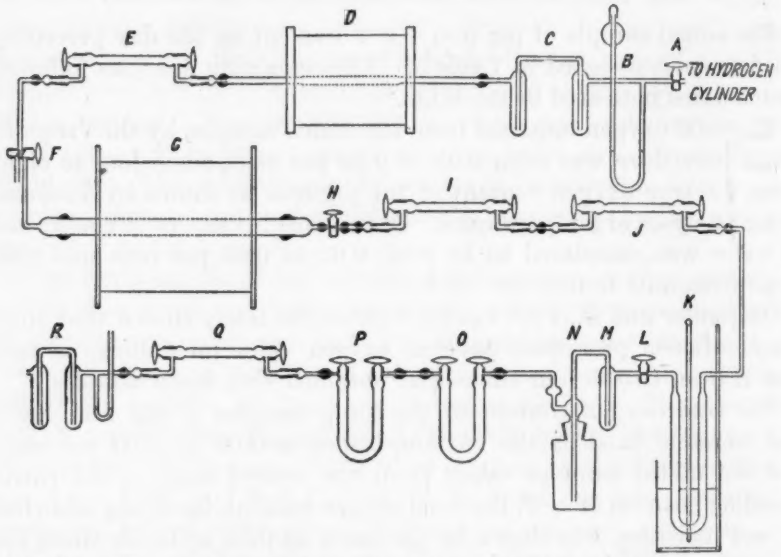

FIG. 2.—*Diagram of apparatus for the determination of oxygen in cast irons by the hydrogen-antimony-tin method*

guarded at each end with phosphorus pentoxide, for the absorption of carbon dioxide. The U-tube at *K* contains iodine pentoxide heated in an oil bath to 150° C. for the oxidation of carbon monoxide to carbon dioxide. The oil bath contains a thermometer and a stirring rod, as indicated. The trap *M* is to guard against any of the solution in *N* passing back into the tube *K*. The wash bottle *N* contains an aqueous solution of potassium iodide (2 g of KI in 180 ml water) for the absorption of free iodine evolved from the tube *K* by the oxidation of carbon monoxide. Tubes *O* and *P* contain, respectively, sulphuric acid and phosphorus pentoxide for the preliminary and final drying of the gas which passes through the potassium iodide wash solution in *N*. The weighed absorption tube *Q* contains ascarite and phosphorus pentoxide for the absorption of

carbon dioxide formed by the oxidation of carbon monoxide from the sample. The open-end manometer following *Q* and the bubble tube and guard tube *R* indicate the pressure and the rate of flow of the hydrogen gas at the exit end of the train.

2. ANTIMONY-TIN ALLOY

The antimony-tin alloy used for mixing with the iron samples was prepared by melting equal weights of antimony and tin in an Acheson graphite crucible in a high-frequency induction furnace. Graphite powder was sprinkled on the surfaces of the melt. The alloy ingot was machined on the lathe to a clean cylinder of metal and then crushed in an iron mortar. The crushed alloy was cleaned with alcohol and ether, and that portion passing through a 6-mesh but retained on a 10-mesh screen was preserved for use in a glass bottle with ground stopper, but without the use of any lubricant on the ground surfaces.

3. DETAILED PROCEDURE

The analyses for oxygen in the pig-iron samples by the hydrogen-antimony-tin method were made generally on 5 g samples of the iron with 10 g of the antimony-tin alloy, heated at 1,200° C. The sample, with the antimony-tin alloy, was placed in an alundum boat which had previously been heated in hydrogen. This boat and its contents were placed at the middle in the porcelain tube within furnace *G*. (Fig. 2.) The temperature of the section of the porcelain tube occupied by the boat was determined by means of a platinum, platinum-rhodium thermocouple whose hot junction was placed between the porcelain furnace tube and the outer alundum core which supported the platinum furnace winding.

It is of the utmost importance that no oxygen, either from the air or from impure hydrogen, shall at any time enter the porcelain tube of furnace *G*. In order to prevent such entrance of oxygen it is best to maintain between runs a pressure of hydrogen within the porcelain tube slightly above atmospheric pressure, or still better, to maintain, if possible, a very slow stream of hydrogen (about 15 bubbles per minute at *C*) through the train as far as stopcock *H* and keep the furnace *G* at its operating temperature. The hydrogen escapes into the air at stopcock *H*.

When it is necessary to allow furnace *G* to stand with no stream of hydrogen flowing, stopcocks *F* and *H* should be closed when the temperature of the furnace is as low as possible and with the hydrogen pressure as high as possible. A new determination must then be begun by sweeping hydrogen through the cold furnace *D* and the train up to stopcock *F*, where the gas escapes into the air. Only after furnace *D* has been heated at its operating temperature for several minutes is the hydrogen stream turned into the sample furnace *G*.

While the train is being swept out, the three absorption tubes, *I*, *J*, and *Q*, are filled, their surfaces cleaned with ether, and then weighed. While waiting for the tubes, hanging in or near the balance case, to come to constant weight the potassium iodide solution in *N* is changed. This renewal of the potassium iodide solution is necessary before each run in order that the concentration of free iodine in the solution shall be kept as low as possible. The ground-glass stopper of bottle *N* is lubricated with moist phosphorus pentoxide. A solid cake of moist phosphorus pentoxide put on the finger and rubbed over the ground-glass surface served better than phosphorus pentoxide moistened to a sirupy consistency. The stopcock *L*, both stopcocks of tube *O*, and the stopcock of tube *P* next to *O* are all lubricated with moist phosphorus pentoxide. Ordinary stopcock grease is not permissible in these locations because of reactions with iodine vapors, causing the formation of products which are taken up in tube *Q* and will be mistaken for carbon dioxide resulting from carbon monoxide derived from the sample. Stopcocks thus lubricated with rather viscous phosphorus pentoxide paste are best lifted very slightly from their seats when they are turned. If they are pressed into their seats on turning, the lubricated joint often is not tight.

The ground-glass connections of tube *Q* and that of tube *J* next to *K* are not lubricated. These connections must be very carefully ground and may be held firmly pressed together by rubber bands. The use of a grease lubricant at these points must be avoided because of the reaction with iodine vapors mentioned above. The use of the phosphorus pentoxide lubricant was not convenient on the type of tube connections employed because of its accumulation in the open end of the train during the repeated inserting and removal of the tubes. All other stopcocks and ground-glass connections are lubricated with a medium hard stopcock grease made of vaseline, crude rubber, and paraffin.

When the absorption tubes have been weighed and the sample and antimony-tin alloy weighed out, the cap of the sample furnace tube is removed at the de Khotinsky seal (the cap next to stopcock *H*) while the flow of hydrogen through the furnace is increased 25 to 50 per cent over the normal rate of about 80 bubbles per minute at *C* (approximately 1.85 liters per hour).

The boat containing the antimony-tin-iron alloy from the previous run, is then removed from the furnace tubes by means of a hooked-end wire and metal tweezers. The fused sample is then removed from the boat and the latter carefully and thoroughly brushed with a stiff bristle brush to remove as much of the fine graphite powder as possible. If the boat is not brushed quite free of graphite each time, an abnormally large amount of carbon monoxide will be indicated by the gain in weight in the third absorption tube in the next succeeding

run. This is caused by an increase in the "hydrocarbon blank." (See IV, 4, (*d*).)

The cleaned boat containing the new sample and antimony-tin alloy is put back at the middle of the furnace tube. The cap is then resealed to the furnace tube and the weighed absorption tube *I* put in place while the hydrogen is still flowing and with the stopcocks of tube *I* open. Then by closing the stopcock at the exit end of tube *I* the train is tested for tightness up to this point. Tube *J* is then put in place and the ungreased ground-glass joint at the exit end of tube *J* is wound tightly with a thin rubber strip (such as a strip cut from a toy balloon). The train as far as the outlet stopcock of tube *P* is now tested for leaks by determining if it will hold a pressure of hydrogen equivalent to about 40 mm of mercury in manometer *B*. If the train is free from leaks, the stopcock at the outlet of tube *P* is opened and the hydrogen is passed through the train at the regular rate (1.85 liters per hour). The gas burner for heating the oil bath, which surrounds tube *K*, is now lighted. After the gas has passed thus for one-half hour and the oil bath has reached 150° C. the third weighed absorption tube *Q* is placed in the train and the current is turned on in the sample furnace *G*.

In all the runs the sample furnace was brought from room temperature to 1,200° C. in approximately two hours. The duration of the run is taken as the time the sample was held at the full temperature of 1,200° C. after the two-hour period required to first reach that temperature. The minimum length of run required for complete recovery of the oxygen determined by this method in any particular class of material was estimated by making runs of increasing lengths of time on similar samples.

In Table 4 are given the results of seven analyses on milled samples of pig iron 4–c–2 in which the duration of the heating at 1,200° C. was varied from 0 to 3 hours. Runs 21, 29, and 47 were made by heating the sample up to 1,200° C., stopping the run as soon as the sample and furnace had just reached that temperature; that is, approximately two hours after the start of the heating from room temperature.

TABLE 4.—*Recovery of oxygen as influenced by duration of heating of sample at 1,200° C.*

Run No.	Duration of heating at 1,200° C.	Oxygen found
	Hours	*Per cent*
21	0	0.022
29	0	.028
47	0	.028
63	1	.058
55	2	.12
57	2	.11
61	3	.10

The values for oxygen shown in Table 4 indicate that not less than two hours heating of the sample at 1,200° C. is necessary for the recovery of all the oxygen determinable by this method. Accordingly, all determinations were made with at least a two-hour heating period, and when working with lump samples the heating period was increased to two and one-half hours.

After a run is completed and the absorption tubes *I*, *J*, and *Q* are removed, air purified by passing through phosphorus pentoxide and ascarite is passed through each absorption tube for one minute (at a rate of about 3 liters per hour) in order to replace the hydrogen. Tube *J* should be swept free of hydrogen by passing the air through it in the direction opposite to that of the flow of hydrogen through the tube as placed in the train on account of the danger of traces of moisture having condensed in the arm of the tube next to tube *I* if, as was the case in the train employed, it is necessary to unseal with a hand-torch flame the de Khotinsky cement joint between *I* and *J*. All three tubes are again carefully cleaned with ether and weighed.

4. BLANKS

It was soon evident that in the hydrogen antimony-tin method of determining oxygen in cast irons there were many sources of oxygen or of other gases which might be absorbed in the weighed tubes and mistaken for oxygen. These sources may be enumerated as follows:

(*a*) The oxygen from the sample; the value it is desired to obtain.

(*b*) Oxygen from air or moisture adsorbed on the alundum boat during the loading of the sample and any oxygen from the reduction of oxides of which the boat is made.

(*c*) Oxygen from oxides in and air adsorbed on the crushed antimony-tin alloy.

(*d*) Hydrocarbons formed from the action of hydrogen on carbides or free graphite. Such hydrocarbons apparently react to some extent with the iodine pentoxide yielding oxidation products which are recovered in the weighed tubes but which do not represent oxygen derived from the metal sample.

(*e*) A possible small but continued reduction of the oxides of the alundum boat even after adsorbed air has been removed.

(*f*) A possible small but continued reduction of oxygen in the antimony-tin alloy after adsorbed air and surface oxidation of the crushed alloy has been removed.

It thus became necessary to make four distinct kinds of runs for each sample of different composition or of different form—that is, millings or lump sample—or of different weight or ratio of sample to alloy. These four types of runs are designated as—

1. Beginning sample run (BSR).
2. End sample run (ESR).

3. Beginning blank run (BBR).
4. End blank run (EBR).

A "BSR" value is obtained according to the regular procedure as described for a typical determination, opening the sample furnace and placing a new sample and portion of alloy in a boat previously used for several runs. Such a run, therefore, includes the oxygen from the sources designated above as *a*, *b*, *c*, and *d*.

An "ESR" value is obtained by the regular heating period on a boat, sample, and alloy remaining from a "BSR" determination without, however, opening the sample furnace tube between the two runs. This run then includes the oxygen from sources designated above as *d*, *e*, and *f*.

The "BBR" value is obtained by making a regular run opening of the furnace tube but putting the proper weight of antimony-tin alloy only in the boat, omitting the sample. Such a run gives the combined values of oxygen from *b* and *c*.

The "EBR" value is obtained by a run after the "BBR" determination without opening the sample tube. This gives the combined values for oxygen from *e* and *f*.

Then, since

$$\text{BSR} = a+b+c+d$$
$$\text{ESR} = d+e+f$$
$$\text{BBR} = b+c$$
$$\text{EBR} = e+f$$

$$\text{BSR}+\text{EBR}-\text{BBR}-\text{ESR} = (a+b+c+d)+(e+f)-(b+c)-(d+e+f)$$
$$= a,$$

the oxygen content of the sample only.

Many preliminary blank runs were made to develop the technique of the method and to indicate the complexity of the blank. It was in the course of this preliminary work that it became evident that wash bottle *N* and drying tubes *O* and *P* were needed between the iodine pentoxide tube and the third absorption tube in order to prevent iodine from passing into the absorption tube; that all traces of oxygen must be kept from entering the sample tube of furnace *G* at any time, even after the tube had cooled to room temperature, probably on account of the ready oxidation of antimony deposited from the vapor in the cooler portions of the tube. Such entrance of oxygen was guarded against by keeping the tube at all times full of hydrogen which had passed over hot copper chips and through phosphorus pentoxide. As a further precaution, the unsealing of the cap for opening the sample tube as well as the resealing after replacing the boat or boat and sample was carried out with a flow of pure hydrogen through the sample tube, made at a sufficiently increased rate, so that the escaping hydrogen, when ignited by the flame of the torch used for softening the cement, should not burn back in the end of the

sample tube. The early blank runs also showed the need for precise control of the temperature and of the duration of the runs. The need of conditioning a new alundum boat by repeated heatings in hydrogen at 1,200° C. or higher was also clearly demonstrated.

5. APPLICATION OF METHOD TO CAST-IRON SAMPLES

The results of the analyses of both milled and lump samples of pig iron No. 4 by the hydrogen-antimony-tin method are given in Table 5. The analyses on milled samples show, in the first place, that a heating period of two to three hours is required for complete reduction, as has already been pointed out in a briefer summary of these same analyses in Table 4. The analyses made with two and three hour heating periods gave for the oxygen content of the milled samples 0.10 to 0.12 per cent. These results are to be compared with the analyses listed in Table 3 where the average oxygen content of this same milled sample was found by the vacuum-fusion method to be 0.07 per cent. This latter value is to be regarded as including somewhat less than the total of the adsorbed air and moisture, since in the vacuum-fusion method the preliminary evacuation of the furnace tube containing the cold sample may well be expected to remove a portion of the less firmly held adsorbed air and water. This preliminary evacuation is carried out through a by-pass, and extracted oxygen or moisture is thus lost. On the other hand, in the hydrogen-antimony-tin method there is no preliminary evacuation when the sample is placed in the cold furnace. The stream of dry hydrogen immediately sweeps over the sample and into the first weighed absorption tube, where any more loosely adsorbed water will be recovered and so must appear as a part of the final result. Some of the adsorbed oxygen which is lost in the preliminary evacuation of the vacuum-fusion method may also be retained by the sample in the hydrogen-reduction method until the heating of the sample has progressed enough to bring about the reduction of the oxygen to water vapor.

In the case of the analysis of milled samples of the pig iron, therefore, the hydrogen-antimony-tin method, when carried out with due regard to the length of the heating period at 1,200° C., to the complexity of the blank correction, and with the technique as described, gave results for oxygen which were of the same order as those obtained by the vacuum-fusion method on the same milled sample. As was shown, however, in the preliminary analyses by vacuum fusion, the oxygen values obtained from milled samples are greatly in error, due to adsorbed moisture and air. The hydrogen-antimony-tin method must, therefore, be applicable to lump samples if it is to give the true values for the oxygen content of a cast iron.

The results of analyses made by the hydrogen-antimony-tin method on solid samples of pig iron 4–b–2 are given as runs 65, 67, 69, and 71 in Table 5. These four analyses gave values of 0.020, 0.013, 0.025, and 0.011, an average value of 0.017 per cent oxygen, to be compared with the average of 0.012 per cent oxygen obtained by the vacuum-fusion method on lump samples of 4–b–3 or with the average of 0.011 per cent oxygen, the average of lump samples of 4–c–3.

Finally, an analysis was made on a sample of a cast iron of high manganese and silicon contents (designated as iron "E") of the following composition:

	Per cent
Carbon	2. 88
Manganese	1. 29
Sulphur	. 047
Silicon	4. 51

This iron showed an oxygen content of 0.043 per cent by the hydrogen-antimony-tin method using a lump sample. (Run 77, Table 5.) Three determinations by the vacuum-fusion method gave values of 0.038, 0.035, and 0.041 per cent oxygen for this same sample, or an average of 0.038 per cent.

The hydrogen-reduction method thus gave results for oxygen slightly higher than the vacuum-fusion method when using lump samples of both pig iron No. 4 and cast iron "E."

TABLE 5.—*Oxygen in cast irons as determined by the antimony-tin-hydrogen method*

Run No.	Type and duration of run	Cast-iron sample	Weight of iron sample used with 10 g Sb–Sn	Oxygen evolved from sample as—			Total oxygen	Oxygen in sample	Blank correction
				H_2O	CO_2	CO			
			g	*0.1 mg*	*0.1 mg*	*0.1 mg*	*0.1 mg*	*Per cent*	*0.1 mg*
21	BSR, up to 1,200° C	4–c–2, milled	5.04	31	3	32	66	0.022	[1](66–35+16–36)
23	ESR, up to 1,200° C	do	5.04	4	7	24	35		
25	BSR, up to 1,200° C	do	5.00	35	7	38	80	[2].050	(80–35+16–36)
27	ESR, up to 1,200° C	do	5.00	6	7	22	35		
29	BSR, up to 1,200° C	do	5.00	35	6	31	72	.028	(72–38+16–36)
47	BSR, up to 1,200° C	do	5.00	36	7	29	72	.028	(72–38+16–36)
48	ESR, up to 1,200° C	do	5.00	6	12	20	38		
49	BBR, up to 1,200° C			19	22	1	42		
50	EBR, up to 1,200° C			7	7	3	17		
51	BBR, up to 1,200° C			9	19	2	30		
52	EBR, up to 1,200° C			6	5	3	14		
55	BSR, 2 hours at 1,200° C	4–c–2, milled	5.00	41	15	112	168	.120	(168–88+9–29)
56	ESR, 2 hours at 1,200° C	do	5.00	4	9	75	88		
57	BSR, 2 hours at 1,200° C	do	5.00	41	15	99	155	.110	(155–80+9–29)
58	ESR, 2 hours at 1,200° C	do	5.00	7	9	64	80		
59	BBR, 2 hours at 1,200° C			4	19	6	29		
60	EBR, 2 hours at 1,200° C			3	1	5	9		
61	BSR, 3 hours at 1,200° C	4–c–2, milled	5.00	34	18	127	179	.104	(179–107+9–29)
62	ESR, 3 hours at 1,200° C	do	5.00	7	12	88	107		
63	BSR, 1 hour at 1,200° C	do	5.00	36	13	55	104	.058	(104–55+9–29)
64	ESR, 1 hour at 1,200° C	do	5.00	7	8	40	55		
65	BSR, 2½ hours at 1,200° C	4–b–2, solid	5.10	12	23	36	71	.020	(71–41+9–29)
66	ESR, 2½ hours at 1,200° C	do	5.10	4	6	31	41		
67	BSR, 2½ hours at 1,200° C	do	5.22	11	23	40	74	.013	(74–47+9–29)
68	ESR, 2½ hours at 1,200° C	do	5.22	3	8	36	47		
69	BSR, 2½ hours at 1,200° C	do	9.41	12	24	61	97	.025	(97–53+9–29)
70	ESR, 2½ hours at 1,200° C	do	9.41	3	8	42	53		
71	BSR, 2½ hours at 1,200° C	do	10.46	13	23	58	94	.011	(94–63+9–29)
72	ESR, 2½ hours at 1,200° C	do	10.46	4	9	50	63		

77	BSR, 2½ hours at 1,200° C	"E," solid	5.33	22	42	53	117	.043	(117–69+17–42)
78	ESR, 2½ hours at 1,200° C	do	5.33	5	17	47	69		
79	BBR, 2½ hours at 1,200° C			12	23	7	42		
80	EBR, 2½ hours at 1,200° C			6	4	7	17		

[1] The figures in this column indicate the values (in 0.1 mg) used for the blank correction in the calculation. The figures in the parentheses in all cases are the expression "BSR–ESR+EBR–BBR" which has already been shown to give the corrected value for oxygen in the sample. The values for EBR and BBR used in obtaining the first 4 results in this table are, respectively, the averages of runs 50 and 52 and of runs 49 and 51. The corresponding values used in calculating the results for the subsequent runs (with the exception of run 77) are those obtained in runs 60 and 59, respectively. These values, although obtained from runs of 2 hours at 1,200° C., are used in runs of both 1 hour and 2½ hours at 1,200° C., since the difference between EBR and BBR is what is actually used in the calculation, and this difference was found to be the same for a given sample (pig iron 4–c–2) for runs up to 1,200° C. and runs held for 2 hours at 1,200° C.

[2] The result of this run, higher than the duplicate runs 21, 29, and 47, is probably in error, due to the fact that the alundum boat used in this run was not carefully brushed free of graphite powder remaining from the previous runs but was only roughly scraped with an iron rod. The value for CO in the third weighed tube is thus quite probably too high on account of an abnormally high "hydrocarbon blank."

V. SUMMARY

A summary of the results obtained for oxygen by the two methods of analysis on both milled and lump samples of pig iron No. 4 and on lump samples only of cast iron "E" is given in Table 6. From this it is seen that both methods gave the same result on millings of pig iron No. 4, but that vacuum-fusion analyses of lump samples of this same pig iron proved that the determinations made by either method on milled samples were greatly in error, due chiefly to adsorbed moisture and air on the pig-iron millings. The analyses on lump samples of this same iron by the hydrogen-reduction method gave an oxygen content slightly higher, by approximately 0.005 per cent, than that indicated by the vacuum-fusion method. In the same way the hydrogen-reduction value for oxygen in cast iron "E" was higher than the vacuum-fusion result, again by 0.005 per cent.

TABLE 6.—*Summary comparison of results for oxygen in cast irons*

Sample No.	Form of sample	Reduction by hydrogen at 1,200° C. with addition of antimony-tin	Vacuum fusion at 1,475° C. in graphite
		Per cent oxygen	*Per cent oxygen*
4–c (2 or 3)	Millings	0.11 (average of 3)	0.07 (average of 7).
4–b (2 or 3)	Lumps	0.017 (average of 4)	0.012 (average of 2).
4–c (3)	do		0.011 (average of 4).
E	do	0.043 (single value)	0.038 (average of 3).

The precision of the vacuum-fusion method, as indicated by the average deviation from the mean of either the blanks for oxygen listed in Table 1 or the last six blanks in Table 2 is 0.0003 g oxygen, or 0.001 per cent oxygen when using a 30 g sample. A similar calculation, based on the average deviation from the mean of the corrected values for oxygen for the first four vacuum-fusion analyses of Table 2 (samples in which segregation of oxygen in the pig iron does not enter), also indicates a precision of 0.001 per cent oxygen.

If the precision of the hydrogen-reduction method is calculated as based on the deviation from the mean in blanks, it will be found that the average deviation from the mean of the net blanks of runs 65 and 67 (Table 5) is 0.0003 g oxygen, equivalent to a precision of 0.006 per cent on a 5 g sample; and that the average deviation in the case of runs 69 and 71 is 0.005 g oxygen, equivalent to 0.005 per cent on a 10 g sample. The precision calculated from the three determinations on milled samples (runs 55, 57, and 61, Table 5) is also 0.006 per cent oxygen. An increase in the size of sample used is of less value in increasing the precision than might be expected, possibly due to the fact that the oxygen equivalent of the "BSR" and "ESR" runs, as well as the value of the net blank, will increase with increase in weight of sample due probably to the increase in the

"hydrocarbon" blank caused by the greater amounts of carbides and free graphite for reaction with hydrogen.

Within the precision of the hydrogen-reduction method, therefore, the agreement obtained between values on solid samples in runs 65, 67, 69, and 71 is all that could be expected. The maximum range in these four determinations is 0.014 per cent. The average deviation from the mean is 0.005 per cent oxygen. The maximum difference in results obtained by the hydrogen-reduction method in check determinations on the milled samples was 0.016 per cent. With the oxygen content of the milled samples at a little over 0.10 per cent this range was not high enough to make the agreement with vacuum-fusion values unsatisfactory. In the case of solid samples, however, containing approximately 0.012 per cent oxygen this same range in hydrogen reduction values is more noticeable and serious.

A point of interest attaches to the results of this work in comparison with the results reported by Thanheiser and Müller [12] as to the influence of silicon on the determination of oxygen by reduction in hydrogen. These investigators found that only a small part of the oxygen in low-carbon iron alloys was obtained by the hydrogen-reduction method (alloying the sample with antimony only) when silicon was present in amounts of 0.1 per cent or more. The results of the analyses made in the present investigation indicated that the recovery of oxygen from a pig iron containing 1.31 per cent silicon and 3.68 per cent carbon was, at least, as complete as by the vacuum-fusion method. It is to be inferred, then, either that the presence of considerable amounts of carbon in the samples used in the present investigation have prevented the retention of the oxygen by the silicon in the sample, as experienced by Thanheiser and Müller, or that the vacuum-fusion method may fall short of complete determination of the oxygen in a high-carbon, high-silicon alloy to the same degree as the hydrogen-reduction method. The first explanation is more probably the correct one as is indicated by the results obtained by Oberhoffer, Piwowarsky, Pfeifer-Schiessl, and Stein [13] on the distribution of oxygen among the gases H_2O, CO, and CO_2 evolved from ferrous alloys of various carbon content when subject to hydrogen reduction analyses. They found that from steels of carbon content ranging between about 0.1 and 1.0 per cent from 40 to 70 per cent of the oxygen was evolved as water vapor and only 25 to 30 per cent as carbon monoxide. When, however, the sample for analysis was a gray iron containing 3.26 per cent carbon, some 80 per cent of the evolved oxygen was combined as carbon monoxide and only 12 per cent as water vapor. The reduction of oxides in the sample by carbon appears to play so large a part in the case of

[12] See footnote 4, p. 703.

[13] See footnote 3, p. 702.

the cast irons used in the present investigation as to make non-applicable the limitation of the hydrogen-reduction method which was found by Thanheiser and Müller to apply in the case of low-carbon steels containing silicon.

VI. CONCLUSIONS

A comparison of the vacuum-fusion and the hydrogen-antimony-tin reduction methods for the determination of oxygen in cast irons resulted in the following observations:

1. The sample used in the hydrogen-reduction method must be a solid sample, in the form of one or two lumps, rather than millings, since samples of the latter form may adsorb air and moisture equivalent to oxygen of four to eight times the real oxygen content of the iron as shown by vacuum fusion analysis.

2. The precision of the hydrogen-reduction method was indicated as 0.006 per cent oxygen using a 5 g sample, and 0.005 per cent using a 10 g sample. This precision is increased but little by using larger samples, since certain factors in the "blank" appear to change with size of sample, and the net value of the blank increases with increasing size of sample. The precision of the vacuum-fusion method was indicated as 0.001 per cent using a 30 g sample.

3. The rather complicated nature of the "blank" for the hydrogen-reduction method was pointed out. This blank required for its proper evaluation no less than four slightly differing types of runs.

4. Within the precision of the method the hydrogen-antimony-tin analysis gave the same values for oxygen as the vacuum-fusion method on samples of two different cast irons whether using millings or lump samples. The precision of the hydrogen-reduction method was, however, of the same order of magnitude as the oxygen content of one of the cast irons used, namely, about 0.01 per cent and about 25 per cent of the oxygen content of the second cast iron employed. The precision of the fusion method, on the other hand, was from about 2.5 to 10 per cent of the oxygen content of the cast-iron samples. The fusion method, therefore, was more satisfactory than the hydrogen-reduction method.

5. The limitation of the hydrogen-reduction method to silicon-free samples, which has been shown to be necessary in the case of low-carbon iron alloys, does not appear to hold for high-carbon iron alloys of the type used in this investigation.

WASHINGTON, May 29, 1928.

NOTE ON THE EFFECT OF REPEATED STRESSES ON THE MAGNETIC PROPERTIES OF STEEL

By M. F. Fischer

ABSTRACT

Changes in the magnetic properties of steel generally accompany changes in the other physical characteristics. This suggests the possibility of detecting and following the progress of a fatigue crack by magnetic methods. It was found, however, that the magnetic changes produced by repeated stresses above the endurance limit are not of a type which can be associated with the characteristic effect of a crack transverse to the direction of magnetization. The similarity of the observed magnetic changes with those brought about by the removal of externally applied static stresses indicates that the observed changes may be produced by the partial relief or redistribution of initially existing internal stresses. The fact that the magnetic changes brought about by understressing are of a similar character though less in magnitude suggests that some of the beneficial effect of understressing may be due to partial stress relief.

CONTENTS

	Page
I. Introduction	721
II. Material and apparatus	722
1. Material	722
2. Testing machine and specimens	722
3. Magnetic testing apparatus	723
4. Methods of measurement	724
III. Observations and results	725
IV. Discussion	729
V. Summary and conclusions	732

I. INTRODUCTION

Burrows [1] once made the statement that a magnetic method may be expected to follow the progress of a fatigue failure in iron or steel. While magnetic analysis has in some cases been successfully used in the detection and study of changes in the physical characteristics of such materials, there is no evidence to substantiate the prediction that it may be successfully applied to the detection of fatigue cracks. Except for the result of a single experiment by Sanford,[2] no evidence is available to indicate that repeated stresses have any permanent

[1] C. W. Burrows, "Some applications of magnetic analysis to the study of steel products," Proc. A. S. T. M., 17, pt. 2; 1917.

[2] R. L. Sanford, Nondestructive Testing of Wire Hoisting Rope by Magnetic Analysis, B. S. Tech. Paper No. 315; 1926.

effect on the magnetic properties of steel. The present work was undertaken, therefore, for the purpose of studying the character of the changes in magnetic properties resulting from the application of repeated stresses and to determine whether or not such changes bear a sufficiently close relationship to the progress of a fatigue failure to warrant further investigation of the possibilities of a magnetic method for the study of fatigue phenomena.[3]

II. MATERIAL AND APPARATUS

1. MATERIAL

Two readily available types of commercial steel were used for a preliminary survey. The samples were taken from two lots of drill rod having about 1 per cent carbon and one lot of cold-rolled machinery steel having a carbon content of approximately 0.13 per cent. The two lots of drill rod showed somewhat different magnetic characteristics and were designated as lot 1 and lot 2.

Had the results of the preliminary work held out hope of following the progress of a fatigue failure by magnetic methods, it would have been necessary to extend the work to a wider range of materials to determine, for purposes of comparison, the endurance limits, static tensile properties, complete chemical composition, metallographic structure, etc., and to study the effect of annealing. Since the magnetic method, as will be shown hereafter, did not follow the progress of the fatigue failure on one hard and one soft steel, it was unnecessary to go to the wider range of materials or to define more closely the materials that were used.

2. TESTING MACHINE AND SPECIMENS

Figure 1 is a photograph of the R. R. Moore[4] rotating-beam testing machine used. Transverse loading causes the longitudinal fibers of the test specimen to be alternately in compression and tension as the specimen rotates. The machine runs at 2,000 r. p. m. and is provided with a revolution counter and an automatic cut-off switch which stops the machine on failure of the specimen.

The specimens used in this machine are easily adapted to magnetic tests. While certain detailed dimensions and form are necessarily fixed by the method of clamping in the testing machine, the general form of the test section of the specimen can be made to suit the specific test requirements. Specimen A of Figure 2 is of the type generally used in the study of endurance properties. The stresses

[3] The recent book by H. F. Moore and J. B. Kommers, The Fatigue of Metals, McGraw-Hill; 1927, describes in detail the many theories of fatigue failure and also contains an extensive bibliography on the subject of fatigue.

[4] R. R. Moore, "Some fatigue tests on nonferrous metals," Proc. A. S. T. M., **25**, 1925.

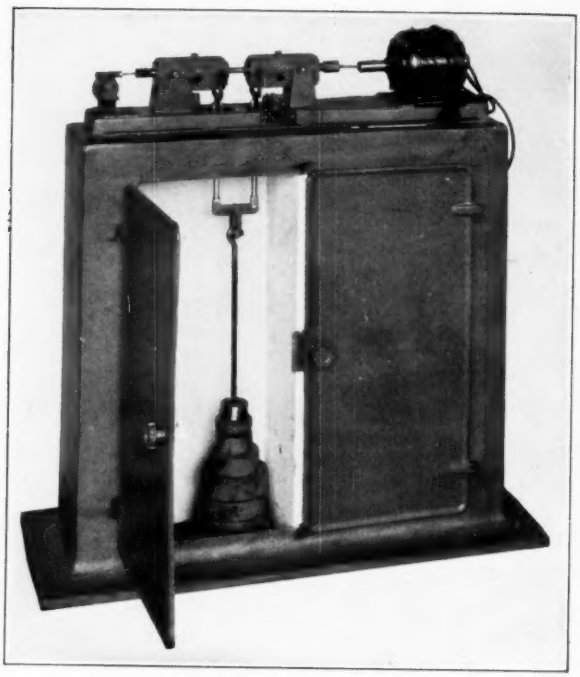

FIG. 1.—*Rotating beam testing machine*

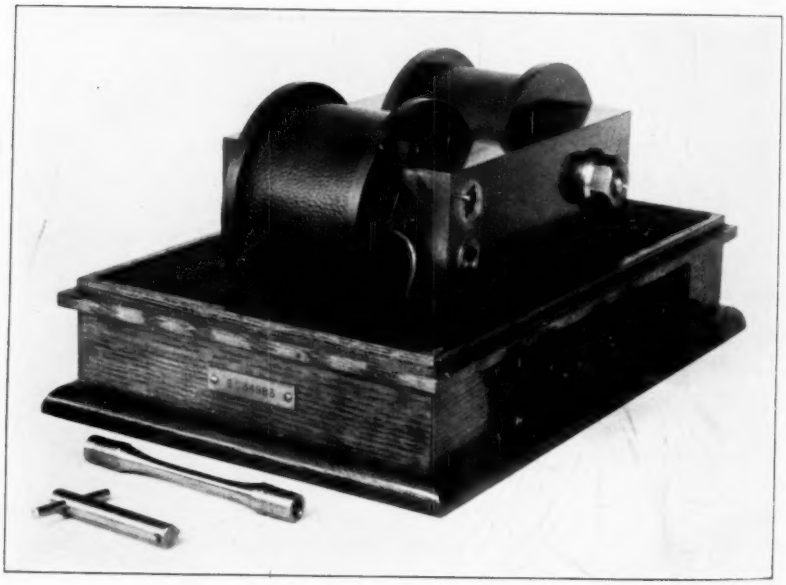

FIG. 3.—*Magnetic comparator*

are greatest at the minimum section, and consequently only a very small part of the material is subjected to the maximum stress range. In order to have a greater proportion of the sample subjected to the maximum stress range, a specimen was designed having a uniform section about 1 inch long. This type of specimen (*B* in fig. 2) was used for the greater portion of the tests. All test specimens were polished longitudinally to remove circumferential scratches, and none broke at the fillet.

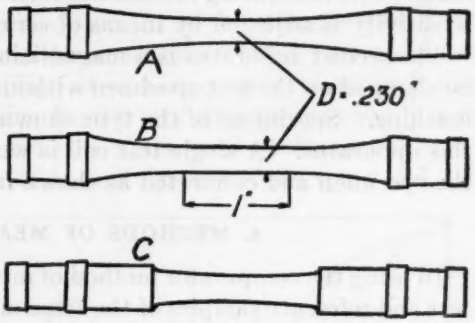

FIG. 2.—*Test specimens*

The sample designated as *C* in Figure 2 was designed to permit of making magnetic tests without removal from the machine. The cylindrical portions near the ends fit into a removable magnetizing yoke.

3. MAGNETIC TESTING APPARATUS

Magnetic measurements can be made by any of several methods. Of the two methods used in the present work, the one by means of which most of the following data were obtained is a modification of the magnetic comparator previously developed and described by the writer [5] for making magnetic measurements on short samples. In this apparatus the sample under examination is compared with a second sample of similar material and properties which is designated as the reference bar. As shown in Figure 3, the comparator consists essentially of an electromagnet with poles and yoke of soft iron. Symmetrically located near the ends of each pole are two holes into which fit the bushings through which contact between the test samples and poles is made. Magnetizing solenoids surround both the yoke and test samples, and test coils of 1,000 turns each surround the test and reference bars. The electrical connections are shown in Figure 4, from which, for the sake of clear-

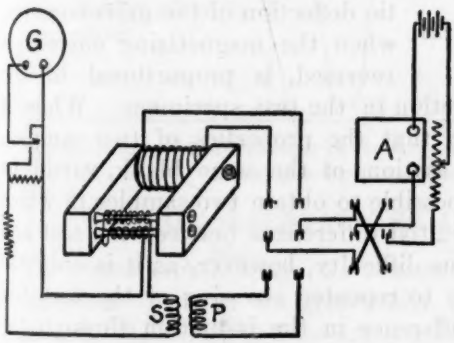

FIG. 4.—*Electrical connections of the comparator circuit*

[5] M. F. Fischer, Apparatus for the Determination of the Magnetic Properties of Short Bars, B. S. Sci. Paper No. 458, 1922.

ness, the magnetizing solenoid over the specimens is omitted. The two magnetizing solenoids are connected in series, aiding, through a reversing switch, ammeter, and control rheostats to a storage battery. The two test coils are connected in series, opposing, through the secondary of a calibrating mutual inductance to the galvanometer whose sensitivity is adjusted by means of series and parallel resistances.

The second apparatus is a magnetizing yoke of soft iron which can be clamped on the test specimen without removing it from the testing machine. Specimens of the type shown in Figure 2 *C* were used with this apparatus. A single test coil is wound on the central section of the specimen and connected as shown in Figure 5.

4. METHODS OF MEASUREMENT

In using the comparator method of measuring the magnetic changes, test and reference samples of the same material are placed in the upper and lower holes, respectively, in the ends of the pole pieces. The reference sample is left in position during the test of all samples of similar material. It can be assumed, without appreciable error, that the same magnetizing force acts simultaneously on both samples when current is flowing in the magnetizing coils. With the test coils properly connected, the ballistic deflection of the galvanometer, when the magnetizing current is reversed, is proportional to the difference in magnetic induction in the two specimens. While it might ordinarily be expected that the properties of two samples, cut from possibly adjoining sections of the same blank, would be the same, it is practically impossible to obtain two samples in which such identity exists. Small initial differences between the test and reference bars cause no serious difficulty, however, as it is only the change in this difference due to repeated stressing of the test bar which is important. The difference in the induction through the bars at corresponding magnetizing forces is measured directly by the comparator. Changes in induction due to any treatment are designated as ΔB. Observations of similar differences in induction for a series of magnetizing currents were made on each test sample before subjecting it to repeated stresses. Measurements were made at the same values of magnetizing currents after each period of stressing. Errors due to possible differences in contact reluctance between the test sample and magnetizing yoke were minimized by

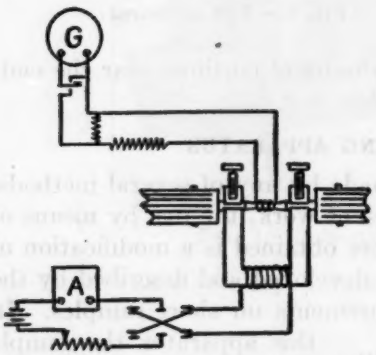

FIG. 5.—*Electrical connections of the single-yoke circuit*

taking the average of several sets of readings, between which the sample was removed from the comparator and reinserted.

In the second method of measurement, using the single yoke, readings were made of the total induction corresponding to a series of magnetizing currents. These tests were made with the load removed. Although the precision of the measurement of the changes was lower in this case than with the comparator, similar results were obtained by both methods. The fact that it is unnecessary to remove the sample from the testing machine for the magnetic measurements is a decided advantage, and the precision of the single-yoke method can probably be improved by a suitable modification of the apparatus.

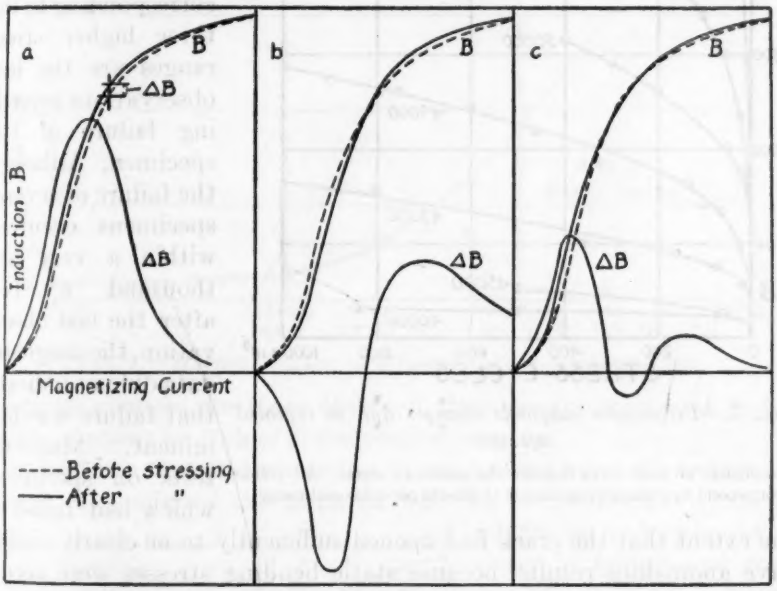

FIG. 6.—*Characteristic changes in the magnetic induction effected by repeatedly stressing samples of different materials*

III. OBSERVATIONS AND RESULTS

The characteristic magnetic changes brought about by the cyclic application of stress are graphically represented by the curves of Figure 6. The dashed lines are the normal induction curves of the unstressed samples. The full lines are the normal induction curves of the same samples after the application of repeated stresses. The changes in induction are represented by the ΔB curves, which are drawn to a larger scale. Curve (*a*) is representative of the drill rod of lot 1, curve (*c*) of the drill rod of lot 2, and curve (*b*) of the cold-rolled steel. For any single value of magnetizing force and type of material, the magnitude of the changes depends both on the value of applied stress and the number of applications.

The samples of drill rod from lot 1 gave, without exception, results of the character indicated by the curves of Figure 6 (*a*). The effects of the magnitude of the stress and the number of its applications are shown in Figure 7, in which each curve corresponds to a different sample, and all points to a magnetizing force of 15 gilberts per cm. The termini of the curves corresponding to the three higher stress ranges are the last observations preceding failure of the specimen. Although the failure of several specimens occurred within a very few thousand cycles after the last observation, the magnetic data did not indicate that failure was imminent. Magnetic tests on specimens which had failed to the extent that the crack had opened sufficiently to be clearly visible gave anomalous results, because static bending stresses were necessarily applied in placing the specimen in the comparator, thus superposing on the normal effects those of the applied static stresses.

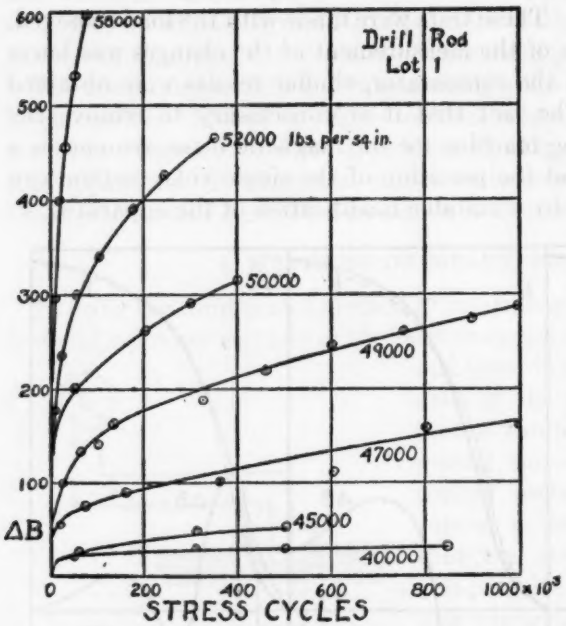

FIG. 7.—*Progressive magnetic changes due to repeated stresses*

The figures on each curve indicate the maximum stress. All points correspond to a magnetizing force of 15 gilberts per cubic centimeter

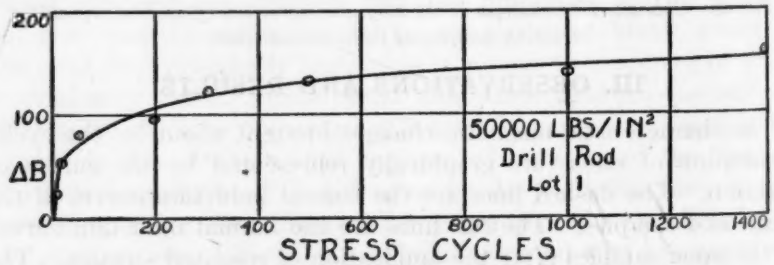

FIG. 8.—*Magnetic changes occurring during the initial cycles of repeated stressing*

Figure 8 shows the magnetic changes in a specimen which was initially rotated by hand and the first observation made after five

cycles of stress. It is probable that some magnetic change would have been observed even after a single cycle.

Figure 9 is taken from the data of Figure 7 and shows the magnetic changes as a function of the maximum stress range. The

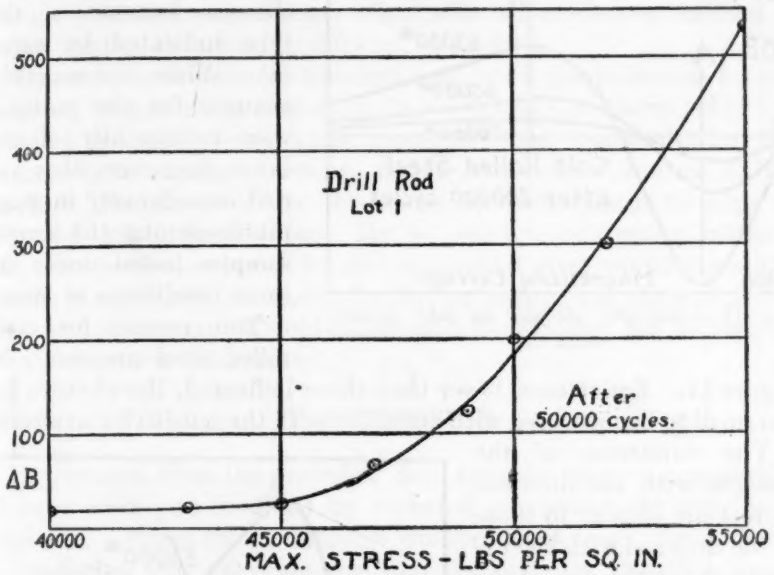

FIG. 9.—*Magnetic changes as a function of the maximum stress*

magnetic changes are those observed after the application of 50,000 cycles of stress to each of the several specimens.

It is known that understressing, in most cases, raises the endurance limit. A sample of this material was run for 10,000,000 cycles at 43,000 lbs./in.^{2} without evidence of failing and then run at a stress of 50,000 lbs./in.^{2} The resulting magnetic changes are shown in Figure 10. The magnetic changes occurring after the application of the higher stress are smaller than those observed in other samples which had been tested at the higher stress alone, although the total change in the present case is of the same order as would have been produced by the higher stress. It is probable that the effect of successively increasing stresses is cumulative, the magnetic changes produced by each depending on the magnitude and number of cycles of application of all preceding stresses.

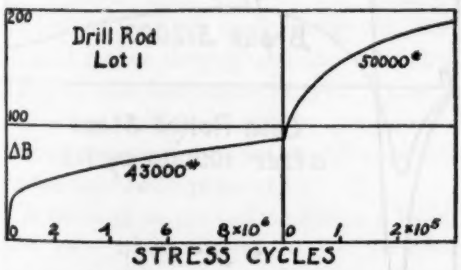

FIG. 10.—*Effect of two different stresses applied successively to the same sample*

Magnetizing force 15 gilberts per cubic centimeter

Magnetic changes produced in drill rod of lot 2 are similar to those indicated in curves (*a*) and (*c*) of Figure 6. The changes taking place in the early part of the test are of the type shown in curve (*c*). As the test proceeds the changes become of the type indicated by curve (*a*). While the magnetic changes for the material were consistently of the same character, they varied considerably in magnitude among the several samples tested under the same conditions of stress.

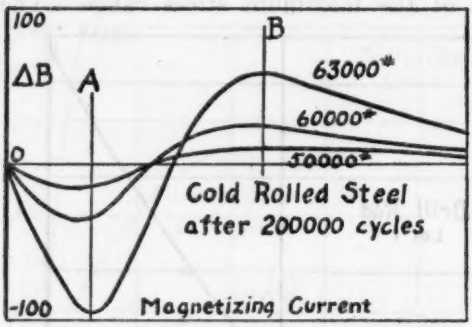

FIG. 11.—*Magnetic changes in cold chilled—rolled steel*

The results for cold-rolled steel are shown in Figure 11. For stresses lower than those indicated, the changes are too small to be measured with certainty with the sensitivity available.

The variations of the changes with the duration of test are similar to those of the drill rod with the exception that the sign of the changes is negative for magnetizing forces in the region A and positive for magnetizing forces in the region B. In Figure 12 the magnetic changes in the sample stressed at 55,000 pounds are much larger than those in the sample stressed at 60,000 pounds, which is contrary to what had heretofore been observed under the same comparative conditions of test. As is evidenced by the relative number of cycles to failure of the two samples, considerable difference may have existed in the initial conditions of the two samples. Similar variation in the endurance properties of apparently identical materials is frequently observed in fatigue testing.

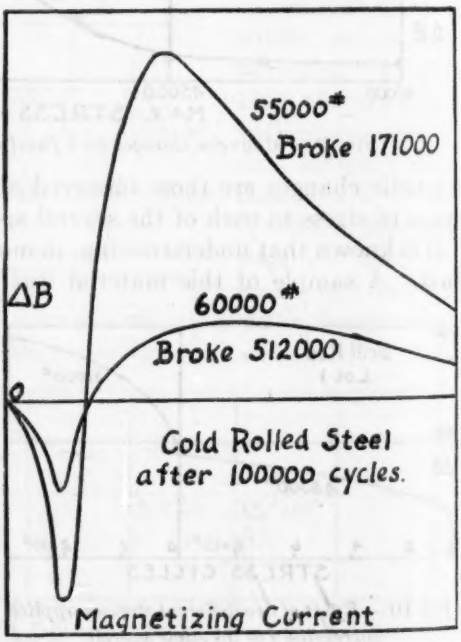

FIG. 12.—*Effect of the initial condition of the material on the magnetic changes and endurance properties*

The fact that at stresses below 50,000 lbs./in.^{2} repeated stress showed no effect upon the magnetic properties of the cold-rolled steel is sufficient to negative the suggestion that arises on looking at Figures 7 and 10, for drill rod, which, by themselves, suggest that the study of magnetic changes might offer an accelerated method of approximately determining the endurance limit.

The endurance limit of the drill rod, lot 1 (as indicated by the breaking of specimens loaded at 50,000 lbs./in.^{2} or above, at a few hundred thousand cycles, while a specimen loaded at 43,000 lbs./in.^{2} apparently has an indefinite life, fig. 10), can not be far from 45,000 lbs./in.^{2} The agreement of this figure with the change of slope in Figure 9 might justify hope for an accelerated testing method, but since a similar curve for the cold-rolled steel would show the change of slope only at 50,000 lbs./in.^{2} or higher, and the endurance limit of 0.13 per cent C cold-rolled steel is obviously not so high as that, the hope is not realized.

IV. DISCUSSION

It is evident from the preceding data that the magnetic properties of some steels are modified by repeated stresses of the type here employed. While the changes are small in most cases, the evidence is conclusive that they are real and permanent. In not a single case, however, are the changes of a character which can be directly associated with the magnetic effects of a crack transverse to the direction of magnetization. Since such a crack constitutes a discontinuity in the magnetic circuit, it would naturally be expected that its presence would cause the apparent magnetic permeability to be lower than that of the unaffected material for all values of induction. In all cases, however, the observed permeability is increased either throughout the whole range of inductions or in certain parts of the induction curve. It is quite probable, therefore, that any effect which might be produced by the presence of cracks is entirely masked by another effect which has a much greater influence on the magnetic properties.

According to prevailing ideas, a fatigue failure starts at a relatively slow rate with respect to the number of repetitions of stress and progresses at a continually increasing rate. The change in magnetic properties starts at the maximum rate and progresses at a continually decreasing rate. This is added evidence that the magnetic change does not bear a direct relation to the progress of the fatigue failure.

It has long been known that the magnetic properties of iron and steel are modified by the application of a static load to the test material. The character and magnitude of such changes depend on the type and magnitude of the stresses, and also on the degree to

which the test sample is magnetized. Figure 13 shows the characteristic magnetic changes which occur in ferrous materials when subjected to static stresses. The ordinates are the changes in magnetic induction due to the load and the abscissas are the magnetizing currents at which the changes are measured.

Curve (*a*) indicates the characteristic magnetic changes due to either a high tensile stress or to a compressive stress of any magnitude. The magnetic changes under these conditions are negative for all magnetizing forces.

Low tensile stresses produce changes of the style represented by curve (*b*). It is to be observed in this curve that the magnetic changes are positive for low values of magnetizing force but become negative when the magnetizing force is increased. When the

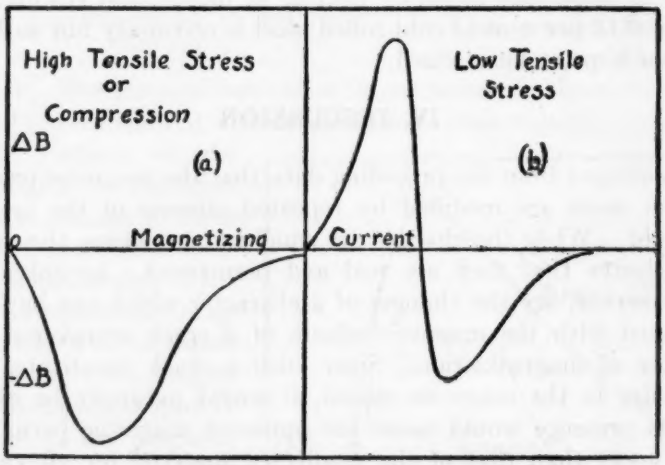

FIG. 13.—*Changes in the magnetic induction* (Δ *B*) *due to the application of static stresses*

magnetizing forces are increased indefinitely, the magnetic changes due to stresses of any type become vanishingly small.

If the applied stresses exceed the elastic limit of the material, permanent magnetic changes of the type shown in Figure 13 (*a*) occur.

Comparison of the curves of Figure 13 and Figure 6 (*a* and *b*) shows that the magnetic changes due to static stress and those brought about by repeated stresses differ mainly in sign. If the data on static stresses had been plotted with signs reversed, thus indicating the effect of stress relieval, it would be seen that the magnetic changes due to repeated stresses are exactly similar in character to those corresponding to the removal of a previously existing static stress. From this it appears that the observed changes in magnetic properties which accompany the application of repeated

stresses are probably associated with the relief or redistribution of initial stresses rather than with the start and development of the crack which ultimately results in failure.

The probability of a change in magnitude or redistribution of initial stresses is suggested by Gough and Hanson,[6] and others in their respective theories of fatigue failure. Direct evidence of the relief of internal stresses by repeated understressing is furnished by some "turning-down" tests made by Moore and Jasper.[7] Strain changes resulting from the removal of surface material were generally smaller in specimens which had previously been understressed than in virgin material.

As shown by the lowest curve of Figure 7, the magnetic changes produced by understressing differ only in magnitude from those effected by overstressing and, therefore, probably have their origin in changes similar to those produced by the higher stresses. The fact that partial stress relief may have occurred under these circumstances suggests that some of the improvement in endurance properties resulting from understressing may be due to such stress relief.

It is to be borne in mind that under cycles of flexural stresses the outside fibers of the test specimens are subjected to the greatest stresses, the maximum stresses in the concentric lamellæ of the test piece being proportional to the cubes of their respective radii and varying from the maximum, both in tension and compression, to zero during each revolution of the specimen. Since the stresses vary across the section in this manner, it is reasonable to suppose that any effect which they might have on the properties of the test bar also varies in an approximately similar manner and that the observed magnetic changes are the resultant of those occurring in all the lamellæ of the test bar. In Figure 9 it is seen that the magnetic changes corresponding to a maximum stress of 43,000 pounds are small. For a maximum stress of 50,000 pounds, the magnetic changes are moderately large. In the latter case, however, only about 10 per cent of the cross-sectional material is stressed above 43,000 pounds, and it is probable, therefore, that the difference in the magnetic changes corresponding to these maximum stresses is contributed almost entirely by the small area in which the stresses exceeded the lower value.

Differences in the character of the magnetic changes which occurred in the several materials studied may be attributed to differences in the magnitude or distribution of the initial internal stresses. The magnetic changes were mainly of the two types shown in curves (*a*) and (*b*) of Figure 6. Curve (*c*) of this figure may be considered as a

[6] H. J. Gough and D. Hanson, "The behavior of metals subjected to repeated stresses," Proc. Roy. Soc., 104A; 1923.

[7] H. F. Moore and T. M. Jasper, "An Investigation of the Fatigue of Metals." Bull. No. 142, Eng. Exp. Sta. Univ. of Ill.; 1923.

combination of curves (*a*) and (*b*). It is not to be supposed that a change of a single type occurs without a compensatory change of another type, but rather that one change, by reason of its magnitude or the volume of material involved, has a predominating influence on the magnetic properties.

V. SUMMARY AND CONCLUSIONS

The results of the present study may be summarized as follows:

1. Repeated stresses of the reversed-bending type affect the magnetic properties of the materials studied.

2. The magnetic changes accompanying repeated stresses are not characteristic of the effect of a fatigue crack transverse to the direction of magnetization.

3. Imminence of failure is not indicated by the magnetic changes.

4. The character of the magnetic changes differs according to the material of which the test sample is made.

5. The magnitude of the magnetic changes for a specific material is a function of the applied stress, the number of cycles of its application, and the values of the magnetizing force at which the changes are observed.

Since the magnetic changes which have been observed can not be associated with a fatigue crack, a basis of explanation was sought in the known effects of static stresses on the magnetic properties of ferromagnetic materials. From the similarity of the observed magnetic changes resulting from the removal of static loads from the test material, the following tentative conclusions appear to be warranted:

1. The magnetic changes brought about by repeated stresses are such as would be caused by the partial relief or redistribution of initially existing internal stresses.

2. The magnetic effects of such stress relief are so large as to mask the small magnetic changes which may directly result from a fatigue crack.

3. The fact that magnetic changes are produced by repeated stresses even below the endurance limit suggests the probability that understressing results in the partial relief or redistribution of the internal stresses. Some of the beneficial effect of understressing may be explained on this basis.

4. Differences in the character of the magnetic changes observed in the different materials can be associated with the difference in type, magnitude, or distribution of the partially relieved stresses.

WASHINGTON, May 16, 1928.

EFFECT OF TWIST ON COTTON YARNS

By A. A. Mercier and Charles W. Schoffstall

ABSTRACT

Yarns were spun in the bureau's experimental cotton mill from 1-inch and $1\frac{1}{16}$-inch staples, middling grade cotton, using single and double roving organizations. Seven counts of combed yarns ($1\frac{1}{16}$-inch staple) and five counts of carded yarns (1-inch staple) were spun. Different twist factors were used for each yarn.

Measurements were made of strength, diameter, angle of twist, and contraction. Correlations of the results graphically with respect to the twist multiplier are shown and discussed. Suggestions regarding the application of these data to the cotton mill are given.

CONTENTS

	Page
I. Factors that affect the properties of cotton material	733
II. Need for definite information	735
III. Purpose and scope	736
IV. Manufacturing procedure	736
V. Testing procedure	738
1. Conditioning	738
2. Sampling	738
3. Breaking strength	738
4. Yarn count	739
5. Diameter of yarn	739
6. Angle of twist	739
VI. Discussion of results	740
1. Breaking strength	740
2. Diameter and angle of twist	744
3. Contraction	745
VII. The use of these data in the mill	745

I. FACTORS THAT AFFECT THE PROPERTIES OF COTTON MATERIAL

The physical properties of a cotton yarn are extremely important, both from the standpoint of quality of product and cost of production. The strength, regularity, or evenness, absorptivity with respect to moisture or dye, the feel or handle, the cleanliness, and other properties of the finished product must each be considered in the selection of the raw material and the proper manufacturing procedure in the mill.

The factors governing the selection of raw cotton as it is related to the properties of the final product have been fairly well established.

The long fibers for the combed yarns used in voiles, lawns, airplane fabrics, etc., the shorter fibers for bagging, blankets, etc.; the selection of the grades according to the type of cloth desired; all these features have been established, at least along approximate lines. No manufacturer would attempt to spin fine yarns on a production basis from low-grade short-stapled cotton, nor would he buy high-grade cotton for such a low-grade fabric as osnaburg.

The quality and cost features are definitely related with the processes and settings of the machines, hence the proper organization of mill procedure is even more important than the selection of the raw cotton. When a mill is being planned for the manufacture of a particular kind of material, such as sheeting, for instance, it is very desirable to know the relation of the twist factors to yarn diameter, strength, angle of twist, etc. The best mill organization from the standpoint of cost in this instance is one which will yield maximum production with minimum idle machinery. The difference of a few turns per inch may necessitate additional spinning frames or other machines which are expensive in both initial cost and operation and occupy valuable space. Having once fixed the operating conditions, the manufacturer can seldom afford to make a change; thus it is of increased importance that the best mill organization be adopted initially.

Some mills are equipped to make any type of material, within certain limits, that is ordered. Here a definite knowledge of the relation of the mill organization to the finished product means the satisfactory completion of the order from the standpoint of both quality and cost of product.

In most cases one property is more important than another, and some sacrifice of the other features may be necessary. This is the case, for instance, in the manufacture of toweling where high moisture absorption and softness of feel must be obtained. Some of the strength is generally sacrificed; but, obviously, some middle ground must be selected, for the towel must be capable of withstanding the rigors of the laundry treatment at frequent intervals. So the highest absorptive quality can not always be attained.

A closer analysis of the situation shows that the absorptiveness and the strength of the yarn each depend largely on one manufacturing factor; namely, the twist. Within limits, the lower the twist the higher is the absorptiveness and the lower the strength.

When the selection of the proper manufacturing organization for the toweling is considered from a cost viewpoint, it is found that the higher the twist the greater the cost of production. Now, if it is known what properties certain twist factors produce, an easy selection might be made of the best mill organization.

II. NEED FOR DEFINITE INFORMATION

The mill managers may fully realize the fact that the twist of the yarn affects the finished product very materially and yet be unable to cope with difficulties arising from this condition. Many mills buying their yarn for weaving or knitting are confronted with this situation. Such terms as "filling twist," "warp twist," and "hosiery twist" are frequently used in the yarn market. (Sometimes the word "yarn" is substituted for "twist.") Agreeing on an exact definition for these terms is not easy.

It is recognized that yarns for hosiery and underwear must be soft and pliable in order to run properly on the knitting machines. The desired properties are gained by using a low number of turns per inch. "Hosiery twist" thus indicates that the yarn has few turns per inch. Many of the defects of cotton hosiery occur because of the lack of definite data or a standard definition for "hosiery twist." For instance, yarn from two different sources, the same yarn count and both "hosiery yarns" according to the marks of the respective yarn mills, may be used on the same knitting machine. Because of the differences in twist practice in different mills there are apt to be dissimilarities in the finished product. If the difference is not apparent in the stitch formation, it will show when the hosiery are dyed. Uneven shades or difficulties in pair matching will frequently occur.

Another example is found in connection with the "filling-twist" yarns and "warp-twist" yarns. Warp yarns are subjected to strain in the loom, and thus, if for no other reason, they must have sufficient twist to make them strong enough to prevent excessive breaking. Filling yarns undergo very little strain in weaving. If a manufacturer wants to make a cloth with as little cost as possible so far as twist is concerned, he uses yarns having the least twist, which, according to practical experience, works satisfactorily on the loom. Generally, yarns bought under designations of "warp twist" and "filling twist" approximate these minimum twists unless a definite twist is specified. This results from the close relation of twist to production cost. Unfortunately the idea of what the minimum should be varies in the different yarn mills, so that the terms which express the degree of twist have only vague meanings.

If definite data regarding the effect of twist on the properties of yarn were established, the relation of the yarn to the finished material and to its intended use would receive more attention and there would follow an improvement in yarn manufacture and trading. A weaving mill could order yarn with a certain twist factor made from cotton having a certain staple and be reasonably sure that, whatever yarn mill made it, it would fulfill definite requirements. This would not be confusing for the yarn mill, for, no doubt, standardization of terminology would be accomplished in due time and "warp twist," "filling twist," "hosiery twist," etc., would have definite meanings.

III. PURPOSE AND SCOPE

The purpose of this paper is to show how twist affects the breaking strength of yarn, the diameter of yarn, the angle of fibers (angle of twist), and the draft necessary to maintain a constant count while increasing the twist.

The raw cotton used was middling grade of 1-inch and $1\frac{1}{16}$-inch staples. The 1-inch cotton was carded and spun into 10s, 15s, 20s, 25s, and 30s yarns. The $1\frac{1}{16}$-inch cotton was combed and spun into 10s, 15s, 20s, 25s, 30s, 35s, and 40s yarn. Both single and double roving organizations were used in carded and combed yarns.

IV. MANUFACTURING PROCEDURE

The cotton was given the usual treatment in the mill processes outlined as follows:

1. Automatic feeder.
2. Vertical opener (600 r. p. m.).
3. Breaker picker (Kirschner, 3-blade beater).
   (*a*) 900 r. p. m., 31 blows per inch, 14 ounces lap.
4. Intermediate picker (rigid, 2-blade beater).
   (*a*) 900 r. p. m., 39 blows per inch, 13 ounces lap.
5. Finisher picker (Rigid, 2-blade beater).
   (*a*) 900 r. p. m., 40 blows per inch, 12.5 ounces lap.
6. Card.
   (*a*) Cylinder, 165 r. p. m.
   (*b*) Licker-in, 390 r. p. m.
   (*c*) Doffer, 10 r. p. m.
   (*d*) Weight of sliver, 55 grains.
7. Sliver lapper.
   (*a*) Feed, 20 slivers of 55 grains each.
   (*b*) Delivery, 1 lap of 430 grains.
8. Ribbon lapper.
   (*a*) Feed, 4 laps of 430 grains each.
   (*b*) Delivery, 1 lap of 400 grains.
9. Comber.
   (*a*) Feed, 8 laps of 400 grains each.
   (*b*) Delivery, 1 sliver of 50 grains.
   (*c*) Waste removed, 23 per cent.
10. First drawing frame.
    (*a*) Combed.
       (1) Feed, 6 slivers of 50 grains each.
       (2) Delivery, 1 sliver of 60 grains.
    (*b*) Carded.
       (1) Feed, 6 slivers of 55 grains each.
       (2) Delivery, 1 sliver of 60 grains.
11. Second drawing frame.
    (*a*) Combed and carded.
       (1) Feed, 6 slivers of 60 grains each.
       (2) Delivery, 1 sliver of 60 grains.

12. Slubber (11 by 5½).
    (*a*) Spindle speed, 745 r. p. m.
    (*b*) Draft, 4.3.
    (*c*) Feed, 1 sliver of 60 grains.
    (*d*) Delivery, 1 roving.
        (1) Count (hanks), 0.6.
        (2) Twists per inch, 0.93.

13. Intermediate (9 by 4½).					
(*a*) Spindle speed (r. p. m.)	990	990	990	990	990
(*b*) Draft	3. 67	5. 5	3. 94	4. 4	5. 5
(*c*) Feed (2 roving, hanks)	0. 60	0. 60	1. 10	1. 10	1. 10
(*d*) Delivery.					
(1) Count (hanks)	1. 10	1. 65	1. 86	2. 20	2. 75
(2) Twists per inch	1. 28	1. 56	1. 66	1. 78	1. 99
14. Fine fly frame (7 by 3½).					
(*a*) Spindle speed (r. p. m.)	1, 250	1, 250	1, 250	1, 250	
(*b*) Draft	6	4. 63	4. 73	5. 9	
(*c*) Feed (2 roving, hanks)	1. 10	1. 65	1. 86	1. 86	
(*d*) Delivery					
(1) Count (hanks)	3. 30	3. 85	4. 40	5. 50	
(2) Twist per inch	2. 19	2. 34	2. 52	2. 83	
15. Jack frame.					
(*a*) Spindle speed (r. p. m.)	1, 425	1, 425	1, 425		
(*b*) Draft	4	4. 7	4. 5		
(*c*) Feed (2 roving, hanks)	3. 30	3. 30	3. 85		
(*d*) Delivery.					
(1) Count (hanks)	6. 60	7. 70	8. 80		
(2) Twists per inch	3. 06	3. 28	3. 55		

16. Spinning frame.
    (*a*) Spindle speed--variable.
    (*b*) Draft---------variable.
    (*c*) Single roving.

(1) Feed (hanks)	1. 10	1. 65	2. 20	2. 75	3. 30	3. 85	4. 40
(2) Delivery (counts)	10	15	20	25	30	35	40

    (*d*) Double roving.

(1) Feed (hanks)	2. 20	3. 30	4. 40	5. 50	6. 60	7. 70	8. 80
(2) Delivery (counts)	10	15	20	25	30	35	40

Beginning with the slubber, the mill organizations were changed to avoid long drafts and to facilitate the work by employing as few processes as possible. The greatest number of changes occurred in the spinning processes, where the draft, twist, and spindle speeds were altered to produce the desired results.

A range of twist was obtained using twist multipliers from 2.5 to 5.0 in increments of 0.25 and from 5.0 to 8.5 in increments of 0.5. The twists per inch for each yarn varied for each twist multiplier according to the formula

$$T = M \times C$$

where T is the twists per inch, M the twist multiplier, and C the yarn count.

The yarns were spun on ring frames, the 10s, 15s, 20s, 25s, and 30s yarns being spun on 1¾-inch rings and the 35s and 40s yarns on 1⅜-inch rings. The spindles were driven from an 8-inch drum by means of tapes which were kept tight by idler pulleys. This method kept the slippage of spindles at a minimum.

As the twist was varied, the draft was changed according to the amount of contraction, so that practically a constant yarn count was maintained. The spindle speed was also changed in order to avoid high speeds on low-twisted yarn and to follow the usual mill procedure for production.

A relative humidity of 65 per cent was maintained throughout the entire period of manufacturing.

V. TESTING PROCEDURE

1. CONDITIONING

The tests were conducted in a room having a constant temperature of 70° F. and a relative humidity of 65 per cent, and after the yarns had been conditioned for at least four hours.

2. SAMPLING

Ten bobbins were taken at random from each lot of yarn. For carded yarns there were 5 different counts, each count having 17 different twists for each of the roving organizations (single and double), making a total of 170 lots. For combed yarns there were 7 counts, each count having 17 different twists for each of the roving organizations, a total of 238 lots. This made a grand total of 408 lots of yarn.

Table 1 shows the number of specimens tested.

TABLE 1.—*Number of specimens tested*

Test	Number of specimens from each bobbin	Number of specimens from each lot	Total number of specimens (408 lots)
Breaking strength, skein	1	10	4,080
Breaking strength, single strand	4	40	16,320
Twist	1	10	4,080
Yarn count	1	10	4,080
Diameter	1	10	4,080
Angle of twist	1	10	4,080
Total	9	90	36,720

3. BREAKING STRENGTH

The breaking strength of the yarn was determined both by the skein (or lea) test and by the single-strand test. The apparatus used for both tests were Scott testers of the inclination-balance type.

The speed of the pulling drum or jaw was 12 inches per minute under no load.

In the skein (or lea) test a skein 120 yards in length was wound on a reel having a perimeter of 1½ yards. This skein, consisting of 80 strands, was then placed on the drums of the testing machine. These drums are 1 inch in diameter. The capacity of the machine. is 300 pounds. Careful handling minimized the overlapping of the yarn and distributed the load, which was applied more or less evenly.

In the single-strand test the yarn was clamped in small jaws of the testing machine. The distance between jaws was 6 inches. The capacity of the machine is 2.2 pounds. Care was taken to avoid disturbing the twist while the specimen was being prepared for the break. Breaks occurring at or in the jaws were disregarded.

4. YARN COUNT

Yarn count was determined by weighing a skein of 120 yards and then making the usual calculations according to the formula

$$C = \frac{Y \times 453.6}{W \times 840}$$

where Y = yards in specimen, W is weight in grains, 453.6 is number of grams in a pound, and 840 is the cotton constant.

5. DIAMETER OF YARN

The yarn was wrapped loosely around a black cardboard 1 inch wide. This was then placed on a rotary stage microscope. The sides of the yarn were brought into focus and made to coincide with the movable wire in the eyepiece. This wire was moved across the field by a screw, one turn of which moved the wire 0.5 mm. The screw had an adjustable drumhead divided into 50 parts, one part therefore being equal to 0.01 mm, one-tenth of which could be easily estimated (0.001 mm). The readings were made at the center of the scale, to insure greater accuracy.

When the wire had been made to coincide with one side of the yarn the readings on the field and drum were noted, and the wire was then moved to the other side of the yarn and the readings again recorded. The difference in each case between these two readings was the diameter of the yarn.

6. ANGLE OF TWIST

The angle of twist with respect to the longitudinal axis of the yarn was measured with the same apparatus used for diameter measurement, by rotating the stage so that the wire in the eyepiece was parallel to the angle of the twist in the yarn.

VI. DISCUSSION OF RESULTS

The test data were very voluminous, as will be noted from the number of tests made as indicated in Table 1. It was deemed advisable to correlate the results graphically rather than tabularly. Attention is therefore directed to Figures 1 to 7. Through the points, as plotted, smooth curves have been drawn.

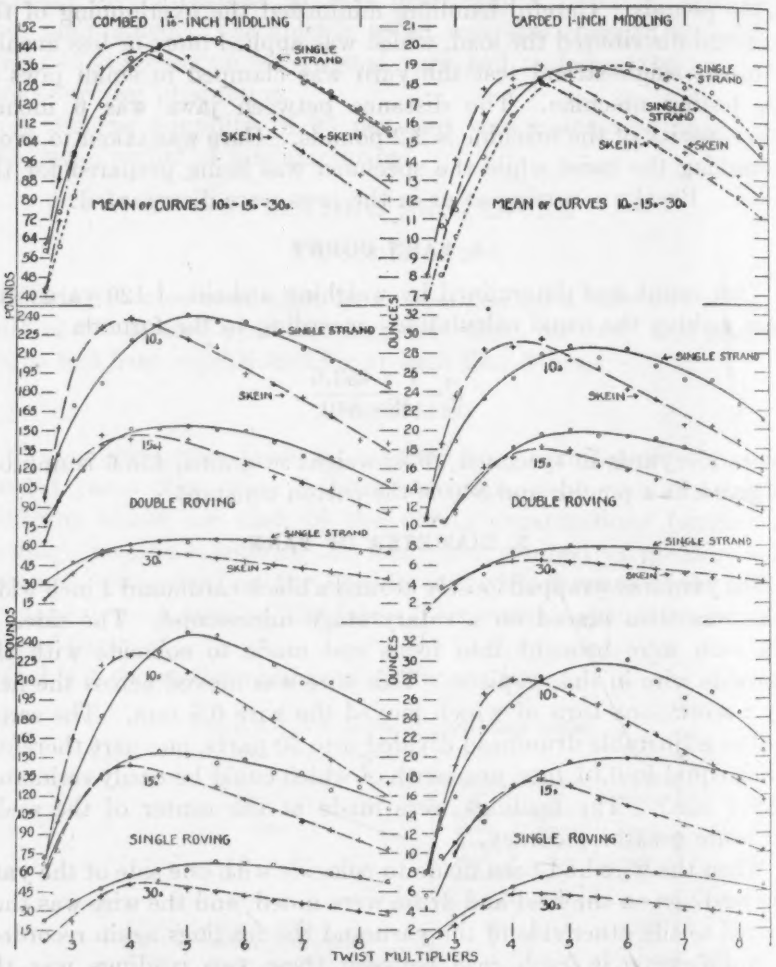

FIG. 1.—*Comparison of skein and single strand breaking strength determinations as affected by twist*

The scale for the skein results is given at the left; the scale for the single-strand is given in the center of the chart. The curves are plotted so that the shapes of single-strand and skein methods may be compared.

1. BREAKING STRENGTH

Figure 1 shows a comparison of the curves obtained by plotting the twist multiplier against the skein and the single-strand breaking strengths. The maximum strength for skein breaks was reached with a twist multiplier of about 4.25, whereas for the single-strand

method the maximum breaking strength was reached with a twist multiplier of about 5.25. This may be partially explained by considering that the single-strand result represents an average of a number of tests (in this case 40), including high, low, and medium breaks, whereas the skein test, although presumably the average of a large number of single-strand tests, is really an average of the medium

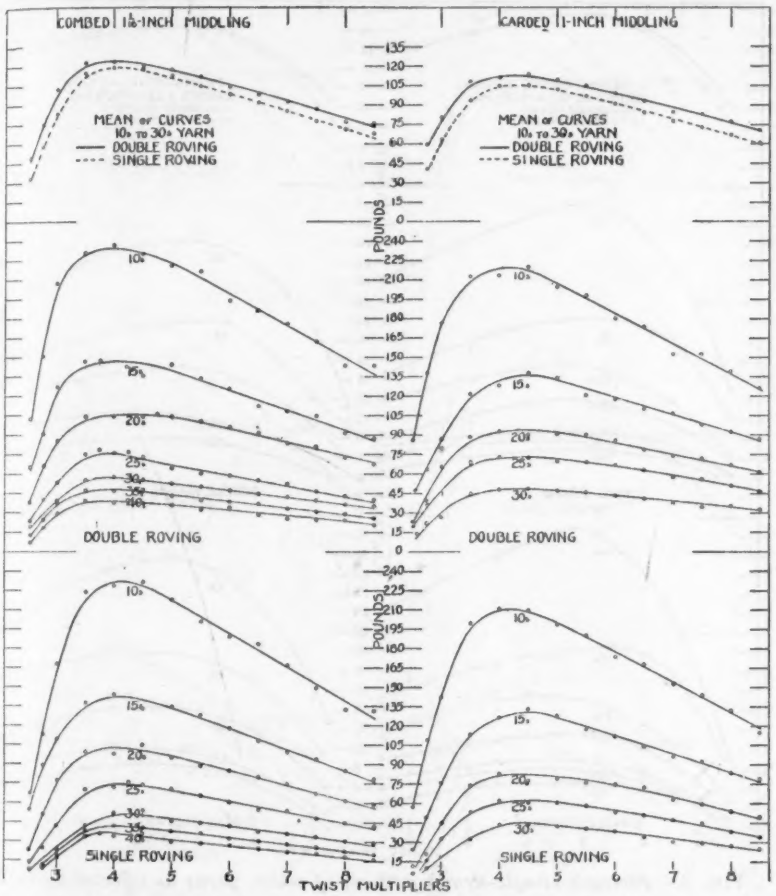

FIG. 2.—*Strength (skein method) of cotton yarns as affected by twist*

Yarns with different twist factors were spun from single and double roving; made of combed 1 1/16-inch and carded 1-inch staples, middling grade cotton. Results are given for the various counts, and a mean of the results is given at the top to show the average gain obtained by using the double roving.

and low breaks. The factors of friction, distribution of tension, and variation in the stretch of the individual yarns appreciably influence the results. At best, the skein tests grade the samples in the same quantitative order as a single-strand test.[1]

The strength tests by the skein method, which are plotted in Figure 2, indicate the benefit obtained by using a double-roving instead of a

[1] Confer Hall, J. Text. Inst., 15, T223; 1925.

single-roving organization. Using low-twist multipliers, the advantage gained is as high as 15 pounds in some instances. The single-strand tests (fig. 3), however, although in general agreement with the above statement in regard to the low-twist multipliers, indicate that little if any advantage is gained for high-twist yarns.

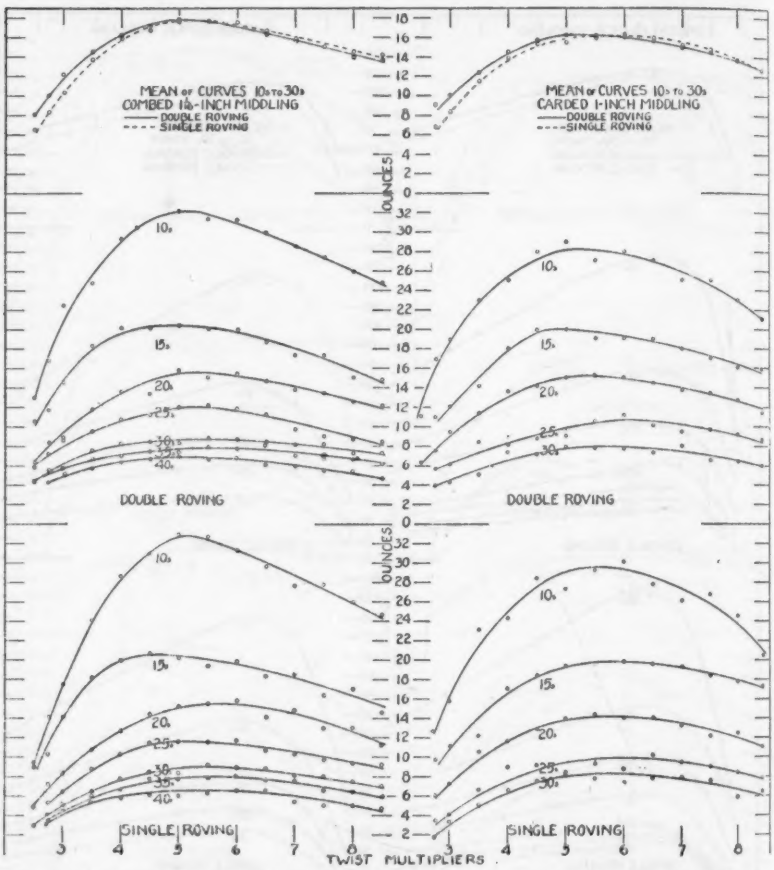

FIG. 3.—*Strength (single-strand method) of cotton yarns as affected by twist*

Yarns with different twist factors were spun from single and double roving; made of combed $1\frac{1}{16}$-inch and carded 1-inch staples, middling grade cotton. Results are given for the various counts, and a mean of the results is given at the top to show the average gain obtained by using the double roving.

The advantage of using the combing process is indicated to some extent in Figure 4, although it is impossible to state how much of the increased strength is due to the greater staple length and how much is due to the combing process.

There is one outstanding fact shown by Figures 1 to 4: The strength of a yarn increases with twist up to a certain point, then decreases as

further twist is added. In a previous bureau paper [2] the following statement occurs:

The twist is an important factor in obtaining the strength of a yarn. In the twisting process the fibers are entwined around and cling to each other so that

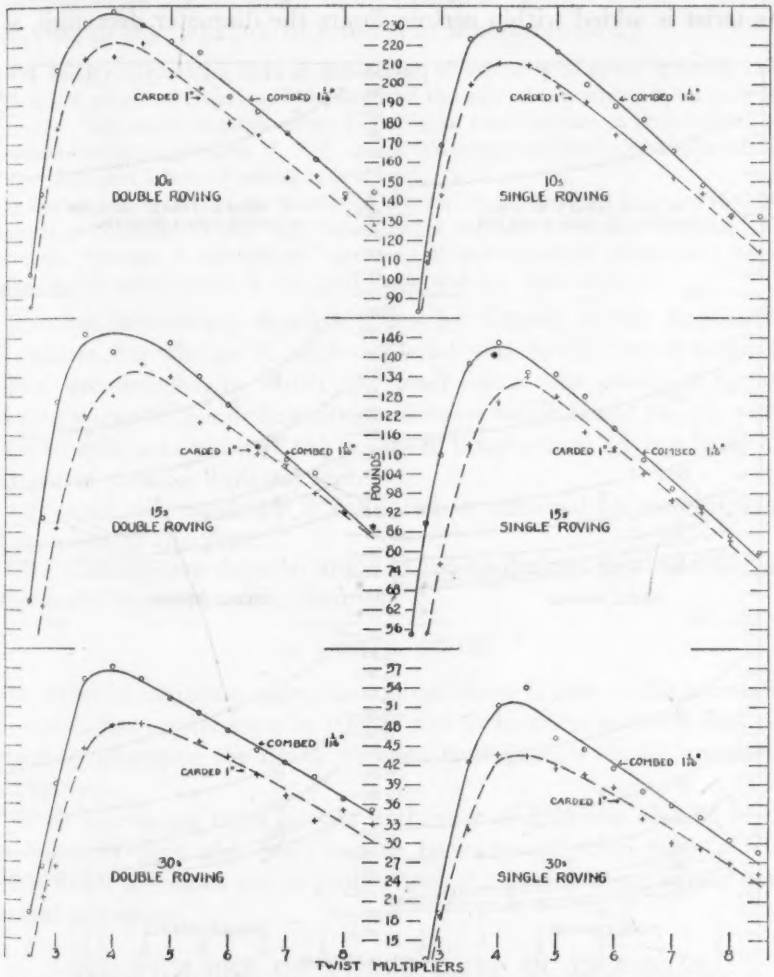

FIG. 4.—*Strength (skein method) of combed and carded cotton yarns as affected by twist*

Yarns were spun from single and double roving. It is to be noted that 1-inch cotton was used for the carded and 1¼-inch for the combed yarn; therefore the curves are not strictly comparable.

they resist efforts to slip by each other. Theoretically the maximum strength is obtained when sufficient twist is given which will, with minimum strain to the individual fibers, prevent any slipping when force is applied in a longitudinal

[2] McGowan, Schoffstall, and Mercier, Effect of Twist on Pima Yarn, B. S. Tech. Paper No. 278, p. 89; Feb. 11, 1925.

direction. Beyond this point the strength decreases, and this decrease can be continued until the yarn breaks under no longitudinal strain, but merely from the shearing action of the twisting.

2. DIAMETER AND ANGLE OF TWIST

The covering power of a yarn is directly affected by the diameter. As twist is added within certain limits the diameter decreases, as is

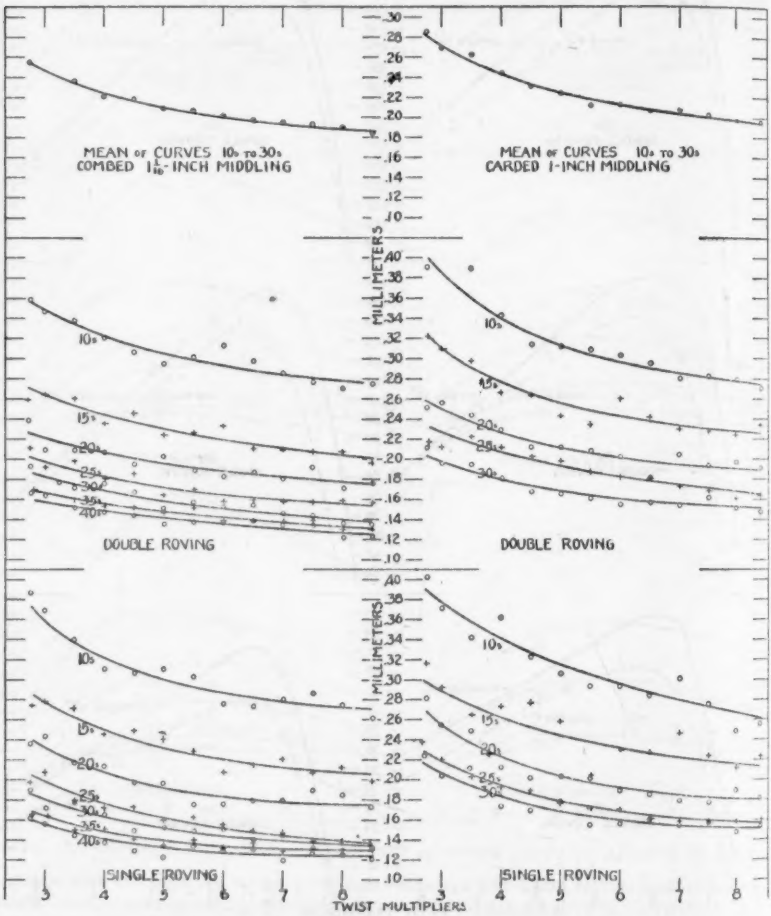

FIG. 5.—*Diameters of cotton yarn as affected by twist*

Groupings of the yarn spun from single and double roving for the carded and combed lots are given; also the mean of the curves.

shown by Figure 5. This feature is important. For example, the yarn for underwear cloth must be soft and make up into cloth in such a way that the interstices between the stitches are a minimum. On the other hand, a voile is made from yarns which form comparatively wide interstices as compared with the surface covered by the yarn itself.

The relation of the angle of twist to the yarn properties is seldom fully realized. There is little doubt that the angle of twist affects light reflection from the surface of the yarn or cloth made from the yarn. While the data in the present study were being collated a paper by Tenney [3] indicated that this feature of yarn testing was receiving attention in other more practical fields. Tenney has the following to say, which is of interest in this connection:

> The theory of parallel lines in the design of cloths is of great interest. The fiber angle, angle of twist, and the angle of the axis of the yarn are all very important. The angle of twist offers not only an exact means of determining the average twist in single yarns * * * but it is a measure of the hardness or softness of the yarn and fabric of which it is a part.
>
> In the design of cotton warp sateens the nearer the parallel fibers of the yarn conform to the angle of the twill the smoother will be the face of the cloth. The difference between a smooth-face and a twill-face sateen is determined by the apposition or coincidence of the twill angle and the fiber angle.

Another interesting example given by Tenney of the application of definite knowledge of angle of twist was in the construction of cotton broadcloths, in which increased luster was obtained by employing yarns with a definite angle of twist which made the ply yarns seem to split into pairs at the points of intersection, giving twice the number of parallel lines per inch.

Luster of silk materials is enhanced or subdued by manipulation of the twist in the yarn.

The quantitative data on angle of twist obtained in this study are graphically represented in Figure 6.

3. CONTRACTION

In order to maintain a constant count in each yarn while increasing the twist, the contraction in length due to increase in twist was corrected by changing the draft. These draft-change curves are shown in Figure 7.

When increasing from a twist multiplier of 3 to one of 4.75 (using the same roving), the draft had to be increased from 9.25 to 9.75. Other draft increases are in proportion, the curves being of the same general character.

VII. THE USE OF THESE DATA IN THE MILL

Questions may arise as to the application of the data here presented in the everyday operation of a cotton mill. Variations from the actual results obtained here may, of course, be expected, even when the same staple of cotton and the same mill organizations are used. Such features as relative humidity in the mill, slippage of spindles,

[3] Tenney, A. M., "Microscopic research in industry," Textile World, p. 2033, Mar. 26, 1927 (a paper read before Committee D-13, Am. Soc. Test. Mat. at Mass. Inst. Tech.; March, 1927).

and variations in test procedure will change the result somewhat. However, it is to be noted that for the most part the data given follow smooth curves very closely, and it should be possible in cases where results are affected by some constant (such as spindle slippage) to interpolate the actual figures from these charts.

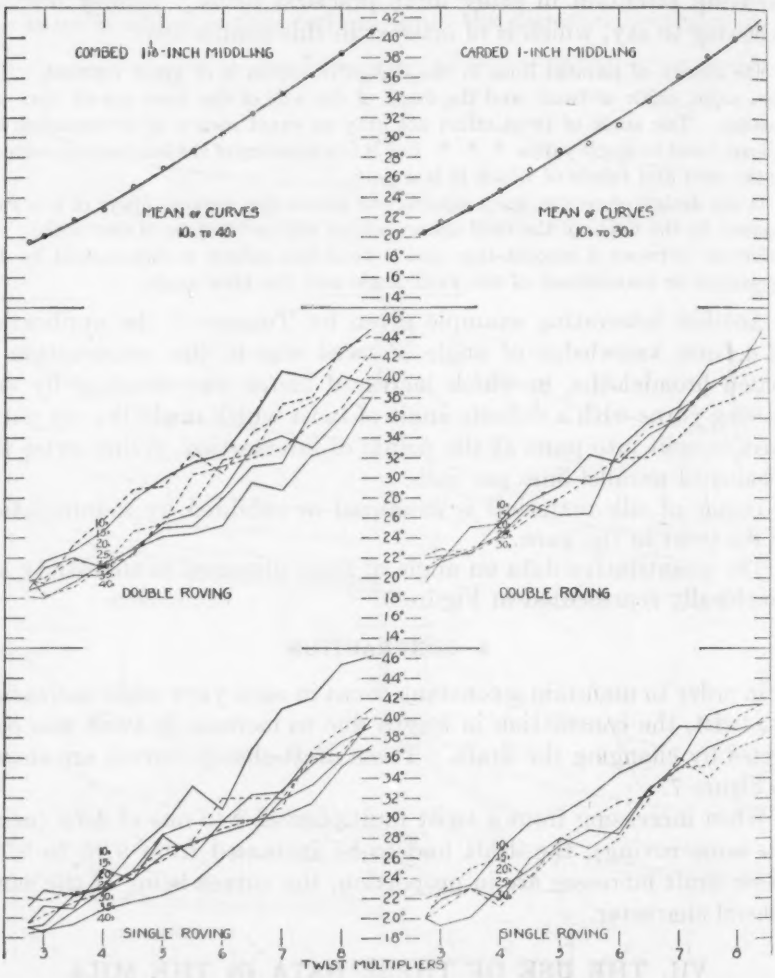

FIG. 6.—*Angle of twist of cotton yarn as affected by twist*

Groupings of the yarn spun from single and double roving for the carded and combed lots are given; also the mean of the curves. Several of the lines connecting the points are broken lines to aid in following the points.

Figure 1 shows markedly the effect of the test method on the result and should enable a mill to some extent to correlate data obtained by either of the two commonly used methods of determining breaking strength. The curves obtained by the two methods separately are shown in Figures 2 and 3. It is believed that the single-strand

method presents a better measure of the breaking-strength relation of the yarn, because the results are an average of a number of breaks, each made separately and including high, low, and medium values.

It was observed that yarn of the twist multiplier which would give maximum strength as indicated by the skein method had less tendency

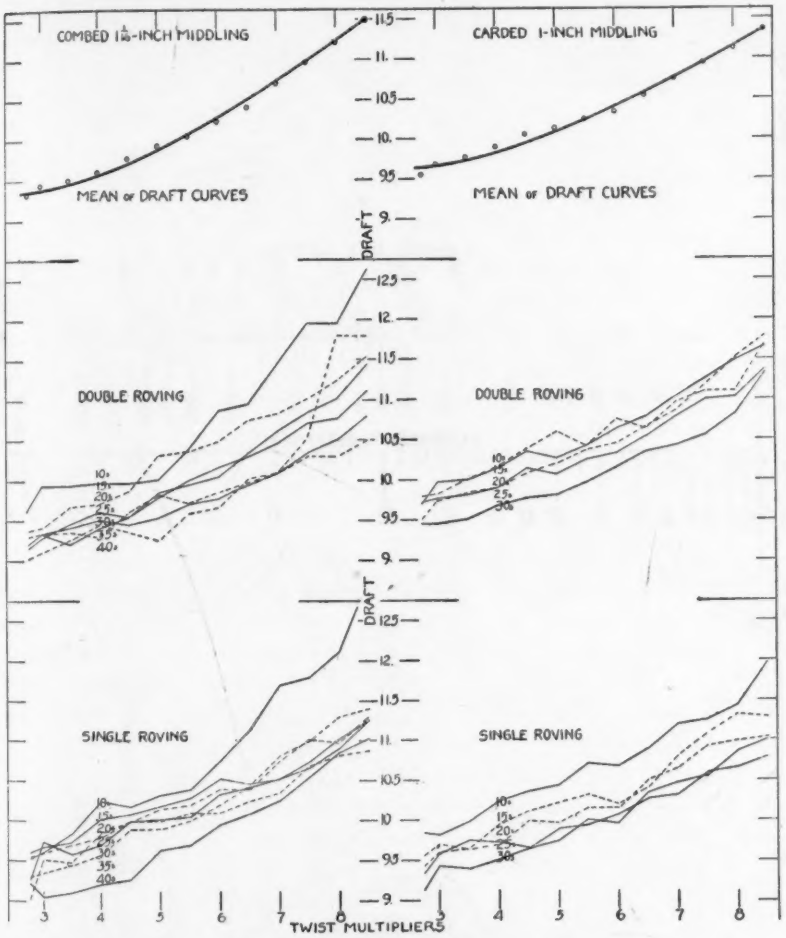

FIG. 7.—*Draft as affected by twist*

The amount of draft necessary to maintain constant counts is plotted against the twist multiplier. Groupings of the yarn spun from single and double roving for the carded and combed lots are given; also the mean of the curves. Several of the lines connecting the points are broken lines to aid in following the points.

to kink. This made it very much easier to handle, and this is, of course, an important factor in the choice of twist multiplier.

Figures 1, 2, and 3 also show that equal breaking strengths can be obtained at two points on the curve, one with a low-twist multiplier, the other with a high. The choice of the proper twist mul-

FIG. 8.—*Chart for determining turns per inch*

To determine turns per inch in a yarn, place straightedge on the count of yarn and on the twist multiplier to be used. The turns per inch are read on the center scale.

FIG. 8.—*Chart for determining turns per inch*

To determine turns per inch in a yarn, place straightedge on the count of yarn and on the twist multiplier to be used. The turns per inch are read on the center scale.

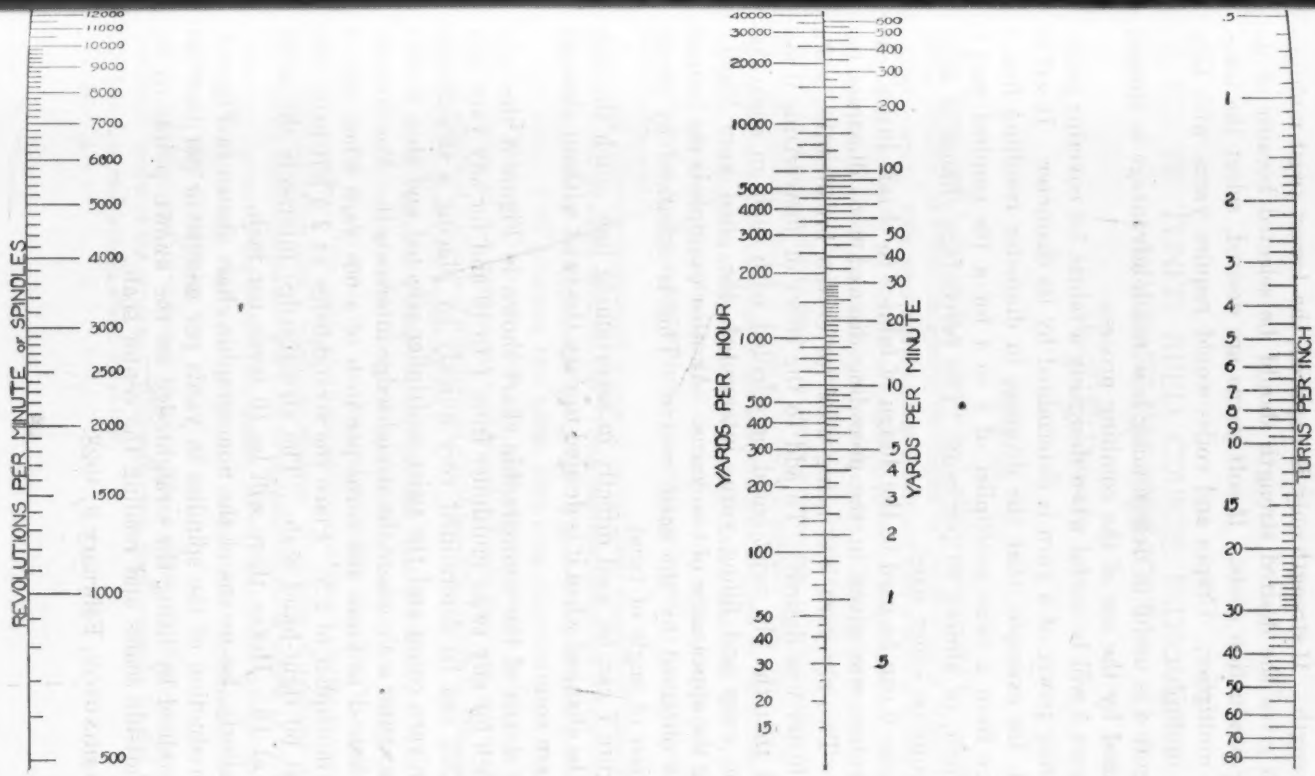

FIG. 9.—*Production chart*

To determine yards per minute or per hour, place straightedge on the revolution of spindle speed at which machine is operating and on the turns per inch. Yards are noted on center scale.

tiplier will depend on what other qualities are desired in addition to strength. If strength only is required, the lowest-twist multiplier which gives the desired strength should be selected because of the lower production costs. If soft yarns are desired, select the lower-twist multiplier. Crêpes and voiles would require yarns with high-twist multiplier.

Figure 4 is useful in determining how much advantage in strength is gained by the use of the combing process.

Figure 5 will be useful when designing a fabric for covering power. Covering power of a yarn is determined by its diameter. It will be noted, for example, that the decrease in diameter resulting from a change from a twist multiplier of 3 to 4 for a 10s combed yarn is 0.04 mm, or almost 10 per cent. The percentage change is about the same on other sizes.

Figure 6 can be used in the design of fabrics to obtain luster. An illustration was given in the preceding discussion to illustrate this case. Two-ply yarn was being used for cotton broadcloths, and a high luster was desired. To add to the effect of mercerizing it was found that the ply twist could be selected with such an angle that as the warp and filling yarns intersected, the plied yarn "split," giving the appearance of two yarns. Another example is the lustrous effects obtained by the satin weave. This is enhanced by proper selection of angle of twist.

Figure 7 can be used directly in ascertaining how much the draft must be changed when it is desired to vary the twist without changing the yarn count.

By means of the nomographic chart shown in Figure 8 the turns per inch for any twist multiplier from 1 to 10 and for any yarn from 1 to 225 can be determined very quickly by placing a straightedge at the yarn count and the twist multiplier selected and then reading on the center scale where the straightedge intersects it. For example, it is desired to know the turns per inch of a 60s yarn when using a twist multiplier of 2.5. Place the straightedge at 2.5 left-hand scale and at 60 right-hand scale. The straightedge intersects the center scale at 19. Hence there will be 19 turns per inch.

Similarly, by means of the nomographic chart shown in Figure 9, the production of the spindles in yards per minute or per hour can be obtained by fixing the straightedge on the known points on the two outside scales and reading the center scale.

WASHINGTON, February 8, 1928.

DESIGN OF TUNED REED COURSE INDICATORS FOR AIRCRAFT RADIOBEACON

By F. W. Dunmore

ABSTRACT

The tuned reed indicator is a simple and reliable instrument for use in connection with the radiobeacon system developed by the Bureau of Standards for guiding aircraft. This beacon system was developed with a view to giving a pilot a visual indication as to whether or not he is flying on a specified course, and if not, to which side and how much he has deviated. This indication is given by two vibrating reeds, the relative amplitudes of vibration of which indicate the position of the airplane with respect to the beacon course. Equal amplitude of the two reeds indicates that the airplane is on the course. The reeds give a continuous indication to the pilot of his position with respect to his course. This indication is obtained without any other effort than a glance of the eye. This feature is particularly valuable, since in time of fog, when the device is most needed, the pilot is very much occupied and can only glance at a course-indicating device occasionally.

The reed indicator consists of a pair of metal reeds capable of vibrating between a pair of small electromagnets. These electromagnets are connected to the output terminals of the airplane receiving set. The free end of each reed carries a white vane. This produces two white lines close together when the reeds vibrate. These two lines are what the pilot observes when holding a beacon course. Owing to the mechanical tuning of the reeds they are extremely free from the effects of all kinds of interference unless the interference is strong enough to block the tubes in the receiving set.

Six types of indicators were constructed and data obtained on each. The final model was one in which the reeds were made of steel with a bimetallic strip on the free end of the reeds for automatically holding the reeds in tune as the temperature varies. The reeds which are strongly polarized vibrate between two electromagnets taken from a telephone receiver. This form of indicator requires less than 1.5 milliamperes and 3.5 volts to operate the reeds with a 11 by 11 mm damper on the end of the reed. This damper served to increase the decrement of the reed, so that any slight changes in the modulation frequencies would not change the reed deflections.

This indicator unit is arranged to plug into a shock-proof mounting on the instrument board of the airplane. With mounting its dimensions are 3½ by 2¾ by 4½ inches, and weighs under 2 pounds.

8431°—28——1

CONTENTS

	Page
I. Introduction	752
II. Choice of modulation frequencies	753
III. Description of several types of indicators	757
1. Experimental type, with marker beacon reed, type A	758
2. Multireed indicator, type B	760
3. Single-coil reed indicator, type C	761
4. Plug-in type of indicator, type D	762
5. Rear-drive, nonpolarized indicator, type E	763
6. Rear-drive, polarized reed, type F	767
IV. Conclusion	769

I. INTRODUCTION

The tuned reed type of visual indicator is a simple and reliable instrument for use on airplanes in connection with the double modulation type radiobeacon.[1] This beacon system was developed with a view to giving a pilot a visual indication as to whether or not he is flying on a specified course, and if not, to which side and how much he has deviated. This indication is given by two vibrating reeds, the relative amplitudes of vibration of which indicate the position of the airplane with respect to the beacon course. The reeds give a continuous reading indication to the pilot, free from the effects of ignition and other interferences, yet they are sufficiently sensitive to operate from the output of an aircraft receiving set and small enough to be placed on the instrument board of an airplane.

The radiobeacon, in connection with which the reed indicator operates, is a transmitting station which sends out 290-kilocycle waves on two loop antennæ. These antennæ are at right angles to each other, and the waves from one are modulated at a certain low frequency, such as 65 cycles, and the other at another low frequency, as 85 cycles. A figure-of-eight characteristic is produced in space, and there are two lines (or four directions) along which the two modulated signals are of equal intensity. These directions are the courses where the two reeds of the visual indicator vibrate with equal amplitudes.

The reed indicator consists of a pair of metal reeds capable of vibrating between a pair of small electromagnets. These electromagnets are connected to the output terminals of the airplane receiving set. The frequencies to which the two vibrating reeds are tuned are the modulation frequencies supplied to the two transmitting antennæ at the beacon station. This paper describes the development of the reed indicators, with special reference to choice of the modulation frequencies.

[1] "Development of radio aids to air navigation." J. H. Dellinger and H. Pratt, Proc. I. R. E., 16, p. 890-920; July, 1928.

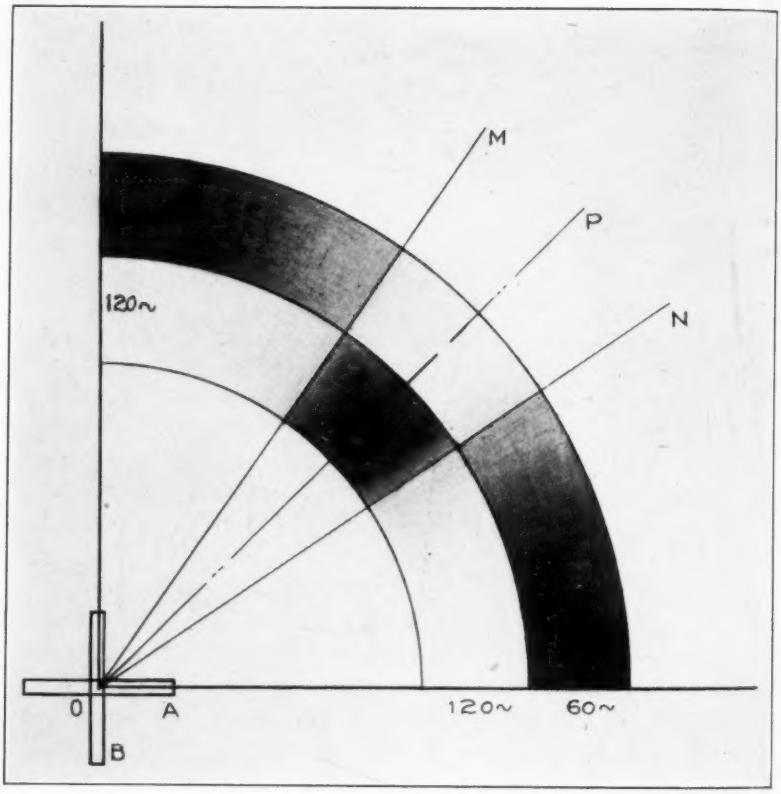

FIG. 1.—*Transmission characteristic of beacon modulated at 60 cycles, push-pull fashion. Degree of shading shows amount of modulation present*

II. CHOICE OF MODULATION FREQUENCIES

The choice of modulation frequencies which may be used in the beacon station is essentially determined by the characteristics of the indicators used on the airplane. In order to obtain an appreciable amplitude of reed vibration in the indicators, it is necessary to use a reed of sufficient length to give at least 1 cm deflection. Low frequencies were, therefore, chosen, of the order of 50 to 100 cycles. Aside from making possible the use of a sufficiently long reed in the indicator, the use of these frequencies had the added advantage that, owing to the narrow side bands when modulating the carrier at two of these frequencies, a change in tuning of the receiving set operating the reeds will not cause an apparent shift in the course due to the relative change in the side band amplitudes. A detuning of the receiving set by 100 cycles throws out both frequencies, while if 500 or 1,000 cycles were used and the set detuned by 500 cycles most of the 500 cycles would be tuned out while much of the side band from the 1,000 cycles would remain.

In the first experiments to determine suitable modulation frequencies 60 cycles was chosen as one frequency, since it could easily be obtained from the power lines. The circuit consists of a master oscillator, the radio-frequency output of which is amplified by two amplifier tubes I_1 and I_2. The plate of I_1 is supplied with high voltage at 85 cycles through transformer F and passes radio-frequency on to one coil antenna modulated at this frequency through coils C and L, while the other tube passes the same radio-frequency modulated at 65 cycles by transformer G to the other coil antenna through coils M and P. In these first tests one center-tapped 60-cycle transformer was used in place of transformers F and G. The effect of this combination was to operate the power amplifier tubes I_1 and I_2 in push-pull fashion, so that radio-frequency power is passed through coils C–L and M–D every other half cycle.

An advantage of the push-pull arrangement is that there can be no coupling between power amplifier circuits or between goniometer stators, since the push-pull circuit causes one power amplifier to be completely inactive while the other is functioning, due to the negative potential on one plate while the plate of the other tube is positive. The effect produced in space is that shown in Figure 1, in which the relative amounts of shading in the outer segment represent the amount of 60-cycle signal present and a similar effect in the inner segment represents the amount of 120-cycle signal present. Since the signals received along the line OP from loops A and B are of equal amplitude and come alternately, two every 60 cycles, the audio-frequency signal in this region will be 120 cycles. In this system, therefore, the second reed was tuned to 120 cycles. With this

method there are two courses for each quadrant, one being along the line ON, where the 60 and 120 cycle modulation are present with equal amounts and the other along the line OM where the two frequencies are likewise present in equal amounts.

It was found during experiments with this system that the two courses could readily be found. In fact, there were really eight courses, two for each quadrant. These were found by rotating the courses through 360° while receiving the 120 and 60 cycle signal at a

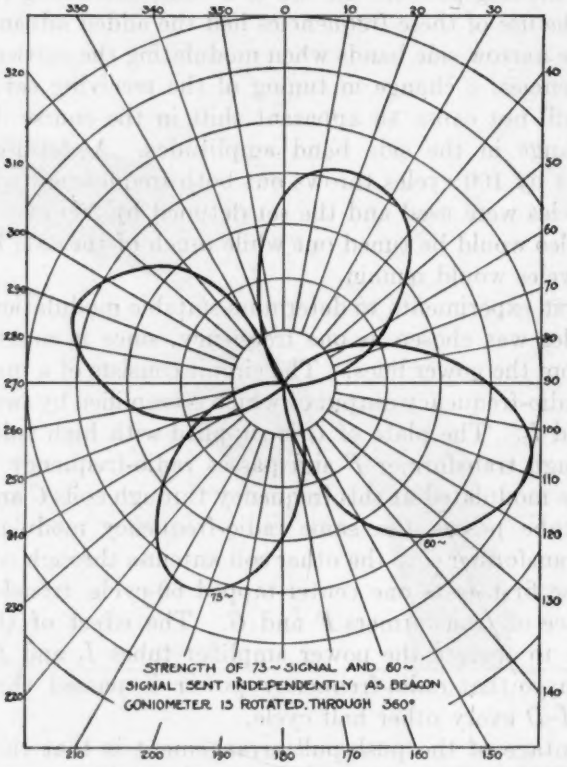

FIG. 2.—*Resultant field with beacon antennas modulated, one at 60 cycles and the other at 75 cycles*

fixed location and watching the reed indicator. In this way all eight courses could be swept through the receiving point. Although the transmitting circuit for this system is simple, several disadvantages were found from the point of view of the reeds. The principal objection was that the 120-cycle reed being tuned to a harmonic of 60 cycles was caused to operate by the 60-cycle frequency. Although the amplitude of the vibration due to this effect was small, it was sufficient to broaden the course. Another disadvantage was that the 120-cycle reed, being considerably shorter than the 60-cycle reed,

gave a much less amplitude of vibration than the 60-cycle reed for an equal audio-frequency input. The sharpness of the course is greater when turning into the 120-cycle zone than when turning in the opposite direction toward the 60-cycle zone. The two courses, OM and ON (fig. 1), might cause some confusion, since they are within 15 or 20° of each other, and the pilot might accidentally shift from one course to the other without knowing it. For these reasons this method of modulation at the beacon was discarded for the one in

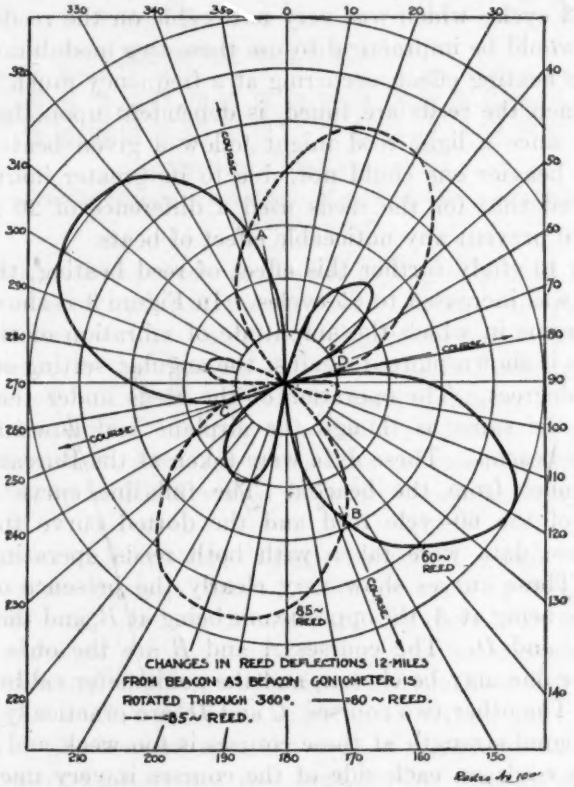

FIG. 3.—*Polar curves obtained by measuring the amplitudes of vibration of the 60 and 85 cycle reeds as beacon course is changed through 360°*

which two sources of audio-frequency modulations were used independently of each other.

The next problem was to determine the two best modulating frequencies. Sixty cycles was again chosen as one frequency, since it could be so easily obtained from the power line and since the length of the reed which tuned to this frequency was sufficient to give ample movement at the free end without being too long to be affected by mechanical vibrations. The other frequency, as first chosen, was

73 cycles. Figure 2 shows polar curves taken using these two frequencies with thermoelements in the output of a radio receiving set. These curves were taken as the goniometer was rotated through 360°, thus swinging the courses past the receiving point. The curve for 60 cycles was taken with the 73-cycle power off and the curve for 73 cycles with the 60-cycle power off. When both frequencies of modulation were applied simultaneously and a reed indicator with reeds tuned to 60 and 73 cycles was put in place of the thermoelement, it was found that the frequencies of 60 and 73 cycles caused a beating effect at 13 cycles which was very noticeable on the reeds; so much so that it would be impractical to use these two modulation frequencies. This beating effect, occurring at a frequency much lower than that to which the reeds are tuned, is dependent upon the inertia of the reeds, since a light reed might follow a given beat frequency, whereas a heavier one could not, due to its greater inertia. Later tests showed that for the reeds used a difference of 20 cycles was sufficient to prevent any noticeable effect of beats.

In order to study further this effect of reed beating, the 73-cycle frequency was increased to 85 cycles. In Figure 3 is shown a set of polar diagrams in which the amplitude of vibration of the reeds in millimeters is shown plotted against the angular setting of the goniometer in degrees. The operation of the reeds under these circumstances is the same as though the airplane had flown completely around the beacon. These data were taken at the Bureau of Standards, 12 miles from the beacon. The full line curve shows the operation of the 60-cycle reed and the dotted curve the 85-cycle reed. These data were taken with both reeds operating simultaneously. These curves show very clearly the presence of the four courses, one being at A, the opposite one being at B, and the other two being at C and D. The courses A and B are the ones which are used; either one may be chosen, and the goniometer calibrated using this one. The other two courses, C and D, are practically worthless, since the signal strength at these courses is too weak and the operation of the reeds on each side of the courses is very uneven. The smaller polar curves within the larger ones are due to coupling between the two power amplifiers and goniometer stator coils. With the courses A and B the amplitude of vibration of one reed drops evenly, while that of the other reed rises in a similar fashion as the pilot deviates from the course. Although the two beacon loops, A and B, are at right angles as well as the goniometer stators and rotors, it will be noted that the minimum of 60-cycle signal and minimum of 85-cycle signal do not occur at points separated by 90°. Instead, this angle is about 60°. From Figure 3 it will be noted that if a pilot deviates from his course at A by 25° to the right, the 60-cycle reed

will decrease in amplitude until it becomes stationary, while the 85-cycle reed would vibrate with nearly maximum amplitude at this point. If he deviates by 35° in the opposite direction to the left, the 85-cycle reed will drop to a stationary position and the 60-cycle reed will be vibrating with maximum amplitude. The effect is shown in more graphical form in Figure 4, which is self-explanatory. From

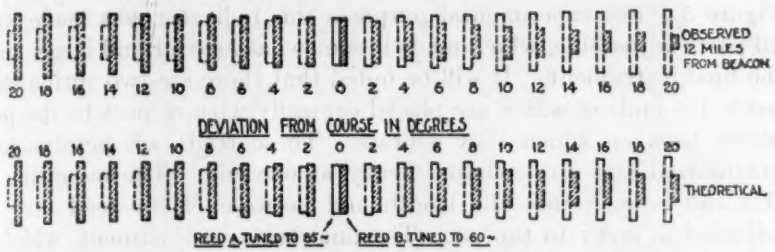
OBSERVED 12 MILES FROM BEACON
20 18 16 14 12 10 8 6 4 2 0 2 4 6 8 10 12 14 16 18 20
DEVIATION FROM COURSE IN DEGREES
20 18 16 14 12 10 8 6 4 2 0 2 4 6 8 10 12 14 16 18 20
THEORETICAL
REED A TUNED TO 85~
REED B TUNED TO 60~

FIG. 4.—*Relative change in amplitude of reed vibrations as airplane deviates from the course*

the operation of the reeds as shown in Figure 4, it is evident that the relative amplitudes of the two reeds enables the pilot to judge to a large extent as to the number of degrees he has deviated from the course either to the right or left and still indicate to him which side he is off. This feature of the reed indicator is very useful, since it is frequently necessary to make large detours to avoid storms or other hazards to flying, in which case the pilot knows at all times to what degree he has deviated from the course and how to turn to return to it.

The particular field strength patterns using the two frequencies of modulation, as shown in Figure 3, were produced by the certain combination of conditions at the beacon transmitter. Instead of being two figure-of-eight's oriented at 90°, they produce a much better field strength pattern with a strong signal in the direction of the two courses and a much weaker one at 90°, thus cutting down interference produced by the beacon; also, the slope of the curves at the intersection is greater than if they had been circles, thus giving a sharper course indication.

Since very good operation of both the beacon and reed indicator was obtained when using 60 and 85 cycles as the modulation frequencies, these two were adopted and the reeds designed accordingly.

III. DESCRIPTION OF SEVERAL TYPES OF INDICATORS

In order to obtain a satisfactory reed indicator suitable for use on aircraft, several models were successively designed and experimented with. These various models are designated below as types A, B, C, D, E, and F. The type F indicator is the most satisfactory of these.

1. EXPERIMENTAL TYPE, WITH MARKER BEACON REED, TYPE A

Several forms of this type of indicator were constructed and tried out. In this type the reeds are permanently magnetized, the driving electromagnets operating on the free end of the reeds. The first one was made using the electromagnets from an ordinary telephone receiver. One of the indicators constructed in this way is shown in Figure 5. For experimental purposes this indicator was made with all parts adjustable, which made it somewhat heavier and larger than the final instrument. It will be noted that there are two spring-steel reeds, the ends of which are placed centrally with respect to the pole pieces between which they vibrate. These reeds are permanently magnetized and are anchored firmly at one end. The mounting at this end is such that the length and position of the reed may be adjusted in order to tune it. The final tuning adjustment, which is very critical, is made by slightly tightening or loosening the screws through the clamps which hold the reeds in place. The tip of the reed is provided with a small light vane painted white, so that when the reed vibrates a clear white line is produced. The 60-cycle reed is approximately 60 mm long, 3.2 mm wide, and 0.28 mm thick. The 85-cycle reed is about 50 mm long, 2.7 mm wide, and 0.28 mm thick. Reeds of this width were necessary in this model, as they are acted upon at their free end by the electromagnets. Since it was necessary that these reeds be operated from the output of the radio receiving set on the plane, it was necessary that they be sufficiently sensitive to give full amplitude of vibration with normal output of the receiving set. This was accomplished by using two electromagnets acting push-pull fashion on a magnetized polarizing reed and by matching the impedance of the reed coils to that of the last tube on the receiving set. When this type of indicator was tried out without extra damping, it was found that it required somewhat less than 2 milliamperes to give full amplitude of vibration. Data taken at 60 cycles on this indicator showed that it had an impedance of 3,180 ohms, the direct-current resistance was 2,200 ohms, and 1.78 milliamperes at 60 cycles caused the 60-cycle reed to deflect 1 cm. The single reed on the right in Figure 5 is the marker beacon reed, to be described in a forthcoming paper. The two extra electromagnet coils for operating this reed were not included in the circuit when the above measurements of resistance and impedance were made.

The white vane on the ends of the reeds was made as light as possible. This was done for two reasons: (1) The greater the weight on the tip of the reed the more susceptible it is to the effect of mechanical vibrations; (2) the lighter the vane on the end of the reed the less the mechanical selectivity, since a weight on the end of a tuned reed acts like inductance in a tuned circuit, the resonance curve is sharper. It is important that the reeds be not too selective, since any slight

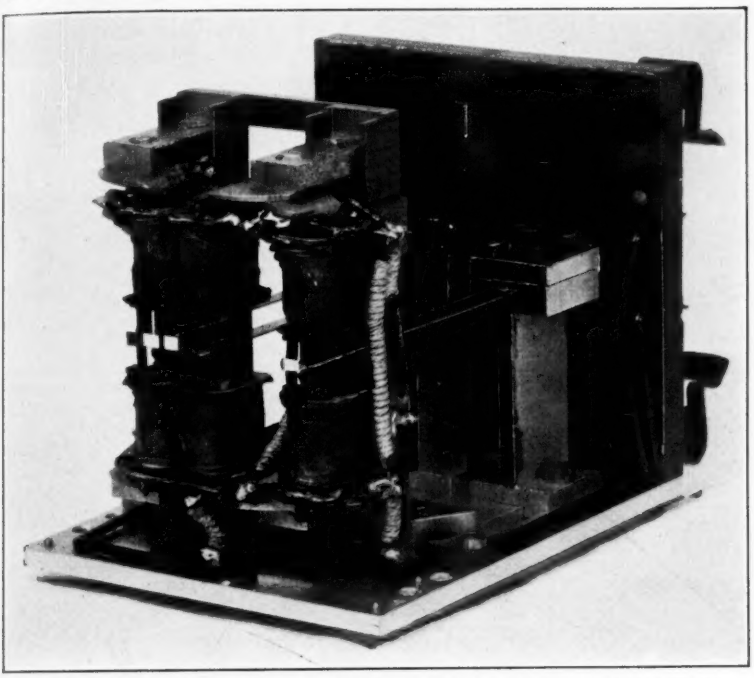

FIG. 5.—*Type A indicator, with forward drive and magnetized reeds*

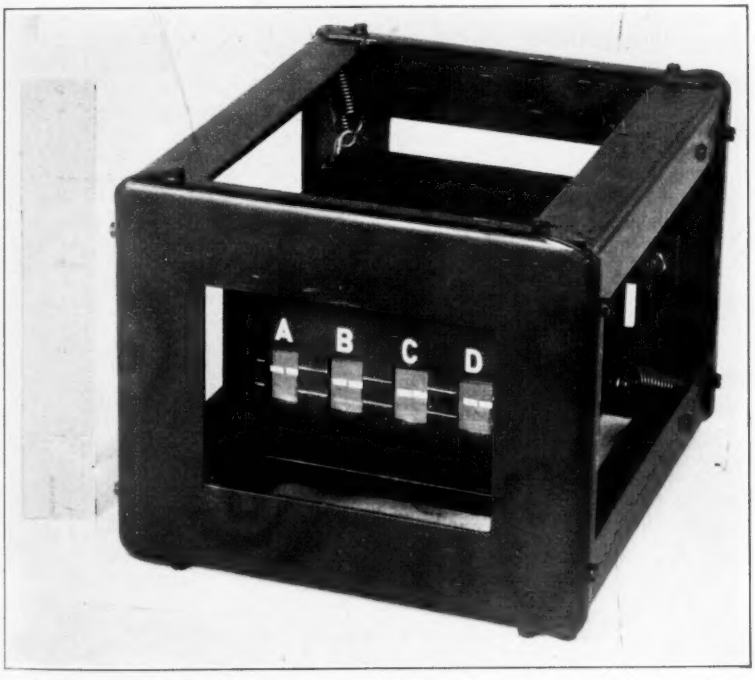

FIG. 7.—*Type B indicator, multi-reed type, with shock-proof mounting*

change in the modulation frequency at the beacon would result in a decreased amplitude of reed vibration, thus causing an apparent shift in course.

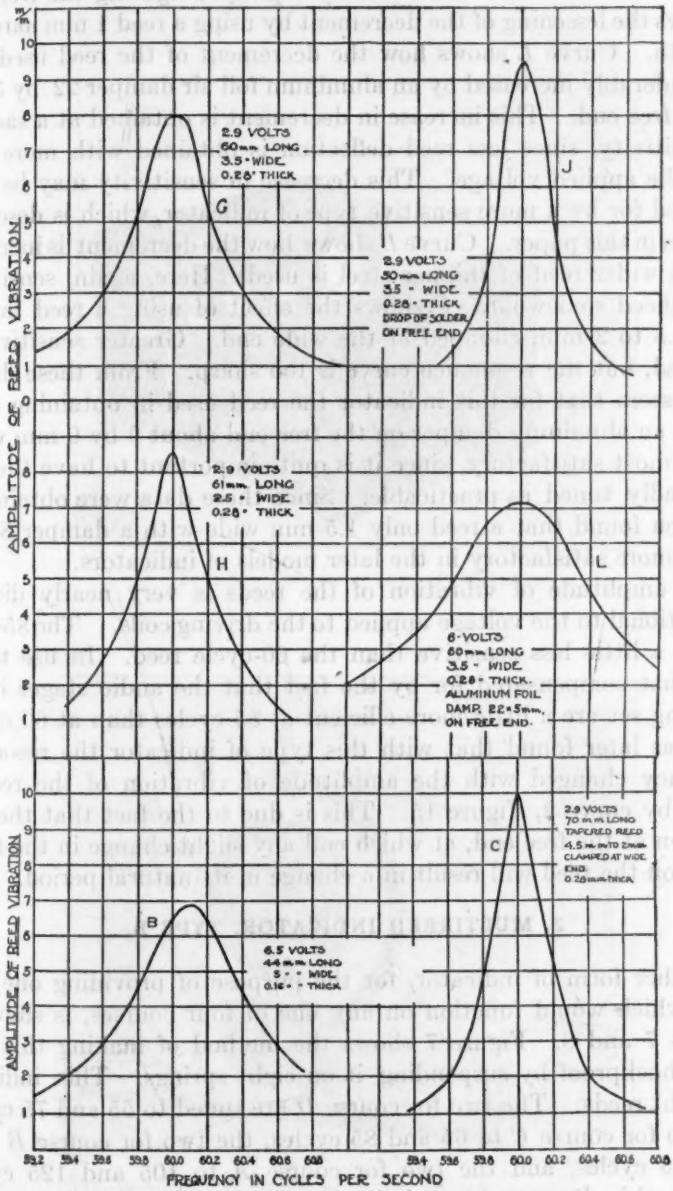

FIG. 6.—*Resonance curves for various reeds*

Because of this a study was made of different types of reeds in order to obtain one with as high a decrement as possible, yet sufficiently sensitive. The resonance curves shown in Figure 6 show

how the reed characteristics in the type A indicator may be varied. Curve *G* shows the resonance curve for a convenient size of spring steel reed without weight on the free end. Curve *J* shows how the decrement of the reed is lessened by slightly weighting the free end. *H* shows the lessening of the decrement by using a reed 1 mm narrower in width. Curve *L* shows how the decrement of the reed used in *G* is considerably increased by an aluminum foil air damper 22 by 5 mm on the free end. This increase in decrement is obtained at a sacrifice of sensitivity, since less reed deflection is obtained with more than twice the applied voltage. This decrease in sensitivity may be compensated for by a more sensitive type of indicator, which is described later on in this paper. Curve *B* shows how the decrement is increased when a wider reed of thinner steel is used. Here, again, sensitivity is sacrificed somewhat. *C* shows the effect of using a reed tapered from 4.5 to 2 mm, clamped at the wide end. Greater sensitivity is obtained, but the resonance curve is too sharp. From these data it would seem that for this indicator the reed used in obtaining curve *G* with an aluminum damper on the free end about 9 by 9 mm would be the most satisfactory, since it is quite important to have the reed as broadly tuned as practicable. Since these data were obtained it has been found that a reed only 1.5 mm wide with a damper 8 by 8 mm is more satisfactory in the later models of indicators.

The amplitude of vibration of the reeds is very nearly directly proportional to the voltage applied to the driving coils. The 85-cycle reed is a little less sensitive than the 60-cycle reed. In use this is somewhat compensated for by the fact that the audio stages in the receiving set are a little more efficient at 85 cycles than at 60 cycles.

It was later found that with this type of indicator the resonance frequency changed with the amplitude of vibration of the reed as shown by curve 2, Figure 15. This is due to the fact that the reed is driven at the free end, at which end any slight change in the forces acting on the reed will result in a change in its natural period.

2. MULTIREED INDICATOR, TYPE B.

Another form of indicator, for the purpose of providing one indicator which would function on any one of four courses, is shown in Figures 7 and 8. Figure 7 shows the method of making this indicator shockproof by suspending it on eight springs. This indicator has eight reeds. The two for course *D* are tuned to 55 and 75 cycles, the two for course *C* to 65 and 85 cycles, the two for course *B* to 95 and 115 cycles, and the two for course *A* to 105 and 125 cycles. This combination made an indicator which might be used on any one of four courses, *A*, *B*, *C*, or *D*, which may be sent out from a given beacon, provided they are sent on slightly different carrier

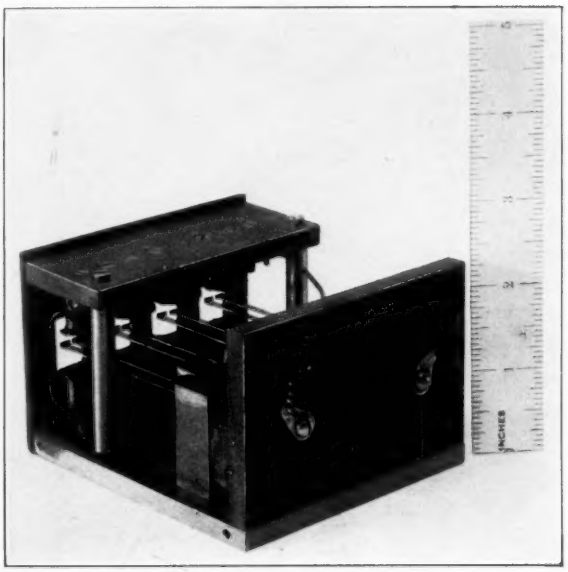

FIG. 8.—*Interior of type B indicator*

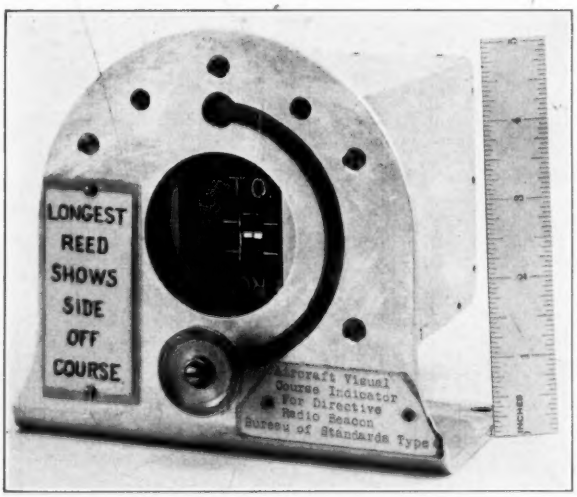

FIG. 9.—*Type C indicator, with pivoted mounting for turning it upside down*

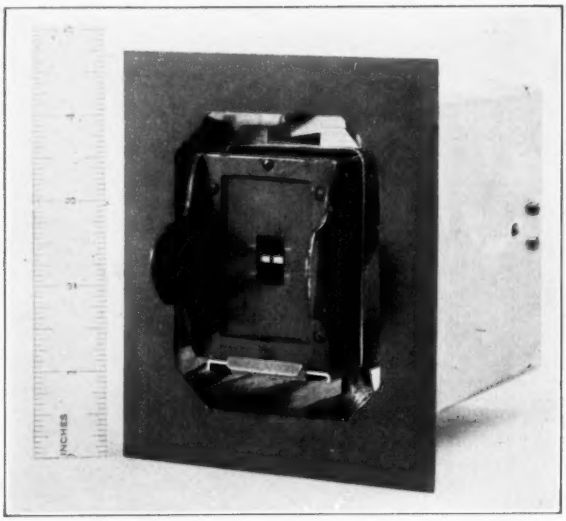

FIG. 11.—*Type D indicator, with shock-proof mounting*

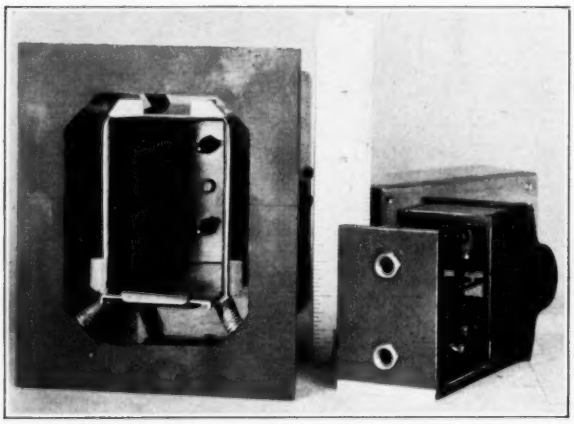

FIG. 12.—*Type D indicator, showing plug-in connection*

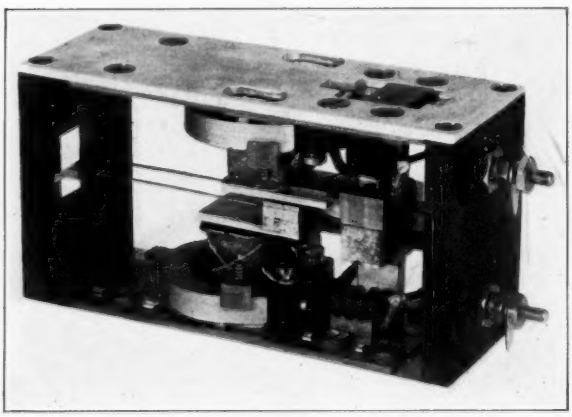

FIG. 13.—*Type E indicator, nonpolarized rear drive*

frequencies. Thus, if the pilot is flying on course *B*, he would observe the second set of reeds only, which would be operated only by the beacon signal when it is oriented on course *B*. When the signal is oriented on courses *A*, *C*, and *D*, the modulation frequency and carrier frequency being changed, *B* reeds are stationary. This type of indicator was found to be rather insensitive due to the necessity of using many electromagnets in series for driving the eight reeds. This might be overcome by a switching device for connecting in circuit any one set of two driving coils.

3. SINGLE-COIL REED INDICATOR, TYPE C

This type of indicator differs considerably in design from the ones described and was made in the attempt to obtain an indicator of greater sensitivity. It is shown in Figure 9. Figure 10 shows the

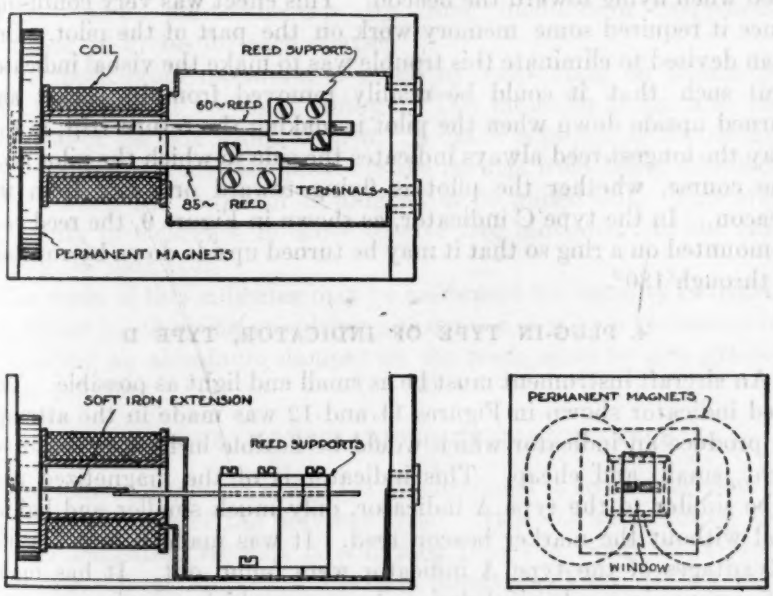

FIG. 10.—*Principle of design of type C indicator*

details of construction. The reeds are not magnetized in this indicator, but both vibrate in the center of the coil of about 12,000 turns of No. 28 enameled wire. The reeds are of spring steel, but the ends within the coil have attached to them a little strip of corrugated soft iron about 1 inch long cut from a telephone receiver diaphragm. The magnets from the telephone receivers are placed at the free ends of the reeds. The polarity of the soft iron tips follows that of the alternating flux within the coil which carries the 60 and 85 cycle frequency. As these soft-iron tips are within the field of permanent

magnets, they are attracted and repelled with the changing flux, causing the reeds to vibrate. This type of indicator gave a deflection of the 60-cycle reed of 13 mm for 1.45 mils of 60-cycle current in the coil. This deflection was without damping. It has an impedance at this frequency of 5,030 ohms and a direct current resistance of 3,100 ohms. This indicator was made shock proof by mounting it in a box lined with light sponge rubber. It was found that the resonance frequency of this indicator changed considerably with amplitude, as shown by curve 3, Figure 15.

During the early trials of these indicators in actual flight tests a rather troublesome feature was found regarding the use of the reed type of visual indicator, since the pilot was required to turn in the direction of the shortest reed to get back on the course when flying away from the beacon, whereas he was required to turn to the longest reed when flying toward the beacon. This effect was very confusing, since it required some memory work on the part of the pilot. One plan devised to eliminate this trouble was to make the visual indicator unit such that it could be readily removed from its socket and turned upside down when the pilot is making the return trip; in this way the longest reed always indicates the side to which the pilot is off the course, whether the pilot is flying toward or away from the beacon. In the type C indicator, as shown in Figure 9, the reed case is mounted on a ring so that it may be turned upside down by rotating it through 180°.

4. PLUG-IN TYPE OF INDICATOR, TYPE D

An aircraft instrument must be as small and light as possible. The reed indicator shown in Figures 11 and 12 was made in the attempt to produce an indicator which would be flexible in its use, sensitive, light, small, and cheap. This indicator is of the magnetized reed type similar to the type A indicator, only much smaller and lighter and without the marker beacon reed. It was made before the disadvantages of the type A indicator were found out. It has many refinements in mechanical design, however, which were incorporated in the later models. Four driving coils similar to those used in the type A indicator are used in this indicator. Figure 11 shows the indicator in position in its shock-proof case, and Figure 12 shows the case and indicator removed. The indicator has two plug terminals and the case two sockets permanently connected to the receiving set. Iu this way the indicator is automatically connected to the receiving set when it is plugged into its shock-proof case. The case is designed for panel mounting. Figure 21 shows the indicator mounted on the instrument board of an airplane. The words "From Beacon" appear right side up, and the words "To Beacon" upside down, showing that it is plugged in for a flight from the beacon. The indicator weighs

½ pound without the shock-proof mounting, and is 1⅝ by 2⅜ by 3 7/16 inches. With the mounting it weighs 1¼ pounds and is 3½ by 2¾ by 4½ inches. As it has but two reeds, it may be used only on one air route, but since it is of the plug-in type it may readily be removed from its shock-proof mounting and a similar indicator plugged in with reeds tuned to the course frequencies of whichever route the plane is to fly over. This type of plug-in indicator has several advantages over the multireed type of indicator. It may be made much smaller and lighter. It is more sensitive, since there are but two reeds to be operated. It may be easily removed from circuit for inspection. It may be quickly plugged in upside down when making the return trip. Any number of different courses may be flown by plugging in an indicator tuned to the desired course frequencies, since it is possible with an indicator as selective as the reed indicator to have the beacon serve several courses simultaneously by using modulation frequencies separated 20 cycles for each course.

The shock-proof mounting is made by suspending an aluminum box on springs at its eight corners. The indicator plugs into the front end of the box which is open. A catch is provided for holding it in. A stop on the rear prevents the springs from being stretched unduly when the indicator is plugged in or pulled out. This stop has plenty of clearance in order to give free movement to the case holding the indicator.

The reeds of this indicator may be calibrated for equality of deflection either by shunting one driving magnet coil with a resistance or by bending an aluminum damper on the reeds so as to give greater or less damping.

5. REAR-DRIVE, NONPOLARIZED INDICATOR, TYPE E

This indicator (shown in fig. 13) was designed to overcome some of the disadvantages of the previous types. It is the same size as the type D indicator, so that it will plug into the same shock-proof mounting. It is somewhat heavier, however. Four driving coils similar to those used in the type A indicator are used in this indicator. It is radically different in design, being somewhat similar to the commercial type frequency indicator which has a number of reeds mounted in a common armature which is actuated by an electromagnet. This design was modified somewhat, since it was found that with the two reeds on a common armature there was a noticeable reaction between them, since the armature was light in weight and the ends of the reeds were not weighted. By putting each reed on a separate armature, each armature being actuated by a separate electromagnet, this trouble was overcome. The two actuating electromagnets were taken from ordinary telephone receivers. These each operate a soft-iron armature to which a reed is attached. The reeds

are only 1.5 mm wide in this indicator. They may be of any desired material, since it is not necessary that it be magnetic. The alloy elinvar was therefore used for the reeds, since the modulus of elasticity of this material is practically independent of the temperature. This is a rather important factor, as will be noted from the data shown. (Fig. 14.) From these data it will be noted that a change in 60° C.

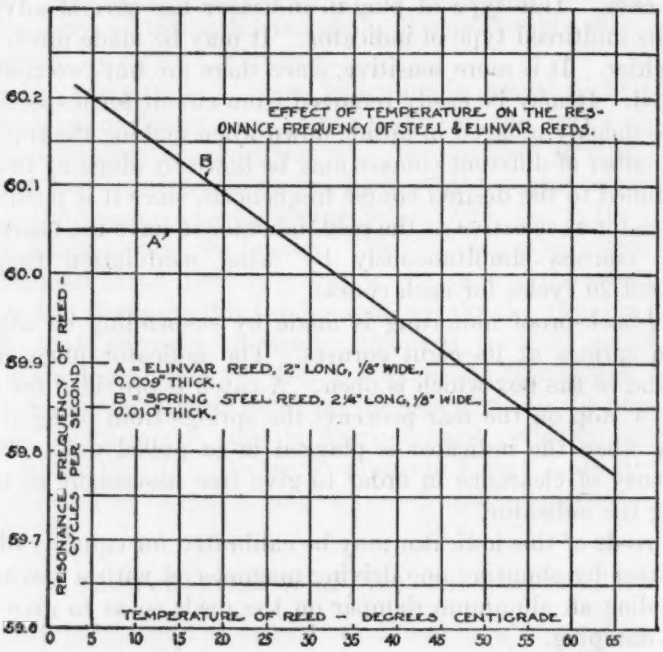
EFFECT OF TEMPERATURE ON THE RESONANCE FREQUENCY OF STEEL & ELINVAR REEDS.
B
A
A = ELINVAR REED, 2" LONG, 1/8" WIDE, 0.009" THICK.
B = SPRING STEEL REED, 2 1/4" LONG, 1/8" WIDE, 0.010" THICK.
RESONANCE FREQUENCY OF REED - CYCLES PER SECOND
60.2
60.1
60.0
59.9
59.8
59.7
59.6
TEMPERATURE OF REED - DEGREES CENTIGRADE
0 5 10 15 20 25 30 35 40 45 50 55 60 65

FIG. 14.—*Effect of temperature on the resonance frequency of steel and elinvar reeds*

of a steel reed in this indicator caused its resonance frequency to change from 60.20 to 59.78 cycles, whereas with a similar change in temperature of an elinvar reed no change in the resonance frequency could be noted. For the steel reed, therefore, the change in frequency with temperature is 0.0117 per cent per degree centigrade. This figure agrees well with the commonly accepted value. Since temperature changes of the order of 60° C. are to be expected on aircraft, it is evident that the use of this material for the reeds in this indicator is an improvement, since it is not necessary to dampen the reed so much in order to hold it in tune with changing temperature. Some damping of the elinvar reed, however, is desirable, in order to hold it in tune in case the modulating frequencies of the tuning forks at the transmitting beacon should drift slightly.

Another advantage of the type E indicator is that the resonance frequency of the reeds in this indicator is not altered by their ampli-

tude. It was found that with other types of indicators when the driving force was applied to the free end of the reed the natural period of the reed was a function of the amplitude. This is shown in Figure 15, in which curve No. 1 shows no variation in the resonance frequency of the reed in the type E indicator when the driving force is applied to the fixed end of the reed even up to a deflection of 12 mm.

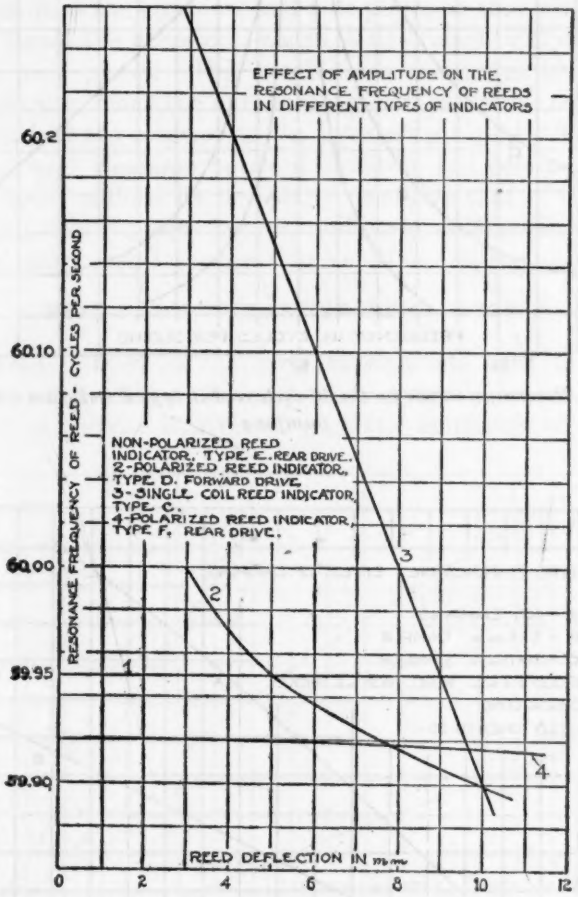

FIG. 15.—*Effect of amplitude of vibration of reeds in different types of indicators*

However, in curve 2, which is for the type D indicator, a change of one-tenth of a cycle was noted for a change in amplitude of the reed from 3 to 10 mm. The period of the reed drops with increasing amplitude. Curve No. 3 for the type C indicator shows an even worse variation. Figure 16 shows the resonance curves for a 60-cycle reed in the type E indicator, with and without damping on the reed. Different voltages were used on the reed coils for each resonance curve.

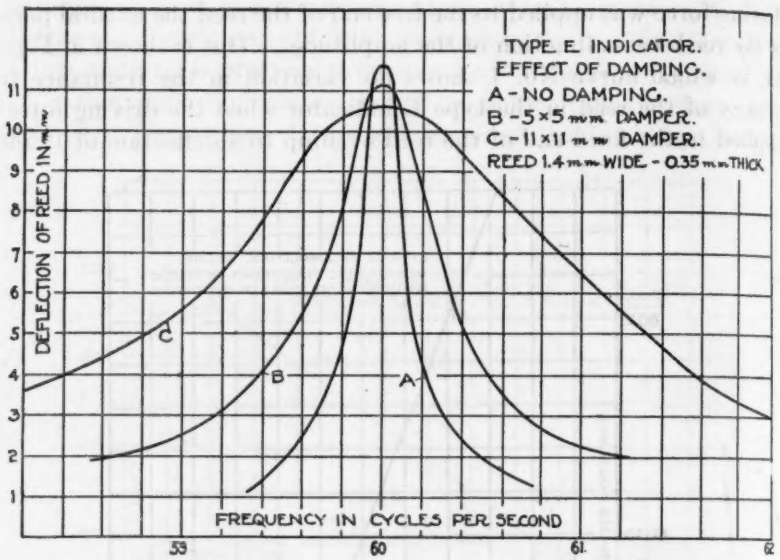

FIG. 16.—*Resonance curves for the 60-cycle reed in type E indicator with different damping*

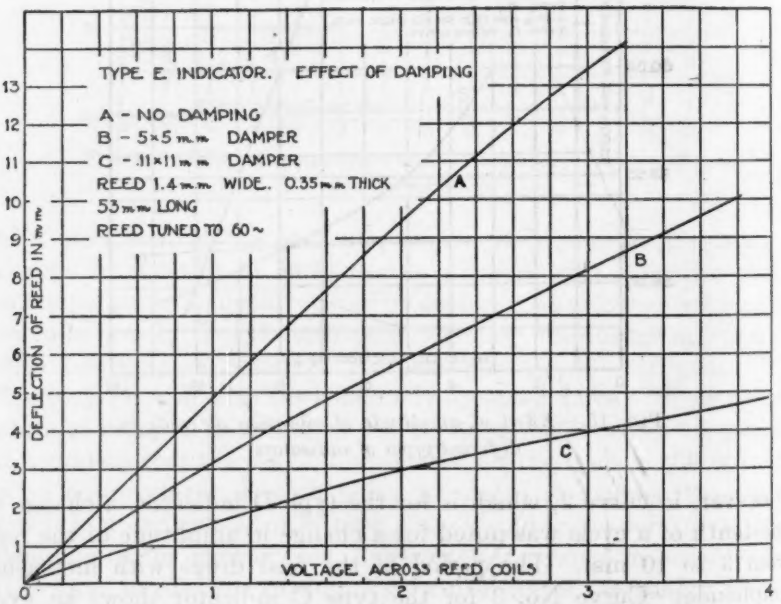

FIG. 17.—*Voltage required to operate 60-cycle reed in type E indicator with different damping*

Figure 17 shows the voltage required to operate the reeds with and without damping.

A disadvantage of this indicator is that, due to the untuned armature, it is not as free from the effects of bad interference as is the other types of indicators.

It is important with the type E indicator to have sufficient spring tension on the spring holding the soft-iron armature and sufficient clearance between the armature and pole pieces so that with a strong interfering signal the armature, which is not tuned, will not chatter against the pole pieces. This trouble can not occur in the other types of indicator, since the only moving element is the reed, which, being tuned, will not respond to the interfering signal. This spring stiffness and large clearance between armature and pole pieces in the type E indicator reduces its sensitivity to nearly that of the type D indicator, but it is requisite in order to obtain satisfactory operation of the reeds under practical operating conditions on the airplane.

6. REAR-DRIVE, POLARIZED REED, TYPE F

It had been noticed in the early experiments with the type A indicator that a permanent magnet, when correctly located near the reed, tended to polarize it, giving it a greater amplitude of vibration.

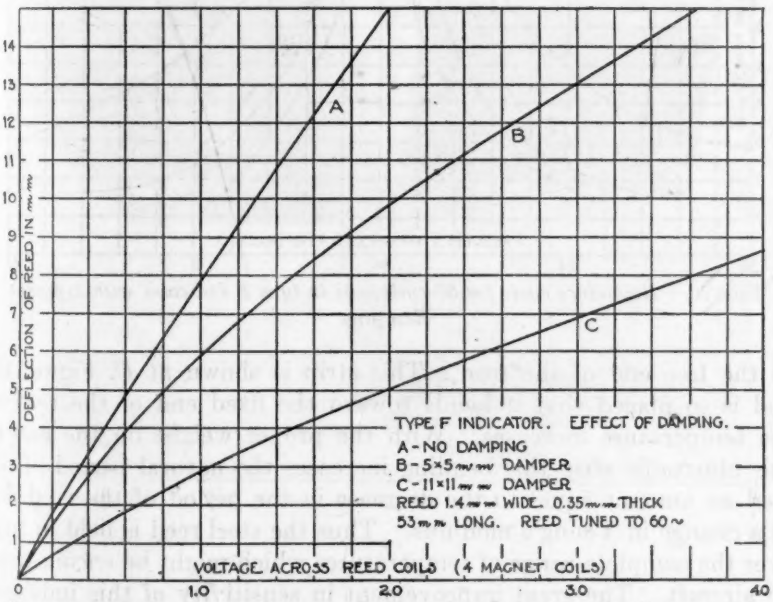
DEFLECTION OF REED IN m/m
VOLTAGE ACROSS REED COILS (4 MAGNET COILS)
A
B
C
TYPE F INDICATOR. EFFECT OF DAMPING.
A - NO DAMPING
B - 5×5 m/m DAMPER
C - 11×11 m/m DAMPER
REED 1.4 m/m WIDE. 0.35 m/m THICK
53 m/m LONG. REED TUNED TO 60 ~

FIG. 19.—*Voltage required to operate 60-cycle reed in type F indicator with different damping*

This feature was made use of in the type F indicator, as shown in Figure 18, in which two permanent magnets, *A* and *B*, strongly

polarize the portion of the reeds directly under the driving electromagnets. These four electromagnets are similar to those used in the types A, D, and E indicators. This greatly increased the sensitivity. In addition to this, since the driving force is applied near the fixed end of the reed, the resonance frequency is practically independent of the amplitude, as shown in curve No. 4. (Fig. 15.) Due to the nature of the drive, being push-pull as in the type A indicator, the selectivity of the type A indicator is preserved in the type F indicator.

Since in this indicator it was necessary to use a magnetic material for the reed in order to polarize it, the metal elinvar could not be used as it is only slightly magnetic. It was found possible to use steel, however, since a method was devised for automatically correcting for the change in natural period of a steel reed due to change in temperature by the use of a small strip of bimetallic material soldered

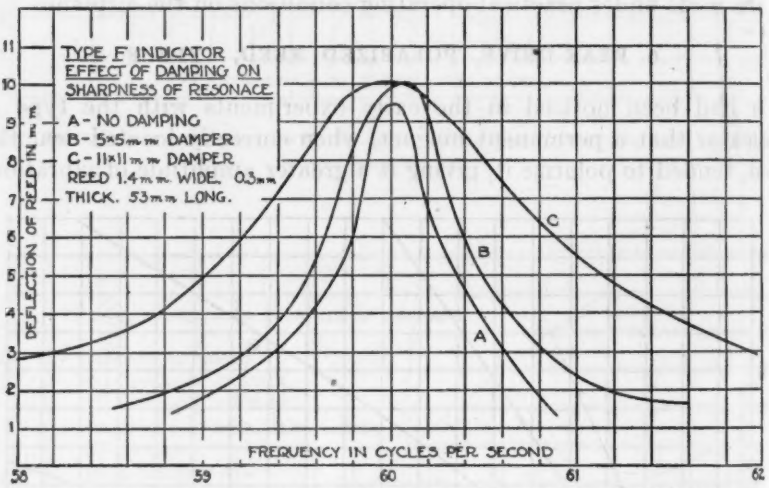

FIG. 20.—*Resonance curve for 60-cycle reed in type F indicator with different damping*

to the free end of the reed. This strip is shown at *C*, Figure 18, and is so placed that it bends toward the fixed end of the reed as the temperature increases. With the proper weight on the end of this bimetallic strip this bending increases the natural period of the reed an amount equal to the decrease in the period of the reed due to a change in Young's modulus. Thus the steel reed is held in tune over the complete range of temperatures which might be encountered on aircraft. The great improvement in sensitivity of this indicator is shown in Figure 19. Figure 19 shows the reed deflection in millimeters plotted against the voltage across the reed driving coils for different sized dampers on the end of the reed. Figure 20 shows the resonance curves for the 60-cycle reed in this indicator under the

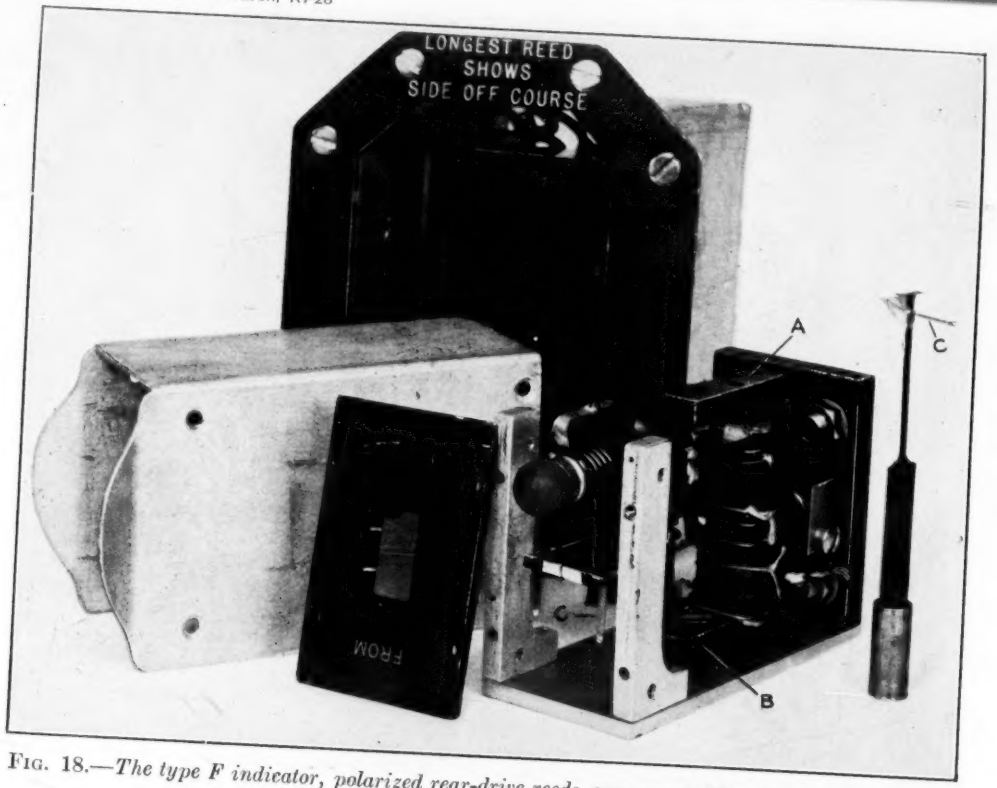

FIG. 18.—*The type F indicator, polarized rear-drive reeds, compensated for effect of temperature*

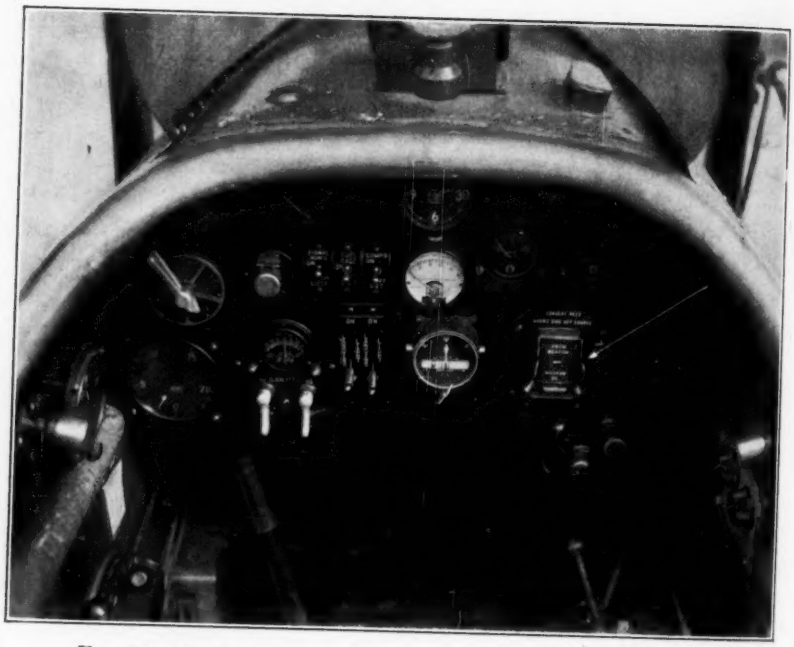

FIG. 21.—*Reed indicator mounted on airplane instrument board*

same conditions of damping. Different voltages were applied to the reed coils for each curve. From Figure 19 it will be seen that even with the greatest damping, which feature, as stated before, is desirable, it is possible to obtain a proper working deflection of 8 mm with only 3.6 volts applied to the reed indicator driving coils and only 1 milliampere in these coils. This is an improvement over the operation of the type E indicator which, as shown in Figure 17, required approximately 7 volts to give the same deflection under the same conditions of damping. Externally the type F indicator looks like the type D indicator shown in Figures 11, 12, and 21. It plugs into the same shock-proof mounting.

IV. CONCLUSION

The results obtained, in general, with the reed indicators in actual airplane flights are given in the paper [2] referred to at the beginning of this paper. Figure 21 shows the visual indicator installed on the instrument board of a De Haviland plane. It is connected in place of the headphones on a 6-tube receiving set installed in the tail of the plane. From the flights made on the radiobeacon course under various conditions, designs of reed indicator and shock-proof mounting were worked out. These flights showed that when ignition interference made aural reception almost impossible the reeds functioned satisfactorily, owing to their insensitivity to any frequency other than that to which they are tuned. For the same reason, other stations, such as the marine beacons, did not interfere with the operation of the reeds, the audio modulation of their signal being 1,000 cycles, while with aural reception trouble was often experienced from this source. One of the most valuable features of the reed indicator is the fact that it gives a continuous indication to the pilot of his position with respect to the course. This indication is obtained without any other effort than a glance of the eye. This feature is particularly valuable, since in time of fog, when the device is most needed, the pilot is very much occupied and can only glance at a course-indicating device occasionally.

The author is indebted to H. Pratt for helpful suggestions in connection with the design of the magnetic circuits in some of the indicators. Acknowledgment is due R. R. Gessford and D. O. Lybrand for constructing the indicator models and for suggestions pertaining to their mechanical design.

WASHINGTON, September 15, 1928.

[2] See footnote 1, p. 752.

THERMAL EXPANSION OF MAGNESIUM AND SOME OF ITS ALLOYS

By Peter Hidnert and W. T. Sweeney

ABSTRACT

This paper gives data on the linear thermal expansion of 6 samples of cast and extruded magnesium and 11 samples of cast and extruded magnesium alloys (magnesium-aluminum and magnesium-aluminum-manganese alloys). The samples of magnesium were investigated over various temperature ranges between −183° and +500° C. and most of the alloys between room temperature and 300° C.

Three types of apparatus were used in this research, and a summary of available data by previous observers on the thermal expansion of magnesium and some magnesium alloys is given.

The following average equation represents the expansion of magnesium between 20° and 500° C.:

$$L_t = L_o\,[1+(24.80\,t+0.00961\,t^2)\,10^{-6}]$$

The coefficients of expansion of extruded magnesium and the alloys investigated are slightly less than those for the cast materials. A comparison of the average expansion curve obtained in the present investigation on magnesium, with data from previous observers, is shown graphically.

The relations between the chemical composition and the coefficients of expansion of the magnesium alloys are shown in a figure. The addition of 0 to 10 per cent aluminum to magnesium causes practically no change in the coefficients of expansion. Small additions of manganese (0.9 and 0.3 per cent) to magnesium and magnesium-aluminum alloys cause slight changes in the coefficients of expansion.

The table in the summary gives a comparison of the average coefficients of expansion of the materials investigated.

CONTENTS

	Page
I. Introduction	772
II. Previous determinations	772
III. Materials investigated	775
IV. Apparatus	775
V. Results	777
1. Magnesium	778
2. Magnesium-aluminum alloys	782
3. Magnesium-aluminum-manganese alloys	788
VI. Summary	791

I. INTRODUCTION

This paper gives the results of an investigation on the linear thermal expansion of pure magnesium, magnesium-aluminum alloys, and magnesium-aluminum-manganese alloys. Magnesium, the lightest structurally used metal, and its alloys are coming into greater prominence for materials of construction where low density and strength are important factors; for example, in aircraft manufacture and for moving parts of gasoline engines.

The earliest available observations on the thermal expansion of magnesium were those by Fizeau in 1869. However, up to the present time no data on the expansion of the alloys mentioned were available.

In the present investigation expansion determinations were made between −183° and +500° C. Six samples of cast and extruded magnesium were examined over various temperature ranges between −183° and +500° C. and 11 specimens of cast and extruded magnesium alloys between room temperature and 400° C. The maximum aluminum content of the magnesium-aluminum alloys is 10.4 per cent, and the maximum aluminum content and maximum manganese content of the magnesium-aluminum-manganese alloys are 4.1 and 0.9 per cent, respectively.

The authors wish to express their appreciation for the cooperation by the American Magnesium Corporation, Niagara Falls, N. Y., and Aluminum Co. of America, New Kensington, Pa. The former furnished the samples of magnesium and magnesium alloys and information about the preparation, and the latter company analyzed the samples used in the investigation. Acknowledgment is due to H. W. Bearce, Wilmer Souder, and H. W. Gillett, of the Bureau of Standards, and J. D. Edwards, of the Aluminum Co. of America, for valuable suggestions.

II. PREVIOUS DETERMINATIONS

The results obtained by previous observers on the thermal expansion of magnesium and some magnesium alloys are summarized in Table 1. In this table, a_t represents the instantaneous coefficient or rate of expansion at $t°$ C., L_t represents the length at $t°$ C., and L_0 the length at 0° C. For additional information the reader should refer to the original papers.

TABLE 1.—*Summary of expansion data on magnesium and magnesium alloys by previous observers*

TABLE 1.—*Summary of expansion data on magnesium and magnesium alloys by previous observers*

Observer	Date	Material	Temperature or temperature range	Coefficient of linear expansion per °C.	Expansion equation	Remarks
			°C.	$\times 10^{-6}$		
Fizeau [1]	1869	Magnesium	40	26.94		
			0 to 100	27.62		
Voigt [2]	1893	do	15.4	25.15	$\alpha_t=[26.05+0.064(t-30)]10^{-6}$ between 15° and 40° C.	
			16.5	25.16		
			32.3	26.26		
			33.0	26.15		
			40.0	26.73		
Stadthagen [4]	1901	Magnalium [5]	12 to 39	23.8		Aluminum-base alloy with about 13 per cent magnesium. (The average coefficient of expansion of pure aluminum [3] is 23.1×10^{-6} for the same temperature range.)
Grüneisen [6]	1910	Magnesium [7]	−183 to 15	21.40		The expansion was determined by comparison with the expansion of platinum. The accuracy is approximately 1 per cent. For two temperature ranges Grüneisen [8] showed that the ratio of the average coefficient of expansion and the average specific heat is approximately constant.
			+17 to 100	26.07		
			19 to 100	26.09		
Hidnert [9]	1919	Magnesium [10] (cast)	−40	24.3	$L_t=L_0[1+(25.03t+0.00892t^2)10^{-6}]$ between −63° and +300° C.	The probable error of L_t is ±0.000007 L_0. The observations on cooling lie below the expansion curve on heating. At the end of the test the specimen was 0.01 per cent shorter than at the beginning.
			−20	24.7		
			0	25.0		
			+20	25.4		
			40	25.7		
			60	26.1		
			80	26.5		
			100	26.8		
			120	27.2		
			140	27.5		
			160	27.9		
			180	28.2		
			200	28.6		
			220	29.0		
			240	29.3		
			260	29.7		
			280	30.0		
Souder and Hidnert [11]	1919	Dow metal [12]	20 to 400	27.0		
Hodgman [13]	1920	Magnesium (cast)	20 to 100	26.86		
		Magnesium (wrought)	20 to 100	26.73		

Footnotes at end of table.

TABLE 1.—*Summary of expansion data on magnesium and magnesium alloys by previous observers*—Continued

Observer	Date	Material	Temperature or temperature range	Coefficient of linear expansion per °C.	Expansion equation	Remarks
			°C.	$\times 10^{-6}$		
Disch [14]	1921	Magnesium [15]	20 to 100	[16] 25.9	$L_t = L_0[1+(25.07t+0.00936t^2)10^{-6}]$ between 20° and 500° C.	The expansion equation was derived by Scheel from the data by Disch and Schulze.
			20 to 200	[16] 27.1		
			20 to 300	[16] 28.2		
			20 to 400	[16] 29.0		
			20 to 500	[16] 29.9		
Schulze [14]	1921	....do.[17]	20 to 100	[16] 25.6		
			20 to 200	[16] 26.9		
			20 to 300	[16] 28.3		
			20 to 400	[16] 29.0		
			20 to 500	[16] 30.0		
Disch [18]	1921	Electron [19] metal	0 to 100	[16] 28.4	$L_t = L_0[1+(28.24t+0.00165t^2)10^{-6}]$ between 0° and 300° C.	
			0 to 200	[16] 28.6		
			0 to 300	[16] 28.7		
Jubitz [20]	1926					For the range from 20° to 40° C. the expansion of worked magnesium (drawn from 10 to 5.5 mm. diameter at 200° C.) is slightly less than the expansion of cast magnesium.
Portevin and Le Chatelier.[21]	1926	Magnesium alloys [22]				The thermal expansion of magnesium alloys is nearly equal to that for pure magnesium. It is increased by the addition of zinc and lead and decreased by copper, nickel, and especially silicon. The expansion of magnesium is also decreased by the addition of aluminum, if the aluminum content is less than the limit of the solid solution. No quantitative data on expansion were given.

[1] Fizeau, Comp. Rend., **68**, p. 1125; 1869; or Pogg. Ann. d. Physik u. Chem., **18** (138), p. 26; 1869.
[2] Voigt, Wiedemann Annalen der Physik und Chemie, **49**, p. 697; 1893.
[3] Hidnert, B. S. Sci. Paper No. 497 (**19**, p. 697; 1925).
[4] Stadthagen, Deutsche Mech.-Ztg., p. 21; 1901.
[5] Al 85.89, Mg 12.71, Si 0.71, Fe 0.46, Cu 0.08 per cent. Density 2.538.
[6] Grüneisen, Annalen der Physik, **33**, p. 33; 1910.
[7] From C. A. F. Kahlbaum (in Germany).
[8] Grüneisen, Annalen der Physik, **33**, p. 65; 1910.
[9] Hidnert, Thesis, George Washington University; 1919.
[10] Mg 99.89, Cu 0.03, Fe 0.08, Chlorides trace, Si, C, Pb, Sn, Zn, Ca, K not detected; other elements present in not more than traces. The density of the sample before the investigation was 1.737 g/cm³ at 20° C.
[11] Unpublished data obtained at the Bureau of Standards in 1919.
[12] Magnesium alloy from Dow Chemical Co., Midland, Mich. The company states that this sample had a calculated composition of approximately 8.5 per cent aluminum, with the balance magnesium.
[13] Hodgman, Physical Review, **15**, p. 218; 1920.
[14] Scheel, Zeitschrift für Physik, **5**, p. 167; 1921.
[15] Temperature coefficient of electrical resistance at 20° C., 3.8 to 3.9×10^{-3}.
[16] Computed from data given by observer.
[17] Same material as used by Disch.
[18] Disch, Zeitschrift für Physik, **5**, p. 173; 1921.
[19] From Chemischen Fabrik Griesheim-Elektron, Frankfurt a. M., Germany. Disch states that electron is an aluminum-magnesium alloy. For additional information consult B. S. Circular No. 346, p. 302.
[20] Jubitz, Zeitschrift für Technische Physik, **7**, p. 522; 1926.
[21] Portevin and Le Chatelier, Comptes Rendus, **182**, p. 382; 1926.
[22] Determinations were made on samples in the drawn and annealed state. The maximum contents of the metals added to magnesium were as follows: Al 7, Cd 6, Cu 13, Mn 4, Ni 15, Pb 5, Si 1.5, and Zn 5 per cent.

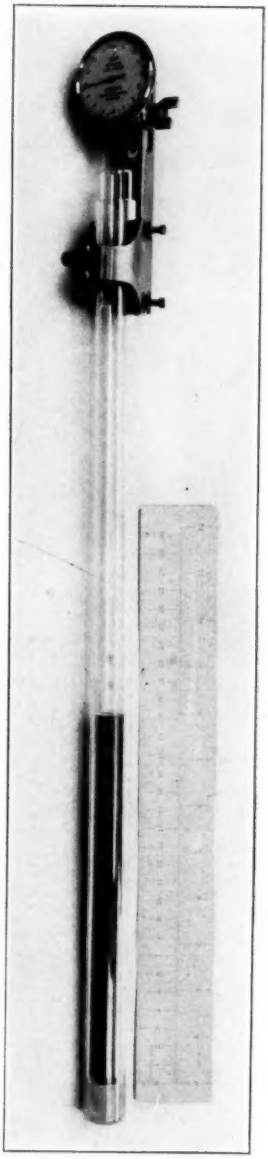

FIG. 1.—*Fused quartz tube expansion apparatus*

[2] Magnesium alloy from Dow Chemical Co., Midland, Mich. The company states that this sample had a calculated composition of approximately 8.5 per cent aluminum, with the balance magnesium.

FIG. 2.—*Fused quartz tube expansion apparatus and auxiliary equipment*

III. MATERIALS INVESTIGATED

The samples investigated are classified into three groups, as given in Table 2. This table also gives the chemical composition of the samples of magnesium and magnesium alloys.

The pure magnesium and the magnesium content of the alloys were of exceptional purity. The magnesium was made by the electrolysis of magnesium oxide dissolved in a fused fluoride bath and was subsequently purified by the sublimation process developed by H. E. Bakken, United States Patent 1594344, August 3, 1926.

TABLE 2.—*Chemical composition of magnesium and magnesium alloys*

Material	Sample	Chemical analyses [1]						Treatment
		Magnesium [2]	Aluminum	Manganese	Silicon	Iron	Copper	
		Per cent	*Per cent*	*Per cent*	*Per cent*	*Per cent*	*Per cent*	
Magnesium	1268A	99.996	([3])	([3])	0.002	<0.001	<0.001	Extruded at 410° C.
	1269	99.99	0.00	0.00	.000	.005	.002	Cast in vacuum furnace at 665° C.
	1269 I [4]							
	1270	99.97	.02	.00	.004	.007	.002	Extruded at 425° C.
	1270A [5]							
Magnesium-aluminum alloys.	1271	95.61	4.36	.00	.004	.018	.007	Extruded at 350° C.
	1272	95.52	4.44	.00	.018	.020	.006	Cast in vacuum furnace at 680° C.
	1273	93.70	6.26	.00	.008	.026	.008	Extruded at 330° C.
	1274	93.73	6.22	.00	.018	.024	.009	Cast in vacuum furnace at 680° C.
	1275	89.58	10.35	.00	.016	.040	.016	Extruded at 330° C.
	1276	89.75	10.19	.00	.014	.034	.008	Cast in vacuum furnace at 680° C.
	1277	90.14	9.75	.00	.068	.033	.012	Extruded at 330° C., held at 425° C. for 8 hours, quenched, and then aged at 175° C. for 72 hours.
	1277A	89.84	10.04	.00	.076	.033	.010	
Magnesium-aluminum-manganese alloys.	1278	95.58	4.10	.27	.014	.025	.011	Extruded at 390° C.
	1279	95.53	4.14	.27	.018	.029	.009	Cast in vacuum furnace at 690° C.
	1280	99.05	.01	.91	.004	.020	.003	Cast at 670° C.

[1] The analysis on sample 1268A was made by J. P. Hancock, of this bureau, and the analyses on the other samples were made by the technical direction bureau, Aluminum Co. of America.
[2] Per cent magnesium determined by difference.
[3] Not detected.
[4] Duplicate of sample 1269.
[5] Duplicate of sample 1270.

IV. APPARATUS

Three types of equipment were used in this research, namely: (*a*) Precision comparator;[1] (*b*) interferometer;[2] (*c*) fused-quartz tube.

Types (*a*) and (*b*) are described in previous bureau publications. A short description of (*c*) follows:

A fused-quartz-tube apparatus was used in some determinations of the expansion of magnesium between −183° and +20° C. The authors have improved this type of apparatus from a similar type

[1] Souder and Hidnert, B. S. Sci. Paper No. 524 (**21**, p. 1; 1926).
[2] Peters and Cragoe, B. S. Sci. Paper No. 393 (**16**, p. 449; 1920).

used abroad and recommend this type for commercial laboratories where data of the highest precision are not necessary. With this equipment, which has been used for various temperature ranges between −183° and +1,000° C., it is possible to obtain an accuracy of better than 2 per cent. A short description of the equipment appeared in Technical News Bulletin of the Bureau of Standards No. 123, page 2; 1927.

Figure 1 shows a fused-quartz tube closed at one end, with a sample (20 cm) in place ready for heating or cooling. A movable

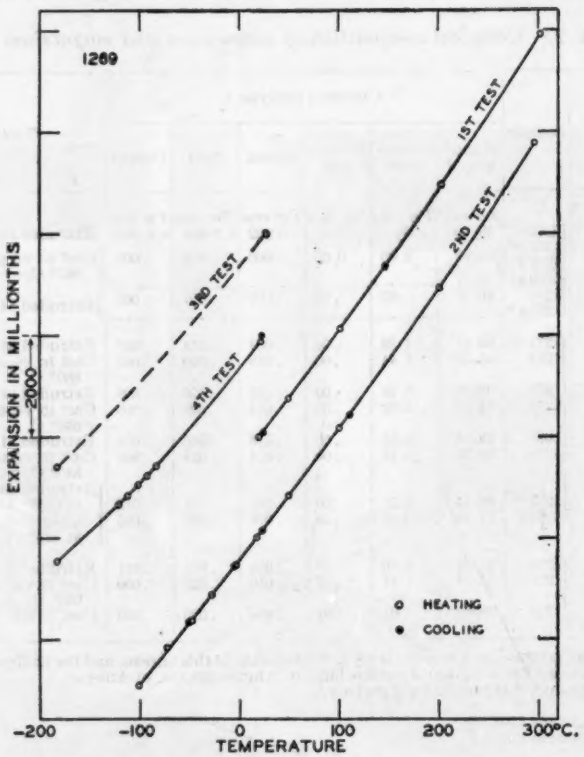

FIG. 3.—*Linear thermal expansion of cast magnesium (99.99 per cent) from −183° to +300° C.*

fused-quartz rod rests on top of the sample and extends above the open end of the tube. The bottoms of the tube and the movable rod are ground concave and the ends of the sample convex in order to secure satisfactory contacts. The top of the movable rod, on which an indicator gauge rests, is flat. Heating is effected by placing the tube containing the sample in a water or oil bath or electrical furnace (fig. 2) extending well above the top of the sample. Low temperatures are secured by using proper cooling baths. In the

present investigation liquid oxygen was used. A thermocouple placed inside the fused-quartz tube near the center of the sample indicates the temperature. An indicator gauge fastened near the top of the tube registers the differential expansion between the sample and an equivalent length (20 cm) of fused quartz. A small correction for the expansion [3] of fused quartz is made.

Figures 1 and 2 show the fused-quartz-tube apparatus and auxiliary equipment.

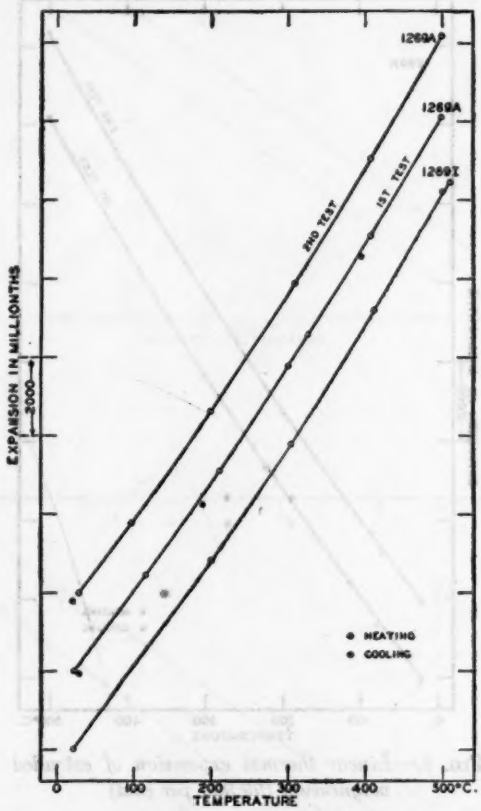

FIG. 4.—*Linear thermal expansion of cast magnesium (99.99 per cent) from 20° to 500° C.*

V. RESULTS

The results obtained on magnesium, magnesium-aluminum alloys, and magnesium-aluminum-manganese alloys are given in the following subsections. The expansion curves of all samples investigated are shown in figures. In all cases the coefficients of expansion were derived from the observations on heating.

[3] Souder and Hidnert, B. S. Sci. Paper No. 524 (21, p. 1; 1926).

1. MAGNESIUM

The linear thermal expansion of six samples of magnesium containing about 99.99 per cent magnesium were investigated over various temperature ranges between −183° and +500° C. Since preliminary work on small pieces of magnesium showed that this metal oxidized in air at about 550° C., the maximum temperature of the expansion tests did not exceed this temperature.

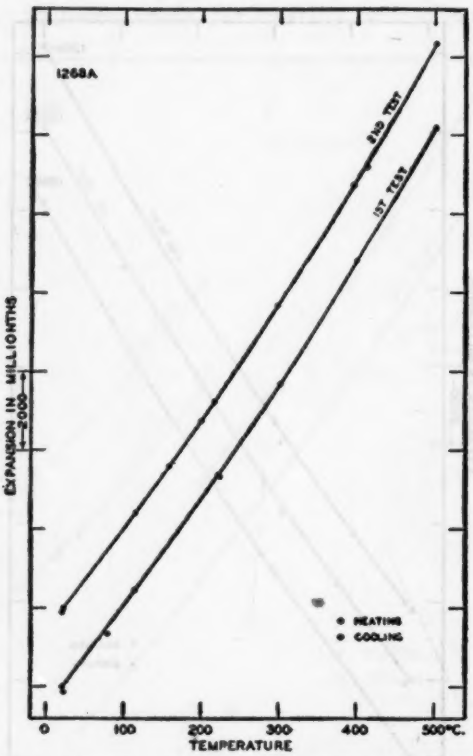

FIG. 5.—*Linear thermal expansion of extruded magnesium (99.996 per cent)*

The results obtained on cast and extruded magnesium are shown in Figures 3 to 7, inclusive. The coefficients of expansion which were derived from the expansion curves are given in Table 3. The last column in this table shows the differences in length before and after the expansion tests. The plus (+) sign indicates an increase in length and the minus (−) sign a decrease in length.

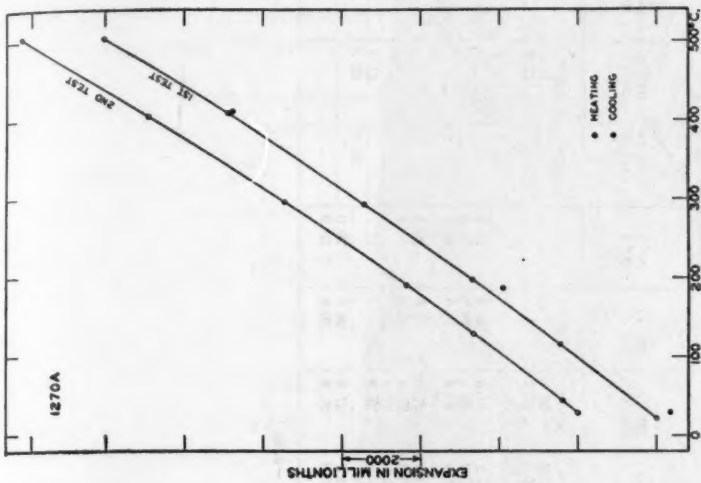

FIG. 7.—*Linear thermal expansion of extruded magnesium (99.97 per cent) from 20° to 500° C.*

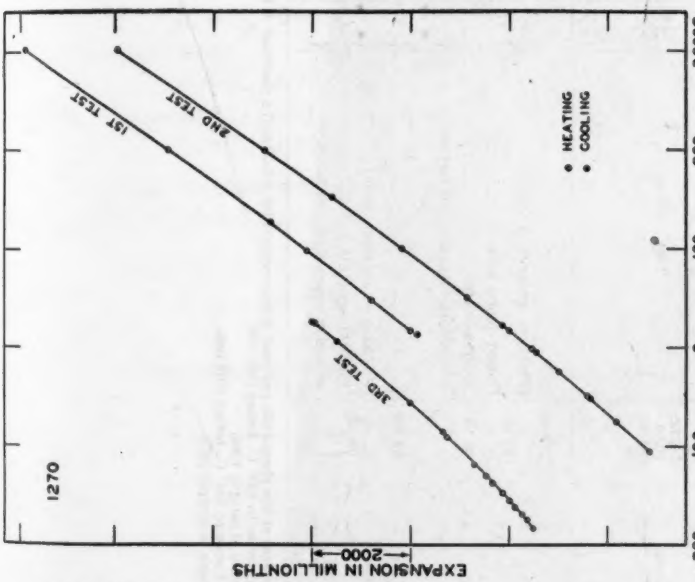

FIG. 6.—*Linear thermal expansion of extruded magnesium (99.97 per cent) from −183° to +300° C.*

TABLE 3.—*Average coefficients of expansion and length changes of magnesium*

Sample	Magnesium content	Test method	Test No.	Average coefficients of expansion per °C.								Change [1] in length due to heat treatment received during test
				20° to 100° C.	20° to 200° C.	20° to 300° C.	20° to 400° C.	20° to 500° C.	−183° to −100° C.	−100° to +20° C.	−183° to +20° C.	
	Per cent			×10⁻⁶	×10⁻⁶	×10⁻⁶	×10⁻⁶	×10⁻⁶	×10⁻⁶	×10⁻⁶	×10⁻⁶	*Per cent*
Cast:												
1269	99.99	Precision comparator (bath)	1	26.1	27.0	28.1						0.00
			2	26.0	27.0	27.9				24.9		.00
		Fused-quartz tube	[2] 3								21.9	.00
			4						18.6	23.1	21.2	−.01
1269 I	99.99	Interferometer	1		27.2	27.8	28.8	29.8				
1269A [3]		Precision comparator (air furnace)	1	26.6	27.0	28.1	28.8	29.6				−.02
			2	26.0	27.0	27.9	29.0	30.1				+.00
Extruded:												
1268A	99.996	do	1	26.4	26.7	27.5	28.6	29.6				−.01
			2	26.2	26.9	27.9	28.9	29.9				−.00
1270	99.97	Precision comparator (bath)	1	26.0	26.9	27.8						−.00
			2	26.0	27.1	27.9				23.5		.00
		Fused-quartz tube	[4] 3						18.5	23.2	21.3	−.00
1270A [5]		Precision comparator (air furnace)	1	26.3	26.7	27.4	28.0	29.0				−.06
			2	26.4	27.0	27.8	28.9	29.9				.00

[1] An increase of less than 0.005 per cent is represented by +0.00 and a decrease of less than 0.005 by −0.00.
[2] Heated twice to 500° C. before this test.
[3] Duplicate of sample 1269.
[4] Heated once to 500° C. before this test.
[5] Duplicate of sample 1270.

Table 4 gives expansion equations for samples 1269, 1269 I, 1269A, and 1268A. These equations were derived, by the method of least squares, from the observations on heating. ΔL represents the expansion or change in length from 20° C. to any temperature t between 20° and 500° C., L_t represents the length of the metal at any temperature t between 20° and 500° C., and L_o the length at 0° C.

TABLE 4.—*Expansion equations of magnesium*

Sample	Test No.	Expansion equations	Probable error of ΔL or L_t
Cast:			
1269, 1269 I, 1269A	1	$\Delta L=25.50\ (t-20)\ 10^{-6}+0.00871\ (t-20)^2\ 10^{-6}$ $L_t=L_o\ [1+(25.15\ t+0.00871\ t^2)\ 10^{-6}]$	$\times L_o$ ±0.000022
1269, 1269A	2	$\Delta L=25.15\ (t-20)\ 10^{-6}+0.01021\ (t-20)^2\ 10^{-6}$ $L_t=L_o\ [1+(24.74\ t+0.01021\ t^2)\ 10^{-6}]$	±.000007
Extruded:			
1268A	1	$\Delta L=24.85\ (t-20)\ 10^{-6}+0.00982\ (t-20)^2\ 10^{-6}$ $L_t=L_o\ [1+(24.46\ t+0.00982\ t^2)\ 10^{-6}]$	±.000025
1268A	2	$\Delta L=25.26\ (t-20)\ 10^{-6}+0.00971\ (t-20)^2\ 10^{-6}$ $L_t=L_o\ [1+(24.87\ t+0.00971\ t^2)\ 10^{-6}]$	±.000016

The following average equations may be given as the most probable second-degree equations for the expansion of cast magnesium and extruded magnesium between room temperature and 500° C.:

Cast magnesium:

$$L_t=L_o\ [1+(24.94\ t+0.00946\ t^2)\ 10^{-6}] \quad (1)$$

Extruded magnesium:

$$L_t=L_o\ [1+(24.66\ t+0.00976\ t^2)\ 10^{-6}] \quad (2)$$

Average of equations (1) and (2):

$$L_t=L_o\ [1+(24.80\ t+0.00961\ t^2)\ 10^{-6}] \quad (3)$$

The average coefficients of expansion for various temperature ranges given in Table 5 were computed from equations (1), (2), and (3).

TABLE 5.—*Average coefficients of expansion of magnesium*

Temperature range (in °C.)	Average coefficient of expansion per °C.		
	Cast magnesium	Extruded magnesium	Average
	$\times 10^{-6}$	$\times 10^{-6}$	$\times 10^{-6}$
20 to 100	26.1	25.8	26.0
100 to 200	27.8	27.6	27.7
200 to 300	29.7	29.5	29.6
300 to 400	31.6	31.5	31.5
400 to 500	33.5	33.4	33.4
20 to 200	27.0	26.8	26.9
20 to 300	28.0	27.8	27.9
20 to 400	28.9	28.8	28.8
20 to 500	29.9	29.7	29.8

The coefficients of expansion of extruded magnesium are slightly less than those for cast magnesium. Jubitz [4] also found that worked magnesium expands slightly less than cast magnesium. The largest variation in the coefficients given in Table 5 is 0.3×10^{-6}.

The instantaneous coefficients or rates of expansion of cast magnesium and extruded magnesium from 0° to 500° C. are shown in Figure 8. The coefficients increase with temperature. The greatest variation (0.3×10^{-6}) in the rates of expansion of the cast and extruded metal occurs at 0° C. Above this temperature the variation decreases with temperature.

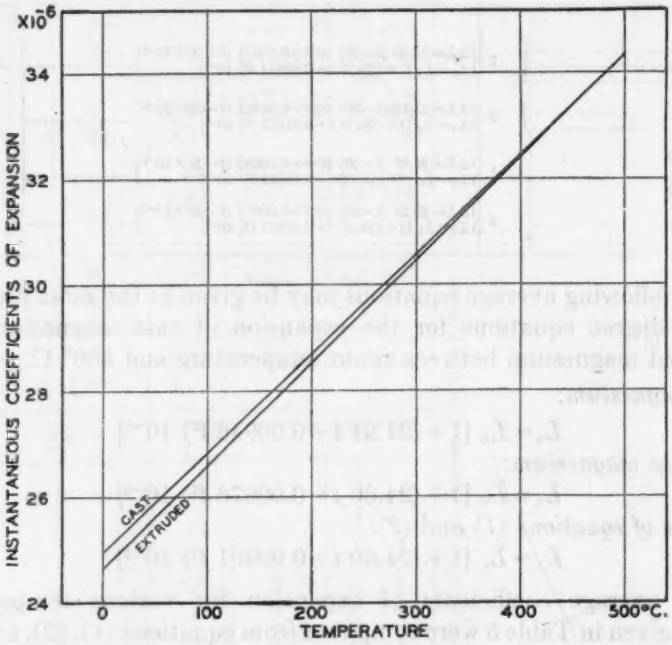

FIG. 8.—*Instantaneous coefficients of expansion of magnesium*

Figure 9 shows a comparison of the average expansion curve obtained in the present investigation on magnesium, with data from previous observers. The curve was derived from equation (3) and the data at low temperatures. The values of nearly all observers show good agreement.

2. MAGNESIUM-ALUMINUM ALLOYS

Eight samples of magnesium-aluminum alloys containing various percentages of aluminum (4 to 10 per cent) were investigated. Al samples except 1277A were investigated by the precision-comparator

[4] See Table 1, p. 773.

method (bath) from room temperature to 300° C. The interference method was used for sample 1277A from room temperature to 400° C.

Figures 10 to 13, inclusive, show the observations obtained on the magnesium-aluminum alloys. The expansion curves of all samples except 1277 and 1277A are regular. The curves for samples 1277 and 1277A which received special heat treatment,[5] show critical regions above 200° C.

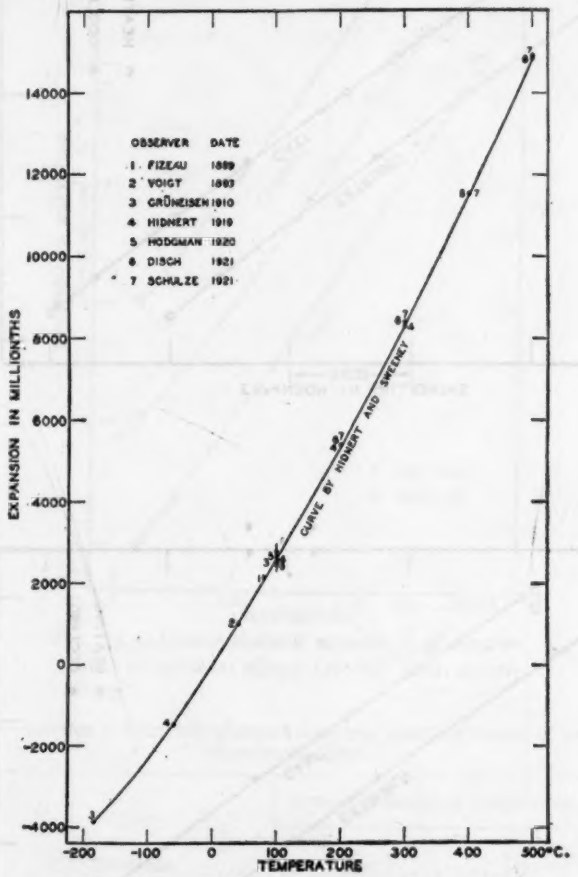

FIG. 9.—*Comparison of the average expansion curve obtained in the present investigation on magnesium with data from previous observers*

The average coefficients of expansion given in Table 6 were derived from the expansion curves of the magnesium-aluminum alloys. This table also indicates the differences in length before and after the expansion tests. The plus (+) sign signifies an increase in length and the minus (−) sign a decrease in length.

[5] Extruded at 330° C., held at 425° C. for 8 hours and quenched, and then aged at 175° C. for 72 hours.

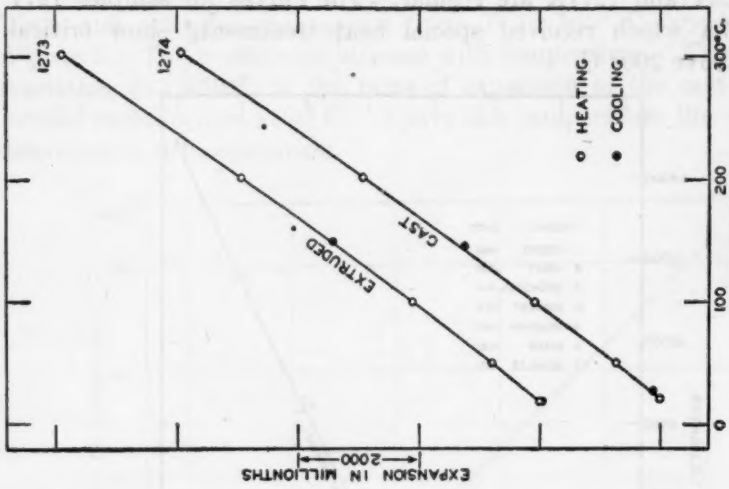

FIG. 11.—*Linear thermal expansion of magnesium-aluminum alloys (6 per cent aluminum)*

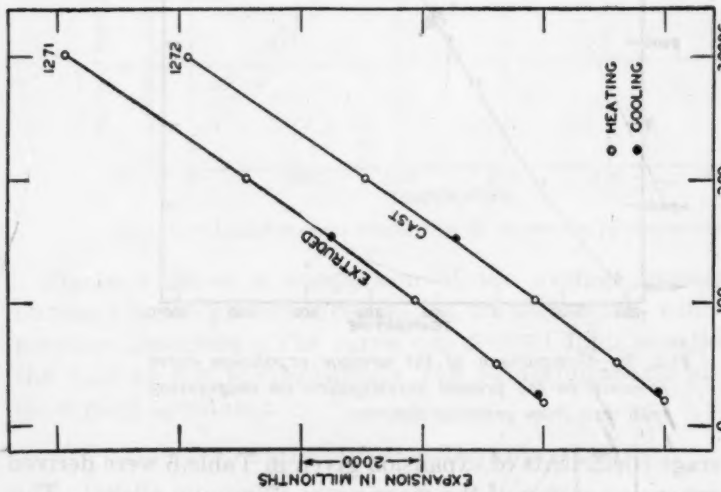

FIG. 10.—*Linear thermal expansion of magnesium-aluminum alloys (4 per cent aluminum)*

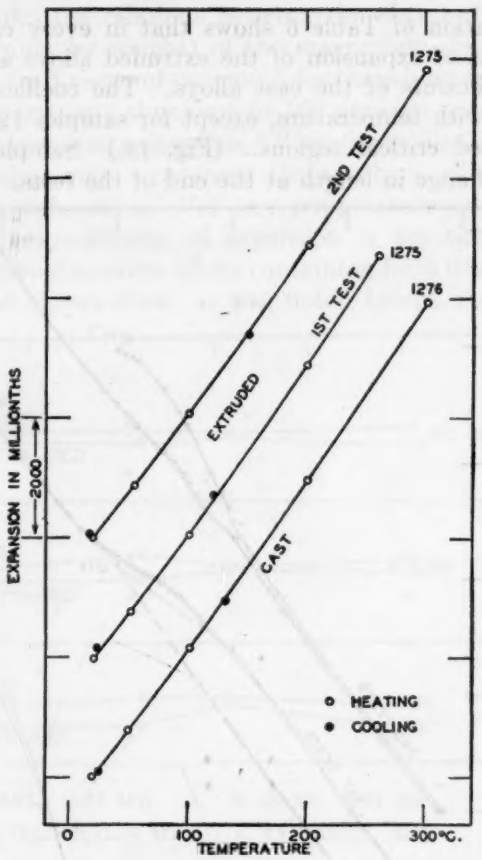

FIG. 12.—*Linear thermal expansion of magnesium-aluminum alloys (10 per cent aluminum)*

TABLE 6.—*Average coefficients of expansion and length changes of magnesium aluminum alloys*

Sample	Aluminum content	Treatment	Average coefficients of expansion per °C.						Change in length due to heat treatment received during test
			20° to 50° C.	20° to 100° C.	20° to 200° C.	20° to 300° C.	200° to 300° C.	300° to 400° C.	
	Per ct.		$\times 10^{-6}$	$\times 10^{-6}$	$\times 10^{-6}$	$\times 10^{-6}$	$\times 10^{-6}$	$\times 10^{-6}$	*Per ct.*
1272	4.44	Cast in vacuum furnace at 680° C.	25.9	26.4	27.4	28.0	------	------	−0.01
1271	4.36	Extruded at 350° C	25.5	25.8	26.9	27.8	------	------	−.01
1274	6.22	Cast in vacuum furnace at 680° C.	25.3	26.4	27.2	28.0	------	------	−.00
1273	6.26	Extruded at 330° C	26.0	26.2	27.1	27.9	------	------	−.00
1277	9.75	Extruded at 330° C., held at 425° C. for 8 hours, quenched, and then aged at 175° C. for 72 hours.	25.3	25.4	26.5	------	14.4	------	−.14
			------	[1] 25.7	27.8	------	29.8	------	+.04
1277A	10.04	Same as 1277	------	26.0	26.1	------	17.0	21.7	------
			------	[1] 25.8	26.9	------	22.6	26.1	------
1276	10.19	Cast in vacuum furnace at 680° C.	25.3	26.2	27.3	28.1	------	------	−.00
1275	10.35	Extruded at 330° C	24.9	25.9	27.2	[2] 28.3	------	------	+.01
			[1] 24.7	25.6	26.9	27.7	------	------	+.01

[1] Values on this horizontal line were obtained on a second heating. [2] From 20° to 250° C.

An examination of Table 6 shows that in every case except one the coefficients of expansion of the extruded alloys are slightly less than the coefficients of the cast alloys. The coefficients of expansion increase with temperature, except for samples 1277 and 1277A, which indicated critical regions. (Fig. 13.) Sample 1277 showed the greatest change in length at the end of the tests.

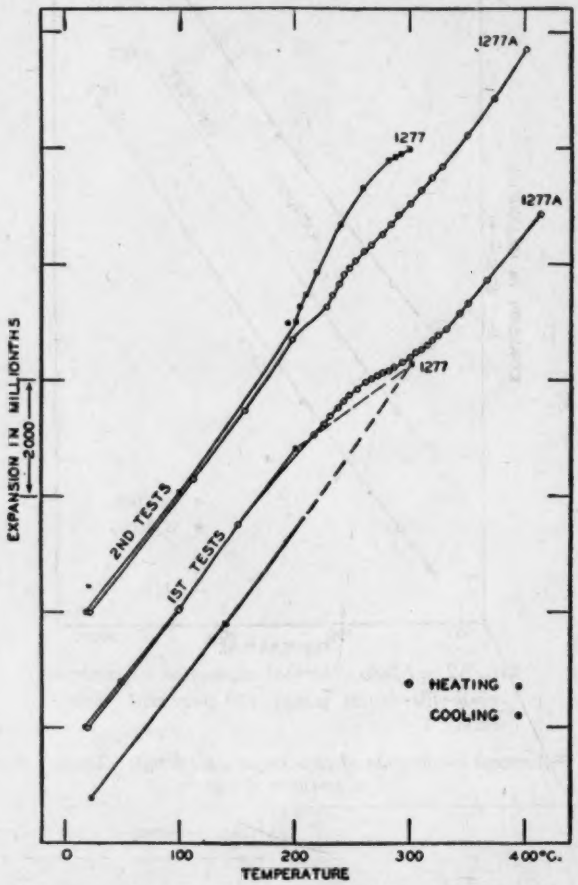

FIG. 13.—*Linear thermal expansion of magnesium-aluminum alloys (10 per cent aluminum)*

Extruded at 330° C., held at 425° C. for 8 hours, quenched and then aged at 175° C. for 72 hours

It is interesting to note that for the range from 20° to 300° C. the coefficients of expansion of these magnesium-aluminum alloys are practically the same as the coefficients of expansion of aluminum-copper alloys [6] containing from 4 to 12 per cent copper. From the point of view of expansion there is therefore no gain or loss in substituting magnesium-aluminum alloys for aluminum-copper alloys used in pistons.

[6] Hidnert, B. S. Sci. Paper No. 497 (19, p. 697; 1925).

Figure 14 shows the relations between the chemical composition (per cent aluminum by weight) of the magnesium-aluminum alloys and the average coefficients of expansion for three temperature ranges. The values for 0 per cent aluminum or 100 per cent magnesium were taken from the previous subsection. This figure also includes data on magnesium-aluminum-manganese alloys, which will be discussed in the following subsection. For any temperature range indicated in the figure, the coefficient of expansion is practically constant for the magnesium-aluminum alloys containing from 0 to 10 per cent aluminum. The curves show, as was noted before, that the coeffi-

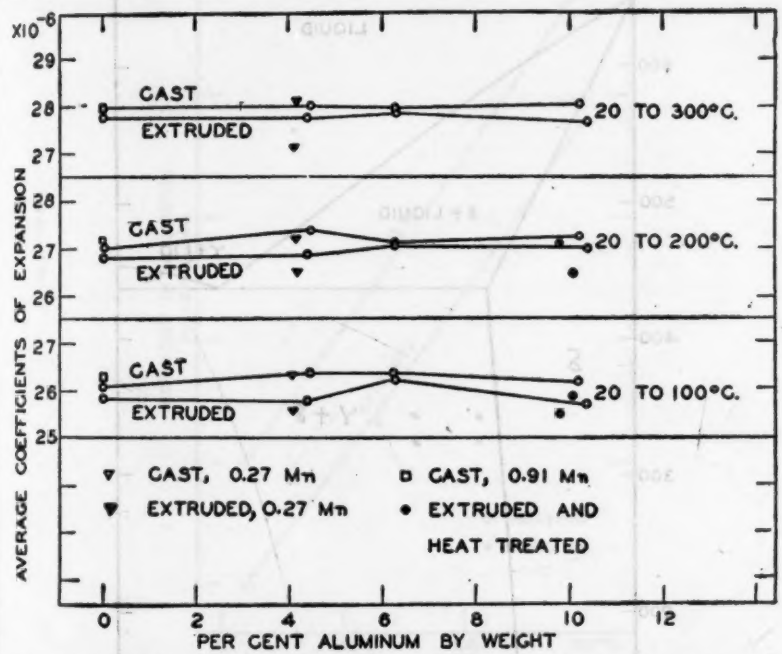

FIG. 14.—*Relations between the aluminum content and the coefficients of expansion of magnesium-aluminum alloys, and some effects of small additions of manganese to these alloys*

cients of expansion of the extruded magnesium-aluminum alloys are slightly less than the coefficients of the cast alloys.

For a comparison of the constitution of the magnesium-aluminum alloys and the coefficients of expansion the reader should refer to Figures 14 and 15. The latter figure shows a portion of the magnesium-aluminum equilibrium diagram determined by Hanson and Gayler.[7] According to the diagram, magnesium retains about 11 per cent aluminum in solid solution at 435° C. and the solubility decreases slightly as the temperature falls. Experiments [8] conducted by the Aluminum Co. of America indicate that the solubility de-

[7] Hanson and Gayler, J. Inst. of Metals (London), **24** (No. 2), p. 201; 1920.
[8] Handbook on Magnesium, American Magnesium Corporation.

creases more rapidly with falling temperature than is indicated by the diagram of Hanson and Gayler. The phase δ is a solid solution of aluminum in magnesium, and γ is the next phase produced by the addition of aluminum to δ. Opportunity for heat treatment by solution quenching and precipitation hardening exists in magesium-aluminum alloys containing about 10 per cent aluminum. (See fig. 13.) The relation between the chemical composition and the

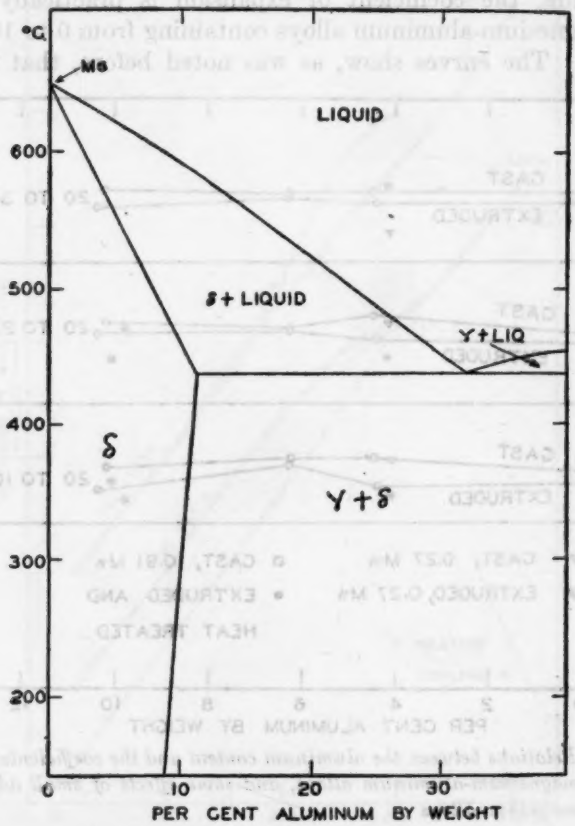

FIG. 15.—*Equilibrium diagram of magnesium-aluminum alloys (after Hanson and Gayler)*

coefficients of expansion for each temperature range shown in Figure 14 is approximately linear.

3. MAGNESIUM-ALUMINUM-MANGANESE ALLOYS

Three samples of magnesium-aluminum-manganese alloys containing less than 1 per cent manganese were investigated by the precision-comparator method (bath) from room temperature to 300° C.

Figures 16 and 17 show the observations. The expansion curves of these alloys are regular.

Table 7 gives the average coefficients of expansion which were derived from the expansion curves of the magnesium-aluminum-manganese alloys. This table also indicates the differences in length before and after the expansion tests. The minus (−) sign signifies a decrease in length.

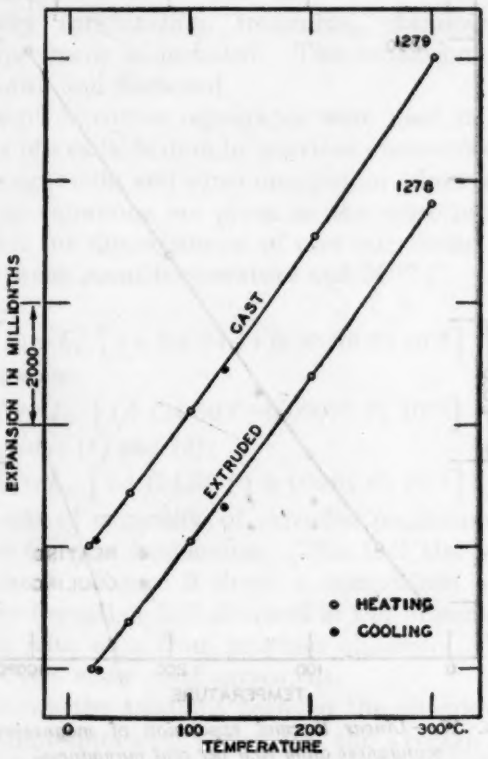

FIG. 16.—*Linear thermal expansion of magnesium-aluminum-manganese alloys (4.1 per cent aluminum and 0.3 per cent manganese)*

TABLE 7.—*Average coefficients of expansion and length changes of magnesium-aluminum-manganese alloys*

Sample	Content		Treatment	Average coefficients of expansion per °C.				Change in length due to heat treatment received during test
	Aluminum	Manganese		20° to 50° C.	20° to 100° C.	20° to 200° C.	20° to 300° C.	
	Per cent	*Per cent*		×10⁻⁶	×10⁻⁶	×10⁻⁶	×10⁻⁶	*Per cent*
1279	4.14	0.27	Cast in vacuum furnace at 690° C.	26.1	26.6	27.3	28.1	−0.01
1278	4.10	.27	Extruded at 390° C	24.9	25.6	26.4	27.2	−.02
1280	.01	.91	Cast at 670° C	26.0	26.3	27.2	27.9	−.01

The coefficients of expansion of the magnesium-aluminum-manganese alloys increase with temperature. The coefficients of the extruded alloy containing about 4 per cent aluminum and 0.3 per cent manganese are less than the coefficients of the corresponding cast alloy. The greatest deviation in the coefficients shown in the table is 1.2×10^{-6}.

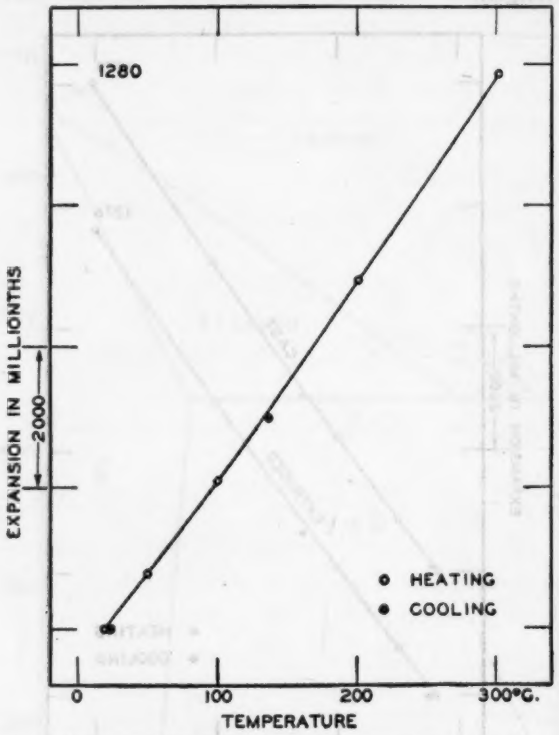

FIG. 17.—*Linear thermal expansion of magnesium-manganese alloy (0.9 per cent manganese)*

Data on the magnesium-aluminum-manganese alloys are shown in Figure 14 of the preceding subsection. The addition of 0.9 per cent manganese to magnesium caused a slight increase in the coefficients of expansion. The coefficients of the extruded ternary alloy containing about 4 per cent aluminum and 0.3 per cent manganese are less than the binary magnesium-aluminum alloys (cast and extruded) containing the same amount of aluminum.

VI. SUMMARY

This paper gives data on the linear thermal expansion of 6 samples of cast and extruded magnesium and 11 samples of cast and extruded magnesium alloys (magnesium-aluminum and magnesium-aluminum-manganese alloys). The samples of magnesium were investigated over various temperature ranges between −183° and +500° C. and most of the alloys between room temperature and 300° C. The previous history (preparation, treatment, chemical composition, etc.) of the specimens is included. The expansion curves of the samples are shown and discussed.

Three types of expansion apparatus were used in this research, and a summary of available data by previous observers on the thermal expansion of magnesium and some magnesium alloys is given.

The following equations are given as the most probable second-degree equations for the expansion of cast magnesium and extruded magnesium between room temperature and 500° C.

Cast magnesium:

$$L_t = L_o \left[1 + (24.94\ t + 0.00946\ t^2)\ 10^{-6}\right] \quad (1)$$

Extruded magnesium:

$$L_t = L_o \left[1 + (24.66\ t + 0.00976\ t^2)\ 10^{-6}\right] \quad (2)$$

Average of equations (1) and (2):

$$L_t = L_o \left[1 + (24.80\ t + 0.\ 00961\ t^2)\ 10^{-6}\right] \quad (3)$$

The coefficients of expansion of extruded magnesium are slightly less than those for cast magnesium. This fact also applies for the alloys investigated. Figure 9 shows a comparison of the average expansion curve (equation (3)) obtained in the present investigation on magnesium, with data from previous observers. The values of nearly all observers show good agreement.

Figure 14 shows the relations between the chemical composition of the magnesium-aluminum alloys and the average coefficients of expansion for three temperature ranges. The addition of 0 to 10 per cent aluminum to magnesium causes practically no change in the coefficients of expansion. The expansion curves of the magnesium-aluminum alloy (10 per cent aluminum) which was extruded and heat treated show critical regions above 200° C. Small additions of manganese (0.9 and 0.3 per cent) to magnesium and magnesium-aluminum alloys caused slight changes in the coefficients of expansion.

A comparison of the average coefficients of expansion of the materials investigated are given for several temperature ranges in the following table. For detailed data the reader should refer to the proper sections of the paper.

TABLE 8.—*Average coefficients of expansion of magnesium and magnesium alloys*

Material	Magnesium content	Average coefficients of expansion per °C.				
		20° to 100° C.	20° to 200° C.	20° to 300° C.	20° to 400° C.	20° to 500° C.
	Per ct.	$\times 10^{-6}$	$\times 10^{-6}$	$\times 10^{-6}$	$\times 10^{-6}$	$\times 10^{-6}$
Magnesium	99.99	26.0	26.9	27.9	28.8	29.8
Magnesium-aluminum alloys	90 to 96	25.4 to 26.4	26.1 to 27.8	27.7 to 28.1	------	------
Magnesium-aluminum-manganese alloys	96 to 99	25.6 to 26.6	26.4 to 27.3	27.2 to 28.1	------	------

WASHINGTON, July 17, 1928.

EQUIPMENT FOR ROUTINE SPECTRAL TRANSMISSION AND REFLECTION MEASUREMENTS

By H. J. McNicholas

ABSTRACT

This paper presents a description of an assembly of apparatus which has been in use at the Bureau of Standards since August, 1924, for routine spectral transmission and reflection measurements. The Koenig-Martens spectrophotometer is used with different light sources, each source being designed especially to meet the required conditions of illumination on the sample, in the measurement of the following quantities as functions of wave length:

1. The *unidirectional normal transmission* of an optically homogeneous (nondiffusing) material in the form of a plate with plane-parallel surfaces.

2. *The normal brightness of a sample by reflected light, relative to the same for a standard material,* when both sample and standard are under equal and completely diffused illuminations.

The sources for transmission measurements are three separate white-lined inclosures, each just large enough to contain, respectively, two 400-watt gas-filled incandescent lamps, two helium lamps, and a quartz mercury-vapor lamp. These sources are conveniently and quickly interchangeable, so that any one of them may be used separately for specific purposes.

A uniform distribution of 156 small gas-filled incandescent lamps on a white diffusely reflecting hemispherical surface provides a source of illumination for reflection measurements which is shown to be equivalent to the desired ideal completely diffused condition.

Accessory equipment includes ventilation apparatus, convenient devices for handling the transmission and reflection samples, standard sectored disks for use with the spectrophotometer, and apparatus for temperature control of liquid transmission samples.

The theory of the Koenig-Martens spectrophotometer is given, along with a discussion of some possible sources of error in the spectrophotometric measurements.

Tests of the accuracy in the measurement of the specified quantities are described.

CONTENTS

	Page
I. Introduction	794
II. Description of light sources	798
1. Source for reflection measurements	798
(*a*) Construction	798
(*b*) Ventilation system	800
(*c*) Cooling of sample	801
(*d*) Illumination and observation of the sample	802
2. Sources for transmission measurements	803
(*a*) Principle of construction	803
(*b*) Tungsten lamp source	805
(*c*) Helium lamp source	906
(*d*) Mercury-vapor lamp source	806
(*e*) Use of transmission sources	806

109431°—28——1

Page
III. Accessory apparatus 807
1. Mechanism for the insertion and interchange of the sample and comparison standard in reflection measurements 807
2. Devices for the support and shifting of transmission samples 809
3. Thermostat for temperature control of liquids 812
4. Sectored-disk attachment 813
IV. Koenig-Martins spectrophotometer 814
1. Theory of the instrument 814
2. Use of the instrument for polarization measurements 823
3. Use of the instrument for reflection and transmission measurements 825
(*a*) The polarization problem: Simplified formulas 825
(*b*) Propagation of error through the formulas 829
(*c*) Choice of formula for routine work 830
(*d*) Use of one quadrant of the circular scale on nicol mounting 833
(*e*) Procedure in measurements 836
4. Further remarks on the instrument and its adjustments 838
(*a*) Stray light 838
(*b*) Photometric field 838
(*c*) Wave-length scale 845
(*d*) Circular scale 846
(*e*) General remarks 846
V. Use of equipment and tests of its performance 846
1. Transmission measurements 846
2. Reflection measurements 850
(*a*) Reflection standards 850
(*b*) Adequacy of absolute illumination on sample 852
(*c*) Equivalence of the illumination to the ideal completely diffused condition 853

I. INTRODUCTION

The measurement of the transmissive and reflective properties of various materials for wave lengths throughout the visible spectral range is a matter of fundamental importance in the work of a colorimetry laboratory, for the data thus obtained under given conditions of illumination and observation constitute a description of the material which is unique and sufficient for the purposes of colorimetry. When multiplied into the spectral energy distribution of the source of illumination, the resulting data are a representation of the entire physical stimulus of the sensation of color (neglecting simultaneous and successive contrast effects) and form the fundamental basis for color specification. The use of these data with the psychophysical data of color vision in the computation of various colorimetric functions has been considered in detail by others. In the establishment of material color standards for various purposes, the spectrophotometric data form a suitable and adequate record of the colors, so that the reproduction of the standards at some future time may be verified without depending on the permanence of the materials originally used. The utility of spectrophotometric equipment and methods in

many fields of research is being recognized by an increasing number of investigators.

A serious disadvantage inherent in the use of visual methods of spectrophotometry lies in the decreased precision of measurement attainable toward both ends of the visible spectrum as a result of the decreased sensibility of the eye to these spectral regions. The difficulty is further enhanced in the blue and violet regions by the relatively lower energy emission of the sources of light commonly used. In some applications of the spectrophotometric data, as in the transformation into the trilinear coordinates of colorimetry, it is often of importance to obtain accurate transmission or reflection data over the spectral range from 380 or 400 to 740 mμ. Sometimes the range from 420 to 720 mμ is sufficient. Unless recourse is had to radiometric methods, the above-mentioned difficulty in the visual method can only be overcome by providing sources of light of sufficient intensity so that the desired photometric precision and range of measurement are obtained.

The transmissive and reflective properties of various materials depend not only on the nature and structure of the material itself, but may also vary considerably with the conditions of illumination and observation. Various transmission and reflection coefficients corresponding to these conditions may therefore be defined and measured to serve particular purposes.

In transmission measurements we are most frequently concerned with the unidirectional normal transmission of light through an optically homogeneous (nondiffusing) medium in the form of a plate with plane-parallel polished surfaces. The beam of light is in this case incident in a direction perpendicular to the surface of the sample; it is partly reflected at the surfaces in a regular manner and partly transmitted by the medium without scattering or appreciable deviation from its original path. The quantity to be measured is the ratio of the total transmitted to the total incident light and is thus defined as the *transmission* (considered now as a magnitude).

In the case of reflection measurements, on the other hand, we are usually concerned with diffusing media, such as papers, painted surfaces, dyed fabrics, etc., for which the incident light is generally reflected in all directions from the surface of the sample. The conditions of illumination and observation must be definitely specified, if unambiguous and reproducible results are to be obtained.

The specification of the illumination for reflection measurements is based upon the following considerations:

1. The absolute illumination on the sample must be sufficient for precise spectrophotometric measurements over the desired range of wave lengths, but the sample must be protected at the same time from excessive heating by the source.

2. The angular distribution of the incident light must be definitely determined by the construction of the source, so that the conditions of illumination may be readily reproduced.

3. It is desirable that the conditions of illumination adopted be also representative of some natural condition of illumination, under which, for instance, the color of various materials is ordinarily observed.

It is difficult to realize all the desired conditions of illumination simultaneously by the use of a single commercial type of lamp. Such illumination will generally be insufficient for spectrophotometric purposes. It is necessary, therefore, to resort to multidirectional illumination of some sort, whereby the combined effect of a number of different light sources is obtained. If no restrictions be placed on the solid angular extent of the incident luminous flux, it is advantageous to place the light sources in an inclosure surrounding the sample, the walls of which are made of a good diffusing material of high reflectance.[1] Furthermore, to make the condition of illumination definite and reproducible, it is expedient to arrange the light sources with reference to the sample so that the illumination on the sample is for all practical purposes *completely diffused*.

No attempt will be made in this paper to discuss the advantages or disadvantages of different conditions of illumination for colorimetric or other purposes. Completely diffused illumination as compared with unidirectional illumination is, perhaps, a closer approximation to the average condition under which the color of a sample is observed (by reflected light) in a well-lighted room or in the open, when the sample is shaded from the direct rays of the sun. In regard to the spectrophotometric measurements, a source for the diffused illumination of the sample may readily be constructed to comply with all of the desired specifications.

If it be desired to measure the total reflected light, some method for the integration of the light flux in all directions from the sample is required. Although suitable methods for this purpose may be applied in certain cases, it is usually most convenient to measure the light reflected in a specified direction from the surface of the sample; and, indeed, this corresponds to the actual condition of use of the eye in observing the color of materials. In this case, however, only a small portion of the total reflected light is directly received by the eye, or by the spectrophotometric observing system, so that a greater light flux on the sample is required in order to obtain the same photometric field brightnesses (hence, the same precision and range of measurement) as may readily be obtained in the above-defined case of unidirectional transmission, wherein the beam of incident light is not broken up or scattered by the sample.

[1] *Reflectance* is defined as the ratio of the total reflected to the total incident light, without regard to directions of incidence or reflection.

The method of observation herein adopted is to view the sample in a direction approximately normal to its surface. The symmetry of both the illumination and the direction of observation with respect to the surface of the sample is an advantage in spectral reflection measurements, which will be evident later in the discussion of these measurements.

The equipment to be described is designed, then, for the measurement of the following quantities:

1. The *unidirectional normal transmission* of an optically homogenous material.

2. *The normal brightness of a sample by reflected light relative to the same for a standard material,* when both sample and standard are under equal and completely diffused illuminations.

In the design and construction of the apparatus for these measurements considerable attention has been given to the matter of convenience in the arrangement and location of the various parts, in the handling of the samples and recording of observations, and to the stability and permanence of the adjustments, in order that the work could be carried on at any time as a routine daily procedure, if desired, with the greatest possible facility and speed and without preliminary adjustments or frequent attention to the working parts. The assurance that a given amount of work may be accomplished in a specified time, without annoying interruptions or uncertainties arising from failures or irregularities in the performance of the apparatus, is a source of the greatest satisfaction to those having to do with a considerable amount of this work.

The equipment has now been in service for nearly four years.[2] Such provisions as have been made to facilitate and expedite the measurements are, if seemingly elaborate, fully warranted, nevertheless, by the use which has been made of this equipment. In addition to determinations of the spectral transmissive or reflective properties of more than 200 samples of various materials submitted during the past four years by outside industrial establishments, private individuals, and other Government departments, an even greater demand for the spectrophotometric data has arisen in various research projects carried on at the Bureau of Standards, particularly those originating in the colorimetry laboratory. These investigations often call for the highest precision and accuracy attainable in the spectrophotometric measurements.

[2] The equipment herein described replaces the old illumination apparatus for transmission and reflection measurements which was in use in the colorimetry section of the bureau prior to the summer of 1924, and described in part in the following papers: B. S. Tech. Paper No. 148, p. 5; 1920; B. S. Tech. Paper No. 167, p. 20; 1920; B. S. Sci. Paper No. 440, pp. 126, 143; 1922; J. O. S. A. and R. S. I., 8, p. 203; 1924.

II. DESCRIPTION OF LIGHT SOURCES

The salient features and general arrangement of the spectrophotometer and illumination apparatus are best illustrated by the photographs in Figures 1 and 2 and by the diagram in Figure 3. The apparatus is built around a wooden framework placed in the center of a small room, which may be darkened, is well ventilated, and devoted exclusively to spectrophotometric work. All switches, rheostats, and other instruments for the control of the lamps, motors, etc., are conveniently assembled on a wall board. Detailed information on the construction of the light sources and accessory parts is given in Figures 4, 5, and 6, to which frequent reference will be made in the description. In the various figures different parts are referred to by number, and a given part is numbered the same in whichever figure and view it may be shown. A general key to the construction is provided, which serves for all of the figures and supplements the description to be found in the text. (See legend to fig. 4.)

The specific requirements in regard to the illumination of the sample, in the particular type of reflection and transmission measurements to be made, are most advantageously met by the use of separate sources especially designed for each kind of work. The advantages of this plan will be brought out in the course of the following description.

1. SOURCE FOR REFLECTION MEASUREMENTS

The source for reflection work is an attempt to realize the ideal condition of completely diffused illumination on the sample to a sufficient approximation for practical purposes, combined with an illumination which is sufficient for precise spectrophotometric measurements throughout the desired spectral range.

(*a*) CONSTRUCTION.—These purposes are served in a satisfactory manner by the following construction:

The sample and comparison standard are placed side by side near the center, and forming a part, of the base of a hollow steel hemisphere (40 cm in diameter), the inner (concave) surface of which is coated with white porcelain enamel (baked), over which a film of magnesium oxide is deposited.[2] The white diffusely reflecting surface thus obtained is studded with 156 small gas-filled incandescent lamps (described in key to construction of apparatus), which are uniformly

[2] The white magnesium oxide "smoke" is easily deposited on a porcelain (or other) surface by holding the surface about 2 inches above the flame of the burning metal. Magnesium metal shavings (as used for Grignard reaction) are generally used, although the ribbon form of the metal may be more convenient in some cases. The shavings are burned in a suitable vessel of brick or iron. The white porcelain surface is first applied to the steel surface in order to avoid the necessity of thick and fully opaque deposits of the oxide, which are more difficult to put on and liable to crack. The relatively good reflecting surface of porcelain is more easily "covered" by the oxide. The eyes of the operator should be protected from the oxide flame by use of dark-yellow glasses.

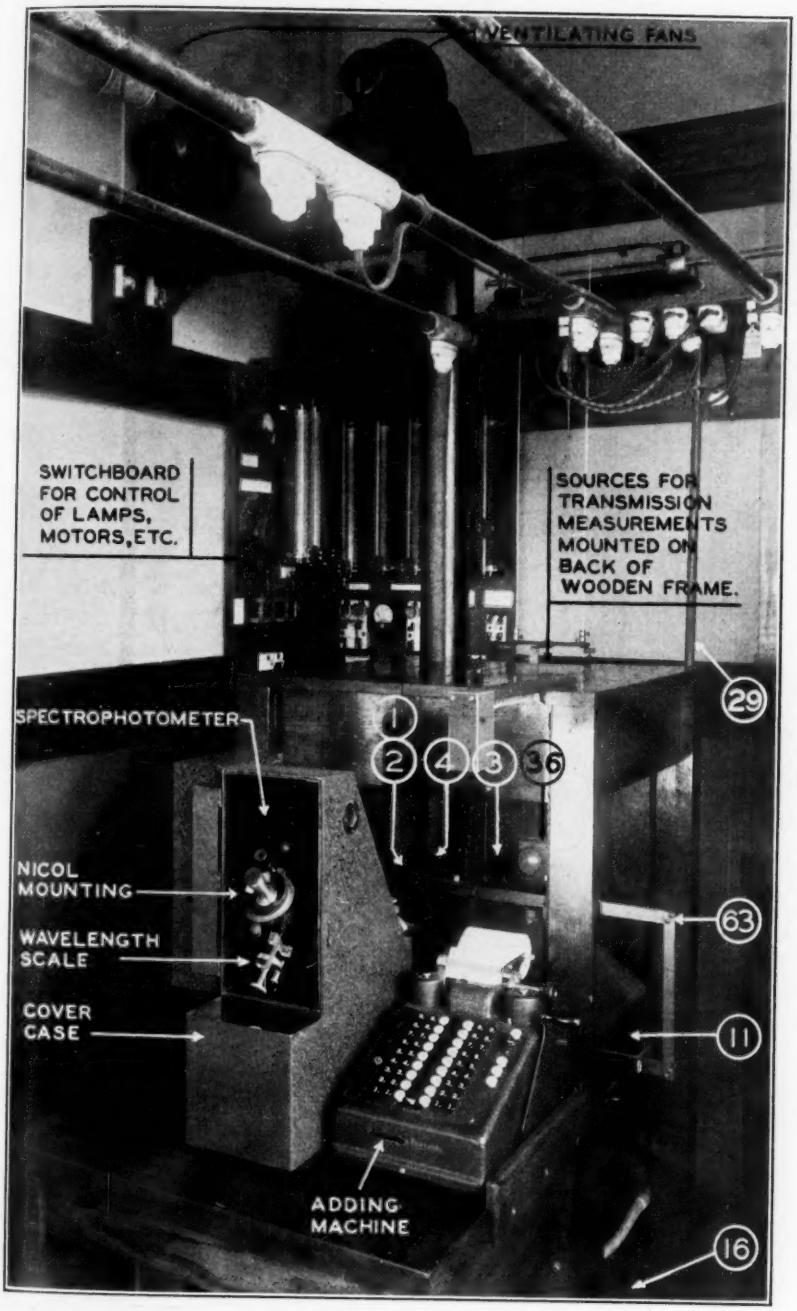

FIG. 1.—*General view of equipment for visual spectrophotometry*

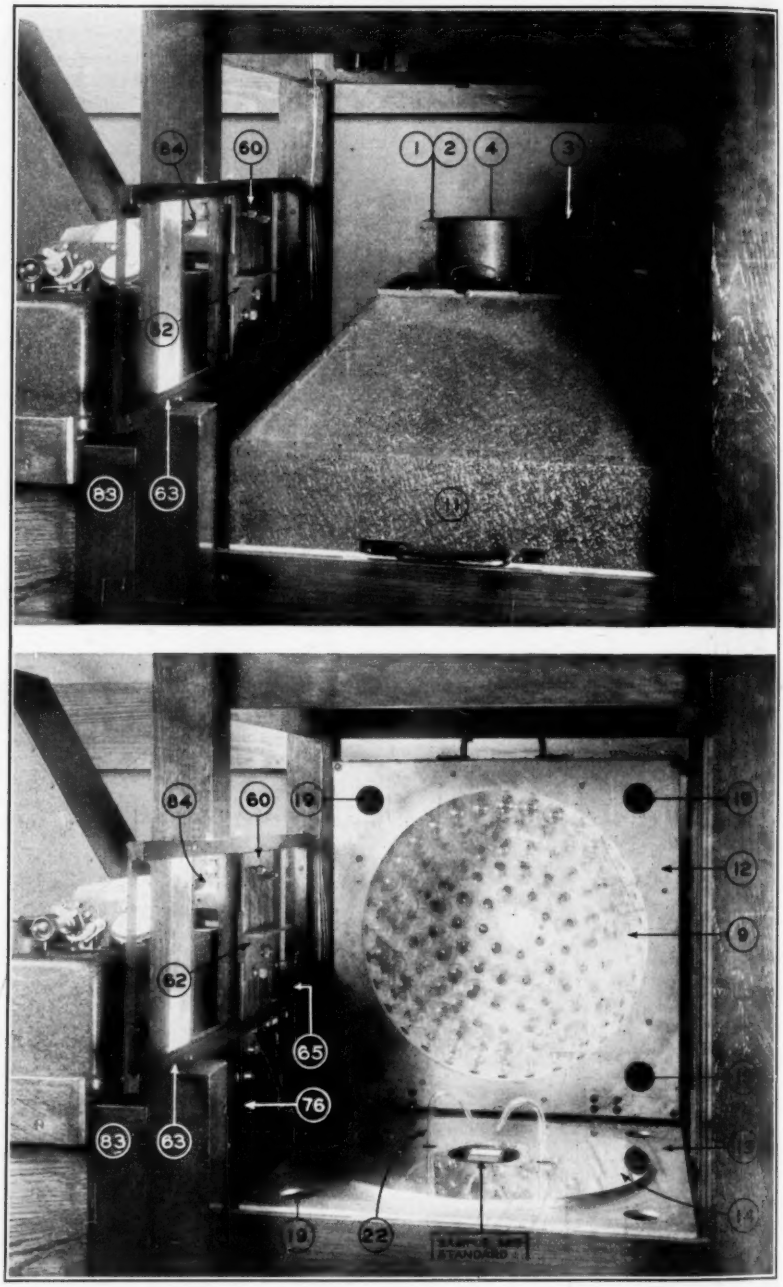

FIG. 2.—*Views of hemispherical source for reflection measurements*

Hemisphere raised in lower photograph, showing arrangement of lamps, mirror base, and parts of ventilation system

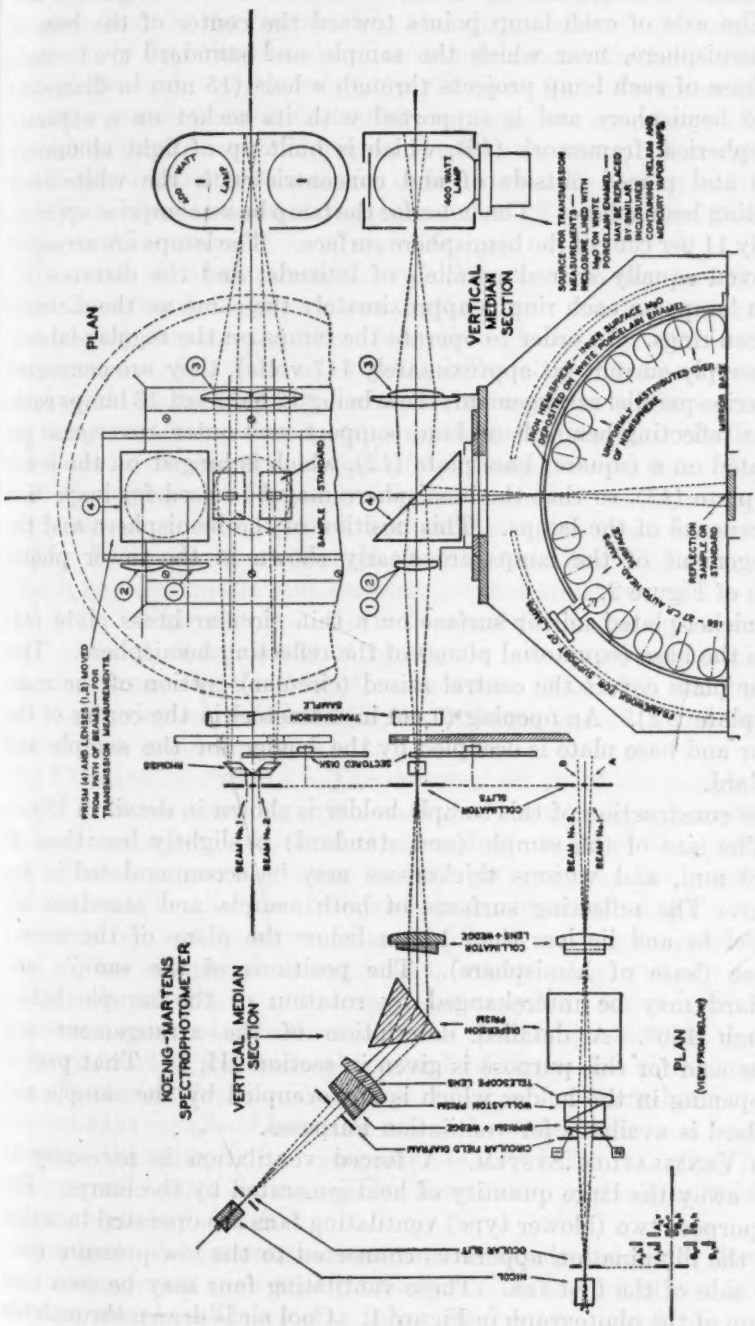
PLAN
VERTICAL MEDIAN SECTION
STANDARD
SAMPLE
400 WATT LAMP
SOURCE FOR TRANSMISSION MEASUREMENTS — ENCLOSURE LINED WITH MgO ON WHITE PORCELAIN ENAMEL — LAMP REPLACED BY SIMILAR ENCLOSURES CONTAINING HELIUM AND MERCURY VAPOR LAMPS
IRON HEMISPHERE — INNER SURFACE MgO DEPOSITED ON WHITE PORCELAIN ENAMEL
UNIFORMLY DISTRIBUTED OVER HEMISPHERE
MIRROR BASE
REFLECTION SAMPLE OR STANDARD
PHOTOCELL FOR SUPPLY OF LAMPS
PRISM (M) AND LENSES (L3) MOVED FROM PATH OF BEAMS — FOR TRANSMISSION MEASUREMENTS.
MIRRORS
SECTORED DISK
TRANSMISSION SAMPLE
COLLIMATOR SLITS
BEAM No. 1
BEAM No. 2
KOENIG-MARTENS SPECTROPHOTOMETER
VERTICAL MEDIAN SECTION
COLLIMATOR LENS + MIRROR
DISPERSION PRISM
TELESCOPE LENS
NICOL

FIG. 3.—*General arrangement of spectrophotometer and separate light sources for transmission and reflection measurements*

(Uniform scale not used throughout the diagram)

distributed over the surface and mounted as shown in Figures 3 and 4. The axis of each lamp points toward the center of the base of the hemisphere, near which the sample and standard are located. The base of each lamp projects through a hole (15 mm in diameter) in the hemisphere and is supported with its socket on a separate hemispherical framework (*10*), which is built up of light aluminum strips and placed outside of and concentric with the white-lined reflecting hemisphere. The holes for the lamp bases comprise approximately 11 per cent of the hemisphere surface. The lamps are arranged on seven equally spaced parallels of latitude, and the distance between lamps on each ring is approximately the same as the distance between rings. In order to operate the lamps on the regular laboratory supply current (at approximately 117 volts), they are connected in a series-parallel arrangement, there being 12 banks of 13 lamps each.

The reflecting hemisphere, lamp support, and outer cover case are mounted on a (square) base plate (*12*), which is hinged on the lower base plate (*13*), so that the hemisphere may be raised for inspection and renewal of the lamps. This position of the hemisphere and the arrangement of the lamps are clearly shown in the lower photograph of Figure 2.

A nickel-plated mirror surface on a thin circular brass plate (*14*) forms the base (equatorial plane) of the reflecting hemisphere. This mirror plate covers the central raised (circular) portion of the main base plate (*12*). An opening (9 cm in diameter) in the center of the mirror and base plate is occupied by the holder for the sample and standard.

The construction of this sample holder is shown in detail in Figure 5. The size of the sample (and standard) is slightly less than 40 by 30 mm, and various thicknesses may be accommodated in the holder. The reflecting surfaces of both sample and standard are parallel to and lie less than 1 mm below the plane of the mirror surface (base of hemisphere). The positions of the sample and standard may be interchanged by rotation of the sample holder through 180°. A detailed description of the arrangement and mechanism for this purpose is given in section III, 1. That part of the opening in the holder which is not occupied by the sample and standard is available for ventilation purposes.

(*b*) Ventilation System.—A forced ventilation is necessary to carry away the large quantity of heat generated by the lamps. For this purpose two (blower type) ventilating fans are operated in series, with the illumination apparatus connected to the low-pressure (suction) side of the first fan. These ventilating fans may be seen near the top of the photograph in Figure 1. Cool air is drawn through the apparatus and the heated air discharged from the room.

It has been found necessary to filter all the air used for ventilation purposes in order to remove dust and dirt, which would otherwise be gradually deposited on the white magnesium oxide coating of the hemisphere and soon appreciably decrease its reflectance. This filtering is accomplished in a satisfactory manner by passing the air through a few overlapping layers of absorbent cotton. The construction of the air filter (*16*) is shown in Figure 4. The layers of cotton are held in place between two square frames of wood covered with a coarse-mesh wire screen.

The course of the air stream through the apparatus may be followed by reference to the various views in Figure 4. Air from the room, after passing through the filter, flows through the pipe (*17*) into the compartment (*18*). This air, which is still cool, now flows around the sample and standard into the hemispherical inclosure and out through the many small annular openings around the bases of the lamps into an outer compartment inclosed by the cover case (*11*). In the lower photograph of Figure 2, four holes (each 4 cm in diameter) may be seen in the base (*12*) of this cover case, one located near each corner. In the same photograph, and in view *B* of Figure 4, four holes of equal diameter and similarly located are shown in the base plate (*13*). When the hemisphere is closed (as in the upper photograph of fig. 2, or in view *A* of fig. 4), the holes in both base plates coincide, permitting the flow of air into four pipes (*20*), which lead from the four openings in base (*13*) to the larger pipe (*21*), and thence direct to the ventilating fans.

(*c*) Cooling of Sample.—The inflow of air about the sample and standard aids considerably in the cooling of the sample and surrounding metal parts, and the outflow around the bases of the lamps is most effective in carrying away the heat generated by the lamps.

The intense irradiation of the sample would cause some materials to become too hot, however, if an additional cooling were not provided. This additional cooling is supplied by a high-velocity jet of air (from the laboratory compressed-air supply line) which is directed from above on the sample through one of the nozzles shown in view *A* of Figure 4 and in the lower photograph of Figure 2. These nozzles are made of clear fused-quartz tubes, which absorb very little of the infra-red heat rays, and hence do not preheat the air stream passing through. Likewise, being transparent to the visible rays, they have no appreciable effect on the angular distribution of the light incident on the sample and standard.

Here, again, the entering air may be dirty or oily and, if not cleaned before using, would soon deposit an appreciable amount of dirt on the reflection sample. The quartz tubes are inserted into brass tubes below the base of the hemisphere; these tubes then lead through a valve (*23*) (purpose described below) to the air filter, and thence to the

supply line. The construction of this air filter is essentially the same as that of the filter described above; it is not shown, however, in any of the figures.

With the lamps operating at normal voltage, there is an expenditure of about 2,800 watts of electric power. The ventilation system (with the lamps in operation) draws 13 cubic feet of air per minute through the hemisphere. With the room temperature at 30° C., a thermometer held in the outgoing stream of air registered 66° C. Two mercury-in-glass thermometers, one with a clear bulb and the other with a blackened bulb, when supported in a vertical position within the hemispherical inclosure with the bottom of each bulb in contact with a reflection sample of black paper, registered 52° and 56° C., respectively, after temperature conditions had become steady with both air streams in operation. When the thermometer bulbs were raised to the center of the hemispherical inclosure, the corresponding readings were 70° and 90° C., respectively.

The actual temperature attained by a sample under these conditions has not been directly measured (as with a thermocouple embedded in the body of the material). The temperature is not excessive, however, and the sample usually feels just warm to the touch. The reflective properties of certain dyed materials occasionally change slightly under the intense irradiation from the hemisphere lamps. This change is probably an actinic effect, however, and not a burning or scorching of the material.

(*d*) Illumination and Observation of the Sample.—With the hemisphere lamps all operating at normal voltage, the absolute brightness of a magnesium carbonate sample observed normal to its surface was found to be 10.8 lamberts.[4] The brightness of this material under completely diffused illumination is practically the same for all angles of view, and its reflectance is close to 98 per cent; hence, the illumination on the sample is 11 lumens per square centimeter.[5]

The path of the beams of light from the sample and standard to the spectrophotometer is clearly shown in the two views of Figure 3. The collimator (entrant) slits of the spectrophotometer are focused on larger slits near the pole of the hemisphere by the lenses (*1*) and (*2*). These hemisphere slits may be seen in the lower photograph of

[4] The absolute brightness was measured in the following manner:

From the construction of the hemispherical illumination apparatus, as depicted in Figure 4, A, it may be seen that it is possible to remove a circular area 5 cm in diameter centering at the pole of the reflecting hemisphere and containing the pair of slits (*15*). This being done, then, a Martens photometer was arranged so that, with the aid of a small total-reflection prism and a lens, the brightness of the magnesium-carbonate sample could be compared in the photometric field with a standard brightness set up outside of the hemisphere. Proper corrections were applied for reflection losses at the optical surfaces between the carbonate and the photometer. A neutral absorbing screen of known transmission was used to decrease the difference between the measured brightness and the standard. The same method was used for the absolute-brightness measurements mentioned later in connection with the description of the transmission sources.

[5] It is of interest to note that the normal illumination of a surface from the direct rays of the noon summer sun (at Washington) is approximately 10 lumens per square centimeter.

Figure 2. (See also at (*15*), fig. 4.) The area of the sample which is observed through the spectrophotometer is semicircular in form and equal approximately to 2 cm². A convergent beam of light normally reflected from this area of the sample passes through the corresponding hemisphere and collimator slits and illuminates one half of the spectrophotometric field. Light reflected from the comparison standard, similarly, illuminates the other half of the field. The comparison of the brightnesses of the sample and standard is fully discussed in sections IV and V.

2. SOURCES FOR TRANSMISSION MEASUREMENTS

(*a*) PRINCIPLE OF CONSTRUCTION.—An intense beam of light is desired for transmission measurements, incident on the sample in a direction approximately normal to its surface. The method often used in spectrophotometry is to focus the incandescent filament of a lamp, or the crater of an arc, through the sample onto the collimator slit of the spectrophotometer. This method may prove very troublesome, however, if, as a result of small irregularities or a nonparallelism of the surfaces of the sample, the image of the source on the collimator slit is shifted when the sample is inserted or removed. Errors of serious magnitude may result in this case if the source is not of uniform intrinsic brightness over a sufficiently large area. Moreover, when a parallel beam through the sample is not used a correction to the illumination of the collimator slit may be necessary, involving the thickness and index of refraction of the sample.

The ideal source for accurate and reliable transmission measurements is a uniformly bright, diffusely emitting surface of sufficient extension so that a beam of light from this source, passing through the collimator slit and filling the photometric field of the spectrophotometer, may then be wholly, or in part, shifted by the slight irregularities of the sample, without changing the illumination of the photometric field. With this source the thickness of the sample has in itself no effect on the illumination of the field.

In the measurements to be made it is assumed that there is no considerable scattering or large-angle refraction of the light during its passage through the sample; that is, we are dealing ideally with the transmission of clear, optically homogeneous materials. Different methods are required for diffusing media. No materials are optically perfect, however, and many of the samples to be measured will slightly scatter or refract the transmitted light. There is, therefore, a considerable advantage in the use of the extended source, for then, if a narrow pencil of rays originating at a given point of the source and forming part of the beam entering the spectrophotometer is scattered out of the beam after the insertion of the sample, it should be

fully replaced by an equal pencil of rays scattered into the beam from an adjacent part of the source.[6]

This type of source offers no particular difficulties in construction, and the required brightness for spectrophotometric work may be readily obtained. Making use of the well-known properties of an inclosure, the walls of which reflect light in approximate accordance with the cosine law, the average total illumination of the wall is given by

$$\frac{F}{A\ (1-R)}$$

where A is the area of the wall, R its average reflectance, and F the total light flux projected into or generated within the inclosure. By placing lamps in as small an inclosure as possible, then, with walls of the highest reflectance attainable, the maximum illumination and brightness of the interior surface is obtained. A portion of this surface, viewed through a suitable aperture into the inclosure, serves as a practical realization of the desired ideal type of source. Care must be taken, however, to insure a sufficiently uniform brightness distribution over an area somewhat larger than the observed portion of the interior wall. Referring to the above formula, it is seen that the average direct illumination of the wall is F/A, but that, as a result of multiple reflections within the inclosure, the total illumination is at least ten times greater, if an average reflectance of 0.9 for the interior surface of the inclosure be assumed. Thus, approximately 90 per cent of the total illumination of the observed spot and surrounding area is due to the multiply reflected indirect component which, in consequence of the reflective properties of the wall, is nearly completely diffused and sufficiently uniform over the required area. The lamps should be arranged inside the inclosure so that the remaining 10 per cent of the total illumination of the observed region, which is received directly from the lamps, is as nearly uniform as possible. Obviously a high value of R is desirable, not only to obtain the highest possible brightness but also to increase the proportion of the indirect illumination, thus insuring a more uniform brightness distribution over the observed portion of the interior surface. The aperture into

[6] This statement is but an application of the Helmholtz reciprocity law to this case of transmission measurements. The application of the law in the analogous case of diffuse reflection has been fully discussed in B. S. J. of Research, **1**, p. 29 (No. 3); 1928.

To make a rigorous application of the law in this case, however, an assumption must first be made in regard to the diffusive properties of the sample. Because of the impossibility of interchanging the directions of the incident and scattered light in strict compliance with the reciprocity law, we must assume that the quantity and angular distribution of the diffused transmitted light for unidirectional normal illumination are practically the same when the light is incident on either surface of the sample. This is generally a valid assumption for the type of sample with which we are concerned. Then, to compensate completely for the light scattered out of the beam in the case here considered, it is only necessary that the solid angle subtended at the sample by the effective aperture into the lamp inclosure be equal to or larger than the solid angular extent of the slightly diffused transmitted light for strictly unidirectional normal illumination. Under these conditions the light entering the spectrophometer is exactly equal to that which would enter the instrument if the sample were made nondiffusing without changing its *transmission*.

the inclosure, through which light passes to the spectrophotomoter, should be as small as possible in order to obtain the highest possible average reflectance of the interior wall. On the other hand, the effective aperture into the inclosure should be large enough to take care of the slight diffusive properties or irregularities of the sample.

The hemispherical source for reflection measurements (previously described) would obviously also serve for transmission measurements, in which case the sample and comparison standard could be replaced by (say) two blocks of magnesium carbonate. As we are primarily interested, however, in a diffusely emitting surface of high and uniform brightness over a limited area, and not particularly concerned with the manner in which this surface is illuminated, a great advantage over the above hemispherical construction is gained by use of a small inclosure, with fewer lamps and a lesser expenditure of electric power.

The sources to be described are designed on the above principles. They are not intended, however, to be of sufficient extension to compensate completely for the light scattered by imperfect samples having badly scratched or poorly polished surfaces. Appreciably lower transmissions may be obtained for such samples than would be obtained with a fully extended (hemispherical) source.

The construction of the sources and their arrangement is shown in Figure 4 (section view A and elevation view B). Three different lamp inclosures are there shown, containing gas-filled tungsten-filament incandescent lamps, helium lamps, and a quartz mercury-vapor lamp, respectively. They are permanently mounted on a plate (*30*), which slides between two vertical guide bars (*31*) and is held in any position by the counterweight (*32*). A handle (*33*) and a spring catch (*34*) are provided, so that either lamp inclosure may be conveniently and easily raised or lowered into position for use in transmission measurements.

(*b*) Tungsten Lamp Source.—The middle inclosure (also illustrated in fig. 3) is an iron box (*36*) coated on its inner surface with white porcelain enamel and "smoked" with magnesium oxide. The box is self-ventilating and just large enough to inclose the bulbs of two 400-watt gas-filled tungsten-filament incandescent lamps (*35*), the bases of the lamps being outside the white-lined inclosure. A sufficient separation between the lamps is allowed for the passage of two beams of light from the back wall of the box through an aperture in the front wall and thence to the spectrophotometer.

This source, giving a continuous spectrum, is used for the greater part of the transmission work. With the lamps operating at normal voltage the brightness of the inner surface, as viewed through the aperture, is 88 lamberts. The lamps are operated in series on 220 volts direct current. The 400-watt lamps may be replaced by 1,000-

watt lamps of approximately the same type and size, if desired. A forced ventilation would then be necessary, however, to prevent an excessive temperature in the lamps, thus greatly shortening their life. An inclosure of the type described in this section could be designed to give a greater interior brightness than is obtained with the present construction.

(*c*) HELIUM LAMP SOURCE.—The form of the two helium lamps (*37*) is clearly shown in views A and B of Figure 4. The discharge tubes are 5 mm in diameter and contain helium gas at a pressure of approximately 10 mm (of mercury). They are connected in series, forming a total tube length of 80 cm, and are operated on a high-voltage transformer.[7] Two aluminum rods (shown in fig. 1) make permanent electrical connection to the lamps by sliding contact with an overhead high-voltage line.

With the exception of their terminal bulbs, the helium lamps are inclosed in a small rectangular box (*38*), the upper, lower, and front sides of which are made of asbestos board (for electrical-insulation purposes combined with good heat-resisting qualities), and the remaining sides are made of aluminum. Two small holes in the top and bottom sides provide for a sufficient ventilation. The inner wall of this inclosure is covered with a thick deposit of magnesium oxide, and an aperture in the front side is provided for the emergence of the light beams to the spectrophotometer. The brightness of the interior surface is approximately 0.5 lambert.

(*d*) MERCURY-VAPOR LAMP SOURCE.—The lower source (fig. 4) is a quartz mercury-vapor lamp (*40*), with the straight portion of its tube inclosed as much as possible in an iron box (*41*), the inner surface of which is also porcelain enameled and coated with magnesium oxide. Light for the sample and spectrophotometer is taken from the back cylindrical surface of the inclosure through an aperture in the front wall.

The mercury lamp, with its inclosing box, is mounted on a circular plate (*42*), which is in turn supported on a hollow bearing, so that the whole lamp may be turned into a vertical position for the purpose of starting. The lamp is operated on the 220-volt direct-current supply line, and the brightness of the interior curved surface is approximately 51 lamberts when the terminal voltage across the arc reaches its usual value of 120 volts.

(*e*) USE OF TRANSMISSION SOURCES.—The course of the light beams from the transmission source to the spectrophotometer is best shown in the upper view of Figure 3. The transmission sample is in position in one of the beams; and the large total-reflection

[7] To operate these lamps in series, a 1-kilowatt, 20,000-volt transformer which was available in the laboratory is used with considerable resistance in the primary circuit. A voltage of 10,000 or less is sufficient for this purpose.

prism (*4*), with lenses (*1*) and (*2*), is moved out of the path of the beams from the transmission sources. (In the lower view these lenses and the prism are in place for reflection measurements.)

The lens combination (*3*) serves the following purposes: (1) The two beams to the spectrophotometer are taken from approximately the same area of the wall of the lamp inclosure, so that any variations in the relative brightness distribution over the interior surface of any one of the inclosures affects both beams equally; (2) the collimator slits of the spectrophotometer are focused approximately in the plane of the aperture into the lamp inclosure. The latter circumstance, combined with the overlapping of the beams inside the inclosure, is an advantage in the design of these sources. The smallest possible aperture into the inclosure may thus be used, so that a maximum area of the wall is conserved for reflecting purposes; also, less free space is needed inside the inclosure for the light beams.

The apertures of the lens combination (*3*) and of the lamp inclosures are made large enough to permit small displacements of either beam (corresponding to the introduction of an imperfect sample) without obstructing the free passage of the beam to the spectrophotometer.

III. ACCESSORY APPARATUS

1. MECHANISM FOR THE INSERTION AND INTERCHANGE OF THE SAMPLE AND STANDARD IN REFLECTION MEASUREMENTS

The adopted method of use of the spectrophotometer (described in Sections IV and V) requires an interchange of the positions of the sample and standard during the course of a reflection measurement, and it is desirable that this operation be performed rapidly and in a manner convenient to the observer.

In addition to the diagram in Figure 5, the sample holder is shown in position for reflection measurements in views A and C of Figure 4. The interchange of the sample and standard is effected by rotation of the holder through 180°. For this purpose the gear teeth on the outer edge of the holder are in mesh with the gear teeth of a drive-wheel (*45*), which is in turn connected through bevel gears (*46*) to the drive shaft (*47*). This shaft may be rotated by the observer from his position at the spectrophotometer by a handwheel (*50*), which is conveniently located to the left of the spectrophotometer cover case (fig. 1) and connected by pulleys (*48*, *49*) and belt to the shaft (*47*). Suitable stops (*6*) on the holder prevent its rotation through more than 180°.

The mechanism for the removal (or insertion) of the holder from the illumination apparatus is explained as follows: From the section view A of Figure 4 it is clear that the weight of the sample holder is carried on the circular shaft (*51*). This shaft has a rack cut into

one side, so that it may be moved up or down by the pinion (*52*) attached to the shaft (*53*). This rack-and-pinion arrangement is operated by the handwheel (*54*) on the shaft (*53*). The latter is normally prevented from turning by the clamp (*55*). To remove the sample and standard, then, this clamp is released and the sample holder lowered until it rests upon a carriage (*56*). This position of the holder is shown in view E of Figure 4. The carriage with the

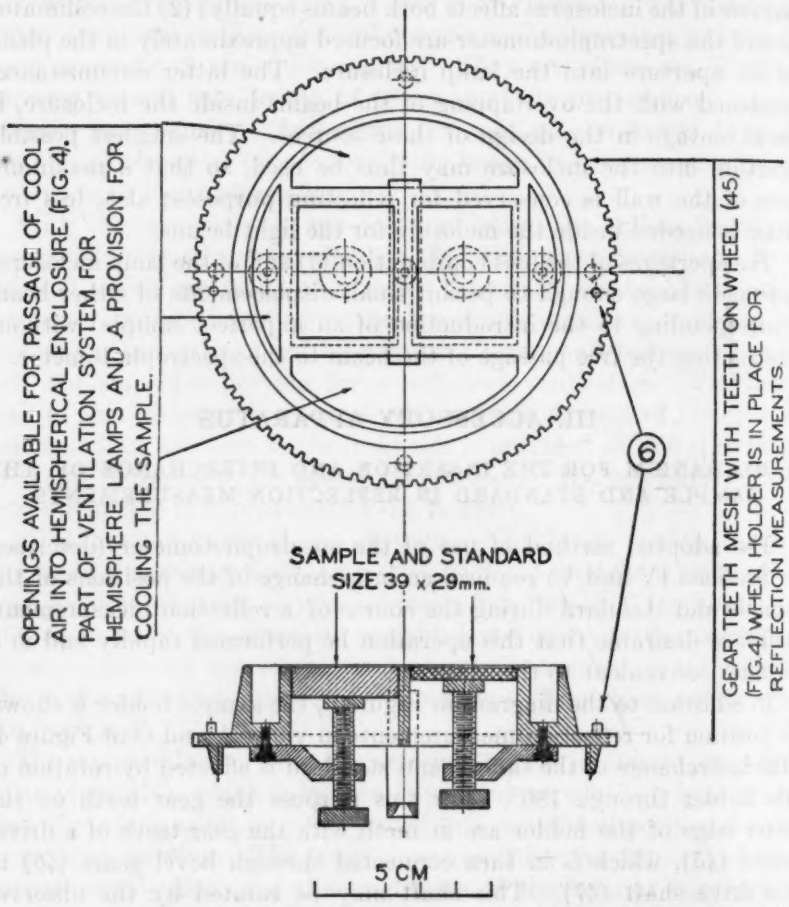
OPENINGS AVAILABLE FOR PASSAGE OF COOL AIR INTO HEMISPHERICAL ENCLOSURE (FIG. 4). PART OF VENTILATION SYSTEM FOR HEMISPHERE LAMPS AND A PROVISION FOR COOLING THE SAMPLE.
GEAR TEETH MESH WITH TEETH ON WHEEL (45) (FIG. 4) WHEN HOLDER IS IN PLACE FOR REFLECTION MEASUREMENTS.
6
SAMPLE AND STANDARD
SIZE 39 x 29mm.
5 CM

FIG. 5.—*Construction of holder for reflection sample and comparison standard*

(Part No. 5 of fig. 4)

holder may now be moved along a track (*57*) by pulling out the rod (*58*) until the holder comes under the door (*59*) (shown open in views C and E). The holder can then be lifted from the carriage and taken out for inspection or change of sample. In the reverse operation of inserting the sample, the holder is raised from the carriage by the shaft (*51*), and the gear teeth on the holder again come into mesh with the teeth of the driving gear.

As the sample and standard are interchanged, the valve (*23*) is simultaneously operated through the levers (*24*) and pins (*6*), so that the high-velocity cooling-air jet is first cut off and then shifted from one of the nozzles (*22*) to the other. The operation of this valve mechanism may be followed in the views C, D, and E. It is designed so that the observer need only be concerned with the proper position of the sample holder on its carriage when being inserted into the apparatus; consequently the air stream is always directed onto the sample and never on the standard. Two reasons for this provision may be mentioned: (1) The comparison standard may always consist of a material requiring no special cooling, so that a greater volume of air is thereby available for the cooling of the sample; (2) the high-velocity air stream impinging continuously on the surface of the standard would be detrimental in the case of some materials which might be used.

2. DEVICES FOR THE SUPPORT AND SHIFTING OF TRANSMISSION SAMPLES

The samples submitted for transmission measurements are likely to vary considerably in size, shape, and thickness, so that a somewhat flexible arrangement for the support of the sample in the beam of light is required, which may be readily adapted to accommodate different samples. As in the case of reflection measurements, the method of use of the spectrophotometer requires the shifting of the transmission sample from one beam to the other, and it is equally desirable in this case that the shifting operation be performed rapidly and in a manner convenient to the observer.

Views of the sample support are shown in Figures 4 and 6, including a vertical median section in Figure 4, A. A brass plate (*60*) carries a double platform (*61*, *62*), which may be raised or lowered to accommodate the size of the sample and to center it vertically in the beam of light. The long platform (*61*) is removable, leaving a shorter platform (*62*), which serves for the majority of samples and does not interfere with the raising of the hemisphere. Three apertures (*68*) in the plate (*60*) allow the passage of the light beams to the spectrophotometer. The plate (*60*) fits into V-shaped grooves in two horizontal guide bars (*63*), forming a track along which the holder may be moved. For this purpose a rack (*64*) and a pinion (in the gear box (*65*)) are provided and operated by a handwheel (*66*), conveniently placed to the left of the observer. As the holder is moved between the stops (*67*) the sample (placed before the central aperture) is shifted from one beam to the other. Upon removal of one of these stops the whole sample support may be moved to the end of the track (*63*), a provision which is very convenient for the mounting and adjustment of the sample on the platform. This position of the holder is shown in Figure 6.

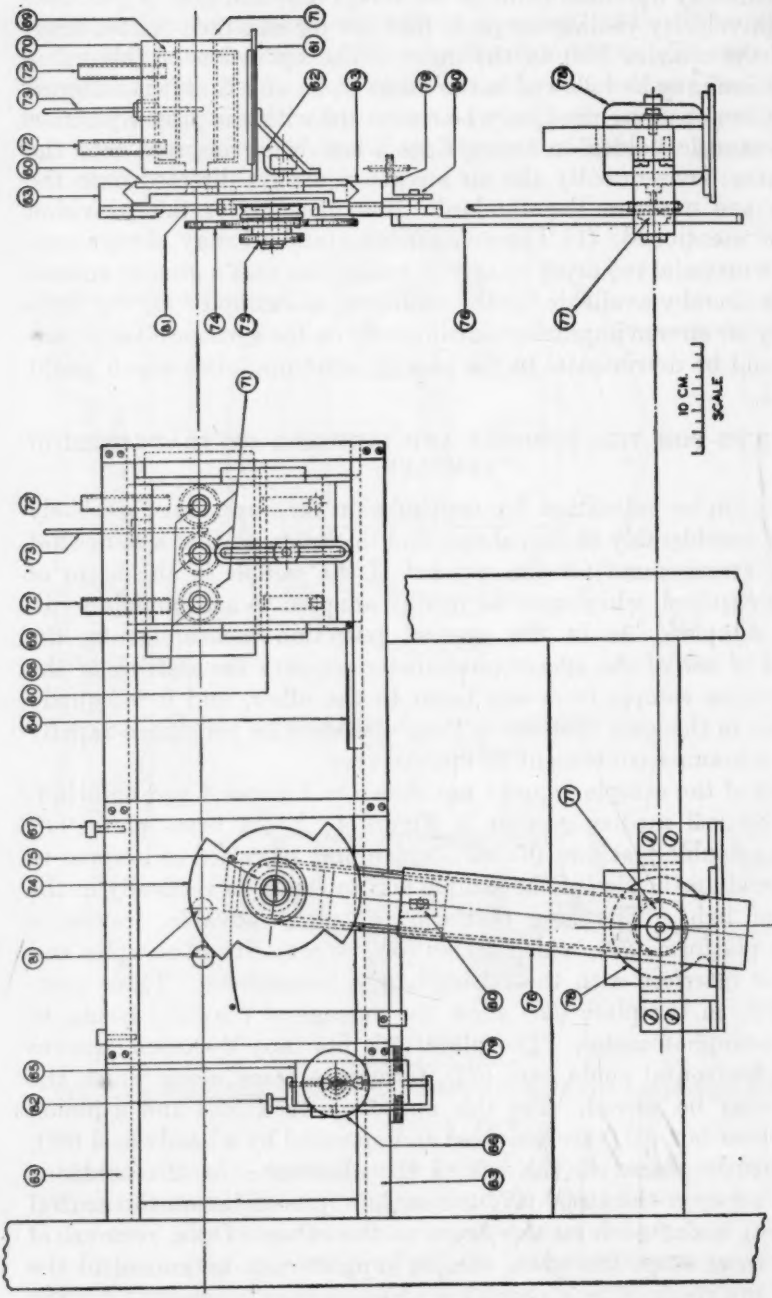

FIG. 6.—*Elevation views showing: (1) Sectored disk attachment and shifting mechanism; (2) constant-temperature box for cells containing liquids, mounted in proper position on support for transmission samples*

(See description of parts in legend to fig. 2)

In the same figure a constant-temperature box (*69*) is also shown mounted in position on the platform of the sample holder. This box is designed particularly for transmission measurements on liquids, such as inorganic salt and dye solutions, in which it is desired to control the temperature of the solution and its solvent to within a degree or two and to cover a range of temperatures approximately 20° above and below the room temperature. The rectangular brass box (*69*) is covered with a heat-insulating material (*70*) and has three cylindrical brass tubes (*71*) passing through, as shown. Water from a thermostat-controlled bath (described later) may be circulated

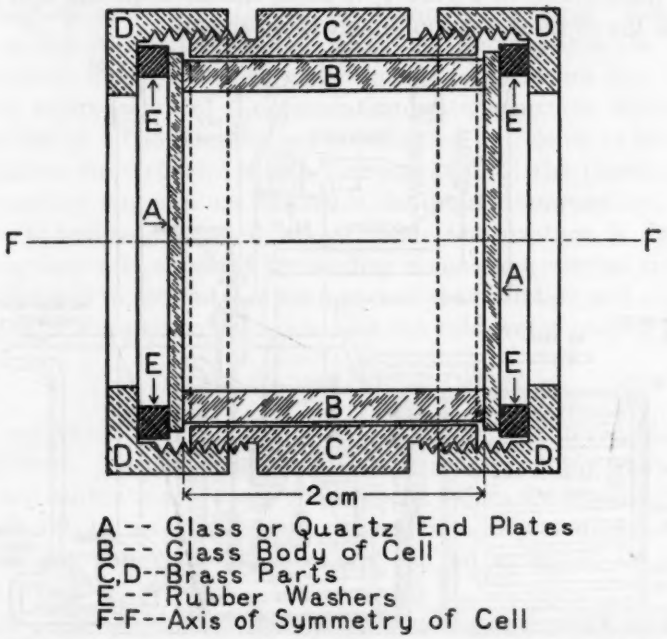

FIG. 7.—*Type of cell used in the measurement of the transmissive properties of liquids*

(Reproduced from B. S. Sci. Paper No. 440)

through the box, thus maintaining the walls of the tubes at an approximately constant temperature, indicated by the thermometer (*73*).

A cylindrical cell (construction fully shown in fig. 7) containing the solution to be measured may be inserted in the central tube of the constant-temperature box with similar cells containing the solvent in the outer tubes. The brass sides of the cell are in contact with the brass walls of the box, and the reading of the thermometer is taken as the temperature of the solution and solvent. While this method would not be satisfactory at temperatures differing greatly from room temperature, it is quite suitable for the purposes to which it is applied.

When the sample holder with the constant-temperature box is moved into position in the light beams, the rack (*64*) engages with its pinion gear, and, as the solution is moved from one beam to the other, one of the solvent cells is always centered in the opposite beam.

3. THERMOSTAT FOR TEMPERATURE CONTROL OF LIQUIDS

A suitable arrangement for this purpose has previously been described in Bureau of Standards Scientific Paper No. 440. The same arrangement, with slight modifications, is installed with the present equipment and is shown in Figure 8. The apparatus does not appear in the photograph of Figure 1, it being mounted on the wall of the room to the right of the equipment there shown.

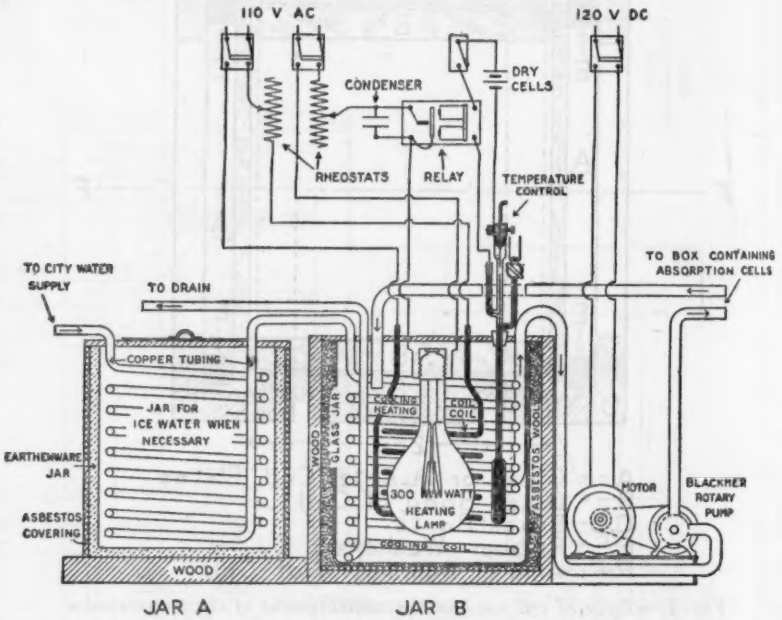

FIG. 8.—*Thermostat and bath arrangement for temperature control of cells containing liquids*

Water from jar *B* is pumped through a few feet of rubber tubing to the constant-temperature box surrounding the transmission cells, and back again to the same jar. This water is maintained at a constant temperature in the following way: A steady stream of cold water (from the city supply) passes through the copper cooling coils in jars *A* and *B* and discharges into the drain. This water may be further cooled, if necessary, by use of ice water in jar *A*, and the volume of water flowing through the coil regulated in accordance with the amount of cooling desired.

Heat is supplied by a 300-watt gas-filled incandescent lamp suspended in jar *B*. The use of a lamp for this purpose affords a quick

means for adding heat to the water, for the radiant energy is instantaneously absorbed by the water over a large surface in contact with the lamp bulb. The current through this lamp is switched on and off as required by the thermostat acting through the relay. When the water in jar *B* is too cool, the contact between the narrow mercury column and a platinum wire in the thermostat is broken by the contraction of the mercury. This interrupts the current through the magnets of the relay, releasing the relay lever and closing the circuit through the lamp. The water in jar *B* now heats up until the expansion of the mercury again closes the circuit through the relay magnets and opens the circuit through the lamp. The continued action of the thermostat, while the pump keeps the water in circulation through the jar and constant-temperature box, maintains the temperature of the circulating water constant within the required limits. The temperature is regulated by raising or lowering the platinum contact wire in the thermostat until the thermometer in the constant-temperature box reads the desired temperature.

When a temperature well above room temperature is desired, better regulation is obtained by sending a constant current through the heating coil to compensate for a part of the radiation and conduction losses in the system. In this case the cold-water cooling is not required.

4. SECTORED-DISK ATTACHMENT

The equipment also includes a set of standard sectored disks of fixed aperture, the transmissions of which are accurately known by mechanical calibration.[8] These transmission values are approximately 80, 70, 60, 50, 10, and 1 per cent, respectively. By combinations of two disks the range of transmissions can be extended to values between 50 and 10 per cent.

The use of these sectored disks in the spectrophotometric measurements is fully discussed in section V, 1. Briefly, they serve two purposes: (1) To test and maintain a check upon the accuracy of the spectrophotometer, and (2) to extend the range of the instrument accurately below 1 per cent, by use of the 10 or 1 per cent disk in the beam opposite the sample. This procedure reduces the difference between the brightnesses compared in the photometric field, with consequent advantages in the measurement of low transmission or reflection coefficients.

Two views of the sectored-disk attachment are shown in Figure 6, and a section through the axis of rotation of the disk and driving motor is contained in Figure 4, A. These views clearly illustrate the construction and mounting of the disk and the position of the

[8] This calibration was made by the Bureau of Standards division of weights and measures and consists in the measurement of the angular opening in each disk. From these data the transmissions of the rapidly rotating disks (assuming the Plateau-Talbot law) are known.

attachment relative to the other parts of the apparatus. The central hole of each disk fits without play on a circular boss carried by the driving pulley. Two small holes in the disk register with two pins projecting from the base of the pulley, in order to prevent slip and possible loosening of the nut due to inertia of the disk during acceleration or deceleration. Two disks may be mounted together on the axle. A 50 per cent sectored disk is shown in position covering one of the apertures (*81*) through which the beams of light pass to the spectrophotometer. The other aperture remains clear.

The disk may be shifted from one beam to the other by a rack-and-pinion arrangement (*79*), which is operated through the gear box (*65*) and handwheel (*66*). The same handwheel is also used for the shifting of the transmission sample; and, by proper adjustment of the vertical position of the knob (*82*) the disk attachment may be placed in gear so as to shift simultaneously either with the sample or in the opposite direction. In the latter case the sectored disk is always in the beam opposite the sample, so that the transmission of the sample is measured relative to that of the disk.

IV. KOENIG-MARTENS SPECTROPHOTOMETER

The type of instrument used for the spectrophotometric measurements is described in papers by Koenig,[9] Martens,[10] Martens and Greenbaum,[11] and has become known as the Koenig-Martens spectrophotometer. The arrangement of some of the optical parts of the instrument [12] in the possession of this laboratory differs slightly, however, from that described in the paper last cited. The optical system is shown in Figure 3; and, to conserve space in this figure, the plan of the optical system is displaced from its proper position relative to the plan of the illumination apparatus.

The theory and method of use of the instrument is given in the following pages, along with a discussion of some possible sources of error in the spectrophotometric measurements.

1. THEORY OF THE INSTRUMENT

A diaphragm placed over the jaws of the (horizontal) collimator slit divides this slit into two parts (*A* and *B*, fig. 3), which are of equal length and width and separated by one slit length from each other. The double collimator slit thus formed is provided with an accurate bilateral adjustment for width.

A Wollaston (double image) prism and a biprism are permanently mounted as a unit on the telescope lens, with the line of intersection

[9] Ann. der Phys. and Chem., **53**, p. 783; 1894.
[10] Verh. der Deut. Phys. Gesellsch., **1**, p. 280; 1899.
[11] Ann. der Phys. (4), **12**, p. 984; 1903.
[12] Purchased from Schmidt and Haensch about 1912.

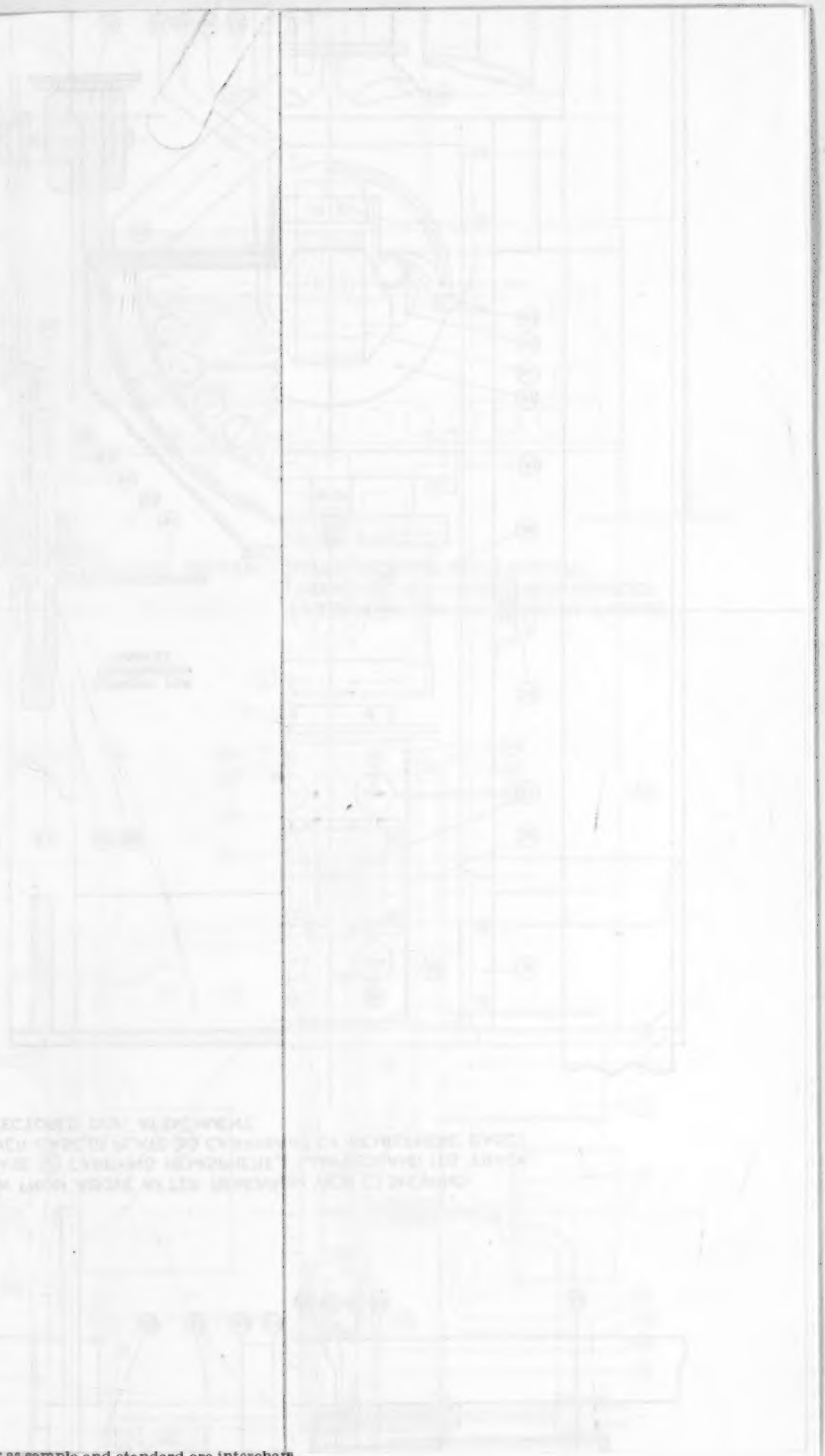

the other as sample and standard are interchan

109431°—28. (Face p. 814.)

UNIV OF MICH

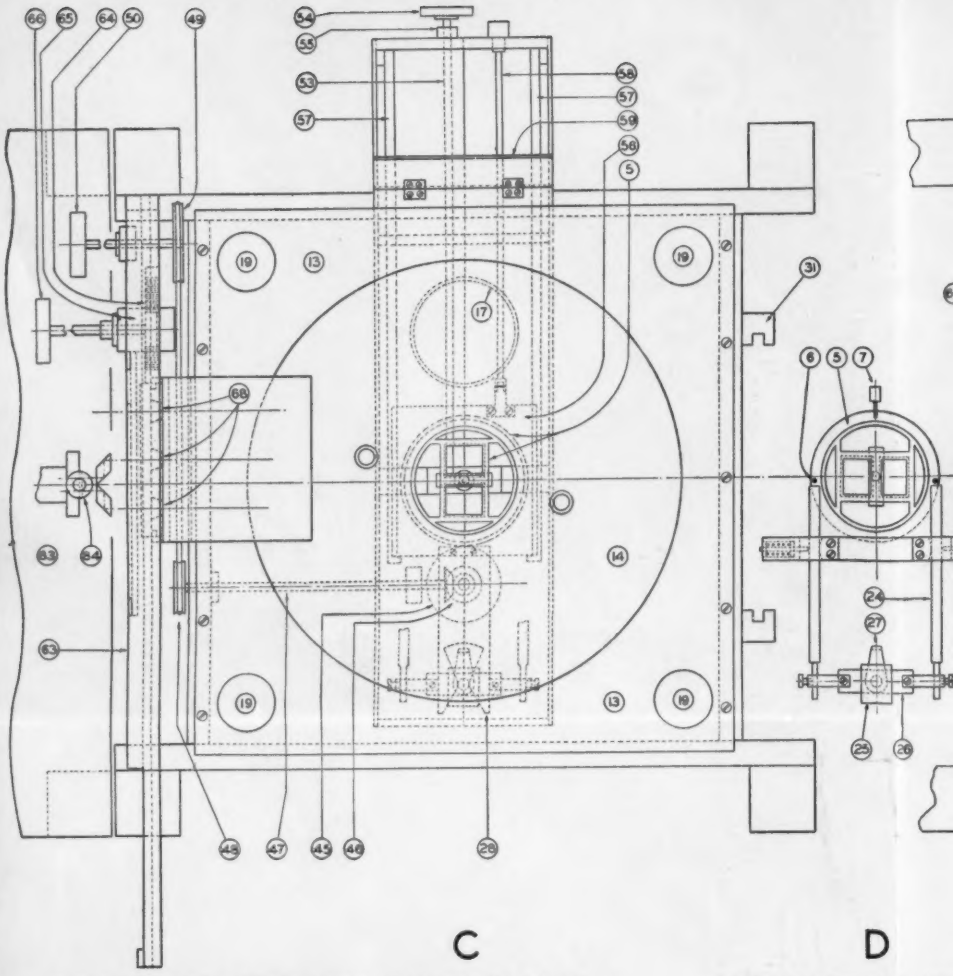

C

VIEW FROM ABOVE AFTER REMOVAL OF FOLLOWING PARTS:
(1) BASE (12) CARRYING HEMISPHERE, LAMP SUPPORT, AND OUTER COVER CASE; (2) PLATE (30), CARRYING TRANSMISSION SOURCES; (3) SECTORED DISK ATTACHMENT.

D

PART OF MECHANISM FOR
OPERATING AIR VALVE (2
(SEE ALSO VIEW E)

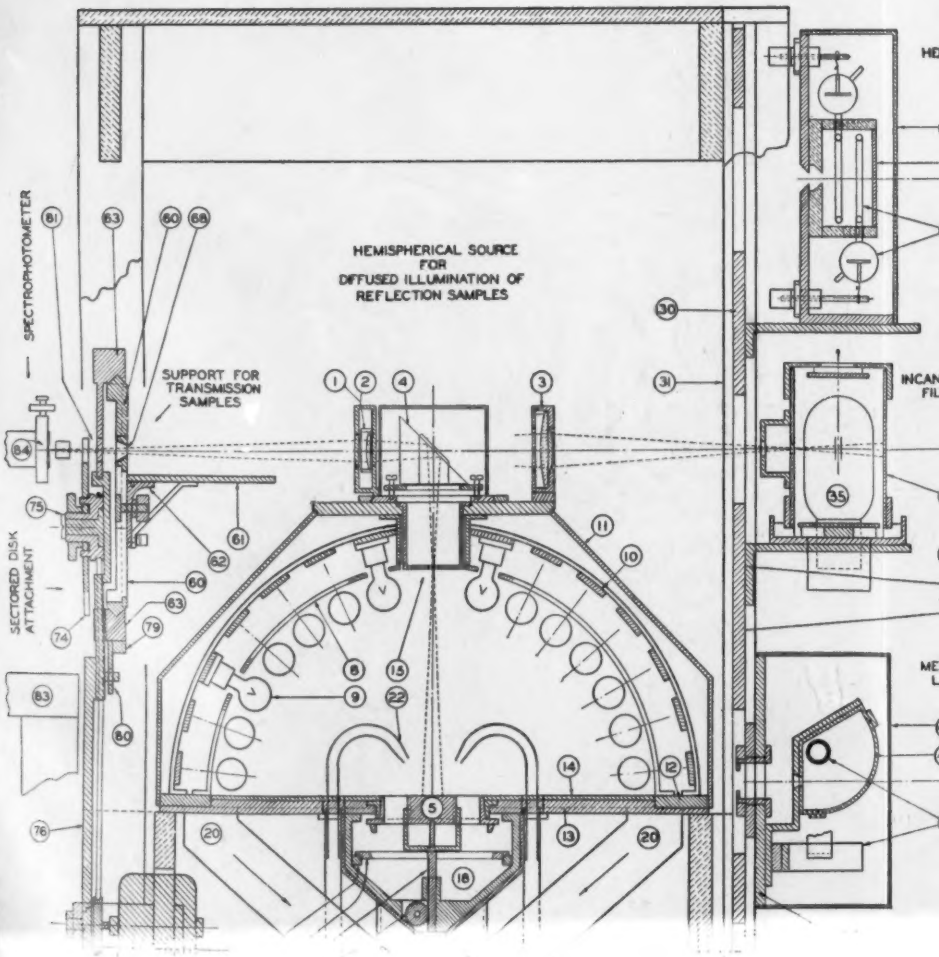
SPECTROPHOTOMETER
HEMISPHERICAL SOURCE FOR DIFFUSED ILLUMINATION OF REFLECTION SAMPLES
SUPPORT FOR TRANSMISSION SAMPLES
SECTORED DISK ATTACHMENT

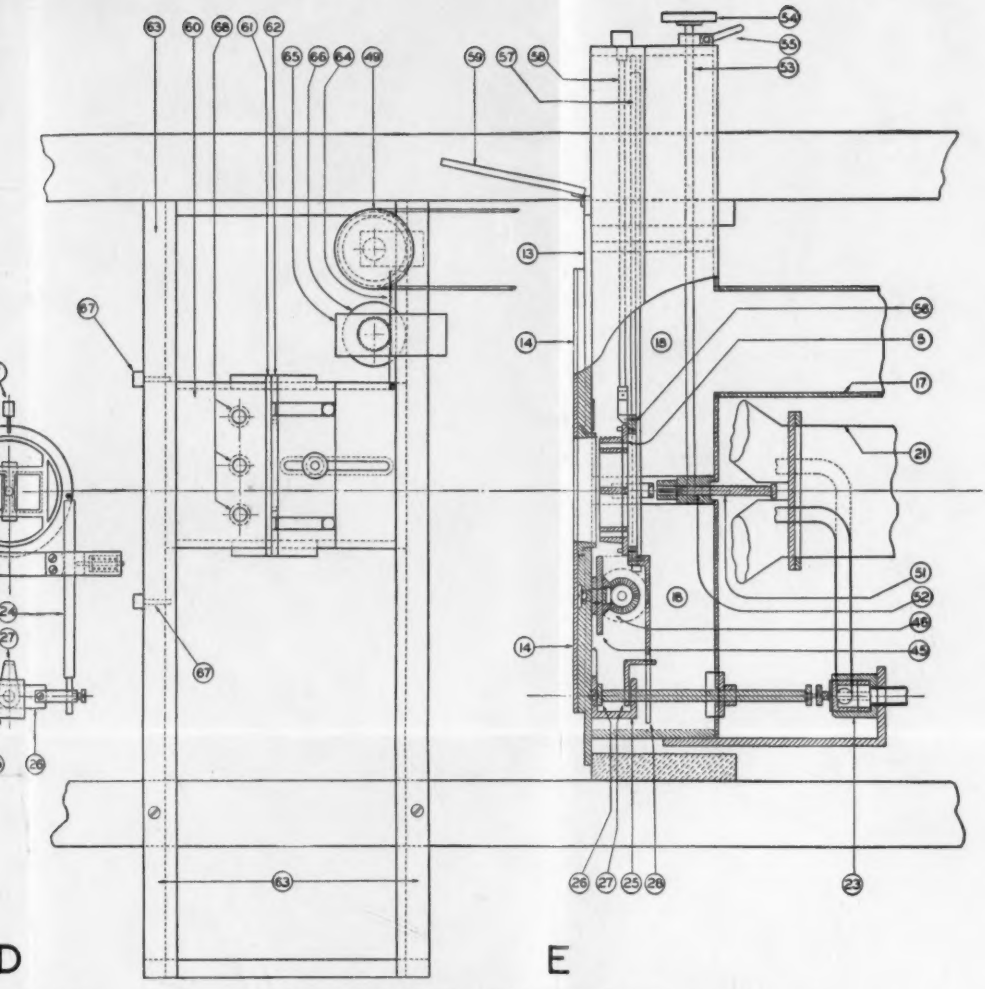

D

E

ANISM FOR
VALVE (23)
E)

ELEVATION (AS PROJECTED FROM VIEW C) SHOWING:
(1) SUPPORT FOR TRANSMISSION SAMPLES AND ITS TRACK;
(2) VERTICAL SECTION THRU PART OF HEMISPHERE BASE
AND COMPARTMENT (18).

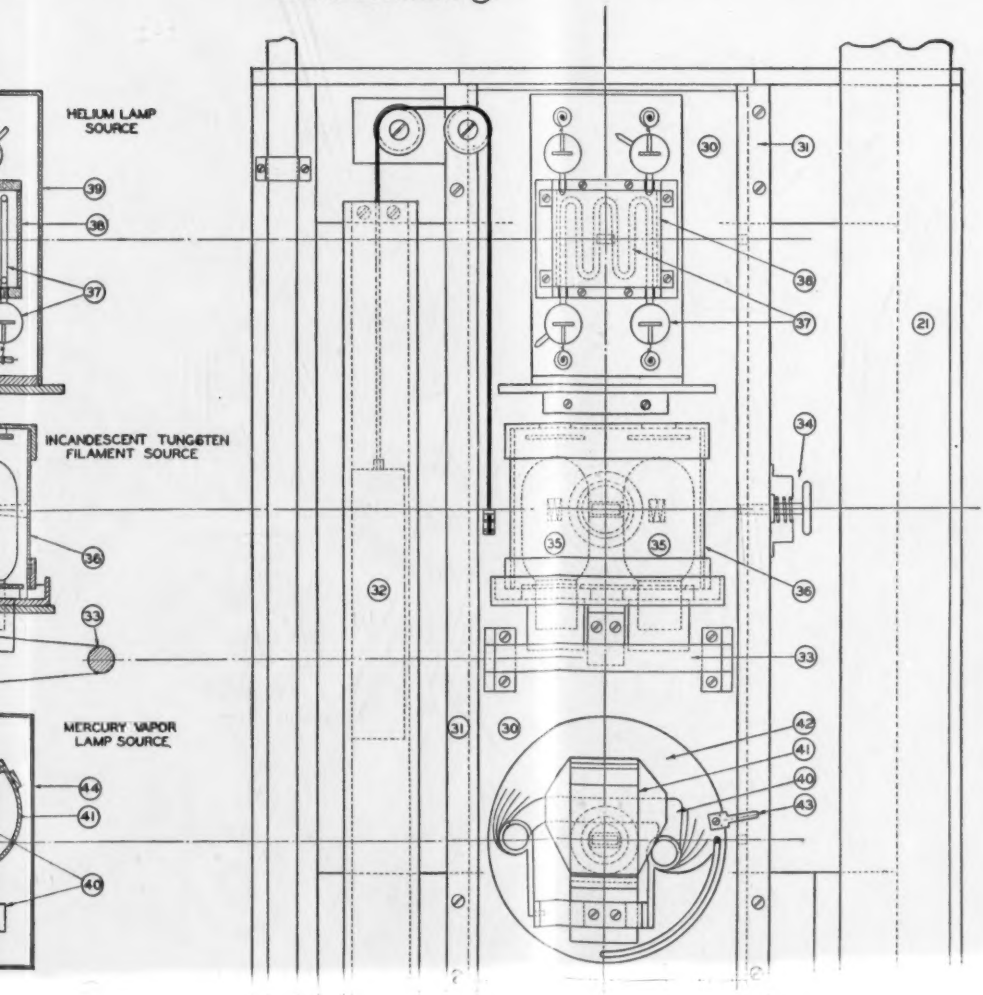

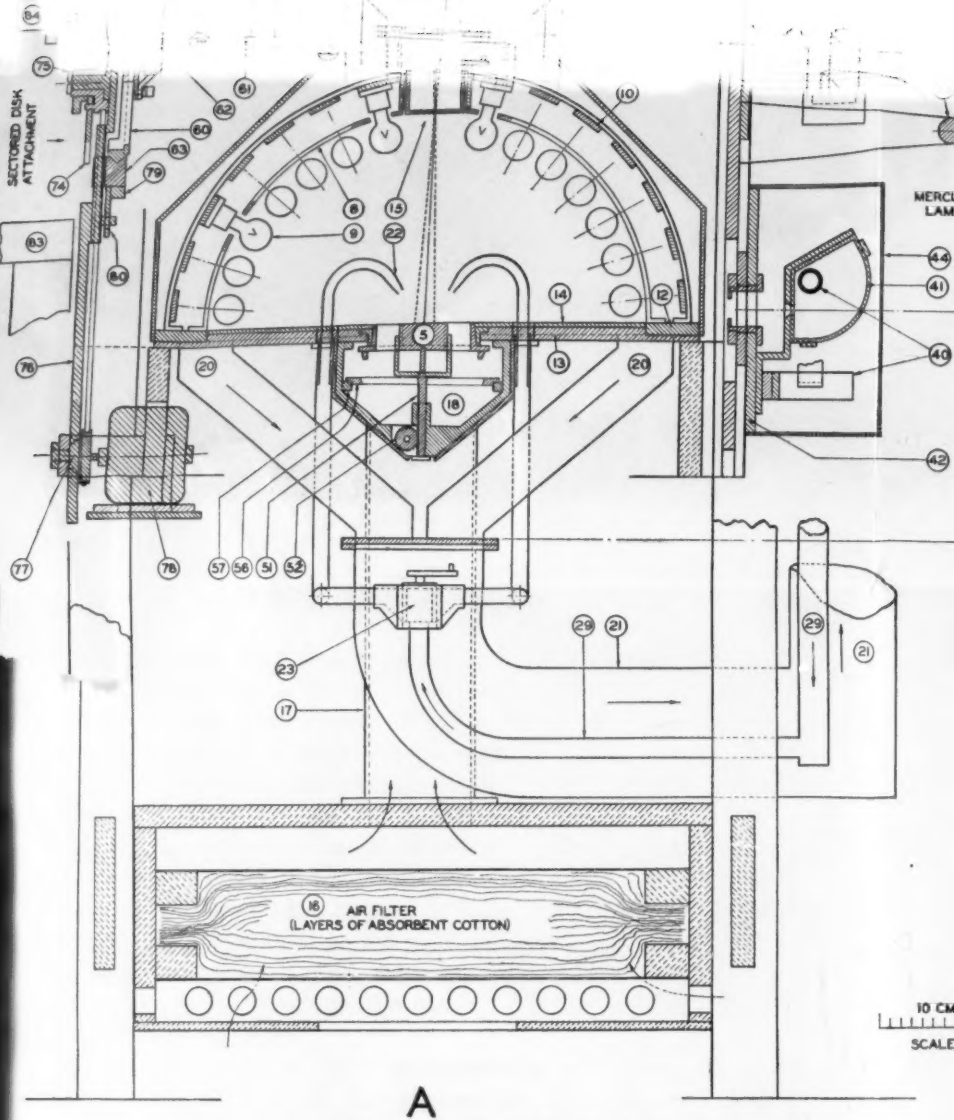

A

VERTICAL SECTION THRU POLE OF HEMISPHERE AND CENTER OF TRANSMISSION SOURCES.

FIG. 4.—*Diagram of illumination apparatus and accessory part*

KEY

1, 2. Lenses focusing collimator slits of spectrophotometer on slits (15), near pole of hemisphere.

3. Lens combination serving the double purpose of focusing the collimator slits of the spectrophotometer approximately at the aperture into lamp inclosures, and causing light for each beam to be taken from the same area of the wall of the inclosure.

4. Right-angle glass prism, reflecting light from sample and standard into spectrophotometer.

5. Holder for reflection sample and standard. (See detailed construction in fig. 5.)

6, 7. Pins and stop to prevent rotation of sample holder through more than 180°. The pins (6) also serve to operate air valve (23) through levers (24). (See views *D* and *E* of fig. 4.)

8. Steel hemisphere, spun from No. 18 gauge sheet enameling stock; diameter, 40 cm. Inner surface covered with two coats of white porcelain enamel (baked), then "smoked" with magnesium oxide deposited from burning magnesium shavings.

9. 9-volt, 27 c. p. (approximately 18 watts) gas-filled automobile headlight lamps; tipless spherical bulb 35 mm in diameter; candelabra screw base.

10. Hemispherical framework for support of lamps. Open construction; built of narrow aluminum strips.

11. Hemisphere cover case.

12. Upper base plate (49 cm square, with circular hole 40.6 cm in diameter) to which reflecting hemisphere, lamp support, and cover case are attached. Plate hinged to lower base plate (13).

13. Lower base plate, supported on wooden framework.

14. Circular mirror; polished nickel plating on brass.

15. Slits near pole of hemisphere through which light beams pass from sample and standard to spectrophotometer.

16. Air filter.

17. Pipe leading from air filter to compartment (18).

18. Air compartment.

19. Holes for passage of hot air from hemisphere into exhaust pipes (20).

20, 21. Exhaust air pipes leading to ventilating fans.

22. Quartz nozzles directing high velocity air stream on to sample.

23. Air valve which automatically shifts air jet from one quartz nozzle to the other as sample and standard are interchanged.

24 to 28. Mechanism for operation of air valv

29. Compressed-air supply line.

30. Plate supporting sources for transmissio

31. Vertical guide bars.

32. Counterweight.

33. Handle.

34. Spring catch, holding plate (30) in prope in transmission measurements.

35. 400-watt 110-volt gas-filled tungsten-filan

36. Lamp inclosure: Iron box, inner surface sphere (8).

37. Helium lamp.

38. Inclosure for helium lamps; inner su oxide.

39. Cover case for helium lamp source.

40. Quartz mercury-vapor lamp.

41. Inclosure for mercury lamp: Iron box w hemisphere (8).

42. Circular plate supporting mercury la plate mounted on hollow bearing through wh photometer.

43. Handle for rotating mercury lamp into

44. Cover case for mercury lamp source.

45. Gear wheel; teeth mesh with teeth on s

46. Bevel gears; one attached to wheel (45)

47. Drive shaft.

48, 49. Pulleys, connected by belt.

50. Handwheel with which observer inte standard.

51. Circular shaft, having teeth cut in one pinion (52). Weight of sample holder suppo

52. Pinion for vertical motion of shaft (51) raised from carriage (56) into position for refle

53. Shaft connecting pinion (52) with handw

54, 55. Handwheel and clamp on shaft (53).

56. Carriage on which sample holder is m shown in view *E* of Figure 4.

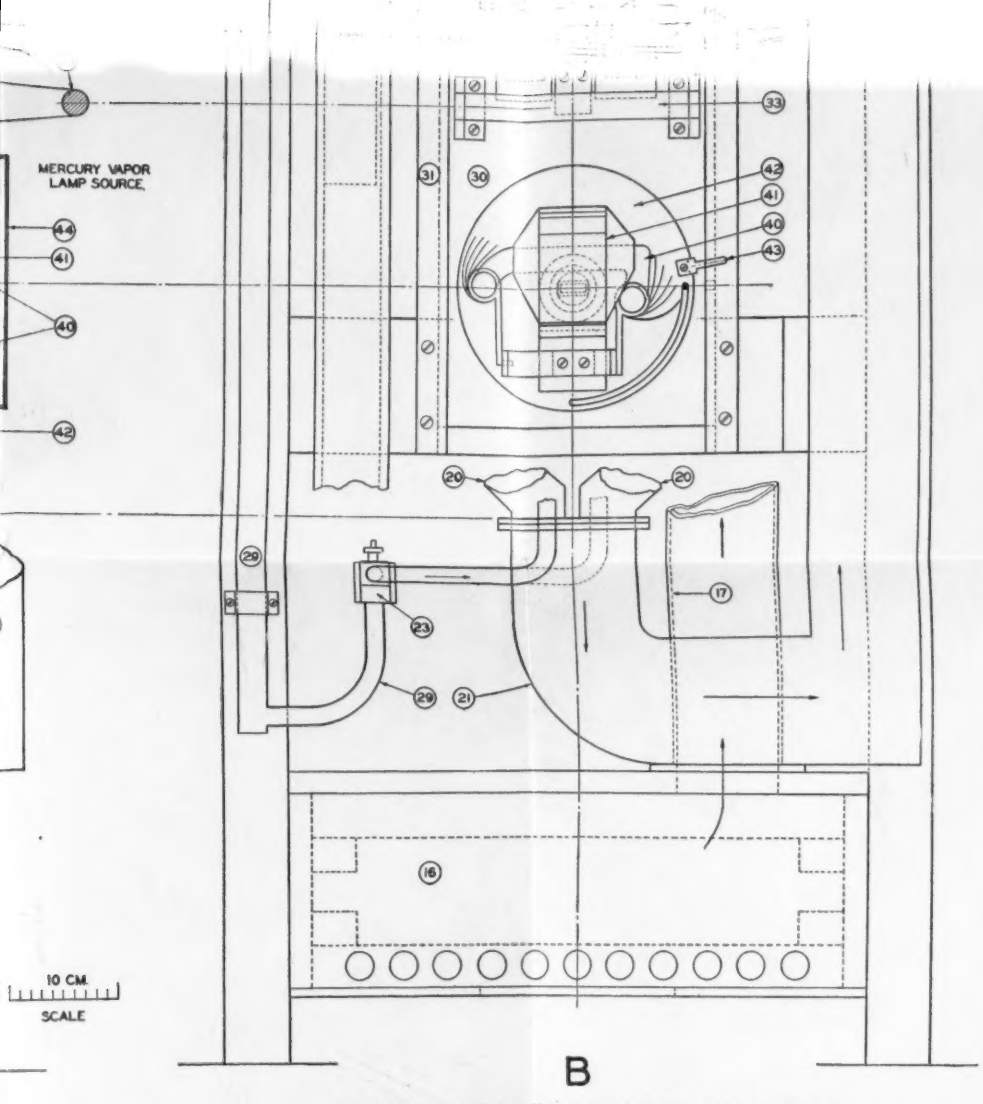

ELEVATION SHOWING: (1) PART OF VENTILATION SYSTEM; (2) CONSTRUCTION AND MOUNTING OF TRANSMISSION SOURCES. (COVER CASES REMOVED FROM HELIUM AND MERCURY LAMPS.)

sory parts for transmission and reflection measurements

KEY

on of air valve.

transmission measurements.

30) in proper position for use of either source

ngsten-filament incandescent lamps.

nner surface same as inner surface of hemi-

; inner surface smoked with magnesium

source.

Iron box with inner surface same as that of

mercury lamp and white-lined inclosure; through which light beams pass to spectro-

lamp into vertical position for starting.

source.

h teeth on sample holder.

wheel (45) and the other to shaft (47).

lt.

server interchanges reflection sample and

cut in one side, which engage with teeth of older supported on upper portion of shaft.

of shaft (51), so that sample holder may be tion for reflection measurements.

with handwheel (54).

n shaft (53).

holder is moved from door (59) to position

57. Track along which carriage slides.
58. Rod to move carriage along track.
59. Door to compartment (18) for insertion and removal of sample holder.
60. Support for transmission samples.
61. Removable platform (for long transmission samples).
62. Short platform; position adjustable vertically on plate (60).
63. Guide bars forming track for sample support.
64. Rack attached to sample-support plate (60); teeth of rack engage with pinion in gear box (65), which is in turn attached to shaft and handwheel (66).
65. Gear box.
66. Handwheel for moving sample support along track (63), thereby shifting sample from one beam to the other.
67. Stops to limit motion of sample support.
68. Apertures in plate (60) for light beams.
69. Constant-temperature box for support and temperature control of cells containing liquids.
70. Heat insulating covering.
71. Three cylindrical brass tubes, passing through constant-temperature box, into which cells are inserted. (Construction of cells shown in fig. 7.)
72. Inlet and outlet tubes for water circulation.
73. Mercury-in-glass thermometer.
74. Sectored disk.
75. Bearing and pulley for rotation of sectored disk.
76. Sectored-disk supporting arm.
77. Bearing about which arm (76) rotates as disk is moved from one beam to the other.
78. Motor with armature shaft centered on axis of bearing (77). Pulley on motor connected by belt to sectored disk pulley (75).
79. Rack attached to sectored disk supporting arm (76); teeth of rack engage with teeth of pinion in gear box (65).
80. Point of attachment of rack (79) to arm (76).
81. Apertures for light beams to spectrophotometer.
82. Knob and lever for throwing rack and pinion of sectored disk attachment into gear with handwheel (66).
83. Spectrophotometer table.
84. Collimator slits of spectrophotometer.

109431°—28. (Face p. 814.)

UNIV OF MICH

of the biprism faces in a vertical plane which is perpendicular to the plane of double refraction in the Wollaston prism and to the refracting edge of the dispersion prism. The biprism surfaces are made on a wedge-shaped piece of glass, which, with a similar wedge on the collimator lens, prevents the passage to the eye of multiply reflected rays from the optical surfaces.

In the following discussion all directions and displacements are referred to two mutually perpendicular planes, the intersection of which forms the axis of the optical system. One of these planes is conveniently chosen as the vertical plane perpendicular to the plane of double refraction in the Wollaston prism. The other plane coincides with the plane of the paper in the plan of Figure 3 and is hereafter called the horizontal plane.

Consider now a beam of light, homogeneous with respect to wave length and composed of all the elementary ray pencils diverging from various points of the collimator slit *A;* the compound bundle of rays is rendered approximately parallel by the collimator lens, is refracted by the dispersion prism, and falls on the surface of the telescope lens. If the Wollaston prism and the biprism were not in the path of this beam, the rays would be converged by the telescope lens to a focus in the plane of the ocular slit, forming a single image of the collimator slit *A*. Similarly, a single image of slit *B* would be formed. The two images would be equally displaced horizontally from the vertical reference plane, the displacement corresponding (with reversed sense) to the displacement of the slits *A* and *B* from the same vertical plane. With the Wollaston and biprism combination in place, however, the beam from slit *A* on traversing the Wollaston prism is split into two distinct beams which diverge slightly from each other in a horizontal plane and are each plane-polarized with their electrical vibrations in vertical and horizontal directions, respectively. Each of the two beams fills the two inclined faces of the biprism, their effective cross section being determined by the circular field aperture. As a result of the horizontal displacement of slit *A* from the axis of the optical system, the parallel beam entering the Wollaston prism is itself slightly inclined to the vertical reference plane. The construction of the Wollaston prism is such that the vibrations are vertical in the least refracted (with respect to the vertical plane) of the two beams emerging from the Wollaston prism. Following this least-refracted beam, we find it again divided into two (similarly polarized) beams by further refraction at the two inclined faces of the biprism. These beams finally form two plane-polarized images of the slit *A* in the plane of the ocular slit, the vibrations in each image being vertical. The images are designated by A_1v and A_2v in Figure 3, and their relative positions in the plane of the ocular slit are indicated in the displaced diagram of this slit

shown in the lower left corner of Figure 3. For clearness in the representation, various slit images are there shown in different planes; actually, they all lie in the plane of the ocular slit. Going back to the more refracted of the two beams emerging from the Wollaston prism, with vibrations in the horizontal plane, it is found to give rise similarly to the two images A_1h and A_2h of the slit A. In the same manner, light entering slit B finally forms the remaining four slit images shown. The angle of the biprism is chosen, with regard to the separation of the slits A and B and the construction of the Wollaston prism, so that two of the eight images overlap at the ocular slit. The designations A_1v and B_2h show that one of these images is formed by light entering slit A and passing through part 1 of the biprism photometric field. It is plane-polarized with vibrations in a vertical plane. The other image is formed by light from silt B passing face 2 of the biprism and is polarized with vibrations in a horizontal plane.

Considering in like manner all the ray pencils of various wave lengths entering the collimator slits, the different refraction of each homogeneous bundle by the dispersion prism results in eight vertical spectral images of slits A and B being formed in the plane of the ocular slit. Two of these spectra overlap at the ocular slit (as explained above), and a beam of light composed of a small equal range of wave lengths from each spectrum passes through the slit to the eye.

The ocular slit, telescope lens, and attached optical parts are mounted in a tube (the telescope tube) which can be rotated about a horizontal axis through the dispersion prism and the ocular slit thus moved to different parts of the spectrum. A scale attached to the tube indicates the part of the spectrum included by the ocular slit.

Looking through the ocular slit one sees, then, the surface of the biprism uniformly illuminated by monochromatic light of small wave-length range, the mean wave length corresponding to the position of the slit in the spectrum. The field of view is limited by the circular field aperture and divided into two equal parts by the line of intersection of the biprism surfaces. The lights in the two parts of the field are plane-polarized in directions mutually perpendicular to each other, the vibrations in the right half (field 1) being vertical. The brightnesses of the two parts of the field are not, in general, the same. Later discussion will show that this may be the result of unequal conditions of the entrant light beams, but is also caused by an unequal transmission of these beams through the instrument. By rotation of a nicol prism between the eye and the ocular slit the light in either part of the field may be extinguished or the principal plane of transmission of the nicol so orientated that the part fields become matched in brightness. This condition is accompanied by a disappearance of the dividing line between the

two parts of the field; and, in fact, this circumstance is used as the criterion for the equality of brightnesses. There will obviously be four positions of the principal plane of the nicol, one in each quadrant of the circle, for which this equality of brightnesses may be established. The mounting of the nicol, with its circular scale, may be seen in Figure 1.

The spectrophotometer is herein used to measure a change in the relative intensities [13] of the two beams of light entering the instrument, for a given wave length, or small spectral range, included in each beam. The measurement is effected by a comparison of the relative intensities of the beams before and after the change has taken place. In the use of any type of spectrophotometer for this purpose the polarizing action of the prism (or grating) dispersion system makes the reading of the instrument depend not only on the relative intensities of the entrant beams but also—to a lesser extent, usually—on the states of polarization of the two beams compared. It is therefore of importance to know under what conditions and to what extent a polarized condition of the entrant beams affects the measurements to be made with the Koenig-Martens instrument. In quest of this information, it will be instructive to consider all possible changes in the relative intensities and states of polarization of the two entrant beams on their independent paths from the source to the eye.

In the use of any one of the transmission sources previously described, let it be assumed that there is a difference between the initial intensities and states of polarization of beams 1 and 2 emitted to the spectrophotometer (fig. 3). Likewise, in the use of the hemispherical source, with an exact duplicate of the comparison standard occupying the position of the sample, the possibility of differences in the initial intensities and states of polarization of the two beams is considered. In the general use of the instrument, then, let the initial intensities and states of polarization of beams 1 and 2 be as represented in Figure 9. Here I_1, R_o, and L'_o represent the initial intensity and component amplitudes,[14] respectively, of beam 1, and I_2, R'_o, and L_o are of corresponding import for beam 2. A numerical expression for the polarization is given later in this section of the paper. The definition must obviously imply a given reference frame.

[13] The form of the beams of light entering the spectrophotometer and filling the photometric field of the instrument is determined by the dimensions of the optical system, and a section perpendicular to the axis of the beam varies in size at different positions along the axis. It is convenient to use the expression "intensity of the beam" or beam intensity for the total luminous flux through a cross section of the beam. At the photometric field this section is equal, of course, in shape and area to that of the field itself.

[14] In these considerations of the state of polarization we are not concerned with any phase differences which may possibly exist between the component vibrations in either beam; only changes in the amplitudes of the components are of interest. The word polarization, as used throughout this paper, refers only to this resolution of all the independent vibrations in the beam along two mutually perpendicular directions (which are not necessarily the principal directions of the vibration), giving the resultant magnitude of the amplitude vectors shown in the figures. The square of the vector sum of these components is proportional to the intensity of the beam.

It is most convenient to resolve the component amplitudes in directions always parallel and perpendicular, respectively, to the vertical reference plane previously defined, so that the directions of the component amplitudes then coincide with the principal directions of vibration in the Wollaston prism.

On passing through the spectrophotometer, both beams traverse optically identical paths. Through the operation of the Fresnel reflection laws at the surfaces of the dispersion prism, however, light with vibrations perpendicular to the refracting edge of the prism (vertical component) is more copiously transmitted than that vibrating parallel thereto. After quadruple subdivision of each beam by the Wollaston and biprism combination (as previously explained), the vertical component amplitude R of the beam passing the ocular

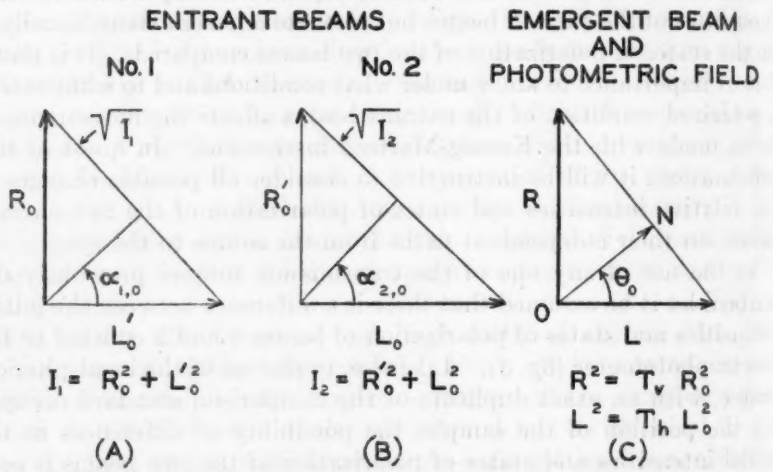

FIG. 9.—*Initial condition of the entrant beams, emergent beam (from ocular slit), and photometric field, before insertion of sample in either beam*

slit from field 1 is a certain fraction $\sqrt{T_v}$ of the vertical component amplitude R_0 of beam 1 before entering the instrument. Similarly, the horizontal component amplitude L of the beam passing the ocular slit from field 2 is a fraction $\sqrt{T_h}$ of the horizontal component amplitude L_0 of beam 2. The components R'_0 and L'_0 of the entrant beams contribute nothing to the intensity of the emergent beam. They are lost in the instrument.

The factors T_v and T_h are the *transmissions* of the optical system as a whole (excluding the nicol) for plane-polarized light with vibrations in vertical and horizontal directions, respectively. Thus, $R^2 = T_v R^2_0$ and $L^2 = T_h L^2_0$.

The quantities R and L are proportional, respectively, to the areas of parts 1 and 2 of the photometric field. These areas are equal, however, and hence the brightnesses in the two parts of the field, as

viewed through the nicol and ocular slit, are proportional, respectively, to the squares of the projections of R and L on the principal plane of transmission of the nicol. Let ON (fig. 9, C) represent the angular position of the principal plane of the nicol, measured (in each quadrant) from the position for extinction of the vertical component amplitude of the emergent beam (position for extinction of light in the right field). Let θ_o be the position of ON when the two parts of the field are matched in brightness; then

$$R^2 \sin^2 \theta_o = L^2 \cos^2 \theta_o$$

or

$$\frac{L^2}{R^2} = \tan^2 \theta_o \qquad (1)$$

When the component amplitudes R_o and L_o of the entrant beams are equal, the angle θ_o is approximately 39° (instead of the ideal 45°, for $T_h = T_v$); hence

$$\frac{T_h}{T_v} = \tan^2 39° = 0.656$$

The difference between the transmissions of two plane-polarized beams with vibrations in vertical and horizontal directions, respectively, is principally the result of the polarizing action of the dispersion prism. The angle θ_o is not constant, but varies slightly with the wave-length setting.

Now, let the initial intensity and state of polarization of beam 1 be changed. This change may be brought about, for example, by the insertion of a transmission sample in the beam or by the replacement of one of the reflection standards by a sample the spectral reflective properties of which are to be determined. Let X represent the fractional reduction in the intensity of the beam in either case. Then the amplitudes R_o and L'_o are both reduced by the factor $\sqrt{X}$. The quantity X is the *transmission* of the sample in the first case, and the *brightness ratio* previously specified (section I) in the second case. The change in the state of polarization of beam 1 may be represented by two factors, a and b', attached, respectively, to the components R_o and L'_o. These factors are not independent of each other, but are related by the equation

$$a^2 R_o^2 + b'^2 L'^2_o = R_o^2 + L'^2_o \qquad (2)$$

The condition of beams 1 and 2 entering the spectrophotometer (entrant beams), the condition of the combined beams passing through the ocular slit (emergent beam), and the brightness relations in the matched photometric field are now as represented in Figure 10.

Let θ_1 be the angular position of the nicol for the equality of brightnesses in the photometric field; then

$$Xa^2R^2 \sin^2 \theta_1 = L^2 \cos^2 \theta_1$$

or

$$a^2X = \frac{L^2}{R^2} \cot^2 \theta_1 = \tan^2 \theta_0 \cot^2 \theta_1 \tag{3}$$

Now, let the transmission sample be shifted to beam 2, or let the positions of reflection sample and standard be interchanged. Then the intensity of beam 2 is reduced by the fraction X, which is the same as in the previous case. The change in the state of polarization of beam 2 may be different than in the previous case but represented in like manner by the factors a' and b, for which

$$a'^2R'^2_0 + b^2L_0^2 = R'^2 + L_0^2 \tag{4}$$

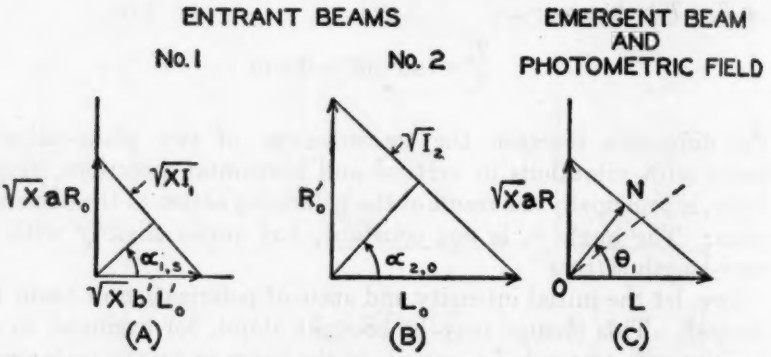

FIG. 10.—*Condition of entrant beams, emergent beam (from ocular slit), and photometric field, after insertion of sample in beam 1*

The corresponding conditions of the beams and the photometric field are now as shown in Figure 11. Let θ_2 be the new position of the nicol for the equality of brightnesses in the photometric field; then

$$R^2 \sin^2\theta_2 = X b^2 L^2 \cos^2\theta_2$$

or

$$b^2X = \frac{R^2}{L^2} \tan^2\theta_2 = \cot^2\theta_0 \tan^2\theta_2 \tag{5}$$

By combination of equations (3) and (5) the angle θ_0 is eliminated; so that we may write

$$ab\,X = \cot \theta_1 \tan \theta \tag{6}$$

From equations (3), (5), and (6) it is evident that any initial differences in the beam intensities or any degree of polarization of the light emitted by the source along beams 1 and 2 does not affect the measurement of X; any *change* in the state of polarization, brought

about by the introduction of a transmission or reflection sample into either beam, must be considered, however, in the measurements. The polarization factors a and b can be expressed in terms of the

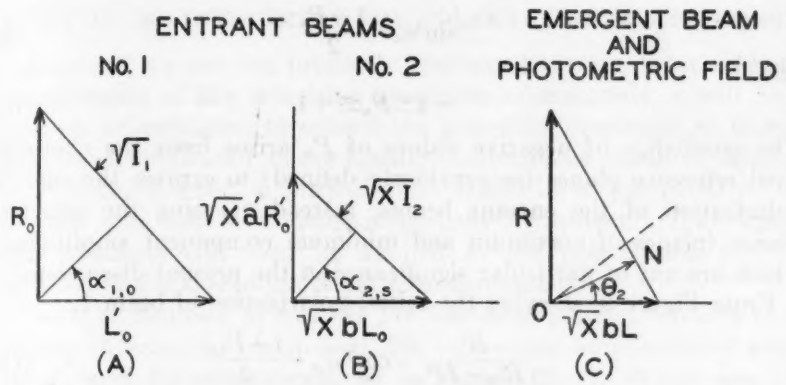

FIG. 11.—*Condition of entrant beams, emergent beam (from ocular slit), and photometric field, after shifting of sample to beam 2*

angles $\alpha_{1,o}$, $\alpha_{1,s}$, $\alpha_{2,o}$, and $\alpha_{2,s}$, of Figures 9, 10, and 11, and also in terms of the directly measurable *fractional polarizations* $P_{1,o}$, P_{1s}, $P_{2,o}$, and $P_{2,s}$. The latter quantities express the states of polarization of beams 1 and 2 before and after the insertion of the sample.

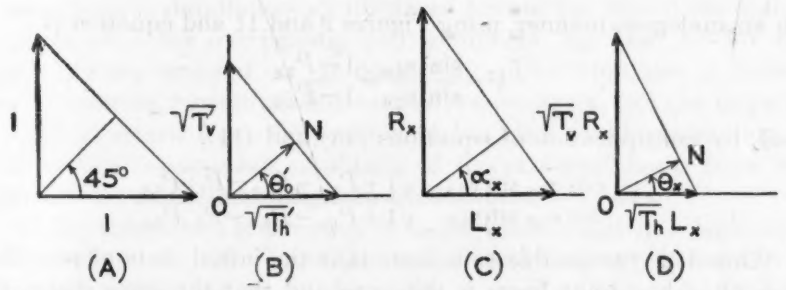

FIG. 12.—*Representation of the states of polarization of the entrant beam and emergent beam (from ocular slit), when the Koenig-Martens instrument is used as a spectropolarimeter with single central slit. (A) and (C), non-polarized and polarized entrant beams, respectively; (B) and (D), corresponding emergent beams and conditions in photometric field*

Let the subscript "x," as in Figure 12 C, refer to any case of polarization an expression for which is desired. The *fractional polarization* is defined as follows:

$$P_x = \frac{R^2_x - L^2_x}{R^2_x + L^2_x} = \cos^2 a_x - \sin^2 a_x = \cos 2a_x \qquad (7)$$

Hence

$$\cos^2 a_x = \frac{1+P_x}{2} \tag{8}$$

$$\sin^2 a_x = \frac{1-P_x}{2} \tag{9}$$

and

$$-1 \leq P_x \leq +1 \tag{10}$$

The possibility of negative values of P_x arises from the choice of fixed reference planes (as previously defined) to express the state of polarization of the entrant beams, instead of using the principal planes (planes of maximum and minimum component amplitudes), which are not of particular significance in the present discussions.

From Figure 9, showing the initial polarization of beam 1,

$$\frac{R^2_o}{R^2_o + L'^2_o} = \cos^2 a_{1,o} = \frac{1+P_{1,o}}{2} \tag{11}$$

and, from Figure 10, after insertion of the sample,

$$\frac{a^2 R^2_o}{a^2 R^2_o + b'^2 L'^2_o} = \cos^2 a_{1,s} = \frac{1+P_{1,s}}{2} \tag{12}$$

Dividing (12) by (11) and using equation (2),

$$a^2 = \frac{\cos^2 a_{1,s}}{\cos^2 a_{1,o}} = \frac{1+P_{1,s}}{1+P_{1,o}} \tag{13}$$

In an analogous manner, using Figures 9 and 11 and equation (4),

$$b^2 = \frac{\sin^2 a_{2,s}}{\sin^2 a_{2,o}} = \frac{1-P_{2,s}}{1-P_{2,o}} \tag{14}$$

and, by multiplication of equations (13) and (14),

$$ab = \frac{\cos a_{1,s} \sin a_{2,s}}{\cos a_{1,o} \sin a_{2,o}} = \frac{\sqrt{1+P_{1,s}-P_{2,s}-P_{1,s}P_{2,s}}}{\sqrt{1+P_{1,o}-P_{2,o}-P_{1,o}P_{2,o}}} \tag{15}$$

When it is permissible to assume that the initial state of polarization of each entrant beam is the same and that the same change in the state of polarization occurs when the sample is inserted in either beam, then

$$a_{1,o} = a_{2,o} = a_o$$
$$a_{1,s} = a_{2,s} = a_s$$

and equations (13), (14), and (15) become

$$a^2 = \frac{\cos^2 a_s}{\cos^2 a_o} = \frac{1+P_s}{1+P_o} \tag{16}$$

$$b^2 = \frac{\sin^2 a_s}{\sin^2 a_o} = \frac{1-P_s}{1-P_o} \tag{17}$$

$$ab = \frac{\sin 2a_s}{\sin 2a_o} = \frac{\sqrt{1-P_s^2}}{\sqrt{1-P_o^2}} \tag{18}$$

The polarization factors a and b are, in general, functions of wave length. The measurement of these quantities is discussed in the following section.

2. USE OF THE INSTRUMENT FOR POLARIZATION MEASUREMENTS

Although we are not primarily concerned in this paper with the measurement of the polarizing properties of materials, it will be of interest, nevertheless, to extend the preceding discussion to include the general application of the Koenig-Martens instrument to polarization measurements, a purpose for which it is particularly well adapted and has been extensively used by others.[15] The theory thus available will then be applied to the polarization problem involved in the spectrophotometric measurements.

Let it be required to measure the fractional polarization of a beam of light entering the instrument, the component amplitudes of which are R_x and L_x, respectively, as in Figure 12, C. There are two methods of use of the instrument for this purpose, corresponding, respectively, to the use of a single central collimator slit or to the double collimator slit arrangement shown in Figure 3.

To use the central-slit method, let the diaphragm previously described as dividing the collimator slit into two parts, A and B, be displaced horizontally until slit A (or slit B) is centered on the axis of the optical system. The A (or B) images in the plane of the ocular slit are simultaneously displaced toward the axis of the optical system until the overlapping pair of images A_1h and A_2v (or B_1h and B_2v) are centered on the ocular slit. The vibrations in fields 1 and 2 are now horizontal and vertical, respectively, but the angle θ_x is still measured from the position of the nicol for the extinction of the vertical component amplitude of the emergent beam (now the position for extinction of light in the left field).

If the instrument is arranged to be movable bodily in a horizontal direction, so that the (now) central slit may occupy either of the positions previously occupied by slits A or B in Figure 3, the light entering the instrument along either beam 1 or beam 2 may then be analyzed in the manner to be described, both before and after the insertion of the sample. The fractional polarization P_x obtained in each case will be the required value of $P_{1,o}$, $P_{1,s}$, $P_{2,o}$, or $P_{2,s}$ in equations (13), (14), and (15).

The absolute intensity of the entrant beam does not enter explicitly into the polarization measurements; hence, the component amplitudes of a nonpolarized entrant beam may each be taken as unity (fig. 12, A). Let θ'_o be the angular position of the nicol for the equality

[15] Woronkoff, G. P., and Pokrowski, G. J., Zeit. f. Physik., **30**, p. 129; 1924 (and in later papers by one or both of these authors). Wawilow, S. J., Zeit. f. Physik., **32**, p. 721; 1925.

of brightnesses in the photometric field when the entrant beam is nonpolarized; then (fig. 12, B)

$$\frac{T_h}{T_v} = \tan^2 \theta'_o \tag{19}$$

where T_h and T_v are again the transmissions of the instrument.

When the entrant beam is polarized, however, with component amplitudes R_x and L_x, respectively, the conditions of the entrant beam and the beam transmitted by the ocular slit (emergent beam) are as represented in Figure 12, C and D. For the entrant beam

$$\frac{L_x}{R_x} = \tan \alpha_x \tag{20}$$

and for the emergent beam

$$\sqrt{\frac{T_h}{T_v}} \cdot \frac{L_x}{R_x} = \tan \theta_x \tag{21}$$

where θ_x is the new angular position of the nicol for equality of brightnesses in the photometric field. Hence

$$\tan \alpha_x = \cot \theta'_o \tan \theta_x \tag{22}$$

If, now, it be possible to rotate the source of polarization relative to the measuring instrument through an angle of 90° about the axis of the entrant beam, or, by any other means, to reverse the magnitudes of the component amplitudes R_x and L_x in Figure 12, C, then the angle θ'_o may be eliminated from the polarization measurements. In the case of a reflection sample, under the symmetrical (nonpolarized) illumination from the hemispherical source, this reversal of the amplitudes R_x and L_x in the reflected beam is effected simply by a rotation of the sample in its own plane through an angle of 90° about the prescribed axis.

Let the subscripts "x" and "y" refer, respectively, to the direct and reverse conditions of the entrant beam; then, in the first case,

$$\tan \alpha_x = \cot \theta'_o \tan \theta_x$$

and in the second case,

$$\tan (90 - \alpha_x) = \cot \theta'_o \tan \theta_y$$

Dividing one equation by the other,

$$\tan^2 \alpha_x = \tan \theta_x \cot \theta_y \tag{23}$$

Hence

$$P_x = \frac{R_x^2 - L_x^2}{R_x^2 + L_x^2} = \frac{1 - \tan^2 \alpha_x}{1 + \tan^2 \alpha_x}$$

$$= \frac{\tan^2 \theta'_o - \tan^2 \theta_x}{\tan^2 \theta'_o + \tan^2 \theta_x}, \text{ by (22)} \tag{24}$$

$$= \frac{\tan \theta_y - \tan \theta_x}{\tan \theta_y + \tan \theta_x}, \text{ by (23)} \tag{25}$$

In the applications of the Koenig-Martens instrument to polarization measurements it is usually not necessary to replace the double collimator slit by a single central slit. The double-slit arrangement may be regarded as effectually but a splitting and separation of the vertical and horizontal component amplitudes of the single entrant beam analyzed above; for, as previously shown, only the vertical component of beam 1 and the horizontal component of beam 2 contribute to the brightnesses of fields 1 and 2, respectively. If the source of the polarized light to be measured is extended over a large enough area and is sufficiently uniform so that the state of polarization of each of the entrant beams is the same, the double-slit arrangement is then equivalent to the use of the single central slit.

The component amplitudes R_x and L_x of Figure 12, C may now be regarded as the vertical and horizontal components, respectively, of beams 1 and 2, and equations (24) and (25) apply without modification to this case. The intensities of the polarized entrant beams need not be the same, provided that the angle θ'_0 (now the angle θ_0 of equation (1)) is determined for the same relative intensities of two nonpolarized entrant beams or that the method of rotating the sample through 90° is used.

The required conditions for the measurement of the polarization of the transmitted or reflected light may be approximately realized with the apparatus herein described by placing two specimens of the same samples orientated in the same way in each beam. It must be assumed, however, that the two specimens are identical, so that the state of polarization of each entrant beam is the same.

3. USE OF THE INSTRUMENT FOR REFLECTION AND TRANSMISSION MEASUREMENTS

(*a*) The Polarization Problem: Simplified Formulas.—In the preceding discussion the general theory of the use of the instrument in the measurement of the relative intensities and states of polarization of the entrant beams has been considered. This theory may now be simplified in its application to the measurement of the particular transmissive and reflective properties previously specified. It will be shown that a quantitative consideration of the polarization factors may always be avoided in the measurement of X with the present illumination apparatus and method of use of the instrument.

The construction of the light sources herein described is such that one would expect to find very little polarization of the light emitted directly to the spectrophotometer. Moreover, any polarization present would be practically the same for all wave lengths. To meet the conditions required in the measurement of the fractional polarization of the light from these sources, it is more convenient and wholly ade-

quate for the purpose to use the Martens [16] polarization photometer (with central aperture) instead of the spectrophotometer.

The general theory and optical principles involved in the construction, operation, and use of this instrument for both relative intensity and polarization measurements are the same as described on the preceding pages for the Koenig-Martens spectrophotometer. The essential difference in the construction of the two instruments lies in the absence of a dispersion system in the Martens photometer. When used with central aperture the instrument measures an average polarization for all wave lengths contained in the entrant beam. The angle θ'_0 (equation (19)) for this instrument is practically 45°; so that equations (24) and (25) both reduce, in this case, to the single equation

$$P_x=\frac{1-\tan^2\theta_x}{1+\tan^2\theta_x}=\frac{\cos^2\theta_x-\sin^2\theta_x}{\cos^2\theta_x+\sin^2\theta_x}=\cos 2\theta_x \qquad (26)$$

Using the Martens photometer, then, in the same manner as described for the spectrophotometer with central slit, it has been found that the initial polarization of the light emitted to the spectrophotometer from the tungsten, mercury-vapor, and helium lamp sources is in each case less than 1 per cent. Under the symmetrical illumination from the hemispherical source, there is no appreciable polarization of the normally reflected light from a sample having no structural regularities differing markedly in mutually perpendicular directions parallel to its surface. The comparison standard used is a material of this type. (See section V, 2.)

In the case of some reflection samples, however, including certain types of textile materials, such as velvets and plushes, there is, in general, an appreciable polarization of the normally reflected light even under completely diffused nonpolarized illumination.

To illustrate the case, the spectral polarization curves of four textile samples have been obtained with the Koenig-Martens instrument, used as a spectropolarimeter with double collimator slit. The curves are shown in Figure 13. In accordance with the theory of polarization measurements, two (square) specimens of each sample were mounted on heavy cardboard and inserted, one in each beam, in the regular position of the sample and standard. The photometric part fields of the instrument were matched with the specimens in the 0 and 90° positions ("x" and "y" positions), giving the angles θ_x and θ_y, respectively. The fractional polarization was then computed by equation (25). The initial (or "x") orientation of each sample was chosen to give the maximum positive polarization of the entrant beams as referred to the vertical plane, so that the data would serve as an illustration of the magnitude of the polarization effect

[16] Martens, F. F., Phys. Zeit. **1**, pp. 299-303; 1900.

which may be obtained in practical cases. In these measurements it is assumed that the state of polarization of the light reflected from each of the specimens is the same. This condition depends, of course, on the uniformity of the two specimens and is fulfilled to a sufficient approximation for these purposes, for an interchange of the specimens from one beam to the other had but slight effect on the angles θ_x and θ_y.

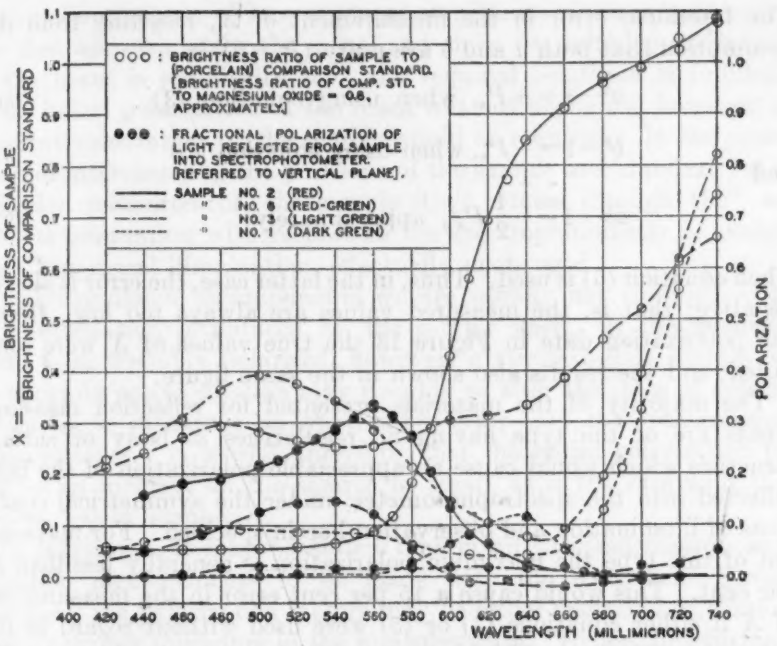
○○○ : BRIGHTNESS RATIO OF SAMPLE TO (PORCELAIN) COMPARISON STANDARD. [BRIGHTNESS RATIO OF COMP. STD. TO MAGNESIUM OXIDE = 0.8, APPROXIMATELY.]
●●● : FRACTIONAL POLARIZATION OF LIGHT REFLECTED FROM SAMPLE INTO SPECTROPHOTOMETER. [REFERRED TO VERTICAL PLANE].
SAMPLE NO. 2 (RED)
" NO. 6 (RED-GREEN)
" NO. 3 (LIGHT GREEN)
" NO. 1 (DARK GREEN)
X = BRIGHTNESS OF SAMPLE / BRIGHTNESS OF COMPARISON STANDARD
POLARIZATION
WAVELENGTH (MILLIMICRONS)
400 420 440 460 480 500 520 540 560 580 600 620 640 660 680 700 720 740
0.0 0.1 0.2 0.3 0.4 0.5 0.6 0.7 0.8 0.9 1.0 1.1

FIG. 13.—*Reflection and polarization measurements made with the Koenig-Martens spectrophotometer, under the specified conditions of illumination and observation*

Samples were chosen from certain textile materials in order to illustrate, particularly, the degree of polarization of the normally reflected light under nearly completely diffused nonpolarized illumination. The orientation of the sample (in its own plane) was chosen to obtain the maximum polarization with reference to the vertical plane.

Samples Nos. 2 and 3 are cotton back, silk cut-pile fabrics (velvets). No. 1 is a warp face sateen silk. No. 6 is a plain weave broadcloth with a silk warp (dyed green) and a rayon filling (dyed pink).

Replacing one of the specimens by the comparison standard, the values of abX for various wave lengths were obtained in the regular way (described later in this section) as the product cot θ_1 tan θ_2 by equation (6).

It is now of interest to determine the difference between the measured quantity abX and the value of X itself. Having shown that the initial polarization of the light emitted to the spectrophotometer by the hemispherical source (light reflected from comparison standard) and by the transmission sources is very small, equations

(16), (17), and (18) may then be further simplified by placing $P_o=0$. Thus

$$a^2=2\cos^2\alpha_s=1+P_s \tag{27}$$

$$b^2=2\sin^2\alpha_s=1-P_s \tag{28}$$

$$ab=\sin 2\alpha_s=\sqrt{1-P_s^2}=1-\frac{1}{2}P_s^2, \text{ approximately} \tag{29}$$

The fractional error in the measurement of X, resulting from the assumption that both a and b are unity ($P_s=0$), is

$$a^2-1=+P_s, \text{ when using equation (3)} \tag{30}$$

$$b^2-1=-P_s, \text{ when using equation (5)} \tag{31}$$

and

$$ab-1=-\frac{1}{2}P_s^2, \text{ approximately} \tag{32}$$

when equation (6) is used. Thus, in the latter case, the error is always negative; that is, the measured values are always too low. From the polarization data in Figure 13 the true values of X were computed, and the results also shown in the same figure.

The majority of the materials presented for reflection measurements are of the type having no regularities in body or surface structure which would cause an appreciable polarization of the light reflected into the spectrophotometer, under the symmetrical conditions of illumination and observation herein specified. For materials not of this type the maximum polarization is generally less than 15 per cent. This would cause a 15 per cent error in the measurement of X if either equations (3) or (5) were used without regard to the polarization factors. Using equation (6), however, in this way, the error is only 1 per cent. Sample No. 2 (fig. 13) represents an extreme case. The polarization of 33 per cent at wave length 560 mμ would cause an error of 5.5 per cent in the measurement of X, if the polarization of the reflected light is not taken into consideration.[17]

As may be seen from the curves of Figure 13, the polarization is generally higher in the spectral regions wherein the material strongly absorbs the incident light. Superposed on this effect, however, there appears to be a general decrease in the polarization for shorter wave lengths.

The polarization errors in the measurement of X may be reduced to negligible proportions by proper orientation of the sample in its own plane, for it is always possible in this way to reduce the polari-

[17] It may be noted that the polarization errors herein considered are not particularly inherent in the use of the Koenig-Martens spectrophotometer. Thus, in the case of another type of spectrophotometer containing no polarizing parts whatever other than the dispersion prism, a 33 per cent polarization of the light reflected from the sample would cause an error of 10 per cent in the measurement of X. Such a spectrophotometer is part of the equipment briefly described later in section V, 2.

zation factors a and b each to unity, leaving the initial state of polarization of the entrant beam unchanged. An inspection of the sample structure will usually be sufficient to determine the reference plane of maximum polarization (positive or negative) under the symmetrical hemispherical illumination, and the sample may then be cut and mounted in the sample holder so that this plane of maximum polarization makes an angle of approximately 45° with the vertical reference plane previously defined (through the optical axis of the spectrophotometer). The component amplitudes of the entrant beam are then approximately the same, and since the initial polarization of the beam is practically zero, the required condition is fulfilled. If the initial polarization of the beam was not negligible, however, a different orientation of the sample would be required. In the operation of interchanging the positions of the sample and standard for a reflection measurement, the sample itself rotates through 180°, so that its orientation with respect to the spectrophotometer is, under the symmetrical illumination, effectually unchanged.

In transmission measurements we are usually not troubled with any polarization introduced by the sample itself. If the incident beam is appreciably polarized, however, a strained-glass sample or an optically active solution may possibly so alter the state of polarization as to introduce an appreciable error into the transmission measurements. It is well, therefore, that the initial polarization of the beams incident on the sample be small, as is the case with the sources herein employed.

In conclusion, it may be stated that in all the transmission and reflection measurements to be made with the equipment herein described, the polarization factors may be either neglected or eliminated by proper procedure in the measurements. Hence the previous formulas for X reduce simply to

$$X = \tan^2 \theta_0 \cot^2 \theta_1 \tag{33}$$

$$X = \cot^2 \theta_0 \tan^2 \theta_2 \tag{34}$$

$$X = \cot \theta_1 \tan \theta_2 \tag{35}$$

(*b*) PROPAGATION OF ERROR THROUGH THE FORMULAS.—It is sometimes desirable to know the precision with which the value of X is determined from a set of readings of the angles of match when using any one of the equations (33), (34), and (35). For this purpose let Z_1, Z_2, and Z be the *fractional probable errors*[18] in the computed values of X by equations (33), (34), and (35), respectively; and let p_0, p_1, and p_2 be the probable errors in the determination of the corresponding angles θ_0, θ_1, and θ_2. Then, in accordance with the general theory of the propagation of error,[19] the following relations

[18] The fractional probable error is here defined as the ratio of the probable error in X to the value of X itself.

[19] Merriman, Method of Least Squares, 8th ed., p. 79.

may be derived (in which the probable errors are expressed in radians):

$$Z_1^2 = 16\ (p_1^2 \csc^2 2\theta_1 + p_o^2 \csc^2 2\theta_o) \tag{36}$$

$$Z_2^2 = 16\ (p_2^2 \csc^2 2\theta_2 + p_o^2 \csc^2 2\theta_o) \tag{37}$$

$$Z^2 = 4\ (p_1^2 \csc^2 2\theta_1 + p_2^2 \csc^2 2\theta_2) \tag{38}$$

Let θ_o, θ_1, and θ_2 be each the mean of n settings of the angle of match. Let $\Sigma\Delta\theta_o$, $\Sigma\Delta\theta_1$, and $\Sigma\Delta\theta_2$ be the sum of the n residuals of θ_o, θ_1, and θ_2, respectively, these residuals being taken without regard to algebraic sign and expressed in circular degrees. The relation between the probable error of the mean of the observed angles and the sum of the residuals is given by the approximate formula[20]

$$p = \frac{0.8453\ \Sigma\Delta\theta}{n\sqrt{n-1}} \tag{39}$$

In routine spectrophotometric measurements, 10 settings are usually made of each angle of match. Placing $n = 10$ in equation (39) and remembering that p in equations (36), (37), and (38) must be expressed in radians, the following formulas are then obtained:

$$Z_1 = 0.002\sqrt{\frac{[\Sigma\Delta\theta_o]^2}{\sin^2 2\theta_o} + \frac{[\Sigma\Delta\theta_1]^2}{\sin^2 2\theta_1}} \tag{40}$$

$$Z_2 = 0.002\sqrt{\frac{[\Sigma\Delta\theta_o]^2}{\sin^2 2\theta_o} + \frac{[\Sigma\Delta\theta_2]^2}{\sin^2 2\theta_2}} \tag{41}$$

$$Z = 0.001\sqrt{\frac{[\Sigma\Delta\theta_1]^2}{\sin^2 2\theta_1} + \frac{[\Sigma\Delta\theta_2]^2}{\sin^2 2\theta_2}} \tag{42}$$

A useful graph for the computation of the probable error by any one of the equations (40), (41), and (42) has been previously published,[21] but is reproduced in the present paper in Figure 14. The legend on this graph clearly explains its use with equations (35) and (42). The symbols X and Z are replaced by T and $(P.E.)_T/T$, respectively, on the graph. Its use with equations (40) and (41) is obviously the same.

(*c*) Choice of Formula for Routine Work.—It is evident that two different methods of use of the instrument are available for the measurement of X. In the first method the two parts of the field are matched with the sample in either beam 1 or beam 2, and again with both beams clear. Equation (33) is used in the first case and equation (34) in the second case. In the second method the two parts of the field are first matched with the sample in (say) beam 1, then again with the sample in beam 2, and equation (35) is used.

[20] Smithsonian Physical Tables, 2d rev. ed., p. 59; 1920.

[21] See paper by Priest, McNicholas, and Frehafer on "Some tests of the precision and reliability of measurements of spectral transmission by the Koenig-Martens spectrophotometer," J. O. S. and R. S. I., p. 211; 1924.

The second method is generally applied in all work with the instrument, chiefly for the following reasons:

1. The possibility of polarization errors are very much reduced, and we may assume that for all ordinary samples no appreciable polarization errors are present in the measurement of X when equation (35) is used.

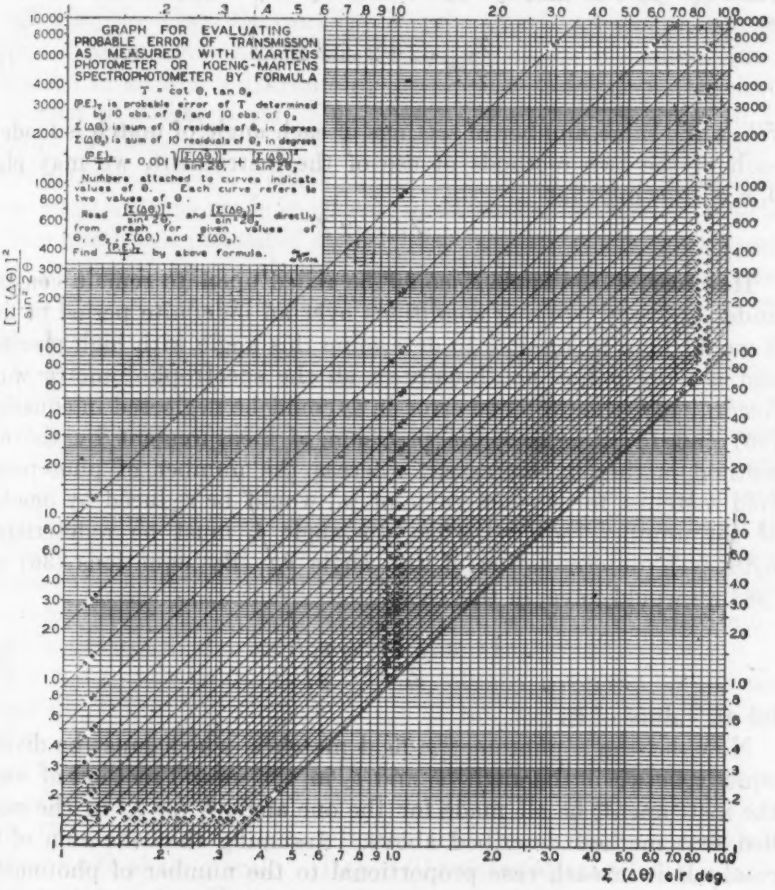
GRAPH FOR EVALUATING PROBABLE ERROR OF TRANSMISSION AS MEASURED WITH MARTENS PHOTOMETER OR KOENIG-MARTENS SPECTROPHOTOMETER BY FORMULA
T = cot θ, tan θ₂
(P.E.)T is probable error of T determined by 10 obs. of θ1 and 10 obs. of θ2
Σ (Δθ1) is sum of 10 residuals of θ1 in degrees
Σ (Δθ2) is sum of 10 residuals of θ2 in degrees
Numbers attached to curves indicate values of θ. Each curve refers to two values of θ.
Read [Σ(Δθ)]²/sin² 2θ and [Σ(Δθ)]²/sin² 2θ directly from graph for given values of θ1, θ2, Σ(Δθ1) and Σ(Δθ2).
Find (P.E.)T by above formula.
[Σ (Δθ)]²/sin² 2θ
Σ (Δθ) clr deg.

FIG. 14.—*Graph for the evaluation of probable errors*

2. In the second method the field brightness at match is nearly the same for both positions of the sample. This is an important consideration in the measurement of low values of X, as it avoids eye strain and consequent loss in photometric precision which would result from alternate settings at widely different field brightnesses.

3. A consideration of the probable errors in X shows that the precision with which the value of X is determined from a set of readings of the angles of match is different for each of the equations

(33), (34), and (35), and that a greater precision of measurement is generally obtained in the second method of use of the instrument.

In the following comparison of the two methods of use of the instrument we are justified in making the following approximations in the preceding formulas for the probable errors: Let $p_o = p_2 = p_1$ in equations (36) and (37), and let $p_2 = p_1 = p$ in equation (38). Place $\theta_o = 45°$, so that $\theta_2 = 90 - \theta_1$ and $Z_2 = Z_1$. Then

$$\frac{Z_1}{Z} = \sqrt{2 + 2 \sin^2 2\theta} \frac{p_1}{p} \tag{43}$$

When the same number of settings of each angle of match is made in each of the two methods of use of the instrument, we may place $p_1 = p$, showing that

$$Z_1 > \sqrt{2}\, Z$$

However, if the angle θ_o could be relied upon to remain constant under ordinary working conditions over an indefinite period of time it would then be feasible to determine this angle with high precision and use the values continually in all the spectrophotometric work. Accordingly, the probable error in θ_o could be neglected in equations (36) and (37), so that the precision of measurement by the first method is thereby increased, whereas the number of photometric field matches, for a given value of p_1, would be reduced by one-half of the number required when the angle θ_o must be redetermined with each determination of the angle θ_1. By equations (36) and (38) we would have, in this case,

$$\frac{Z_1}{Z} = \sqrt{2} \frac{p_1}{p} \tag{44}$$

for all values of θ_1.

Now, let the n photometric field matches, which must be divided equally between the angles θ_1 and θ_2 in the second method of use of the instrument, be all made for the one angle θ_1 (or θ_2) in the modified first method described above. Assuming that the sum of the residuals is in each case proportional to the number of photometric matches, we may evaluate the ratio p_1/p by equation (39), showing that

$$\frac{p_1}{p} = \frac{1}{\sqrt{2}} \cdot \frac{\sqrt{n-1}}{\sqrt{n-1/2}}$$

Hence, in this case, $Z_1 = Z$, approximately, when n is fairly large, say about 10 or 20.

Whereas some advantages might be derived from the use of equations (33) or (34) with the Martens photometer under certain experimental conditions, it is probable that the modified first method would

not be satisfactory and reliable for general use in routine spectrophotometric measurements with the equipment herein described. As previously mentioned, the angle θ_0 varies slightly throughout the spectrum and would be subject to change with the deposition of dust or with the formation of slight diffusing films on the optical surfaces, particularly those surfaces outside of the instrument, where the beams of light to the spectrophotometer are completely separated.

(*d*) Use of One Quadrant of the Circular Scale on the Nicol Mounting.—As previously stated, angles of match can be obtained in all four quadrants of the circular scale when the sample is placed in either beam. In order to eliminate all errors in the reading of these angles, such as may be caused by eccentricities of the circular scale and vernier of the nicol mounting, it is necessary to average settings made in all four quadrants of the circle. The use of four quadrants instead of one slightly complicates the experimental procedure, with the result that more time is consumed in the measurements. In routine work, therefore, it is desirable to avoid this complication, if possible.

To investigate the relative importance of these errors, let the true angular position of the principal plane of transmission ON of the nicol be given by the (imaginary) θ scale shown in Figure 15. This scale is fixed in position relative to the instrument and is accurately centered on the axis of rotation of the nicol. Angles are measured in each quadrant from the position of ON for the extinction of light in the right field. Assuming that the vibrations in the plane-polarized beams entering the nicol from fields 1 and 2 are exactly at right angles to each other, then the angular position of the nicol for extinction of light in the left field is exactly 90° on the θ scale.

Let the ϕ scale be the circular scale actually engraved on the nicol mounting. The following assumptions are made in regard to this scale:

1. The engraving of the scale is accurate, all divisions being exactly 1° apart.

2. The center O' of the graduated circle is slightly eccentric with the center O of the θ scale. Hence O' rotates about O with rotation of the nicol.

3. When the nicol is set in position for extinction of the right field (zero position, as in fig. 15), there is a small angular displacement of the whole ϕ scale relative to the θ scale, and a displacement of the vernier so that its zero line may not coincide with either the zero or 90° marks of the ϕ and θ scales. The ϕ scale rotates with the nicol, the (single) vernier being attached to the body of the instrument. The angular displacements of both the index and the ϕ scale relative to the θ scale cause errors in the reading of θ which are constant (numerically) over the whole circle. In the discussion of these

errors, however, we can regard the position of the index as exactly coincident with the 90° mark on the θ scale and include both displacements in a single rotation of the ϕ scale.

The errors in the reading of the angular positions of the nicol are caused, then, by the combined effect of the linear and rotary displacements of the ϕ scale relative to the θ scale.

It is evident that there is only one angle of match, θ, for which the readings in opposite quadrants of the ϕ scale are exactly 180° apart. At this value of θ the center of the ϕ scale lies on the line connecting the zero of the vernier with the center of the θ scale. For all other angles of match the reading in one quadrant will be as much too large

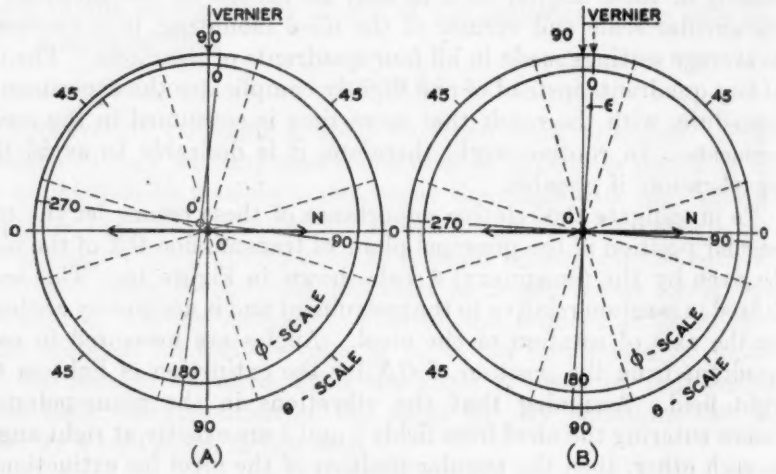

FIG. 15.—*Illustration of errors in the circular scale on nicol mounting (Koenig-Martens spectrophotometer)*

Double arrow *ON* represents principal plane of transmission of nicol. *O* indicates axis of rotation of nicol. Θ scale (imaginary) gives true angular position of *ON*. Φ scale is the circular scale actually engraved on nicol mounting. (*A*) shows combined effect of eccentricity of centers and rotatory displacement of Φ scale relative to Θ scale. (*B*) shows rotatory displacement only. The dotted lines indicate positions of *ON* for a photometric field match in each of the four quadrants, and corresponding angles read with the vernier.

as the reading in the opposite quadrant is too small, so that the error resulting from an eccentricity of the centers is eliminated by averaging the two readings in opposite quadrants. The error caused by a pure rotation of the ϕ scale relative to the θ scale is, on the other hand, eliminated by proper averaging of readings in adjacent quadrants. Let subscripts I, II, III, and IV denote readings made in the first, second, third, and fourth quadrants, respectively. Then

$$2\theta = \frac{\phi_{\mathrm{I}} + (\phi_{\mathrm{III}} - 180)}{2} + \frac{(180 - \phi_{\mathrm{II}}) + (360 - \phi_{\mathrm{IV}})}{2}$$

or

$$4\theta = 360 + \phi_{\mathrm{I}} - \phi_{\mathrm{II}} + \phi_{\mathrm{III}} - \phi_{\mathrm{IV}} \tag{45}$$

It is evident that the same small angular increment added to each value of ϕ in the above formula leaves the value of θ unchanged. Thus, by combining angles of match made in all four quadrants in the above manner, all errors in the reading of the value of θ on the ϕ scale are eliminated.

The amount of the eccentricity and rotary displacement of the ϕ scale relative to the true θ scale may be determined from readings of the angles of match in each of the four quadrants of the circle, when a low transmission sample (for instance) is placed alternately in each beam. The θ values will be the same in adjacent quadrants, but the readings on the ϕ scale will generally not be equidistant from the 0, 90, 180, or 270° marks. Let the subscripts 1 and 2 refer to the positions of the sample in beams 1 and 2, respectively. The angular differences between the 0, 90, 180, and 270° marks on the ϕ scale and the corresponding positions on the θ scale are denoted by the general symbol $[\theta-\phi]$ and given by the following equations:

$$[\theta-\phi]_{\phi=0}=180-\frac{1}{2}(\phi_{2,\mathrm{IV}}+\phi_{2,\mathrm{I}}) \tag{46}$$

$$[\theta-\phi]_{\phi=90}=90-\frac{1}{2}(\phi_{1,\mathrm{I}}+\phi_{1,\mathrm{II}}) \tag{47}$$

$$[\theta-\phi]_{\phi=180}=180-\frac{1}{2}(\phi_{2,\mathrm{II}}+\phi_{2,\mathrm{III}}) \tag{48}$$

$$[\theta-\phi]_{\phi=270}=270-\frac{1}{2}(\phi_{1,\mathrm{III}}+\phi_{1,\mathrm{IV}}) \tag{49}$$

These differences are the result of both sources of error mentioned above and will not generally have the same value. (Fig. 15, A.) Let ϵ be the average of the four values of $[\theta-\phi]$ thus obtained. Then ϵ represents the rotational displacement of the scale as a whole, and the residuals are an indication of the eccentricity of the center. If the eccentricity of the ϕ scale is negligible or zero, however, the $[\theta-\phi]$ differences are the same for all parts of the scale. In this case (the sample being stationary in either beam)

$$4\epsilon=720-\phi_{\mathrm{I}}-\phi_{\mathrm{II}}-\phi_{\mathrm{III}}-\phi_{\mathrm{IV}} \tag{50}$$

True values of θ can then be obtained by applying the constant correction ϵ to the readings of ϕ, as made in one quadrant only, or by adjusting the vernier into coincidence with the zero mark on the ϕ scale when the nicol is set for the extinction of light in the right field.

To test the accuracy of the scale on the particular instrument herein used, angles of match have been made in all four quadrants in the measurement of the transmission of the 1 and 10 per cent sectored disks. The mounting of the disks has been described, and their use

with the instrument will be further discussed in section V, 1. The $[\theta-\phi]$ differences in equations (46), (47), (48), and (49) were found to be practically the same for this particular scale, and the value of ϵ was 0.24°. In Table 1, columns 3, 4, 5, and 6, the transmissions are recorded as computed from the corrected angles of match, using each quadrant separately. In column 8 the transmissions are computed from the averaged angle as given by equation (45). The purpose of this table is to show that it is not necessary to make readings in more than one quadrant of the circular scale in routine spectrophotometric work with this particular instrument. Errors introduced by neglecting the small correction to the scale readings are reduced by use of equation (35) instead of either of equations (33) or (34), for the angles of match are then more nearly equally distant from 45°, and the same small increment added to both θ_1 and θ_2 causes counteractive changes in the cotangent and tangent. If the scale correction ϵ were neglected in the computation of the transmissions in column 3 of Table 1, the values obtained would be on the average about 1.8 per cent lower than the values in column 8. In the measurements of the 10 per cent sectored disk the values would be lower by only 0.4 per cent. By care in the adjustment of the vernier the above errors may be further reduced. An error of 0.2° is of no importance unless very low values of X are being measured, so that θ_1 and θ_2 are close to 90 or 0°, respectively. Readings in these parts of the scale are therefore avoided by use of the sectored-disk attachment.

In routine work with the instrument, then, readings of the angle of match are made only in the first quadrant of the circular scale. An occasional check is made on the adjustment of the vernier.

TABLE 1.—*Transmission measurements with the Koenig-Martens spectrophotometer, using four quadrants of the circular scale on the nicol mounting*

Sample	Wave length	$T=\cot(360-\phi_1-\epsilon)\tan(360-\phi_2-\epsilon)$ (for quadrants I and IV) $T=\cot(180-\phi_1-\epsilon)\tan(180-\phi_2-\epsilon)$ (for quadrants II and III) $4\epsilon=720-\phi_1-\phi_{II}-\phi_{III}-\phi_{IV}$					$T=\cot\theta_1\tan\theta_2$ $4\theta=360+\phi_1-\phi_{II}+\phi_{III}-\phi_{IV}$
	$m\mu$	T_I	T_{II}	T_{III}	T_{IV}	T_{Mean}	
1 per cent sectored disk	490	0.00855	0.00848	0.00845	0.00840	0.00847	0.00848
	530	.00873	.00848	.00860	.00862	.00861	.00860
	570	.00873	.00855	.00869	.00884	.00870	.00870
	610	.00866	.00854	.00846	.00873	.00860	.00860
	650	.00867	.00838	.00863	.00849	.00854	.00856
10 per cent sectored disk	530	.0994	.0995	.0993	.0996	.0994	.0995
	530	.1005	.1004	.0999	.1000	.1002	.1002
	610	.0984	.1005	.0990	.1004	.0996	.0996

(*e*) PROCEDURE IN MEASUREMENTS.—The usual procedure in a transmission or reflection measurement at a given wave-length setting is as follows: After the wave-length scale has been set to the desired position, 5 settings of the angle of match θ_1 are made in the

first quadrant with the sample in (say) beam 1. The sample is then shifted to beam 2, and 10 settings of the angle θ_2 are made. Returning the sample to beam 1 again, the group of 10 settings of θ_1 is completed. As these readings are made they are immediately recorded by the observer on an (8-place) adding machine, the keyboard of which is split so that θ_1 and θ_2 may be recorded in separate columns. This machine is shown in Figure 1, conveniently situated for the observer's right hand. After the two sets of readings at a particular wave length are completed, a pull on the lever adds these readings, and thus records the mean angles. When a complete set of measurements have been made at various wave lengths throughout the spectrum, the values of X are computed with a special slide rule having a cotangent and tangent scale.[22]

In the case of some reflection samples the intense illumination from the hemispherical source may, as previously noted, cause changes in the reflective properties of the sample during the course of the measurements. In order to detect these changes and to make an

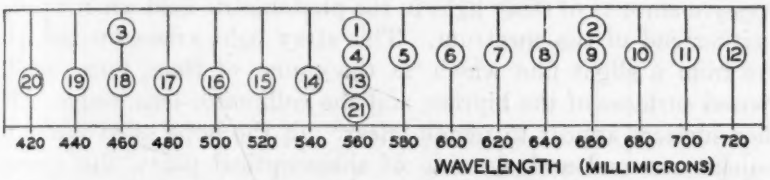

FIG. 16.—*Order of determinations with respect to wave length, generally followed in reflection measurements*

approximate correction therefor, a definite predetermined order of observation with respect to wave length is always followed. The procedure may vary with the type of sample to be measured and with other conditions; but the order of observation generally followed is depicted in Figure 16 and represents a minimum set of observations for a given reflection sample. If the determinations 1 and 4 (at wave length 560) show no change, for instance, but a definite difference is found between determinations 2 and 9 (at wave length 660), one may generally assume, to a first approximation at least, that the change has been progressive with time and that proportional changes have taken place at the intervening or adjacent wave lengths. Sometimes the reverse changes are noted. If there is reason to suspect that the sample is particularly subject to change in the blue region of the spectrum, the series 13 to 20 may precede 4 to 12. A more elaborate arrangement of the observations may be devised in particular cases.

[22] Made to order by Keuffel & Esser Co., Hoboken, N. J., after design by I. G. Priest at the Bureau of Standards.

It is difficult to establish any fixed order of observation for all samples or rules for the correction of the data. The experience and judgment of the observer determines the exact procedure followed with a given kind of material, type of reflection curve, or other circumstances. Usually the changes, when they do occur, are not more than a few per cent of the value measured, and the approximate corrections derived from a study of the observed changes at a few chosen wave lengths are better than none whatever. The nature of the materials usually does not warrant more accurate data than are obtained in this way. In cases wherein a large change does occur it is often desirable to repeat some of the measurements with the use of a new and unexposed sample of the material.

4. FURTHER REMARKS ON THE INSTRUMENT AND ITS ADJUSTMENTS

(*a*) STRAY LIGHT.—Although the optical parts of the instrument are well inclosed by the manufacturer, it was formerly necessary to remove some of these parts during the course of each year in order to clean the optical surfaces and thus prevent the appearance of an excessive amount of stray light in the photometric field when working in either end of the spectrum. This stray light arises for the most part from a slight film which, in the course of time, forms on the exposed surfaces of the biprism and the collimator-lens wedge. The other surfaces appear to remain clear. In the hope of avoiding the frequent removal and cleaning of these optical parts, the spectrophotometer has been inclosed in a dust-proof and approximately moisture-proof box, which is shown in Figure 1. (Door shown open ready for measurements.) This housing prevents the accumulation of dust on the instrument and has proved very effective in retarding the development of stray light in the photometric field. Several glass light filters are provided, having transmission bands in different regions of the spectrum. These filters may be placed between the eye and the nicol and practically eliminate any small amount of stray light present.

(*b*) PHOTOMETRIC FIELD.—Under ordinary conditions of measurement and with the sources of light herein employed the photometric field of the instrument is well-nigh perfect, with a complete disappearance of the dividing line when both parts of the field are matched in brightness. The photometric precision of the brightness matches is believed to be as good as can be obtained with any other type of photometric field used in spectrophotometry.

There is one experimental condition, however, under which very imperfect field conditions will be obtained unless care is taken in the adjustment of the lens—Wollaston—biprism combination (hereafter referred to by the letters LWB). This condition often arises in transmission or reflection measurements on materials exhibiting a strong

selective absorption, so that the spectral distribution of the light entering one of the collimator slits of the instrument is varying rapidly with the wave length in certain regions of the spectrum, whereas the variation with wave length of the light entering the other collimator slit is comparatively small. The extremely rapid variation in the spectral light distribution of the entrant beam may be accompanied by an appreciable variation in brightness across the corresponding half of the photometric field, this variation being always in a direction parallel to the dividing line (vertical). The brightness in the other half of the field will, on the other hand, appear sensibly uniform. This brightness variation may be directly attributed to two possible causes, both producing the same effect. These causes are: (1) The inaccurate focusing of the telescope lens, and (2) the spherical aberration present in the lens system of the instrument.

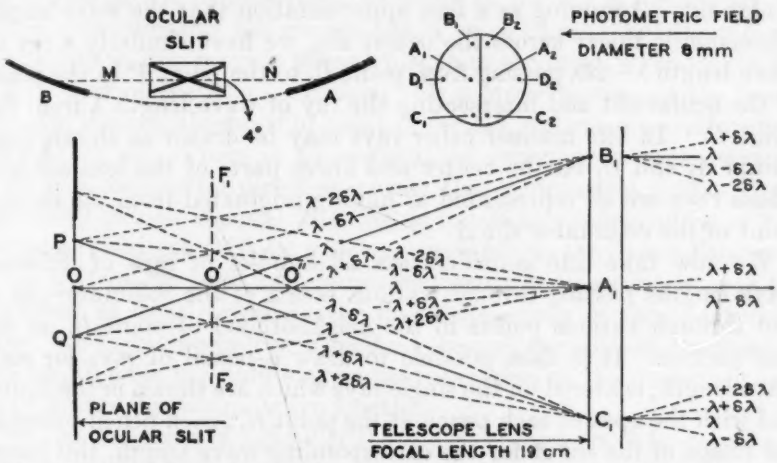

FIG. 17.—*Conditions resulting in a nonuniform brightness distribution over the photometric field*

An explanation of the effect will now be given, along with the proper procedure to be followed in the adjustment of the LWB combination in order that the above causes may have a minimum effect on the uniformity of the brightness distribution over the photometric field.

In the first part of this discussion all defects which may be present in the lens system of the instrument will be neglected. The LWB combination is regarded as a perfect lens. We recall, however, that, as viewed through the ocular slit, the lens surface is divided into two equal parts by the line of intersection of the biprism faces (dividing line in photometric field; see fig. 17, upper right) and each part is independently illuminated by light entering the corresponding collimator slit (fig. 3). Let the wave-length scale of the instrument be set for a particular wave length λ and let the entrant beams be heterogeneous with respect to wave-length composition.

Consider a homogeneous bundle of rays of wave length λ entering the instrument through the central point of the collimator slit A. These rays may be assumed in the present discussion to be incident on the telescope lens, in Figure 17, as a parallel beam which is itself parallel to the axis of the lens; they are brought to a focus at the point O' on the axis and in the focal plane F_1F_2 of the lens. Let the ocular slit, which is centered on the axis of the lens, be displaced a distance OO' from its correct position in the focal plane. Consider, now, another homogeneous bundle of rays of wave length $\lambda-\delta\lambda$, originating also at the central point of the slit A. These rays will be slightly inclined to the axis of the telescope lens and also brought to a focus at a point in the plane F_1F_2. The wave-length difference $\delta\lambda$ may be so chosen that the ray which passes through the point B_1 near the periphery of the lens will also pass through the central point O of the ocular slit. Assuming as a first approximation that the wave-length dispersion is linear across the ocular slit, we have similarly a ray of wave length $\lambda-2\delta\lambda$ passing from point B_1 to the point P in the plane of the ocular slit and intersecting the ray of wave length λ from the point C_1. In like manner other rays may be drawn as shown from points A_1 and C_1 on the center and lower parts of the lens surface. These rays are all represented as having originated from the central point of the collimator slit A.

We now take into consideration all bundles of rays of different wave lengths passing through various points of the collimator slit A and through various points in the neighborhood of point B_1 on the lens surface. It is then possible to draw a pencil of rays for each wave length, centered on the single rays which are shown in the figure, and with the apex of each pencil at the point B_1; each pencil subtends the image of the slit A for the corresponding wave length, this image being here considered as formed only by rays passing through the surface of the lens in the immediate neighborhood of the point B_1. The slit images for different wave lengths are displaced vertically relative to one another to form a sharply focused spectrum in the plane F_1F_2, but a slightly out-of-focus spectrum in the plane of the ocular slit. Considering all the rays passing through any other small area of the lens surface, as at points A_1 and C_1, a similar construction of rays may be made. It is evident from Figure 17 that the various spectra thus formed by various portions of the telescope lens coincide exactly in the plane F_1F_2, but are not coincident in the plane of the ocular slit. The spectrum formed in the latter plane by the upper part of the lens, at B_1, is shifted downward toward the longer wave lengths by an amount $\delta\lambda$, relative to the spectrum formed by the central part of the lens. Similarly, the spectrum formed by the lower part of the lens, at C_1, is shifted upward toward the shorter wave lengths by (approximately) the same amount. In addition to

the vertical shift, there is also a lateral shift of each spectrum relative to the spectrum formed by the central part of the lens, this shift depending on the horizontal distance from the center of the lens of the image-forming portion under consideration. As will be shown later, the effect of the horizontal shift on the brightness variation across the photometric field is entirely negligible.

Looking through the ocular slit at a central portion of lens surface in the neighborhood of point A_1 (or A_2, fig. 17), one sees this area illuminated by light of mean wave length λ, but extending over a spectral range depending primarily on the widths of the collimator and ocular slits being used. The image on the retina of the eye is formed with all the homogeneous ray pencils, previously defined, originating at points in the area about A_1 and subtending the whole or a part of the ocular slit. The image of an upper portion of the lens surface in the neighborhood of point B_1 (or B_2) is formed with light of approximately the same range of wave lengths, but the mean wave length in this range is lower by $\delta\lambda$ than the mean wave length λ at the center of the lens. Similarly, for a lower portion of the lens surface in the neighborhood of point C_1 (or C_2), the mean wave length is higher by $\delta\lambda$. There is no appreciable variation in mean wave length in a horizontal direction across the photometric field. The angle QB_1O (which is equal to PC_1O) is practically independent of λ; but the wave-length shift $\delta\lambda$, which corresponds to the linear distance OP (or OQ) in the spectrum, increases rapidly with an increase in λ as a result of the decrease in the linear dispersion in the spectrum toward the longer wave-length region. Hence, the shift in the mean wave length over the photometric field increases as the ocular slit is moved toward the longer wave lengths.

Now, let the spectral light distribution in beam 1 (say) be decreasing very rapidly with the wave length, whereas the variation with wave length of the light in beam 2 is, on the other hand, comparatively small. Then, if the nicol is set for equality of brightnesses at A_1 and A_2, where the mean wave length is λ, there will be an appreciably lower brightness in the upper part of field 1 at point B_1, where the mean wave length is $\lambda-\delta\lambda$, and a higher brightness at C_1, where the mean wave length is $\lambda+\delta\lambda$. Unless the ocular slit is very badly out of focus, the small wave-length shift $\delta\lambda$ will cause no appreciable difference between the brightnesses at points A_2, B_2, and C_2.

It is obvious from Figure 17 that the magnitude of $\delta\lambda$ may be increased or decreased by moving the ocular slit parallel to the axis of the lens, so that the distance OO' is increased or decreased. Thus, when OO' is zero, $\delta\lambda$ is also reduced to zero; hence, the photometric field must appear uniform in brightness. When the slit is moved in beyond the point O', the brightness gradient across the field is, of course, reversed.

We will now consider the effect of any spherical aberration which may be present in the lens system of the instrument. In order to use Figure 17 for this purpose, any effect of the collimator lens will not be represented. The spherical aberration of this lens would but increase the effect introduced by the telescope lens. Chromatic aberration and other defects in the optical system are of minor importance in this connection, and are therefore neglected in the following discussion.

Let a narrow pencil of rays of wave length λ, passing through the central part of the lens, be brought to a focus at O', as before. As a matter of convenience in the diagram, we may choose the distance $O'O''$ to represent the longitudinal aberration of the lens. Then, a pencil of rays of wave length λ from a peripheral part of the lens at B_1 will be brought to a focus at a point slightly above the axis of the lens on the line B_1O''. (The locus of all the foci of these narrow pencils of rays from various portions of the lens would form the caustic surface of the lens for the wave length λ.) Similarly, a ray B_1O' of wave length $\lambda-\delta\lambda$ may be drawn coincident with the ray of wave length λ in the previous discussion. The ray C_1O' is now of wave length $\lambda+\delta\lambda$, and, likewise, other rays shown in the diagram are shifted in wave length by the same amount $\delta\lambda$. It is evident that the previous discussion applies identically to this case, so that the aberration effect is minimized by moving the center of the ocular slit to the point O''.

It is probable that the aberration effect is small, if not negligible, and that the focusing effect accounts for the greater part of the brightness gradient which may be observed in the photometric field under the conditions described above.

As illustrated in Figure 17 (upper left), the images of the two collimator slits do not coincide over their entire length. At their closest contact they make an angle of approximately 4° with each other. It is of interest to consider what relation, if any, this crossing of the images may have on the focusing (or aberration) effect discussed above. This crossing of the images is a result of the curvature in the plane of the image, introduced by the action of the dispersion prism. If the biprism and Wollaston prism were removed from the instrument, the images of the two (separated) collimator slits would lie on the arc of a circle as shown at A and B in the figure. The Wollaston and biprism combination, however, in addition to dividing these images into eight separate images, as previously explained, shifts them horizontally, causing two of them to overlap as shown at the center of the ocular slit. The horizontal shift of the spectra formed by the lateral portions of the telescope lens would obviously result only in a slight difference between the mean wave lengths at corresponding points, such as D_1 and D_2, in the lateral areas. The

crossing of the images will also broaden the total wave-length range included by the ocular slit. In this respect it is equivalent to a widening of the ocular slit in the diagram. This does not change the distance OO' or therefore the value of $\delta\lambda$. The actual range of wave lengths above and below the average is increased, however, equally over all parts of the lens. If the rapidly varying spectral light distribution in the entrant beam is not a linear function of the wave length, it is possible that the brightness gradient across the lens may thereby be slightly increased or decreased. Experiment shows, however, that a change in the ocular-slit width, or a decrease (by use of a diaphragm) in the length of the slit, has very little effect on the appearance of the field.

The brightness gradient is never present when a homogeneous source, such as the mercury arc, is used for the illumination of the collimator slits. If the collimator-slit images were exactly parallel to the ocular-slit jaws, however, and if the edge of the ocular slit were then allowed to encroach slightly on the image of the spectral line, a brightness gradient across the lens would be observed. This is evident from a consideration of the λ rays only in Figure 17, letting the distance PQ represent the image of the collimator slit formed by the central portion of the telescope lens. The shifted image formed by a peripheral portion of the lens is obviously partly cut off by one edge of the slit, causing a decreased brightness in the corresponding part of the photometric field. (The duplication of this pattern for infinitesimal wave-length steps, as when a continuous-spectrum source is used, results in the somewhat different brightness gradient previously discussed.) It may be noted that the shift of the slit images is greatly exaggerated in the diagram. Unless the slit is very far from the plane F_1F_2, a rather nice adjustment of its edges would be necessary in order to observe any brightness gradient across the field, when a line-spectrum source is used. The crossing of the slit images, however, never permits the required relation to exist.

The brightness gradient can not be completely eliminated in the Koenig-Martens spectrophotometer, owing to the asymmetry introduced into the optical system by the wedges on the collimator and telescope lenses. In Figure 18 it is shown that the rays passing the upper parts of the telescope lens suffer excessive refraction and cross the axis of the lens between the point O' and the lens. Similarly, the rays passing the lower parts of the lens cross the axis slightly beyond the point O'. The aberration, if present, is consequently also greater for the upper parts of the lens and less for the lower parts than that previously represented in Figure 17. There is no position of the ocular slit, therefore, for which the whole field is equal in brightness to the central portion. With the center of the

slit at O' the brightness gradient from the central toward the lower portions of the photometric field is reversed, whereas the gradient toward the upper portions is not entirely eliminated. Hence, it is evident that both the lower and upper parts of the field will be somewhat darker than the central part.

This condition of the photometric field is not serious, and the importance of the residual brightness gradient, considered as an inherent defect in this particular type of instrument, must not be overrated or adjudged by the length of the discussion here given to it. The residual effect is only occasionally observed in transmission measurements under the condition previously stated. It is entirely absent when the mercury-vapor or helium lamp sources are used, as previously explained. In the case of reflection measurements the required condition of the entrant beam is rarely present. The effect introduces no error in the spectrophotometric measurements, if only

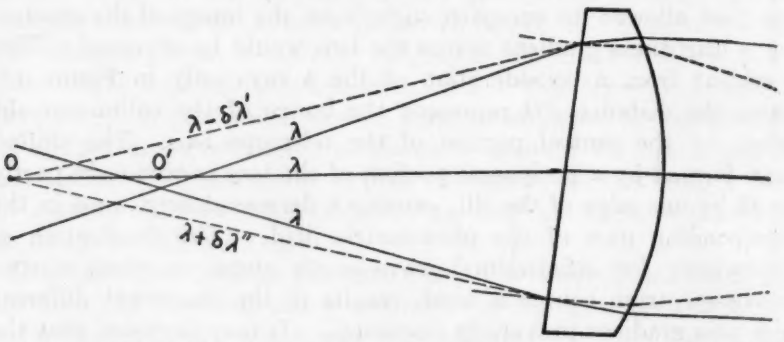

FIG. 18.—*Effect of the asymmetry of the lens system on the brightness gradient across the photometric field*

the central portion of the photometric field (which is free from the disturbing effects above described) is used for the brightness matches. But the precision of the settings of the angle of match is somewhat reduced, owing to the decreased area of the field and the decreased length of the dividing line which may be used.

The brightness gradient may well become a serious matter in the use of the Koenig-Martens spectrophotometer, however, if more than ordinary care is not taken in the adjustment of the distance of the *LWB* combination from the ocular slit. The slit being stationary in this instrument, the *LWB* combination must be moved along the axis of the telescope tube. The ordinary method of adjustment, using an eyepiece to view the ocular slit and adjusting the position of the lens so that the image of a spectral line is apparently as sharp as possible, is not sufficiently sensitive for the purpose. A better adjustment may be made in the following manner:

The condition for the appearance of the brightness gradient is first established by inserting the proper type of (transmission) sample in one of the entrant beams. A high-transmission red glass with a sharp cut-off in the orange region of the spectrum is a suitable sample for this purpose. If the wave-length scale is set to a wave length on the steep slope of the transmission curve, the brightness gradient will generally be visible when the continuous-spectrum source of light is used. The *LWB* combination is mounted in a brass tube which fits snugly into the telescope tube and is held in place by a clamping screw. Loosening this screw, the combination may be moved along the axis of the tube and also rotated about this axis. The combination is moved toward or away from the slit until the brightness gradient is reduced to a minimum. During this operation the center of the photometric field may be kept matched in brightness by rotation of the nicol; also, the angular position of the combination must be properly maintained such that no color difference appears between the two halves of the field. This color difference appears when the two line images of the collimator slits (fig. 17, upper left) are not crossing approximately at the center of the ocular slit, for it is evident that when this condition is not fulfilled the two spectra formed with all the light passing fields 1 and 2, respectively, are then shifted vertically and in opposite directions relative to each other. The mean wave length of the small spectral range transmitted by the ocular slit is then different for each spectrum, and consequently for each half of the photometric field. The image will cross at the center of the slit when the intersecting line of the biprism surfaces (dividing line in the photometric field) is perpendicular to the line *MN*.

The final adjustment of the angular position of the *LWB* combination may be made more accurately by removing the red glass from the entrant beam and setting the wave-length scale in the neighborhood of wave length 580 mμ, for in this region of the spectrum a small change in wave length produces a maximum change in color. The final adjustment is best made, however, by illuminating the collimator slits with a line-spectrum source (such as the mercury-vapor lamp), then replacing the nicol with the eyepiece in order to view the slit images in the plane of the ocular slit, and finally making any rotation of the *LWB* combination necessary to obtain a crossing of the images at the center of the slit. The complete adjustment of the *LWB* combination is easily accomplished, and when once made is very stable.

(*c*) Wave-Length Scale.—Occasional attention to the adjustment of the wave-length scale is necessary. For this purpose the eyepiece is again used to view the ocular slit. Using the homogeneous light from the helium and mercury-vapor lamps, the check or recali-

bration of the scale is quickly made by finding the scale reading for which the crossed images of the collimator slits are centered on the ocular slit.

(*d*) CIRCULAR SCALE.—The circular scale on the nicol mounting is large enough (75 mm in diameter) so that tenths of a degree may easily be estimated or read with the vernier. A low-power reading lens is provided for this purpose. This scale, with its single vernier, is sufficiently accurate for photometric purposes (when the regions close to 0 and 90° are avoided, as previously discussed). Successive settings of the nicol can not generally be made closer than 0.2°; and in consequence of some obscure subjective vagaries of the human visual system the mean of a number of settings of the angle of match may vary as much from time to time.

(*e*) GENERAL REMARKS.—The instrument is compactly made and is convenient to use. As shown in the vertical median section of Figure 3, the refracting edge of the dispersion prism is horizontal, giving the telescope tube an upward slant. The observer thus takes a convenient and natural position at the instrument, which adds considerably to his comfort during a long continuous series of observations, and hence to the quality of his work. The greatest disadvantage in this type of instrument is the waste of light inherent in the nature of the optical system. Some minor mechanical imperfections do exist, as in the construction of the ocular slit; because of the method employed for the mounting of the nicol prism this slit is somewhat inaccessible and is not provided with a means for quick and accurate adjustment in width. Whereas some improvements in the construction of its mechanical parts could be suggested it is doubtful if such changes would increase the general accuracy of measurement attainable with the instrument. Other matters in visual spectrophotometry would warrant a corresponding consideration.

V. USE OF EQUIPMENT AND TESTS OF ITS PERFORMANCE

1. TRANSMISSION MEASUREMENTS

The tungsten lamp (continuous spectrum) source is for obvious reasons used in the greater part of the transmission work. The maximum brightness of this source (88 lamberts) is more than sufficient for measurements in the more luminous region of the spectrum, so that the lamps are usually operated below normal voltage, except in the blue and extreme red ends of the spectrum or for low-transmission samples.

Many of the materials presented for transmission measurements (such as dye solutions, colored glasses, etc.) often exhibit rapid variations of transmission with wave length (steep transmission

curves) in certain regions of the spectrum. In these cases a small spectral range (narrow collimator and ocular slits) must generally be used in order to avoid slit-width errors[23] in the measurements. Except on the steep sides or near the minima or maxima of strong absorption bands, a spectral range of about 5 mμ is generally safe for all spectrophotometric work. The slit widths on the Koenig-Martens instrument corresponding to a 2 and 5 mμ spectral range [24] are given in Table 2. By experience the observer learns to adjust the slit widths to suit the conditions of measurement, thus obtaining in many instances the advantage of greater field brightness when needed without introducing appreciable errors in the work.

TABLE 2.—*Widths of ocular slit on the Koenig-Martens spectrophotometer, for the inclusion of a given wave length range of pure spectrum*

Wave length	Slit widths in mm for spectral range of—		Wave length	Slit widths in mm for spectral range of—	
	2 mμ	5 mμ		2 mμ	5 mμ
mμ			mμ		
720	0.04	0.10	520	0.12	0.30
680	.05	.12	480	.16	.40
640	.06	.14	440	.23	.58
600	.07	.18	420	.29	.71
560	.09	.23	400	.36	.91

In this connection the measurements with the helium and mercury-vapor lamp sources are of special value as checks on the measurements made with the heterogeneous (tungsten lamp) source. With the homogeneous light from these sources the slits may be opened wide without danger of slit-width errors and with a proportional gain in field brightness. The distribution of the Hg and He wave lengths usually permits a check on the steep part of the transmission curves.

The availability of the Hg lines at wave lengths 436 and 405 mμ is of further advantage in supplementing the continuous-spectrum source in the blue and violet regions of the spectrum, where the field brightness with the latter source is usually too low for best photometric work. Using these homogeneous radiations, however, precise measurements may be made at the corresponding wave lengths for transmissions as low as 1 per cent at wave length 405 mμ and lower at 435 mμ. This matter is of considerable importance in the computa-

[23] See discussion of slit-width errors in papers by Nichols and Merritt, Phys. Rev., **30**, p. 328; 1920. Hyde, E. P., Astrop. J., **35**, p. 237; 1912.

[24] The spectral range included by the ocular slit is somewhat indefinite until further conditions are specified. The data in Table 2 are computed from the wave-length calibration curve of the instrument and represent the ocular-slit widths which would include a given range of a pure spectrum such as would be formed if the collimator slit were very narrow. When the collimator-slit width is equal to that of the ocular slit, the actual range of wave lengths in the transmitted light is doubled, owing to the overlapping of collimator-slit images at the ocular slit; but a greater part of the total radiant energy transmitted by the ocular slit is distributed among the wave lengths contained in the pure spectrum range given in Table 2.

tion from the spectrophotometric data of the trichromatic coordinates of the color of the transmitted light, as well as in other applications of the spectrophotometric data. The change to the helium or mercury-vapor sources is rapidly and conveniently made, as previously explained.

As an indication of the precision and accuracy of the measurements with the spectrophotometer and transmission sources herein described, the measured transmissions of the 1, 10, 50, and 80 per cent sectored disks are shown in Figure 19 along with the fractional probable errors in the transmission as computed by equation (42). The precision of measurement depends to some extent, of course, on the general brightness level of the photometric field. In order, therefore, that the field brightnesses in these tests be representative of general working conditions with the heterogeneous source, a spectral range of 5 mμ was maintained at all wave lengths with the following exceptions: At wave lengths 700, 720, 740, and 760 mμ the ranges were 7, 10, 16, and 18 mμ, respectively. With the mercury-vapor lamp source, slits as wide as possible were used for wave lengths 436 and 405 mμ. In this way a greater field brightness is obtained at these wave lengths than can be obtained with the heterogeneous source and narrow slits. For wave lengths 546 and 578 mμ (576.9 + 579.1 mμ) the field brightness with the wide slits was too great for eye comfort. In these cases the slits were either narrowed or a neutral low-transmission screen placed before the nicol. The precision of the measurements made with the Hg lines at wave lengths 436 and 405 mμ is, in general, as good, even for low-transmission samples, as that obtained with the heterogeneous source in the more luminous regions of the spectrum.

The horizontal broken lines in Figure 19 represent the known transmissions of the disks as given by angular measurements of the sector openings.[25] These values are given in the figure and are known to be accurate within one unit in the last decimal place. The accuracy of the measurements with the spectrophotometer is indicated by the general proximity of the points to horizontal lines. Occasional wide departures, which do not appear to be caused by inherent instrumental errors, are common in spectrophotometric work and are often difficult to explain. Measurements on these disks, made by other observers in this laboratory on various occasions, are in good agreement with the above data. The data, as a whole, show no systematic error in the measurements at any wave length and for transmission values down to 10 per cent. Measurements on a sectored disk having a known transmission of 0.0154 have been reported in a previous publication.[26] These measurements indicate no discrepancies in the direct measurement of low-transmission values of this magnitude.

[25] See footnote 8, p. 813.

[26] See footnote 21, p. 830.

In the case of the 1 per cent sectored disk (accurate transmission = 0.88 per cent), however, the measurements herein reported are consistently too low by an average value of about 2 per cent. Referring to the data in Table 1, it is evident that this error is not caused by the inaccuracies there considered in the circular scale of the nicol mounting, for it is not eliminated by the averaging of the readings made in the four quadrants. In the previous discussion of errors in the circular scale it was assumed that the plane-polarized vibrations entering the nicol from fields 1 and 2 were strictly at right angles to each other; also, that the transmission of the nicol prism for a plane-polarized beam followed exactly the cosine-square law. Neither of these conditions may be accurately fulfilled, and the discrepancies,

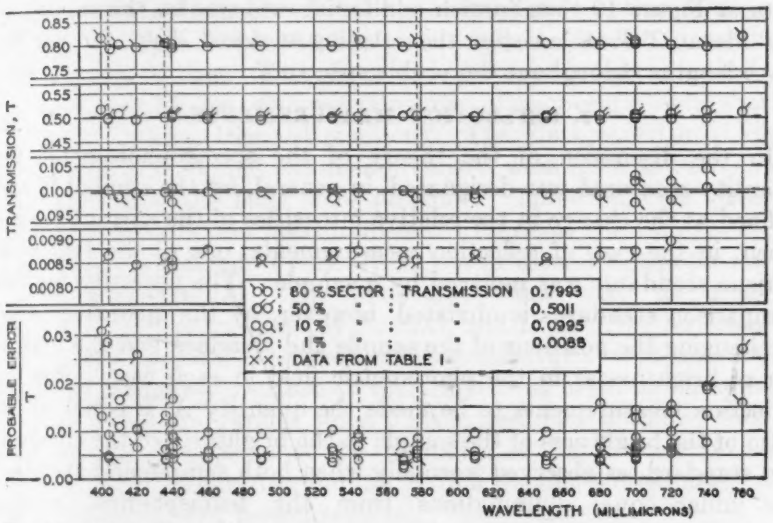

FIG. 19.—*Test of precision and accuracy of measurements with the Koenig-Martens spectrophotometer (using transmission sources)*

though small, may readily give rise to the error observed in the direct measurement of such low-transmission values.

These errors are avoided, however, by use of the 1 or 10 per cent sectored disk in the beam opposite the sample, as previously described. In this way transmissions in the neighborhood of 0.001 are measured with accuracy, for all wave lengths at which a sufficient field brightness may be obtained.

To test the accuracy of the mechanical calibration of the 1 per cent sectored disk, its transmission was measured with the spectrophotometer relative to that of the 10 per cent disk. The following substitution method was used in order to avoid readings on the circular scale near 0 and 90°: A glass having a transmission of approximately 10 per cent was mounted in the regular manner in one beam, with the 1 per cent sectored disk mounted in the other beam.

The transmission of the disk was then carefully measured (for wave length 530 mμ) relative to that of the glass by the usual method of interchanging the glass and sector in the beams. Ten readings of each angle of match were made in each quadrant of the circular scale. The 10 per cent disk was then substituted for the 1 per cent disk and likewise measured relative to the same glass (without disturbing the position of the glass on the sample holder). From these data the transmission of the 1 per cent disk was computed, using the known transmission of the 10 per cent disk, as given by both mechanical and photometric calibrations (fig. 19). A value of 0.00880 was obtained, which is in excellent agreement with the mechanical calibration.

Assuming the accuracy of the photometric measurements, the data in Figure 19 then furnish additional evidence for the validity of the Platau-Talbot law (for the rotating sectored disk) for various wave lengths throughout the visible spectrum.

2. REFLECTION MEASUREMENTS

In the discussion of the theory of the spectrophotometer the quantity measured was designated, in general, by the symbol X and defined as the change in the relative intensities of the entrant beams, when, in the case of reflection measurements, one of the two comparison standards was replaced by a sample. The necessity for two comparison standards is obviated, however, by the operation of interchanging the positions of the sample and standard and the matching of brightnesses in the photometric field in each case. For the reflection measurements to be made the quantity X is equal to the ratio of the brightness of the sample to the brightness of the comparison standard, as observed normally when both sample and standard are under equal illuminations from the hemispherical source. Actually, the absolute illuminations on the sample and standard need not be the same, such inequalities being effectually eliminated in either of the two methods of use of the instrument. (See Section IV, 3.) The brightness ratio may depend, however, on the degree of diffusion of this illumination. This matter will be fully discussed later in this section.

(*a*) REFLECTION STANDARDS.—The comparison (or "working") standard which has been in use for some time is an opaque porcelain plate having a fine-ground (matt) reflecting surface. The choice of this particular material was purely a matter of convenience and serviceability. Its absolute reflectance is fairly high and approximately nonselective with respect to wave length; it is durable, withstands the heat from the lamps without special cooling, and may be removed for cleaning as frequently as desired.

In order to express the reflective properties of a given material in terms of a more definite and reproducible material, however, a magnesium oxide film is used as the primary reference standard for

all spectral reflection work. This material is used pending the development of a more suitable material or means for the absolute evaluation of the working standard.

The magnesium oxide standard is prepared by allowing the oxide from burning metallic magnesium to deposit upon a plane matt porcelain plate to a thickness such that a further increment in thickness would produce no change in the reflective properties. A magnesium oxide film so prepared is a good diffuser and has a reflectance almost unity (approximately 0.98), with very little, if any, selectivity with respect to wave length.

No extensive study of the permanence or reproducibility of this standard has been made. In order to calibrate the working standard, however, measurements of its brightness relative to that of the oxide have been made (with the equipment herein described), using five different oxide films. These films were prepared in the prescribed manner from two different commercial sources of magnesium metal shavings (as used for the Grignard reaction). The films varied in thickness from 0.36 to 0.50 mm, and measurements were made in each case on the same day the films were prepared. Three different observers participated in these measurements. Three of the films were prepared and measured (by H. J. M.) soon after the equipment was completely installed. The other two films were prepared and measured two years later (by K. S. G. and D. B. J.). No consistent differences between these various determinations were found which could be definitely ascribed to real differences between the reflective properties of the various films. From the data obtained thus far, this standard appears to be reproducible, under the prescribed conditions of preparation and use, within the limits of accuracy of the spectrophotometric measurements.

Under the specified conditions of illumination and observation, then, let

$B_0 \equiv$ brightness of primary MgO standard,
$B_0' \equiv$ brightness of working standard,
$B_x \equiv$ brightness of test sample.

In routine reflection measurements the quantity B_x/B_0' is directly measured. B_0'/B_0 is the result of the calibration of the working standard in terms of the primary standard. The final expression of the reflective properties of the sample is then computed as

$$\frac{B_x}{B_0} = \frac{\text{Brightness of sample}}{\text{Brightness of MgO standard}} = \frac{B_x}{B_0'}\frac{B_0'}{B_0} \tag{51}$$

This ratio is, of course, a function of the wave length.

Referring to the discussion of Absolute Methods in Reflectometry in Bureau of Standards Journal of Research, vol. 1, No. 3, it is of interest to note in this connection that the brightness ratio measured

in the present paper may also be expressed (in the terminology of the paper cited) as the apparent normal reflectance of the sample relative to that of the standard under the given conditions of completely diffused illumination. Also, in accordance with the reciprocity law of Helmholtz, the quantity measured is the reflectance of the sample relative to that of the standard for unidirectional normal illumination. If the absolute spectral reflective properties of the standard were known, the absolute spectral reflectances of the sample would then be determined. Equipment is now being assembled with which the standard may be calibrated in absolute reflective terms, if desired.

(*b*) ADEQUACY OF ABSOLUTE ILLUMINATION ON SAMPLE.—The nature of the materials usually presented for reflection measurements is such that the above brightness ratio does not generally exhibit such rapid variations with wave length as does the transmission of many glasses, solutions, etc. In other words, reflection "curves" are not generally so steep as transmission curves. Without danger of appreciable slit-width errors, then, wider slits may generally be used in reflection measurements, with a corresponding gain in photometric field brightness. Another characteristic of reflection samples is that a measurable quantity of light is always reflected into the spectrophotometer at all wave lengths. Under completely diffused illumination this quantity is rarely less than 2 or 3 per cent of that reflected by the comparison standard. Hence the photometric field brightness at a given wave length is never reduced below a certain limit.

These characteristics of the reflection samples have a bearing on the adequacy of the hemispherical source herein described, in regard to the absolute illumination on the sample. Although, for a given value of X and given widths of the instrument slits, the spectrophotometric field brightness with this source is not as high as that obtainable with the transmission sources, the illumination on the sample and standard is sufficient, nevertheless, for good photometric precision in the measurements throughout the brighter region of the spectrum. When proper advantage of the permissible slit widths is taken, measurements of sufficient precision may always be made over the whole spectral range from 700 or 720 to 420 mμ.[27]

[27] An arrangement providing completely diffused illumination from a mercury-vapor lamp is desirable to supplement the above heterogenerous illumination, so that accurate measurements may be made on any sample at wave lengths 405 and 436 mμ (as obtained in the case of transmission measurements). Apparatus has been installed in the laboratory, however, with which the desired brightness ratio may be measured under approximately 45° illumination from the mercury-vapor lamp. The Martens photometer is used in this case with selective filters to isolate the various spectral lines. Proper precautions are also taken to avoid polarization errors in the measurements. When the diffusive properties of the sample are not widely different from those of the comparison standard, the normal brightness ratios obtained under these conditions of illumination are practically the same as obtained under completely diffused illumination. With this equipment the field brightness at wave length 405mμ is wholly adequate for precise reflection measurements on all samples.

This arrangement of apparatus was designed and assembled by Dr. K. S. Gibson especially for use in measurements made for the Munsell Research Laboratory on 70 representative samples from the Munsell Color System (B. S. test 46045; 1926). The method has subsequently been further developed and applied by W. D. Appel. See American Dyestuff Reporter (Sample Swatch Quarterly), p. 49; Jan. 23, 1928.

The hemisphere lamps are usually operated at a voltage considerably below normal, except in the end regions of the spectrum or for low-reflection samples.

(*c*) Equivalence of the Illumination to the Ideal Completely Diffused Condition.—The measurements described on the sectored disks are a proof of the accuracy of the spectrophotometer in the measurement of the normal brightness ratio of the sample to the standard under the actual conditions of illumination from the hemispherical source. The question now arises whether or not the numerical value thus obtained truly represents the desired brightness ratio under the ideal condition of completely diffused illumination. This ideal condition would be realized if all elements of the hemispherical inclosure were of equal brightness. Obviously, the condition is not rigorously satisfied in the actual construction of the hemispherical source, but the tests to be described will show that the illumination obtained with the present construction is practically equivalent to the desired condition of illumination for the reflection measurements to be made on different kinds of materials.

If the sample and comparison standard have very nearly the same diffusive properties [28] (but not necessarily the same reflectance), the normal brightness ratio would be the same for any condition of illumination. When the diffusive properties of the sample differ widely from those of the standard, however, the brightness ratio may depend to a considerable extent on the condition of illumination.

Assuming that the illumination is not a sufficient approximation to the desired condition, then the error in the measurement of the normal brightness ratio of the sample to the standard depends essentially on the following considerations: (1) The degree and nature of the departure of the illumination on the sample from the desired completely diffused condition, and (2) on the diffusive properties of the sample and comparison standard.

The comparison standard is usually a fairly matt diffusely reflecting material. The samples, on the other hand, may represent various stages of mixed diffuse and specular reflection varying from nearly perfect diffusion on the one extreme to pure specular reflection (mirror sample) on the other.

In the test of the illumination apparatus and in the choice of samples for this purpose we are not particularly concerned with the absolute reflectance of the test samples (or standard), or with the spectral composition of the incident and reflected light. These matters play no essential rôle in the test and enter into consideration

[28] Two samples will be considered to have the same diffusive properties under given conditions of illumination when the relative angular distributions of the reflected light flux—compared always at the same wave length—are practically the same for each sample. The diffusive properties depend to a large extent on the absolute reflectance of the sample; hence, when the latter property varies markedly through the spectrum the diffusive properties change accordingly.

only implicitly through their relation to the diffusive properties of the test samples. For example, a sample of black paint with a smooth, glossy surface will approximate closely to the mirror sample, because very little light is reflected diffusely from the body of the material. Given a similar material, however, with a white pigment instead of the black, the large quantity of body reflection accompanying the surface reflection will bring the sample closer in type to the perfect diffuser. Likewise, the diffusive properties of a colored sample may be quite different for different parts of the spectrum.

A practical test of the adequacy of the hemispherical arrangement herein described, as a source of completely diffused illumination for the prescribed purposes, has been made in the following manner:

1. A separate source of diffused illumination was available, which was known by independent tests to be a very close and sufficient approximation to the completely diffused condition of illumination for these purposes.

2. A group of samples was chosen representing various degrees of departure from the perfectly diffusing sample on the one hand and a mirror sample on the other. The color of these samples being unimportant, a group of neutral samples was used of which the reflective properties were already known from the results of a previous investigation.

3. The brightness ratios of the test samples to the (porcelain) comparison standard were measured for both sources of diffused illumination and the results compared. An agreement between the two sets of measurements is then considered as a sufficient proof of the equivalence of the two illuminations for the intended purpose.

The known source for completely diffused illumination used in this test is part of an equipment now being assembled for the study of various problems involving the reflective and transmissive properties of diffusing materials. A complete description of the source and the spectrophotometric apparatus used with it will be given in a forthcoming publication of the bureau series. In the following brief description of this new equipment only those features are mentioned which have a bearing on its application to the present problem:

1. The source for completely diffused illumination is constructed in a manner somewhat similar to that described in the present paper, the essential difference respecting the illumination on the sample being the interposition of a milk-glass hemisphere between the lamps and the sample.

2. The sample and standard are not mounted side by side and compared simultaneously, but either one may be placed alone at the center of the base of the milk-glass hemisphere and the normal brightness of the sample observed with a spectrophotometer through

a small hole at the pole of the hemisphere. The sample may also be observed at 12° from the normal (and at five other angles).

3. The spectrophotometer [20] differs in type from the Koenig-Martens instrument and uses a comparison source, separate from the hemispherical source, for the illumination of one half of the photometric field. The other half of the field is illuminated by light reflected from either the sample or the standard under the (completely) diffused illumination from the milk-glass hemisphere. The desired brightness ratio is obtained by alternate substitutions of the sample and standard.

4. The relative brightness distribution over the inner concave surface of the milk-glass hemisphere may be measured directly from the position of the sample and is known to be constant within definite limits, so that the degree of approximation to the ideal completely diffused condition of illumination on the sample is also definitely known.

This illumination is as nearly completely diffused as any of three diffused illuminations previously described by the author in connection with a study of some absolute methods in reflectometry. (B. S. J. Research, **1**, No. 3, fig. 4.) In that work a group of samples was used, approximately neutral in color, and representing various degrees of departure from the perfectly diffusing sample. The reflective properties of these samples were found to be the same under each of the three diffused illuminations above referred to. Hence it was concluded that the three illuminations were each a sufficient approximation to the completely diffused condition for all practical purposes. The reflective properties of the samples were not analyzed with respect to wave length, however, as a spectrophotometer was not used in the investigation. Hence the measurements therein made can not be compared directly with measurements which might be made on the same samples with the Koenig-Martens spectrophotometer and the illumination apparatus here under test. Different quantities are measured in each case. This previous work is referred to here as a proof of the equivalence of the illumination from the milk-glass hemispherical source to the ideal completely diffused condition of illumination, in order that the equipment briefly described above may be justly applied to the present test of the source of diffused illumination used with the Koenig-Martens spectrophotometer. Furthermore, the samples therein employed form a series such as is required in this test. The samples actually used, however, are not the identical samples employed in the previous work, but very similar pieces from the same stock or kind of material;

[20] The type of instrument used is described by C. W. Keuffel, J. Opt. Soc. and Rev. Sci. Inst., **2**, p. 403; 1925.

so that the data and curves in the paper cited serve as a good description of the reflective properties exhibited by the test samples. These samples are all of a type showing no appreciable polarization of the light reflected to the spectrophotometer.

The brightness ratios, as measured with both sources of diffused illumination, are given in Table 3. From the preceding discussion it is evident that complete measurements for various wave lengths throughout the whole visible spectrum are not essential to this test. Measurements have been made only at wave lengths 480, 580, and 670 mμ. Slit widths on each spectrophotometer corresponding to a 10 mμ spectral range were used to insure an entirely adequate field brightness and thus a maximum photometric precision in all the measurements. The use of neutral samples avoids the possibility of any slit-width errors or other uncertainties incident to the measurement of brightness ratios varying rapidly with the wave length. The magnesium-carbonate, white-felt, and **M** samples have a matt surface, whereas the **V** samples are photographic papers having a smooth, very glossy surface.

TABLE 3.—*Test of the diffused illumination used for reflection measurements, showing its equivalence to the ideal completely diffused condition of illumination*

Sample [1]	Wave length	$\frac{B_s}{B_o}$ = Brightness of sample / Brightness of (porcelain) comparison standard measured under the illuminations from—							
		Source used with Koenig-Martens spectrophotometer (shown in figs. 3 and 4)				Milk-glass hemispherical source for completely diffused illumination (briefly described in text)			
		Determinations—			Mean	Determinations—			Mean
		1	2	3		1	2	3	
Magnesium carbonate block	480	1.232	1.231	-------	1.232	1.255	1.214	-------	1.235
	580	1.230	1.250	-------	1.240	1.260	1.232	-------	1.246
	670	1.294	1.304	-------	1.299	1.307	1.300	-------	1.303
White felt	480	.756	.758	0.752	.755	.773	.770	0.760	.768
	580	.846	.850	.832	.843	.853	.858	.854	.855
	670	.918	.936	.932	.928	.946	.932	.923	.934
Black felt	480	-------	.0305	.0276	.0290	-------	.0283	.0297	.0290
	580	.0261	.0260	.0256	.0260	.0259	.0256	.0241	.0252
	670	-------	.0327	.0327	.0327	-------	.0346	.0355	.0350
M-2 (matt paper)	480	.618	.638	-------	.628	.626	.636	-------	.631
	580	.630	.630	.636	.632	.628	.638	-------	.633
	670	.626	.634	-------	.630	.614	.645	-------	.630
M-8 (matt paper)	480	.0598	.0584	-------	.0591	.0518	.0581	.0615	.0668
	580	.0526	.0532	-------	.0529	.0502	.0497	.0504	.0501
	670	.0577	.0578	-------	.0578	.0578	.0564	.0589	.0577
V-I-A (glossy paper)	480	.856	.855	.858	.856	.876	.857	.846	.860
	580	.878	.867	.868	.871	.876	.880	.874	.877
	670	.944	.924	.940	.936	.940	.943	.933	.939
V-4	480	.2030	.2080	.2030	.2047	.2020	.2005	.2036	.2020
	580	.2008	.2065	.2083	.2052	.2090	.1985	.1985	.2020
	670	.2114	.2170	.2078	.2121	.2060	.2105	.2048	.2071
V-5	480	.0745	.0718	-------	.0732	.0788	.0845	-------	.0816
	580	.0782	.0798	-------	.0790	.0785	.0784	.0792	.0787
	670	.0848	.0852	-------	.0850	.0846	.0934	-------	.0890
Silvered-glass mirror	580	1.096	1.085	-------	1.090	1.082	1.084	-------	1.083

[1] See B. S. J. Research, **1**, No. 3, for complete description of the samples and their reflective properties. The **M** samples are gray painted cardboard (matt surface). The **V** samples are glossy photographic papers.

The measurements on the mirror and glossy samples, in particular, show quite conclusively that the desired condition of illumination is approximated so closely, with the hemispherical illumination apparatus here under test, that further approximation to the ideal condition would not appreciably alter the observed brightness ratios.

When the glossy samples are observed normally with the milk-glass hemispherical source, there is a noticeable effect on the observed brightnesses caused by the (black) observation hole at the pole of the hemisphere. The effect is not appreciable with the hemispherical construction used with the Koenig-Martens spectrophotometer, because of the greater spread of the beams and the narrowness of the hemisphere slits (15, fig. 4). Consequently, the measurements with the milk-glass hemispherical source were made on all the samples at an observation angle of 12° from the normal. However, the previous study of these test samples shows that, with the exception of the white-felt sample only, the brightnesses under approximately completely diffused illumination are sensibly the same for 0 and 12° angles of observation. The slightly higher value obtained for the white-felt sample with the milk-glass hemispherical source is in accordance with the reflective properties of this material.

In the measurement of very glossy samples it is evident that a greater part of the light reflected into the spectrophotometer originates from the polar region of the hemisphere. Consequently, it is particularly important that the average brightness of the source in this region be approximately equal to the average brightness of the whole hemisphere. The filtering of the air which is drawn through the hemisphere for ventilation purposes is an important matter in the maintenance of the desired condition of illumination.

A set of reflection samples which have been calibrated under a known source of completely diffused illumination are a desirable adjunct to the equipment, in order to test and maintain an occasional check on the conditions of illumination.

Many features of the equipment herein described represent the accumulated experience of the colorimetry laboratory of the Bureau of Standards in regard to the requirements for visual spectrophotometry. In this respect the author gratefully acknowledges miscellaneous contributions and suggestions by I. G. Priest and K. S. Gibson which are embodied in the design of the apparatus.

WASHINGTON, January 22, 1928.

EFFECT OF TEMPERATURE CHANGE ON THE COLOR OF RED AND YELLOW LOVIBOND GLASSES[1]

By Deane B. Judd[2]

ABSTRACT

The spectral transmission at 12 wave lengths in the visible spectrum of two Lovibond glasses (35Y and 7.2R) has been carefully determined at 15° C. and at 40° C. From these spectral transmission data the color changes corresponding to the temperature interval of 25° C. have been computed. It was found, both for 35Y alone and for the 35Y+7.2R combination, that an increase of 25° C. is the practical colorimetric equivalent of adding 0.2 in Lovibond red units. This difference is almost negligible in the color grading of cottonseed oil.

Preliminary work on two samples of cottonseed oil indicates that the oil changes in color with change in temperature even less than the glasses do. If all oils behave like these two samples, only extreme variations (more than 15° C.) in temperature need be taken into account in color grading cottonseed oil with Lovibond glasses.

CONTENTS

	Page
I. Introduction	859
II. Method of measurement	860
III. Results	861
IV. Summary	866

I. INTRODUCTION

The present paper is a minor contribution to the program which has been in course at the Bureau of Standards for a number of years, and which has for its goal the attainment of agreement in color grading cottonseed oil. Considerable progress has been made in standardizing the Lovibond glasses themselves,[3] and a start has been made toward standardizing the observers who use the glasses.[4]

[1] A preliminary synopsis of certain of the experimental results herein reported has appeared in the Oil and Fat Industries for April (p. 115) and May (p. 152); 1928.

[2] This work was carried out at the instance of Irwin G. Priest and with the advice of Dr. K. S. Gibson, who had made some preliminary measurements, which he put at the disposal of the present author.

[3] Report on calibration of sixteen Lovibond red glasses of nominal value 7.6, by I. G. Priest, Cotton Oil Press; January, 1921. The Lovibond Color System, I. A Spectrophotometric Analysis of the Lovibond Glasses, by K. S. Gibson and F. K. Harris, B. S. Sci. Paper No. 547; Feb. 17, 1927. (Copies may be obtained from the Government Printing Office, Washington, D. C., at 15 cents each.) Standardizing the red and yellow Lovibond glasses, by Irwin G. Priest and K. S. Gibson, J. Opt. Soc. Am. and Rev. Sci. Inst., 16, p. 116; 1928. A study of 129 Lovibond red glasses with respect to the reliability of their nominal grades, by Deane B. Judd and Geraldine K. Walker, Oil and Fat Inds., 5, p. 16; 1928. See also Oil and Fat Inds., p. 433, December, 1927; p. 27, January, 1928; p. 58, February, 1928; p. 92, March, 1928; p. 114, April, 1928; p. 152, May, 1928; p. 184, June, 1928; p. 220, July, 1928.

[4] Tests of the color sense of A. O. C. S. members and data on sensibility to change in Lovibond red, by Irwin G. Priest, Oil and Fat Inds., 5, p. 63; 1928. A much more comprehensive test was carried out at New Orleans in May, 1928, and a report of the results is in preparation.

It is well known, however, that the absorption characteristics of many glass filters, and, hence, the color of those filters, change with temperature. If an oil were graded with a set of glasses at (say) 25° C. at one time, and by the same observer at another time with the same set of glasses at 50° C. (that is, the oil at 25°, the glasses at 50°), it might reasonably be expected, on account of the temperature change of the glasses, that the two grades would not agree.[5] Whether the amount of this disagreement would be important or negligible, or whether it would result in too high or too low a grade for the oil, can not be predicted. It is the purpose of the present paper to give results of tests framed to decide these points.

II. METHOD OF MEASUREMENT

Determination of the relative spectral transmission [6] of two glasses ($35Y_{BS10289C}$ and $7.1R_{BS10288C}$)[7] separately and in combination were made for the following wave lengths: Hg 405, Hg 436, 470, Hg 492, He 502, 530, Hg 546, 560, Hg 578, He 588, 620, and 680 mμ, 20 settings entering into each determination. The spectrophotometer used was the Koenig-Martens instrument equipped with a thermostat for control of the temperature of the sample.[8] A single set of measurements consisted of one determination made at each of the above wave lengths with the sample at 15° C., then one determination for each wave length with the sample at 40° C., and, finally, one determination at each of wave lengths 405, 436, 492, 502, 546, 578, and 588 mμ with the sample again at 15° C. Two sets each were made for the three filters (that is, for the two separate glasses and their combination). Special precautions were taken to insure accurate setting of wave length; and, at the low temperature (15° C.) frequent inspection was made to be sure that no moisture had collected on the cover glasses.

---

[5] It should be remarked that we consider the effect of changing the temperature of the glasses alone, not the oil, because the scope of this paper does not include a study of the oils graded in practice by Lovibond glasses. The working situation, as above stated, is of more than academic interest, however, because there is some reason to believe that many oils either do not change color on being heated (see footnote 18, p. 865) or, at least, change much less than the glasses, in which case the temperature of the oil is a matter of indifference. Furthermore, if there exist oils whose color does change significantly with temperature, still the condition of having the glasses hotter than the oil sample is a technically important one because often in practice, many samples of oil are graded consecutively against the same 35Y glass which soon attains the temperature of the tintometer, while each oil sample, remaining a relatively short time in the tintometer, fails to heat to much above room temperature.

[6] The actual spectral transmissions were not measured because it was found necessary to cover the glasses being tested with two pieces of clear glass. This was done so that the glass itself could be kept at all times at the temperature of the thermostat undisturbed by currents of air from the room. The relative spectral transmissions that were obtained are very close to the actual spectral transmissions because the reflection losses due to the two cover glasses were compensated for by two plates of glass in the comparison beam.

[7] These numbers (35 and 7.1) are the numerals engraved by the maker.

[8] This instrument forms a part of the regular equipment of the colorimetry section of the Bureau of Standards. It is described in full in Bureau of Standards Journal of Research, 1 (No. 30); 1928, by H. J. McNicholas, "Equipment for Routine Spectral Transmission and Reflection Measurements."

TABLE 1.—*Spectral transmissions for 35Y, 7.2R, and 35Y+7.2R and change of spectral transmission with temperature (θ)*

[The values of T_λ are *not* exactly the ones adopted as standard by Priest and Gibson. They refer to actual glasses—35Y B.S. test 41980 and 7R B.S. test 41969—which approximate 35Y and 7.2R on the Priest-Gibson scale.]

λ in mμ	35Y		7.2R		35Y+7.2R	
	T_λ	$\left[\frac{dT_\lambda}{d\theta}\right]_\lambda$	T_λ	$\left[\frac{dT_\lambda}{d\theta}\right]_\lambda$	T_λ	$\left[\frac{dT_\lambda}{d\theta}\right]_\lambda$
		$\times 10^3$		$\times 10^3$		$\times 10^3$
380	0.000	0.000	0.449	+0.012	0.000	0.000
90	.000	.000	.456	+.012	.000	.000
400	.000	.000	.463	+.012	.000	.000
10	.000	.000	.468	+.011	.000	.000
20	.000	.000	.473	+.011	.000	.000
30	.000	.000	.475	+.010	.000	.000
40	.000	.000	.476	+.010	.000	.000
450	.000	.000	.475	+.010	.000	.000
60	.003	−.001	.471	+.010	.001	.000
70	.022	−.022	.460	+.010	.010	−.010
80	.081	−.050	.436	+.011	.035	−.020
90	.187	−.080	.393	+.014	.073	−.027
500	.313	−.103	.333	+.017	.104	−.027
10	.434	−.095	.256	+.018	.111	−.016
20	.540	−.078	.184	+.015	.099	−.006
30	.623	−.065	.147	+.009	.092	−.004
40	.682	−.050	.167	+.004	.114	−.006
550	.720	−.037	.253	−.006	.182	−.013
60	.738	−.025	.378	−.018	.279	−.023
70	.742	−.015	.495	−.019	.367	−.022
80	.735	−.005	.589	−.019	.433	−.017
90	.719	+.005	.661	−.017	.475	−.009
600	.698	+.014	.713	−.015	.498	−.001
10	.671	+.020	.752	−.013	.505	+.006
20	.645	+.023	.780	−.011	.503	+.010
30	.620	+.020	.800	−.008	.496	+.011
40	.602	+.017	.815	−.006	.491	+.010
650	.591	+.013	.828	−.004	.489	+.008
60	.590	+.007	.838	−.002	.494	+.005
70	.599	±.000	.847	−.001	.507	−.001
80	.611	−.008	.855	.000	.522	−.007
90	.617	−.013	.860	.000	.531	−.011
700	.629	−.016	.866	.000	.545	−.014
10	.650	−.018	.870	.000	.566	−.015
20	.678	−.019	.873	.000	.592	−.016

III. RESULTS

From the values of relative spectral transmission so obtained for the three filters, it has been possible, by averaging and interpolation, to obtain for every 10 mμ the change in spectral transmission (T_λ) per degree change in temperature (θ). This quantity $(dT_\lambda/d\theta)_\lambda$ is tabulated (see Table 1) for 35Y, 7.2R, and 35Y+7.2R,[9] together with the approximate values of spectral transmission for those filters.[10]

[9] This Lovibond red numeral, and those which follow, refer to the red scale established by Priest and Gibson, J. Opt. Soc. Am. and Rev. Sci. Inst., **16**, p. 116; 1928.

[10] The transmissions given are for illustrative purposes only; they do not represent accurately the particular glasses studied, but rather 35Y B. S. test 41980 and 7R B. S. test 41969 which may be taken as typical of the spectral transmission that an average Lovibond glass of grade 35Y (or 7.2R or 35Y+7.2R) yields. This is the type of spectral transmission to which the temperature coefficients of spectral transmission $(dT_\lambda/d\theta)_\lambda$ apply. The quantities in Table 1 are not independent, of course, but are connected, for each wave length, by the relations:

$$T_{35Y+7.2R} = (T_{35Y})\ (T_{7.2R})$$

and

$$(dT/d\theta)_{35Y+7.2R} = (T_{7.2R})\ [(dT/d\theta)_{35Y}] + (T_{35Y})\ [(dT/d\theta)_{7.2R}]$$

It is plain that these results really refer only to the specific Lovibond glasses tested and only for the temperatures 15 and 40° C. If we are to apply these results to all Lovibond glasses of about these grades and to all ordinary temperatures, as would be convenient, we must accept the following assumptions: (1) The spectral transmissions of these Lovibond glasses for all wave lengths are assumed to vary in a *sensibly linear* way with temperature; and (2) *all* Lovibond glasses of about these grades are assumed to change in spectral transmission with temperature approximately as have the two which were studied. It is reasonable to suppose that the first assumption is correct because the changes in transmission found are so small [11]; we expect the second to hold because the same coloring materials [12] enter into all sets of Lovibond glasses.

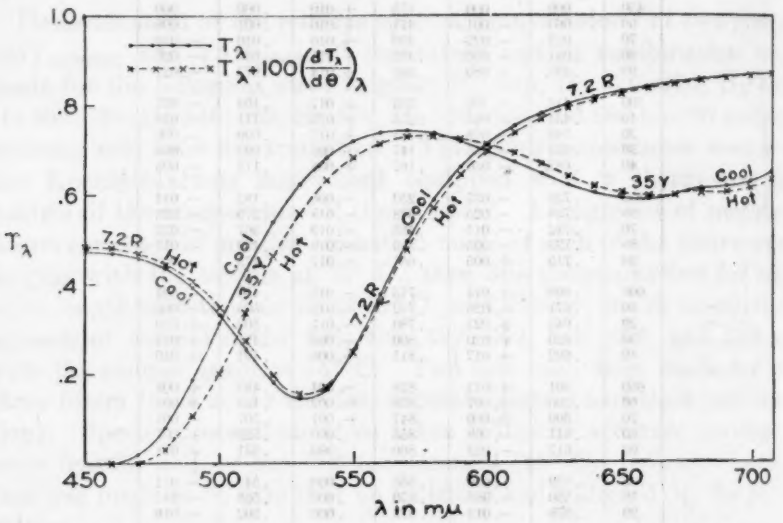

FIG. 1.—*Spectral transmission of 35Y glass and 7.2R glass at different temperatures*

Increasing the temperature of either the red or the yellow Lovibond glass shifts the curve of spectral transmission toward longer wave lengths, but the change of the yellow glass is considerably greater.

Figure 1 serves to illustrate the results presented in Table 1. The solid curves are plotted from the spectral transmissions plus 100 times the change in transmission per °C. rise in temperature. The solid curves of spectral transmission may be taken as typical of 35Y glasses and 7.2R glasses at about 20° C.; if the two assumptions just discussed are correct, the dotted curves may be taken as typical of

[11] The largest change found was 0.001 per °C. This amounts to 0.025 in transmission for the 25° temperature interval studied. A change of 0.005 in transmission is about the *smallest whose direction can be determined with certainty* from two determinations of 20 settings each.

[12] The Lovibond filters are all flashed glasses; the absorbing material in the yellow glasses is principally silver; in the red glasses, gold. (See J. W. Lovibond, On a new method of colour analysis by means of the tintometer, J. Soc. Chem. Ind., **9**, p. 15; 1890). The effect of temperature change on the light-absorbing properties of these kinds of glasses apparently has never before been studied.

the same glasses at about 120° C.[13] It may be noted that the effect of increasing the temperature of the glasses is to shift the curve of spectral transmission somewhat toward the red. Both glasses show this sort of shift, but the shift for the 35Y glass is perhaps four or five times as great as that for the 7.2R glass.

The next problem is to convert these changes in spectral transmission into colorimetric terms. It may be seen that the 35Y glass or the combination 35Y+7.2R must become more reddish on being heated, but we wish now to know how much this increase amounts to in Lovibond units. Accordingly, we assume that the glasses are illuminated by sunlight (Abbot-Priest sun) and compute the color characteristics of the transmitted light.[14] Table 2 shows the results of this computation for 35Y and 35Y+7.2R, both for the spectral transmissions given in Table 1, and for those which are typical of the glasses after a rise of 25° C.[15] The symbols in the first column refer to the trilinear coordinates (r, g, b), the dominant wave length (Λ), the colorimetric purity (P), and the transmission for Abbot-Priest sun (T_s). It will be noticed that, in both cases, heating the glasses results: (1) In a redder color (note that the r-coordinate has increased at the expense of the g and b coordinates; note also that the dominant wave length and purity have increased) and, (2) in a darker color (note the decrease in transmission for sunlight).

TABLE 2 [1]

	35Y			35Y+7.2R		
	Normal temperature	25° above normal	Change	Normal temperature	25° above normal	Change
r	0.5035	0.5073	+0.0038	0.5961	0.5994	+0.0032
g	.4595	.4580	−.0015	.3782	.3768	−.0014
b	.0370	.0347	−.0023	.0257	.0239	−.0018
Λ	575.97m	576.43	+.46	587.2	587.4	+.2
P	.931	.935	+.004	.951	.953	+.002
T_s	.622	.614	−.008	.268	.265	−.003

[1] These computed quantities are based on the Optical Society of America visual response functions as extrapolated by Priest and Gibson (J. Opt. Soc. Am. and Rev. Sci. Inst., **10**, p. 230; 1925). The standard "neutral" stimulus taken is Abbot-Priest sun (J. Opt. Soc. Am. and Rev. Sci. Inst., **12**, p. 479; 1926).

NOTE.—The data for r, g, b, Λ, P, and T are *not* the standard values for the Priest-Gibson scale. They are to be understood merely as characterizing particular glasses (35Y B. S. test 41900 and 7R B. S. test 41900) which are approximate realizations of the standard 35Y and 7.2R.

[13] Of course, the glasses are not ordinarily used at such high temperatures as 120° C., but if a small temperature difference (say 10°) were taken, the transmission differences plotted on the graph would be too small to be easily apparent. Figure 1, therefore, serves to illustrate the kind of transmission changes which occur, though to a proportionally smaller degree, for usual temperature differences (say 10 or 20° C.).

[14] For methods of computing from spectral transmission, the trilinear coordinates (r, g, b), dominant wave length (Λ), colorimetric purity (P), and transmission for sunlight (T_s), see: J. Opt. Soc. Am. and Rev. Sci. Inst., **6**, p. 527; 1922; **9**, p. 503; 1924; **13**, p. 123; 1926; and **13**, p. 133; 1926, particularly the first one cited.

[15] The transmissions typical of the glasses 25° C. above normal are computed as $T_\lambda + 25\,(dT_\lambda/d\theta)_\lambda$. This temperature difference is chosen because it is about the maximum difference which may be expected to arise in the ordinary use of the Lovibond glasses. It is also the difference at which the glasses were measured for change in spectral transmission.

Now, if a small amount of Lovibond red were added to these filters the resulting combination would also be redder and darker. It might conceivably turn out that heating the glasses is the exact colorimetric equivalent of adding a certain amount of Lovibond red to them; and if this should be the case, a convenient way of specifying the temperature effect would be its equivalent in Lovibond red. In order to find out how the color changes specified in Table 2 compare with the color changes produced by adding Lovibond red to the filters, the r and g trilinear coordinates from Table 2 are plotted on the same graph (fig. 2) with the r and g trilinear coordinates of the ideal red scale (established by Priest and Gibson) in combination with a glass that is an approximate 35Y.

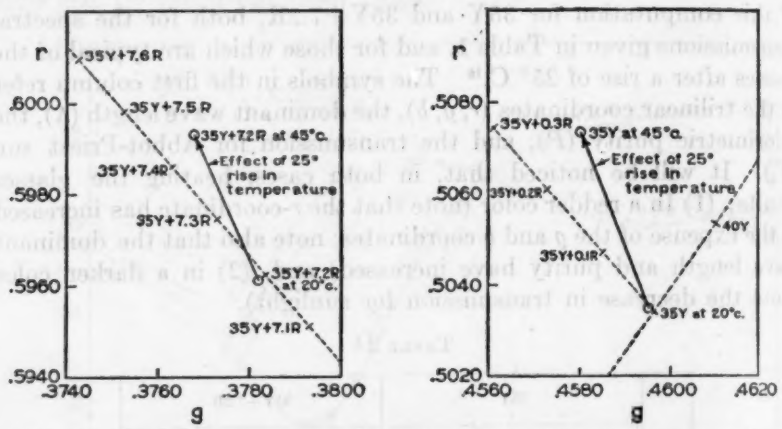

FIG. 2.—*Graphic representation of the color change of the 35Y glass and the 35Y+7.2R combination due to change in their temperature*

The color change produced by heating the red and yellow Lovibond glasses is nearly the same in both cases as is produced by adding Lovibond red, but it is not exactly the same kind of change. An increase of 25° C. is practically equivalent in either case to the addition of 0.2 in Lovibond red units.

Examination of Figure 2 shows that, both for 35Y and for 35Y+7.2R, heating the glasses is not exactly equivalent to the addition of Lovibond red, but that it is nearly equivalent. Heating either the 35Y or the 35Y+7.2 R filter 25° C. above normal is nearly equivalent to adding 0.2 Lovibond red. In more specific terms, a 35Y glass at 50° C. would be a very close hue match [16] for the 35Y+0.2R combination (on the Priest-Gibson scale) at 25° C. The saturation equivalence would not be perfect, but probably the satura-

[16] Although Figure 2 suggests strongly that the temperature effect expressed in Lovibond red units is very nearly the same at 35Y+7.2R as it is at 35Y, it is not obvious why we may say that 35Y at 45° C. has the same hue as 35Y+0.2R at 20° C. This assertion is based on the fact that r/g for 35Y at 45° C. is nearly the same as r/g for 35Y+0.2R at 20° C. It has been shown by Abney (Proc. Roy. Soc., A., 83; 1909) that constant r/g for these colors is synonymous with constant hue. To show that the hue change due to temperature change (that is, the change in r/g due to temperature change) is the same as the hue change due to the addition of a given amount of Lovibond red both at 35Y and at 35Y+7.2R, we proceed to compute for these two colors how much Lovibond red (ΔN) must be added to produce the same increment in hue ($\Delta r/g$) as was produced by raising the temperature 25° C. We have at hand the trilinear coordinates (r, g, b) for all values of N on the 35Y+NR scale (some of these are shown in fig. 2); hence we can compute r/g as a function of N. From this curve (which is sensibly linear for ΔN=0.2) we may obtain $dN/d(r/g)$

tion difference would be too small to be detected. A perfect hue and saturation match would result if some Lovibond yellow (perhaps about three units) were added as well as the 0.2 Lovibond red. This three units of Lovibond yellow is not perceptible with certainty, however. Since a rise in temperature of 25° C. is very closely equivalent in hue and saturation to the addition of 0.2 Lovibond red unit both at 35Y and at 35Y+7.2R, it is probably safe to conclude that this equivalence holds all along the 35Y+NR scale from 35Y up to 35Y+7.2R, or, perhaps, further.

It has also been shown that a rise of 25° C. makes the 35Y glass darker by 0.008 (see Table 2) and the 35Y+7.2R combination darker by 0.003. If 0.2 in Lovibond red units were added to 35Y [17] the transmission for sunlight would decrease by 0.012, which is not far from the darkening (0.008) produced by heating the glass 25° C. If the 0.2 in Lovibond red units were added to the 35Y+7.2R combination, the transmission for sunlight would decrease by 0.004 which is not far from the darkening (0.003) produced by heating the combination 25° C. Hence, we may conclude that not only is a rise in temperature by 25° C. of any of the glass combinations between 35Y and 35Y+7.2R practically equivalent in hue and saturation to the addition of 0.2 in Lovibond red units, but also that it is practically equivalent in brilliance (brilliance is degree of lightness or darkness) as well.[18]

---

for any value of N, though, to be sure, we shall need this value only for $N=0$ and for $N=7.2$. The required increments in Lovibond red (ΔN) may be computed as:

$$\Delta N=\Delta(r/g)\ [dN/d(r/g)]$$

			35Y	35Y+7.2R
See Table 2	Normal temperature	r	0.5035	0.5961
		g	.4595	.3782
	25° C. above normal	r	.5073	.5904
		g	.4580	.3768
	Normal temperature	r/g	1.0958	1.5762
	25° C. above normal	r/g	1.1076	1.5908
		$\Delta r/g$	.0118	.0146
		$dN/d(r/g)$	17.1	13.5
		$\Delta N=\Delta(r/g)\ [dN/d(r/g)]$	$.20_2$	$.19_7$

From these numerical results, it is concluded that the hue change due to temperature change of 25° C. is closely equal to the hue change produced by adding 0.2R, both at 35Y and at 35Y+7.2R.

[17] It is not meant to add a 0.2 red glass to the 35Y glass in the usual way because the resulting combination would be darker by about 8 per cent of its transmission from reflection losses, alone, due to the two added surfaces. If this addition of 0.2 in Lovibond red units is to be thought of as the combination of an actual red glass of 0.2 Lovibond grade (on the Priest-Gibson scale) with the 35Y glass, the conclusions about to be made will only be valid if these two glasses are in optical contact so that the loss in transmission due to two additional reflecting surfaces will be avoided.

[18] It may well be pointed out here that if the oil to be measured by these glasses should change in the same way with temperature as the glasses do, it might not be necessary to take any account of the change of the glasses. It would only be necessary to keep the oil and the glasses at about the same temperature. However, two samples of oil, measured in the same way the glasses were measured, did not show any certain change in hue or saturation. Both samples of oil became somewhat lighter on heating (increase in the transmission for sunlight of about 0.020), and did not, on cooling, darken quite to their original state. If the observer who reads the oils mistakes darkness for redness, this nonselective change in transmission might be important; for, to get a corresponding change in transmission for sunlight on the 35Y+NR scale, nearly a whole Lovibond red unit must be taken. Furthermore, this change is in the opposite direction from that shown by the glasses; that is, the two oils studied grew lighter, the glasses grew darker, on being heated. The conclusions based on the change of the absorbing characteristics of oil due to change in temperature are valid only for the two samples studied. It is not justifiable to assume, as was done in the case of the glasses, that all cottonseed oils are like the two samples studied, because, unlike the glasses, the oils do not contain unvarying coloring materials.

IV. SUMMARY

1. The changes in spectral transmission produced by heating a Lovibond 35Y glass and a Lovibond 35Y + 7.2R glass combination have been determined for the temperature interval of 15 to 40° C.

2. From the changes in spectral transmission the color changes resulting from the glass filters illuminated by sunlight have been computed by making use of the Optical Society of America visual response functions.

3. It is shown that, for Lovibond glasses between 35Y and 35Y + 7.2R on the Priest-Gibson scale, an increase in temperature of 25° C. is practically equivalent to the addition of 0.2 in Lovibond red units.

WASHINGTON, June, 1928.

For a list of previous research papers appearing in Volume 1, BUREAU OF STANDARDS JOURNAL OF RESEARCH, see pages 3 and 4 of cover